

Small Molecule Inhibitors of the p53-MDM2 Protein-Protein Interaction

by

Ross Patrick Fitzgerald B.Sc. M.Sc. H.Dip.

**A Thesis Submitted to the School of Pharmacy
University of Nottingham
In Fulfilment of the
Requirements for the degree of
DOCTOR OF PHILOSOPHY**

**GEORGE GREEN LIBRARY OF
SCIENCE AND ENGINEERING**

**Supervisor, Prof. Peter M. Fischer
Industry Supervisor, Dr. Daniella Zheleva
Co-Supervisor, Dr. Weng C. Chan**

University of Nottingham

October, 2009

CONTENTS

| | |
|---|------|
| Small Molecule Inhibitors of the p53-MDM2 Protein-Protein Interaction | i |
| ACKNOWLEDGMENT | vi |
| ABBREVIATIONS | vii |
| ABSTRACT | viii |
| 1. Introduction..... | 1 |
| 1.1 Cancer | 1 |
| 1.2 Tumorigenesis..... | 2 |
| 1.3 Cancer treatment | 3 |
| 1.4 The p53 tumor suppressor..... | 4 |
| 1.4.1 Discovery of p53 | 5 |
| 1.4.2 Structure of p53..... | 5 |
| 1.4.3 Function of p53 | 6 |
| 1.5 p53 activation in cancer therapy | 9 |
| 1.5.1 p53 is activated by traditional chemotherapy and radiation therapy..... | 9 |
| 1.5.2 Reactivation of mutant p53 | 10 |
| 1.5.3 Non genotoxic activation of wt p53..... | 12 |
| 1.5.4 Upstream targets in the p53 pathway | 12 |
| 1.5.5 Downstream targets in the p53 pathway | 13 |
| 1.6 MDM2..... | 14 |
| 1.6.1 MDM2: Structure | 14 |
| 1.6.2 MDM2: p53 regulator and oncogene | 14 |
| 1.6.3 Targeting MDM2 to reactivate p53..... | 16 |
| 1.7 The MDM2-p53 PPI | 17 |
| 1.7.1 Peptide antagonists of the MDM2-p53 PPI | 20 |
| 1.8 Small molecule antagonists of the MDM2-p53 PPI | 23 |
| 1.9 Therapeutic Window | 34 |
| 1.9.1 MDMX: a possible barrier to p53 reactivation? | 36 |

| | | |
|--------|--|----|
| 1.9.2 | Conclusion | 38 |
| 1.10 | Aims of this project..... | 38 |
| 1.11 | Fluorescence polarization binding assay..... | 39 |
| 1.11.1 | Loss of assay sensitivity..... | 40 |
| 2. | Bisarylsulfonamides | 42 |
| 2.1 | Introduction | 42 |
| 2.2 | Discovery | 43 |
| 2.3 | Early development SAR and binding hypothesis | 45 |
| 2.3.1 | Replacing the 4-nitro and 5-chloro substituents..... | 45 |
| 2.3.2 | Alternatives to the Thiophene Ring System | 47 |
| 2.3.3 | Modifying the <i>N</i> -Substituents | 47 |
| 2.3.4 | SAR Summary | 51 |
| 2.3.5 | Binding hypothesis..... | 52 |
| 2.4 | Results and Discussion..... | 55 |
| 2.5 | Developing the <i>N</i> -substituents | 55 |
| 2.5.1 | <i>N</i> -Aryl Substitution Pattern..... | 56 |
| 2.5.2 | <i>N</i> -Picolyl groups | 59 |
| 2.5.3 | <i>N,N</i> -disubstituted sulfonamides | 60 |
| 2.5.4 | Increasing rigidity; α -branched benzyl substituents..... | 62 |
| 2.6 | Replacing the 5-chloro-4-nitrothienylsulfonamoyl group | 66 |
| 2.6.1 | 5-alkyl substituents | 67 |
| 2.6.2 | Replacing the 5-chloro group with bromine and hydrogen | 68 |
| 2.6.3 | 5-amino substituents | 69 |
| 2.6.4 | The 5-thioacetate starting point..... | 71 |
| 2.7 | Conclusions..... | 74 |
| 3. | Shape based virtual screening for new leads..... | 76 |
| 3.1 | Introduction | 76 |
| 3.1.1 | Virtual screening | 76 |

| | | |
|--|--|-----|
| 3.1.2 | Virtual screening and p53-MDM2 | 78 |
| 3.2 | Shape based virtual screening with ROCS | 78 |
| 3.3 | Validation of ROCS. | 80 |
| 3.4 | Virtual screening work flow for this project | 81 |
| 3.4.1 | Database selection and preparation | 81 |
| 3.4.2 | Database preparation; multi-conformer generation | 84 |
| 3.4.3 | Query selection and preparation..... | 85 |
| 3.4.4 | Performing the screen | 88 |
| 3.4.5 | Hit selection for actual screening. | 89 |
| 3.4.6 | Screening: binding and cell assays..... | 112 |
| 3.4.7 | Functional assays | 115 |
| 3.5 | Conclusions and future work | 117 |
| 3.5.1 | Evaluation of the ROCS screen..... | 117 |
| 3.5.2 | Developing the hits | 119 |
| 3.5.3 | Investigating the other hits..... | 123 |
| 4. | Scaffold Hopping..... | 124 |
| 4.1 | Introduction | 124 |
| 4.2 | 1,5-Benzodiazepiene-2-ones | 125 |
| 4.2.1 | Computational Docking | 125 |
| 4.2.2 | Synthesis and testing | 126 |
| 4.2.3 | Conclusion | 129 |
| 1,3-Dihydrobenzimidazol-2-one based inhibitors | | 131 |
| 4.2.4 | Background | 131 |
| 4.2.5 | Ligand design and synthesis..... | 133 |
| 4.2.6 | Physico property prediction | 135 |
| 4.2.7 | Docking into MDM2..... | 137 |
| 4.2.8 | Synthesis | 138 |
| 4.2.9 | FP Binding Assay and SAR | 139 |

| | | |
|--------|---|-----|
| 4.2.10 | Conclusions and Future work | 141 |
| 5. | Experimental..... | 144 |
| 5.1 | Synthesis, General Methods..... | 144 |
| 5.2 | Computational Methods..... | 216 |
| 5.2.1 | General methods..... | 216 |
| 5.2.2 | Command lines, parameter files and prefixes..... | 216 |
| 5.2.3 | Spiro-oxindole query preparation | 217 |
| 5.2.4 | Nutlin and Benzodiazepiene query preparation..... | 218 |
| 5.2.5 | Database preparation..... | 218 |
| 5.2.6 | Omega .param file examples..... | 220 |
| 5.2.7 | Example of the ROCS Parameter file used in this screen..... | 221 |
| 5.2.8 | The Filter file used in this project, blockbuster_drug.txt..... | 222 |
| 5.2.9 | Example PVM.conf..... | 229 |
| 6. | Bibliography | 230 |

ACKNOWLEDGMENT

First and foremost I want to thank my main supervisor Prof. Peter Fischer for giving me the opportunity to work on this project and for continued inspiration, support and encouragement. My Industrial supervisor Dr. Daniella Zheleva at Cyclacel for her supervision and help with the assays, continued backing of the project, new ideas and making me very welcome on my visits to Dundee. My second supervisor Dr. Weng C. Chan for much input to the chemistry and a number of timely tips that prevented a lot of futile experiments. Dr. Ian Withers for facilitating the virtual screening and Lee Hibbett (the second best technician in the world!) for excellent technical support. At Cyclacel I would like to thank Dr. Graeme Thomson, Ms. Christine Tosh, for running the assays described in this project and Dr. Mark Thomas, and Dr. Campbell McInnes for assistance with molecular modelling. I am very grateful to Cyclacel and The University of Nottingham for funding this project.

On a personal note I would like to thank my many friends both at home and in Nottingham. I can't name every individual but I will single out a few who were particularly influential and supportive or just great friends over the course of this project. Ciara, Barry and Kevin for encouragement advice and helping me get my feet on the ground when deciding to do this project. All of the CBS staff and students particularly my friends Katharina, Sophia, Paulina Mike Mazanetz, Ian Hutch, Graham, Charlie L, Charlie M, Jim, Carol and Chrissie. Christophe and Geeta who I had the pleasure of sharing an office with during my time in Nottingham. Barrie Kelham and all the active members of the problem sessions. Special thanks to Shailesh, Sarah, Aditi and Lee and Ian W for assistance whilst finishing and writing up it is much appreciated. My colleagues John (the other second best technician in the World!), David and Áine in ITT-Dublin for support and tolerance above and beyond the call of duty whilst writing up. I'll be easier to work with in the future, I promise!

To Fiona, for so much love encouragement, patience, positivity, belief and general wonderfulness.

I especially want to thank my family, my parents Rita and Pdraig my brother and sister Dylan and Clare and my Aunt Carmel, for unending support without which I would not have had the opportunities I've had. I cannot (and do not) thank you enough.

ABBREVIATIONS

| | |
|------------------|--|
| Apaf-1 | Apoptotic protease activating factor 1 |
| ARF | Alternative reading frame |
| ATM | Ataxia telangiectasia mutated |
| ATR | Ataxia telangiectasia and Rad3-related |
| Bax | Bcl-2 associated protein X |
| Bcl-2 | B-cell lymphoma-2 |
| cDNA | Complimentary DNA |
| Chk1 | Checkpoint kinase 1 |
| Chk2 | Checkpoint kinase 2 |
| DCM | Dichloromethane |
| DDB2 | DNA damage binding protein 2 |
| DIPEA | Diisopropylethylamine |
| DMAP | Dimethylaminopyridine |
| DNA | Deoxyribonucleic acid |
| EGFR | Epidermal growth factor receptor |
| FP | Fluorescence polarization |
| GADD45 | Growth arrest and DNA damage 45 gene |
| HBTU | O-Benzotriazole-N,N,N',N'-tetramethyl-uronium-hexafluoro-phosphate |
| HDM2 | Human double minute 2 |
| iNOS | Inducible nitric oxide synthase |
| IP | Intellectual Property |
| kDa | Kilo Daltons |
| L | Leucine |
| MDM2 | Murine double minute 2 |
| NAD ⁺ | Nicotinamide adenine dinucleotide |
| NES | Nuclear export signal |
| NLS | Nuclear localization signal |
| NoLS | Nucleolar localization signal |
| PIG-3 | p53 induced gene 3 |
| PPI | Protein-protein interaction |
| SAR | Structural activity relationship |
| Sirt1 | Sirtuin 1 |
| Sirt2 | Sirtuin 2 |
| SPS | Solid phase synthesis |
| SV40 | Simian virus 40 |
| TEA | Triethylamine |
| TFA | Trifluoroacetic acid |
| THF | Tetrahydrofuran |
| UV | Ultra violet |
| VEGF | Vascular endothelial growth factor |
| WHO | World Health Organisation |
| wt | Wild type |
| XIAP | X-linked inhibitor of apoptosis |
| XPC | Xeroderma pigmentosum complementation group C |

ABSTRACT

In Chapter 2, bis- and tris- arylsulfonamides, were investigated as possible inhibitors of the p53-MDM2 protein-protein interaction (PPI). The lead compound, **19**, inhibited the PPI, in a fluorescence polarisation (FP) based competitive binding assay with IC_{50} 26.4 μ M and the most potent analogue, **66**, with IC_{50} 3 μ M. The active compounds in this series, possess a 5-chloro-4-nitro-2-sulfonamoyl substituted thiophene ring that is very susceptible to S_NAr reactions at the 5-position. Analogues of **19** and **66** were prepared to investigate the SAR of these inhibitors. No improvements in activity or structural activity relationship (SAR) consistent with MDM2 binding were observed and no active analogues without the reactive functionality were found. These compound are no longer being investigated.

Chapter 3 describes a 3-D shape-based virtual screening campaign to find new lead compounds. Using queries based on the established Nutlin, benzodiazepine and spiro-oxindole inhibitors, the ZINC database was screened using the program ROCS to find compounds that have good shape similarity (measured by 3D Tanimoto) and similar functional group overlap to the query molecules. 155 compounds were purchased and tested 16 of which inhibited the MDM2-p53 PPI in the FP assay at IC_{50} ranging between 48.22 and 140.42 μ M. Three analogues, **156**, **168** and **180**, induce low levels of p53 induction in cells using a Luciferase based reporter gene assay with most the potent compound, **180**, showed 5.75 fold induction at 8.89 μ M. A number of the hit compounds warrant further investigation.

Chapter 4 describes the investigation 1,5-benzodiazepine-2-ones and 1,3-dihydrobenzimidazolin-2-ones as novel scaffolds on which to base potential p53 inhibitors. A small series of analogues of each class were prepared and their ability to disrupt the MDM2-p53 PPI determined using an FP assay. None of the 1,5-benzodiazepine-2-ones showed any inhibition of the PPI at concentrations up to 500 μ M. Some of the 1,3-dihydrobenzimidazolin-2-one based compounds showed low levels of inhibition with the most potent analogue, **214** having IC_{50} 196.18 μ M. These inhibitors showed some SAR based on the size of substituents and the presence of a 6-chloro substituent that has been shown to considerably enhance the activity in other classes of inhibitor. Compounds of this type warrant further investigation using a more diverse compound library.

1. Introduction

1.1 Cancer

According to the World Health Organisation (WHO), 7.6 million deaths worldwide were due to cancer in 2005. This number is predicted to rise to 11.5 million by 2030, with lung, stomach, colorectal, liver and breast cancers being respectively responsible for the most deaths. The prevalence of different cancers varies on the basis of geographic location, age and gender. Many risk factors associated with various cancers have been identified including genetic predisposition, certain viral and bacterial infections as well as environmental and lifestyle factors with tobacco use being the single most important risk factor. It has been suggested that 40% of cancers are preventable.²

Cancer occurs when cells proliferate abnormally and independently from the signals that normally control them. Whilst it is common to classify cancers based on the organ or tissue they affect, on a genetic and biochemical level cancers are very heterogeneous. The aberrations responsible for abnormal growth can vary considerably between two cancers in the same tissue and conversely, be similar in those occurring in different parts of the body. The term cancer really refers to over 200 different diseases in which the genetic and biochemical backgrounds may be considerably different. Because of this what cures one cancer may have little or no effect on another. The need for new therapeutic strategies is nowhere more important than in oncology. Despite the identification of potential drug targets drug approval rates have dipped alarmingly over the last few years.³ It has however been suggested that while the quantity of drugs being approved may be decreasing that their quality may in fact be improving as ongoing research aims to better understand what occurs within specific diseases and develop appropriate ways to treat them.⁴

1.2 Tumorigenesis

How and when cells divide, stop dividing, differentiate and die are very tightly controlled processes that allow each and every multi celled organism to become what and indeed who, their genetic blueprint says they should be. Each cycle of mitosis is very tightly regulated by various checkpoints that ensure it occurs correctly and that when defects occur they are not passed on to the daughter cells. However, it is possible that the genes which code for the various components that regulate these processes become mutated such that tumour suppressors, which normally restrict growth, experience loss of function and oncogenes, which promote growth, experience increased function. Sufficient deactivation of tumour suppressors and activation of oncogenes causes cells to proliferate uncontrollably resulting in cancer.

Tumorigenesis, whereby normal cells become malignant cancers, is not a single event but rather a process where by cells acquire a number physiological capabilities that allow them to grow and function independent of the controls and signals of the organism to which they belong. Hanahan and Weinberg have described six of these acquired capabilities, most of which are usually required for Tumorigenesis, as “the hallmarks of cancer”.⁵ These capabilities are; self-sufficiency in growth signals, insensitivity to growth-inhibitory (antigrowth) signals, evasion of programmed cell death (apoptosis), limitless replicative potential, sustained angiogenesis and tissue invasion and metastasis. Owing to how successful cell-cycle check points are, mutations are a very rare event. The number of genetic lesions required to achieve the six hallmarks of cancer varies depending on the tumour suppressors and/or oncogenes involved. However, as these checkpoints are lost, the genome becomes increasingly unstable and prone to more mutations which in turn allow more of the hallmarks to be acquired.

1.3 Cancer treatment

Traditionally cancer treatment is based on surgery, radiotherapy or chemotherapy with cytotoxic agents. Often combinations of these approaches are used. The side effects synonymous with radiation and chemotherapy arise as a result of their genotoxic mode of action and poor selectivity for cancer cells over normal cells. The side effects may be acute such as hair loss, nausea or fatigue or chronic leading to infertility, disrupted endocrine function and the occurrence of secondary unrelated tumours later in life.^{6,7} As cancer cells are very similar to the cells that they originate from the targets of cancer drugs are also found in normal cells making selective treatment of cancer difficult to achieve. Most chemotherapeutic agents are genotoxic and target DNA or cellular components associated with replication. Their selectivity is due to their increased accumulation in rapidly dividing cells. As a result slow growing cancer cells can be resistant to treatment and rapidly dividing normal cells such as bone marrow and hair follicles accumulate high levels of anti cancer drugs and are adversely affected. Only the seriousness of cancer allows drugs with such a poor therapeutic index to be used.

Advances in the understanding of genetics at a molecular level have made it possible to identify the specific defects responsible for individual cancers. Coupled with better understanding of the biochemical roles and structures of the proteins and enzymes coded for by these genes, these defects present potential targets for drug intervention to restore correct function. If suitable drugs can be developed it should make it possible to reinstate the body's natural defences against cancer. So far, only a small number of these target specific drugs have been developed. Examples include Imatinib (Gleevec®) which inhibits the BCR-ABL tyrosine kinase expressed in Chronic myelogenous leukemia,⁸ Gefitinib (Iressa®) and Erlotinib (Tarceva®) which inhibit the EGFR tyrosine kinase that

is overexpressed or mutated in some cancers^{8, 9} and Lapatinib (Tykerb®) which is effective in breast cancers in which ERBB2 receptors are overexpressed.¹⁰ While they show excellent clinical activity, without the toxicity of cytotoxic agents, their use is limited to a small number of cancers in which their specific target is significant. Developing drugs that target the most common aberrations in all cancers is highly desirable. One such target is the tumor suppressor p53.¹¹⁻¹³

1.4 The p53 tumor suppressor

The p53 tumour suppressor protein is at the centre of the cells defence mechanisms against cancer. In response to genotoxic stress or DNA damage p53 coordinates various cellular responses, including cell cycle arrest and apoptosis, to ensure that the integrity of the genome is maintained. So important is the role of p53, it has been bestowed the title “Guardian of the Genome”.¹⁴ Loss of p53 function directly results in the acquisition of a number of the hallmarks of cancer such as apoptosis, insensitivity to growth signals, limitless replicative potential and sustained angiogenesis. Furthermore without a functional p53 pathway the genome becomes less stable making it more susceptible to further mutation and the acquisition of more cancer hallmarks. The p53 pathway is believed to be compromised in most, if not all, cancers.¹⁵ Its reactivation is therefore a very attractive strategy for non-genotoxic cancer therapy. The following sections present an overview of p53, its function, the various ways it can be lost and approaches under investigation by which it may be restored. This is followed by more detailed discussion of the subject of this work, inhibition of the protein-protein interaction between p53 and its main regulator and oncogene, MDM2.

1.4.1 Discovery of p53

p53 was first described in 1979 as a 53 kDa protein that co-immunoprecipitated with the SV40 large T-antigen by a number of groups investigating cancer causing viruses.^{16, 17} Subsequently, high levels of p53 were observed in other types of cancer cells but not in non-transformed cells. These observations lead to the belief that p53 was involved in transformation and was in fact an oncogene and it was not until 1989 that its role as a tumour suppressor was established.^{17, 18}

Initial studies into p53 function supported the idea that it is an oncogene. Primary cells transfected with p53 underwent transformation and when introduced to p53 null cells they showed increased *in vivo* tumorigenic properties. However, conflicting observations established an association between the incidences of p53 mutation in human cancers indicating that functional p53 was required for tumour suppression^{19, 20} and that p53 actually prevented transformation.^{21, 22} The conflict was resolved when it was discovered that the p53 cDNA clone used in the initial experiments was derived from transformed cells that contained dominant negative mutations. Experiments performed with wild type p53 clones did not exhibit the transforming effects observed in the original experiments establishing p53 as a tumour suppressor protein.²³⁻²⁵

1.4.2 Structure of p53

The structural features and functional activities of p53 have been conserved across several species of vertebrates and invertebrates for over one billion years.²⁶⁻²⁸ Human p53 consists of 393 amino acids and although it obtained its name from its apparent molecular weight of 53 kDa when it was discovered, its actual molecular weight is 43.7 kDa. The difference arises as p53's migration on gels is retarded by the presence of a proline rich domain.²⁹ The protein can be divided into three structural regions; the amino

terminal region, the central region and the carboxy terminal region. Within these are a number of functional domains; the *N*-terminal region contains the transactivation domain (residues 1-42) and a proline rich domain (residues 63-97), the central domain (residues 102-292) contains the sequence specific DNA-binding regions and the carboxy terminal contains the tetramerisation domain (residues 323-356) and negative regulatory domain (residues 360-393) (Figure 1). p53 exists and functions as a tetramer. This explains why mutations are dominant negative and introduction of mutant p53 caused transformation of cells in early experiments as, depending on the location of the mutation, one mutant sequence may be sufficient to abolish the function of the entire tetrameric unit.³⁰

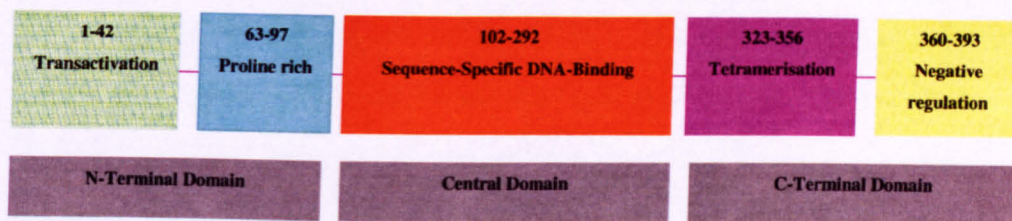


Figure 1 Domain structure of p53

1.4.3 Function of p53

The tumour suppressor activities of p53 are manifold. It is most well known as the central node and regulator of the p53 pathway controlling cell cycle arrest and apoptosis in response to genotoxic damage or cellular stress (Figure 2) These functions allow it to halt the cell cycle so DNA repair can take place or kill the cell if the damage is irreparable. As a sequence specific, DNA-binding transcription factor p53 control's over 100 transcription targets and much of its tumor suppressor activity results from their expression.³¹

p53 is both unstable and tightly regulated (discussed in Section 1.5.5.1). Under normal unstressed conditions p53 exists at barely detectable concentrations. In response to genotoxic stress, DNA damage, UV radiation or hypoxia a number of enzymes such as ATM, ATR Chk1 and Chk2 signal to p53 by effecting various post translational modifications that increase its stability and disrupt interactions with its negative regulator MDM2 and result in its subsequent accumulation.³²⁻³⁴ This in turn leads to the transcription of downstream targets that, depending on the severity of the threat to the genome, will either halt cell replication, temporarily through cell cycle arrest, or permanently by induction of senescence or programmed cell death (apoptosis).

p53 initiates cell cycle arrest at the G1/S and G2/M cell cycle checkpoints.^{35, 36} The main mechanism by which p53 induces cell cycle arrest is by transactivation of the p21 protein, a cyclin dependent kinase inhibitor, resulting G1/S arrest.³⁷ Ptpv/ESP also associated with G1/S arrest is also a p53 transcription target.³⁸ A number of genes associated with G2/M arrest, GADD45, 14-3-3- σ and Gtse1(B99) have been identified as p53 transcription targets.³⁹⁻⁴¹

p53 induces apoptosis through both the transcription dependent and independent pathways.^{42, 43} The transcription dependent pathways involve the transcription of pro-apoptotic genes such as Bax,⁴⁴ Bid,⁴⁵ PUMA,⁴⁶ NOXA,⁴⁷ Apaf-1,⁴⁸ FAS,⁴⁹ and KILLER (DR),⁵⁰ among many others.³¹ Following DNA damage, p53 has been found to re-locate to the mitochondria where it can directly associate with anti-apoptotic proteins effecting apoptosis by the transcription-independent mechanism.^{45, 51-54}

What governs whether the p53 response leads to cell cycle arrest or apoptosis is still unclear. It may be cell-specific and dependant on the nature and strength of the genotoxic stimulus.^{55, 56} However, it does appear that low levels of p53 induce cell cycle

arrest and higher levels induce apoptosis such that arrest and repair occur first and if the damage is too severe to be repaired, further p53 accumulation results in apoptosis.

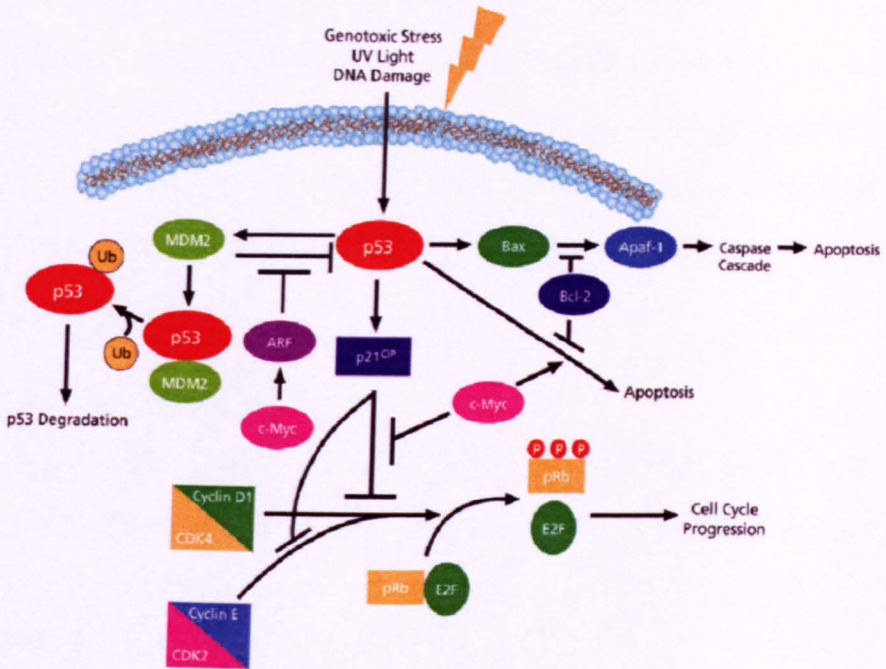


Figure 2 The p53 pathway protects the cell and initiates cell-cycle arrest and apoptosis in response to genotoxic stress. p53 is auto regulated via a negative feedback loop with MDM2. MDM2 acts as an E3 ubiquitin ligase leading to proteosomal degradation of p53.

Another means by which p53 can prevent the proliferation of defective cells is by induction of senescence. Senescence (telomere shortening) is an irreversible cellular state of proliferation and differentiation arrest that is associated with aging and tumour prevention. Initial work indicating the involvement of p53 in regulating senescence showed that cells deficient in p53 had a longer lifespan than their wild type counterparts. However, the cells did eventually enter a senescent state indicating that p53 has a role in the timing and initiating of senescence.^{57, 58}

p53 has also been associated with regulation of DNA repair. It has been shown, that when exposed to radiation mouse lymphoid or myeloid cell lines, in which p53 is mutant or absent, have severely impaired ability to rejoin double strand breaks.⁵⁹ It was also found that in human primary fibroblasts with mutant p53 there was a reduced ability to induce apoptosis and repair DNA.⁶⁰ Co-localisation of p53 to damaged DNA in response to exposure to a variety of stresses has been shown using in situ end labelling of cells.⁶¹ Two DNA repair proteins, XPC and DDB2 were identified as being p53 transcription targets.⁶²

1.4.3.1 Regulator of Angiogenesis

The exact role of p53 in angiogenesis has not been completely defined. However, it is known that p53 down-regulates the angiogenic process by regulating various factors. The anti-angiogenic factor, thrombospondin-1 is induced by p53^{63, 64} and the vasculature growth promoters VEGF and iNOS are down regulated.^{65, 66}

1.5 p53 activation in cancer therapy

The functions of p53 are ablated in most, if not all, cancers as a means of evading apoptosis either by disabling p53, directly through mutation or deletion, or indirectly by alterations of various components of the pathways that regulate p53.⁶⁷ The following sections are a brief summary of the role of p53 in current cancer therapy and novel approaches currently under investigation to activate it.

1.5.1 p53 is activated by traditional chemotherapy and radiation therapy

Radiation treatment and the majority of drugs currently used to treat cancer are genotoxic. They kill cells by damaging their DNA which, as mentioned earlier, activates p53. So even though the mechanisms by which they exert their effects on DNA are well

understood, much of their anti cancer activity is due to induction of p53. This is borne out by the fact that cancers not expressing wt p53 are often aggressive, difficult to treat and associated with poor prognosis.^{68, 69-71}

As discussed in Section 1.3, the development of non-genotoxic targeted therapies, especially those that reactivate p53, is highly desirable. A number of diverse strategies are being investigated for the non-genotoxic activation of p53 depending on how its function is lost.^{11, 72, 73} Some of these are considered briefly in the following sections before a more detailed discussion of the p53-HDM2 protein-protein interaction.

1.5.2 Reactivation of mutant p53

In approximately 50 % of cancers p53 function is lost directly through mutation of p53, making it the most mutated gene in cancer.⁷⁴ Over 2,000 p53 mutations have been characterised in human cancers. 95 % of p53 mutations occur in the core DNA-binding domain and 75 % are missense mutations that tend to be at specific hot spots with mutation patterns correlating well with tumour type and specific mutagen exposure.^{75, 76} Mutations can be at the residues involved in DNA contact or be structural, disrupting local or global protein conformation. As p53 is a relatively unstable protein, with a melting point of 44°C and a half life of just 9 minutes at body temperature, it is easily destabilised by mutation.^{75, 77} It has been shown that activity of p53 can be restored in cells harbouring a temperature sensitive mutant protein by slightly lowering the incubation temperature.¹⁸ As mutant p53 occurs in approximately half of all cancers and is associated with poor prognosis, restoration of its function is highly desirable. A number of diverse approaches to treating cancers with mutant p53 are being investigated.^{11, 72}

1.5.2.1 Gene therapy

Where p53 function is lost through mutation, reinsertion of wt protein through gene therapy would appear to be the most obvious and general solution to the problem. Whilst this approach has been investigated extensively it is not straight forward. Gene therapy itself is still very much an idea in development and has many issues that need to be overcome. A specific issue that arises for p53 is that both the newly introduced and existing mutant sequences will make up the tetrameric protein structure required for DNA binding and the mutant will still dominate activity so reactivation will not occur.³⁰ One approach is to modify the introduced p53 so it can only form tetramers with itself and in doing so create an active protein.^{11, 73}

The first ever gene therapy, known as Gendicine, has been approved in China for the reinsertion of functioning p53 via an adenovirus vector for the treatment of head and neck cancer.^{78, 79} This approval was granted on the back of one small clinical trial (120 patients). Used in conjunction with radium treatment, it was shown to bring about significantly increased tumour regression over radium alone. The only side effect was a fever in 30% of patients from which all recovered. However, given the size of the clinical trial and that it is unclear how it works, further investigation will be required before it receives widespread acceptance. The approach is currently undergoing clinical trials in The United States under the name Advexin. The validity of this approach will be determined in time but this does indicate that gene therapy is a step closer and provides further evidence that p53 reactivation is viable for the treatment of cancer.^{12, 13}

1.5.2.2 ONYX-015

The absence of wt p53 has been investigated as a means of setting tumour cells apart from healthy ones. In one such approach an engineered oncolytic virus

(ONYX-015) is used to kill cancer cells. As the virus cannot survive in the presence of wt p53 it inhibits it by coding for the p53 inactivating protein, E1B. In the engineered virus E1B is deleted so it cannot replicate in normal cells hence allowing it to selectively replicate inside, then lyse and kill cancer cells deficient in wt p53.⁸⁰ While Onyx-015 has shown promise both for safety and efficacy in clinical trials in conjunction with genotoxic chemotherapy for the treatment of head and neck cancers⁸¹ efficacy as a single agent was limited.⁸² A similar virus, known as H101, was recently approved in China to be used in conjunction with radiation for the treatment of head and neck cancers.^{82, 83}

1.5.2.3 Pharmacological rescue of mutant p53

Some mutations destabilise the conformation of p53 required for DNA binding. Pharmacological stabilisation of the mutant protein using peptides and small molecules has been investigated and has shown promise for reactivation of p53 with a number of the most common mutations.^{12, 13} These molecules bind to either the core DNA binding or tetramerisation domains of p53. They stabilise its active conformation and have been shown to restore p53 activity in cells.⁶⁸⁻⁷¹

1.5.3 Non genotoxic activation of wt p53

There are many potential therapeutic targets within the p53 pathway for the treatment of tumours that retain wild type (wt) p53. These can be upstream of p53 in the enzymes responsible for activating it in response to genotoxic damage, downstream of p53 at the effectors of apoptosis or at the proteins that regulate its levels.

1.5.4 Upstream targets in the p53 pathway

By interacting with the upstream components of p53 that control its various post translational modifications it may be possible to induce a non-genotoxic response. The

Tenovin series of compounds are inhibitors of the NAD⁺ dependent histone deacetylases SirT1 and SirT2 that deacetylate p53 at L³⁸² resulting in its destabilisation and deactivation. Inhibiting deacetylation by SirT1 and T2, the Tenovin compounds induced p53 in a non-genotoxic manner and suppressed xenograft tumor growth *in vivo*.⁸⁴

1.5.5 Downstream targets in the p53 pathway

p53 is at the centre of a complex cell cycle regulation system.⁸⁵ In order to bring about its anti tumour properties it requires a functional downstream pathway.⁸⁶ This downstream pathway presents a host of targets whereby it may be possible to directly bring about the effects of p53 such as cell cycle arrest or apoptosis. This approach may be useful where wt p53 is not present and cannot therefore initiate this response or where the actual defect occurs downstream of p53 at or above the particular drug target. Important approaches being extensively investigated are the use of cyclin-dependent kinase inhibitors that mimic p21 to induce cell cycle arrest,⁸⁷ inhibitors of the PPI's between the Bcl-2 anti-apoptotic proteins, and their pro-apoptotic counterparts to promote apoptosis in cells where these proteins are overexpressed,⁸⁸⁻⁹⁰ or direct activation of caspases by the use of Smac mimetics to disrupt the interaction of the anti apoptotic protein XIAP with the caspases.^{91,92}

1.5.5.1 Targeting the regulation of p53: MDM2

Targeting the regulatory pathways of p53, namely by inhibiting its main inhibitor, MDM2, is a very active area of research and the subject of this thesis. It is discussed in detail in the following sections.

1.6 MDM2

Because p53 has strong growth-suppressive activity, it must be tightly regulated to allow normal cellular to function. It is regulated by one of its own transcription products, known as murine double minute-2 (MDM2). The corresponding human protein is sometimes referred to as HDM2 but here the abbreviation MDM2 is used regardless of species. Targeting the regulatory pathways of p53, namely by inhibiting the activities of MDM2, is a very active area of research.

1.6.1 MDM2: Structure

MDM2 is a 491 residue protein. The N-terminus contains the p53-binding domain from amino acids 19-108. The NES and NLS (nuclear export signal and nuclear localisation signal) domains are found between residues 178 and 192. The central acidic domain spanning residues 237-300 immediately followed by the zinc finger domain from residues 301-332. At the at the C-terminus, there is a ring finger domain residues 433-488 that also includes the nucleolar localisation signal (NoLS) between residues 464-471).⁹³

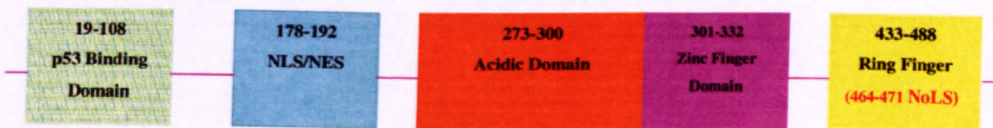


Figure 3 The domain structure of MDM2.

1.6.2 MDM2: p53 regulator and oncogene

MDM2 was first identified as an oncogene in the mouse cell-line (3T3DM) that co-precipitated with p53.^{94, 95} Further evidence of its relationship with p53 came from

experiments which showed that MDM2^{-/-} knockout mice are not viable but MDM2^{-/-}/p53^{-/-} mice are.^{96, 97} It is now known that, as MDM2 is a transcription product of p53, they control each others levels by means of a negative feedback loop.(Figure 2)^{15, 98, 99} MDM2 interacts with p53 and maintains it at low basal levels via three distinct mechanisms: (a) a protein-protein interaction (PPI) between MDM2's N-terminus and the transactivation domain of p53 that physically blocks its transcription factor activity;¹¹⁰⁰ (b) acting as an E3 ubiquitin ligase labelling it for protozoa degradation;¹⁰¹ and (c) facilitating its nuclear export removing it from its site of action.¹⁰²

Depending on the nature of genotoxic or non-genotoxic stress a cell may experience, the negative regulation of p53 by MDM2 is interrupted in several different ways resulting in p53 accumulation and subsequent cell cycle arrest and/or induction of apoptosis. The functions of MDM2 in p53 suppression are inhibited upon association with the ARF protein, which is induced upon oncogenic stress (Figure 2).¹⁰³ Similarly, MDM2 is inhibited upon ribosomal stress by the ribosomal proteins L5, L11, and L23.^{104, 105} Both p53 and MDM2 are regulated through posttranslational modifications, including ubiquitinylation,¹⁰⁶ sumoylation, and multi-site phosphorylations by a range of kinases, especially the DNA damage-induced kinases.¹⁰⁷ In response to genotoxic stress these posttranslational modifications inhibit p53-MDM2 binding allowing p53 to accumulate and exert its tumour suppressor activities.^{33,34}

p53 function can be ablated through direct overexpression of MDM2 (in *ca.* 7 % of cancers).¹⁰⁸ MDM2 overexpression due to gene amplification is especially frequent (*ca.* 30 %) in human osteogenic sarcomas and soft tissue sarcomas.¹⁰⁹ For the approximately 50% of all cancers that retain wild-type p53¹¹⁰, and especially those in which it is overexpressed, MDM2 is a potential target for therapeutic intervention to restore normal

p53 function by non-genotoxic means. The three mechanisms by which MDM2 exerts its effects on p53 each offer distinct possibilities and the search for inhibitors of them is a very active area of research. The ultimate goal would be to discover small molecules as an orally available, non-genotoxic, mono-therapeutic means of inducing p53 accumulation or at least increasing the p53 response to current chemotherapy such that lower doses of harmful agents are required.

1.6.3 Targeting MDM2 to reactivate p53

Most research effort has been focused on directly inhibiting the MDM2-p53 PPI. As this target is the focus of this thesis, both the PPI and progress made at discovering inhibitors of it are discussed in detail in Section 1.7.

The E3 ubiquitin ligase activity of MDM2, that leads to proteasomal degradation of p53, is a distinct target that can be used to rescue wt p53.¹¹¹ JNJ-26854165 was the first MDM2 inhibitor to enter clinical trials (Figure 4).¹¹² This compound first appeared in the public domain as it entered clinical trials and very little about its discovery or development has been disclosed. It has since emerged that its mode of action is inhibition of MDM2's ubiquitin ligase activity. It elevates p53 levels and induces apoptosis.^{113, 114} A number of other ubiquitin ligase inhibitors have been identified that stabilise p53 and induce the p53 mediated apoptosis. While some of these show off-target toxicity and others require further evaluation, they do provide support for the concept of inhibiting the E3 ubiquitin ligase activity of MDM2 to activate p53.¹¹⁵

As of yet no specific inhibitors of the third mechanism by which MDM2 regulates p53, facilitating its nuclear export, have been described.¹¹⁶ Leptomycin B does inhibit nuclear export of p53 resulting in its accumulation and associated tumour suppressor

activity.¹¹⁷ However the molecular target of Leptomycin B is CRM1 which is an export factor for numerous proteins.¹¹⁶ Leptomycin was withdrawn from phase 1 clinical trials due to undesirable side effects.¹¹⁷ However, specific inhibition of p53 export may still be a useful way to restore its tumour suppressor function.

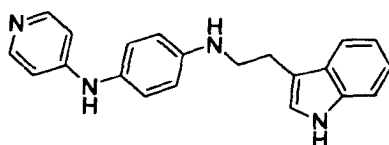


Figure 4 JNJ-26854165 is the first reported MDM2 inhibitor to enter clinical trials. It is believed to have unique mode of action to the well described inhibitors.

1.7 The MDM2-p53 PPI

Given that p53 and MDM2 exist and operate within the cell nucleus, suitable inhibitors would need to be small molecules to have the membrane permeability required to access the target. This would also facilitate oral administration. Prior to elucidation of the structure of the MDM2-p53 PPI it was thought that PPI's would have large poorly defined interfaces and it would not therefore be possible to inhibit them using such drug-like molecules. However, the X-ray co-crystal structure, between the MDM2 N-terminus and an 11-mer peptide of residues 16-27 from p53's transactivation domain, showed that the bulk of the interaction involves just three hydrophobic residues of p53 buried in a well defined hydrophobic cleft in MDM2, of a size that could be filled with a druglike molecule (Figure 5).¹ This observation lead to the notion that PPI's could be reduced to hot-spots^{103, 108, 109, 118, 119} and a wider acceptance of PPI's as tractable targets for druglike molecules.

The fact that all proteins and their binding sites are flexible is also evident from structural studies with MDM2. The elucidation of the apo-structure of MDM2 showed that the well defined binding pocket is in a closed conformation and opens upon binding to p53.¹²⁰ The driving force for the interaction would appear to be the stabilization of both MDM2 and of the amphipathic helix of p53 that supports and projects the three main binding residues into the cleft. This study also shows the presence of a flexible lid which covers the cleft in the apo structure but is displaced upon binding a p53 peptide.

The solved crystal structures of MDM2 bound to peptides are truncated at the *N*-terminus so do not include the lid. Comparison of the MDM2 conformations in the various bound structures (Figure 5, Figure 10 and Figure 11) clearly demonstrates that the small-molecule inhibitors bind to MDM2 so that it adopts a similar conformation as it does upon binding p53. However, more recent NMR studies that focus on the lid dynamics of the apo, peptide bound and small molecule bound structures,¹²¹ show that the lid of the binding site is displaced upon binding a long peptide but not upon binding the small molecule inhibitor Nutlin or a shorter peptide sequence. This is also evident in the X-ray structure of the benzodiazepine series of small molecule inhibitor in which some of the lid structure is maintained and very clearly adopts a helical structure that lies over the leu26 pocket (Figure 11).¹²² Complete displacement of the lid by peptides that extend beyond the deep cleft of the binding site is to be expected as they will occupy this area. These observations indicate that maintaining intramolecular contact between the lid and the binding site is energetically favourable when occupied by small molecules. The presence of the lid may need to be considered during inhibitor design especially when considering the placement of solvent exposed groups as the binding site will be more closed than it appears in crystal structures such as 1YCR.¹ In the apo-state the lid is in

equilibrium between major closed and minor open conformations. This dynamic may be important in molecular recognition allowing potential ligands access to the binding site. Molecular dynamics experiments also indicate that aromatic-aromatic interactions between the incoming peptide and residues at the perimeter of the binding site may be important initial interactions for molecular recognition.¹²³ The importance of this observation may be relevant in inhibitor design as all of the best inhibitors possess at least two aromatic rings.

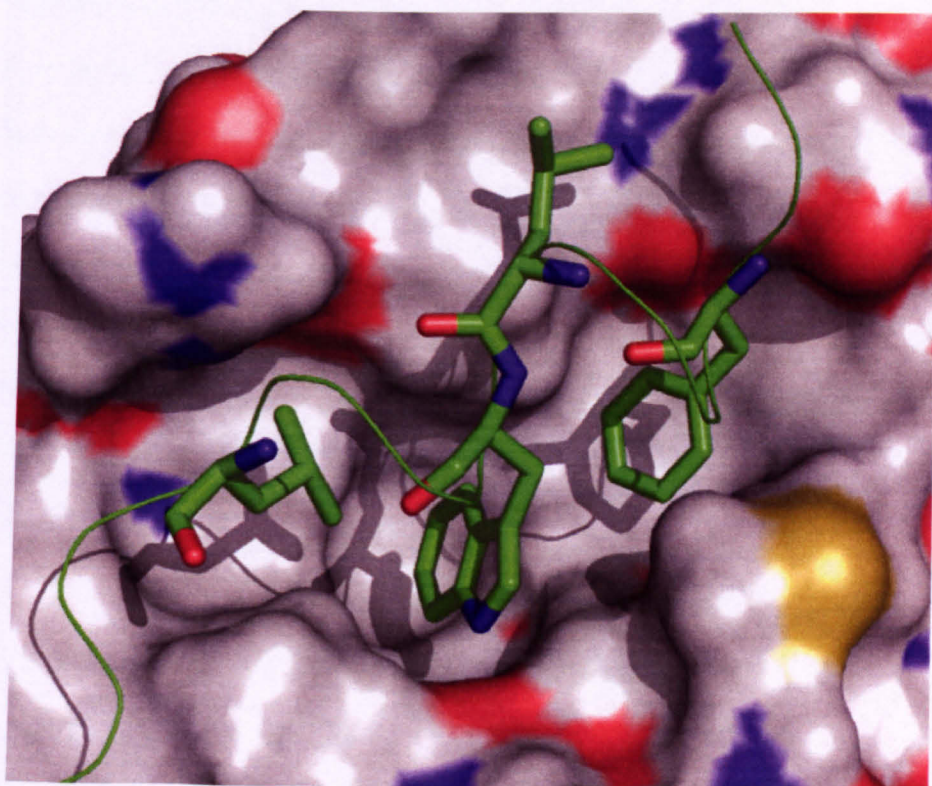


Figure 5 The p53-MDM2 interaction (PDB code: 1YCR)¹ MDM2 is shown as a grey CPK surface, p53 backbone as a green ribbon and p53 residues F¹⁹, W²³, L²⁴ and L²⁶ as green CPK sticks.

1.7.1 Peptide antagonists of the MDM2-p53 PPI

Considerable work has been done with peptides that has increased understanding of structural aspects of the MDM2-p53 PPI.¹²⁴⁻¹²⁶ These studies defined the basic pharmacophore and SAR required by PPI inhibitors. The observations made during this work have been influential in the development of the small molecule MDM2 inhibitors since discovered.

The wt-p53 sequence of the p53 peptide that binds to MDM2 is ¹⁶QETFSDLWKKLLF²⁷. Screening of phage displayed peptides led to the discovery of a 12 amino acid peptide MPRFMDYWEGLN (known as the 12-1 peptide) that exhibited a 28-fold potency increase over the corresponding wt sequence.¹²⁷ Interestingly only the three deeply buried residues are conserved. The basic pharmacophore feature of all potent ligands is indeed three suitably oriented hydrophobic groups. This is generally regarded as the minimum requirement of an inhibitor of this PPI. A very simple pharmacophore model defining the spatial arrangement of three hydrophobic groups (Figure 6) was proposed by Wang et al who used it as the first part of a virtual screening campaign that lead to the discovery of an inhibitor with nM activity (compound 1).¹²⁸

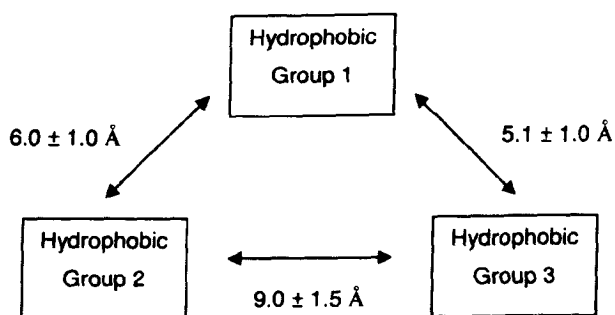


Figure 6 The basic pharmacophore of the PPI as used to screen for the Quinolinol inhibitors 1 ¹²⁸

Truncation and the use of artificial amino acids to explore various structural features of peptide based inhibitors lead to an 8 amino acid peptide (Figure 7) that showed an IC_{50} of 5nM inhibition of the PPI representing a greater than 1700-fold increase in affinity for MDM2 over the 12 amino acid wt-sequence.¹²⁹ The three deeply buried residues are again conserved and chloro-substitution at the 6-position of the tryptophan residue showed that better occupancy of the binding site resulted in increased hydrophobic contacts between ligand and target with very substantial potency gains. Aryl-halides are a common structural feature of the optimized small molecule inhibitors. The helix stabilizing amino acids, Aib and Ac_3C show the importance of a rigid scaffold in presenting the binding residues such that they have good shape complementarity with the binding site. The increases in affinity brought about by Pmp and Glu residues indicate that further polar contacts can be made outside of the cleft.

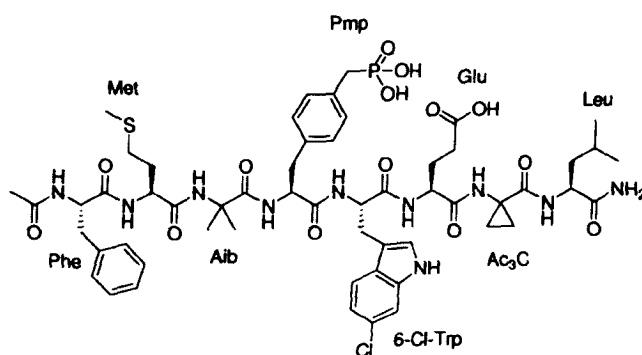


Figure 7 Optimised potent peptide inhibitor.

The co-crystal structure of this peptide bound to MDM2 was solved showing that it binds in the expected manner (Figure 8).¹³⁰ This peptide also induces apoptosis in MDM2-over-expressing cancer cells via non-genotoxic p53 activation.¹³¹ Being a

peptide this highly potent inhibitor lacked sufficient membrane permeability to be of use therapeutically. It did however show that inhibition of the MDM2-p53 PPI had the desired effect in cells and provided precedent for further investigation of the concept. Furthermore its structural features have been inherited by subsequent small molecule inhibitors. The most potent inhibitors are those that mimic the optimised peptide most closely.^{132, 133}

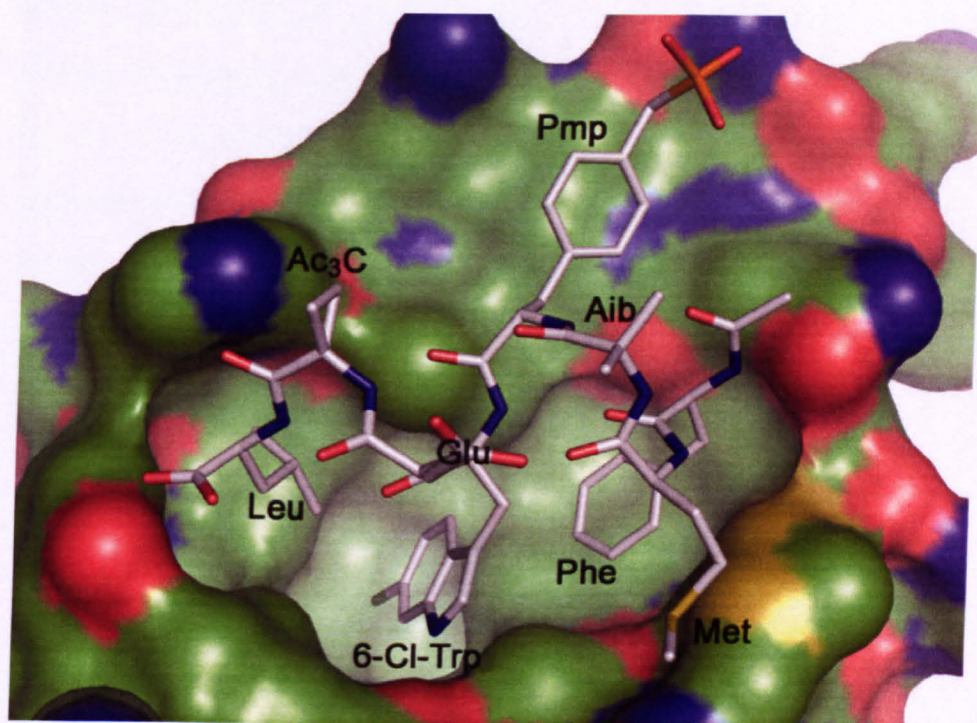


Figure 8. MDM2-binding mode of an optimised p53-derived peptide. Residues of the p53 peptide (grey CPK sticks) are labelled (Ac₃C, cyclopropylglycine; 6-Cl-Trp, 6-chloro-tryptophan; Pmp, phosphonomethylphenylalanine; Aib, aminoisobutyric acid). MDM2 is shown as a green CPK surface. Constructed from PDB entry 2GV2.¹³⁰

1.8 Small molecule antagonists of the MDM2-p53 PPI

Over twenty distinct classes of small molecule inhibitors of this interaction have now been described.¹³⁴ Of all the small molecule inhibitors described, three are of particular importance (Figure 9). The Nutlins,¹³⁵ 1,5-benzodiazepine-2,4-diones (BDPD's)¹³⁶⁻¹⁴⁰ and the spiro-oxindoles^{132, 141} all bind MDM2 with nM affinity and induce cell cycle arrest and or apoptosis consistent with the target rationale. Typically, these compounds are only active in cells that express wt-p53, and upon treatment the expression of p53 transcription products such as p21, MDM2, PIG-3 and PUMA can be observed. Importantly, the presence of posttranslationally unmodified p53 shows that they act in a non-genotoxic manner. Furthermore, optimised analogues from these compound series have all been shown to cause tumour regression in xenograft mouse models.

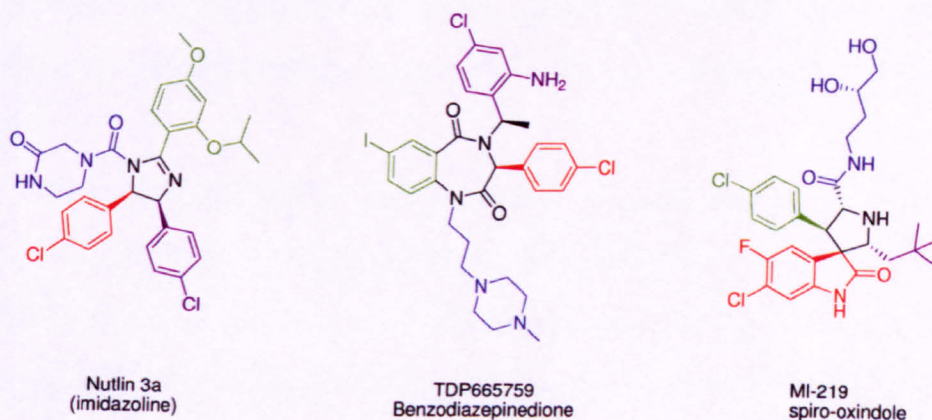


Figure 9. Chemical structures of potent small-molecule p53-MDM2 interaction inhibitor compounds. The groups that interact with the F¹⁹, W²³, and L²⁶ subsites of the p53-binding cleft of MDM2 are shown in green, red, and purple, respectively, compare to Figure 8. Solubilising groups are indicated in blue.

Although chemically distinct, these three potent inhibitors all adhere to the basic hydrophobic three-pronged pharmacophore model. Each uses a unique, rigid, heterocyclic scaffold to project three lipophilic groups into the three sub pockets of the binding site that are occupied by the F¹⁹, W²³ and L²⁶ side chains of p53. As these interactions are predominantly hydrophobic, altering the size of the lipophilic binding groups in order to optimally fill the binding site in a shape-complimentary manner greatly increases affinity. Potent members of all three inhibitor chemotypes bear halide-substituted aromatic groups positioned to maximise these contacts. Indeed the Nutlins, and most of the BDPD analogues rely entirely on hydrophobic contacts for their affinity.¹³⁵⁻¹⁴⁰ Several compounds contain chloro phenyl substituents that closely mimic the 6-Cl-Trp modification discussed above in the context of peptide inhibitors.

Efforts to increase polar interactions have also been shown to increase potency. When the *o*-amino group was added to the benzodiazepines to make a new polar contact, not made by the peptides, lead to increased affinity.¹³⁷ The spiro-oxindoles are built around an oxindole ring that has a H-bond donor and closely mimics the W²³ residue of p53.¹⁴¹

Because the p53-binding cleft of MDM2 is highly hydrophobic, minimal non-peptide inhibitors are by necessity very lipophilic and thus lack aqueous solubility. Throughout their development all of these inhibitors have evolved to bear a solvent exposed polar-group to improve aqueous solubility. The compounds have tolerated the addition of these differently. In the case of the benzodiazepines addition of these groups improves cellular potency but at the expense of some binding affinity. To date, no medicinal chemistry development of the Nutlins has been disclosed. However, the solvent exposed group is the main variation between the 3-compounds presented in the

original report¹³⁵ and a review of the patent literature suggests considerable dependence of biological activity on the nature of this group.¹⁴² In the case of the spiro-oxindoles however, addition of a solubilising group to the core structure immediately resulted in increased binding and cellular activity and further optimization lead to development of the most potent inhibitors described to date.¹³²

Whether solubilising groups just act as property improving appendages or become an additional pharmacophoric feature depends largely on their attachment point. Comparing the docked pose of MI-219 (Figure 12) and the crystal structures of the p53 peptide (Figure 5) shows that the chain mimics hydrophobic contacts made by L²² of p53. The polar groups are thought to mimic polar contacts made by the Pmp or Glu residues of the optimized peptides. The crystal structures of Nutlin-2 (Figure 10) and BDPD (Figure 11) show that their solubilising groups face to the opposite side of the binding site and could not make the same interactions. Given that the lid structure is now known to be closed upon small molecule binding it begs the question does this interact with solvent exposed groups on these inhibitors?

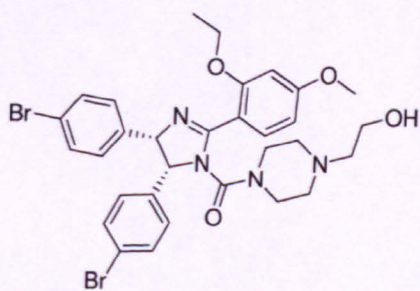
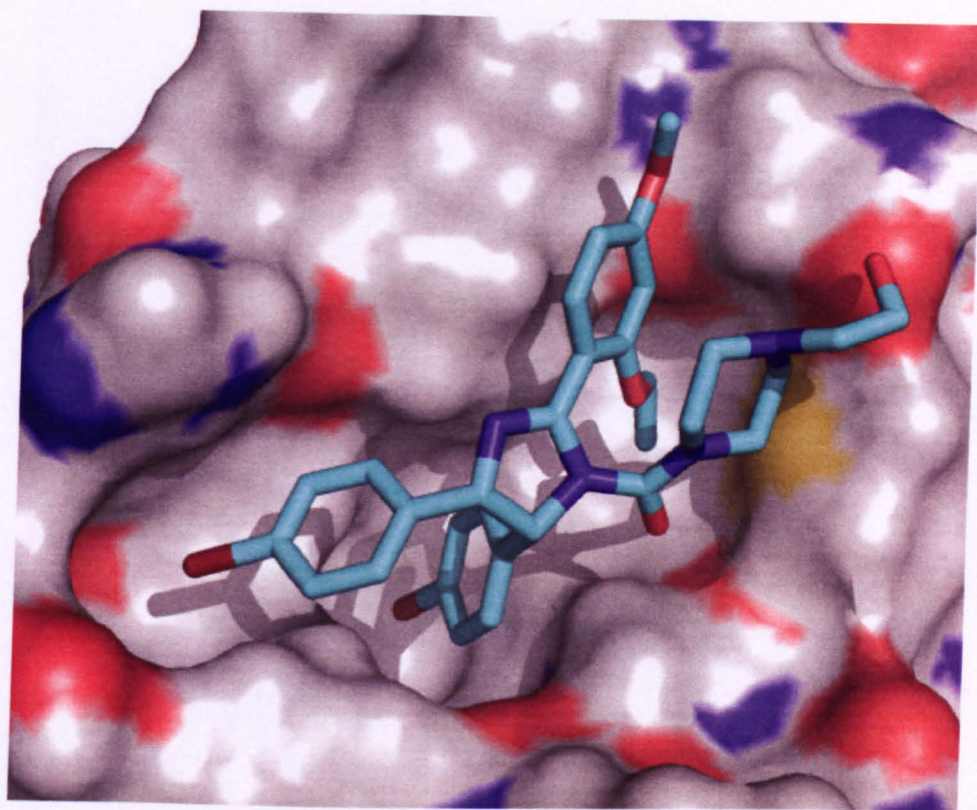


Figure 10 X-ray co-crystal structure of Nutlin-2 (shown as cyan CPK sticks) bound to MDM2 (PDB code: 1RV1)¹³⁵ MDM2 is shown as a grey CPK surface

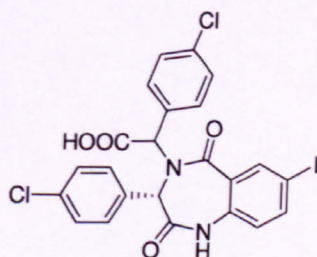
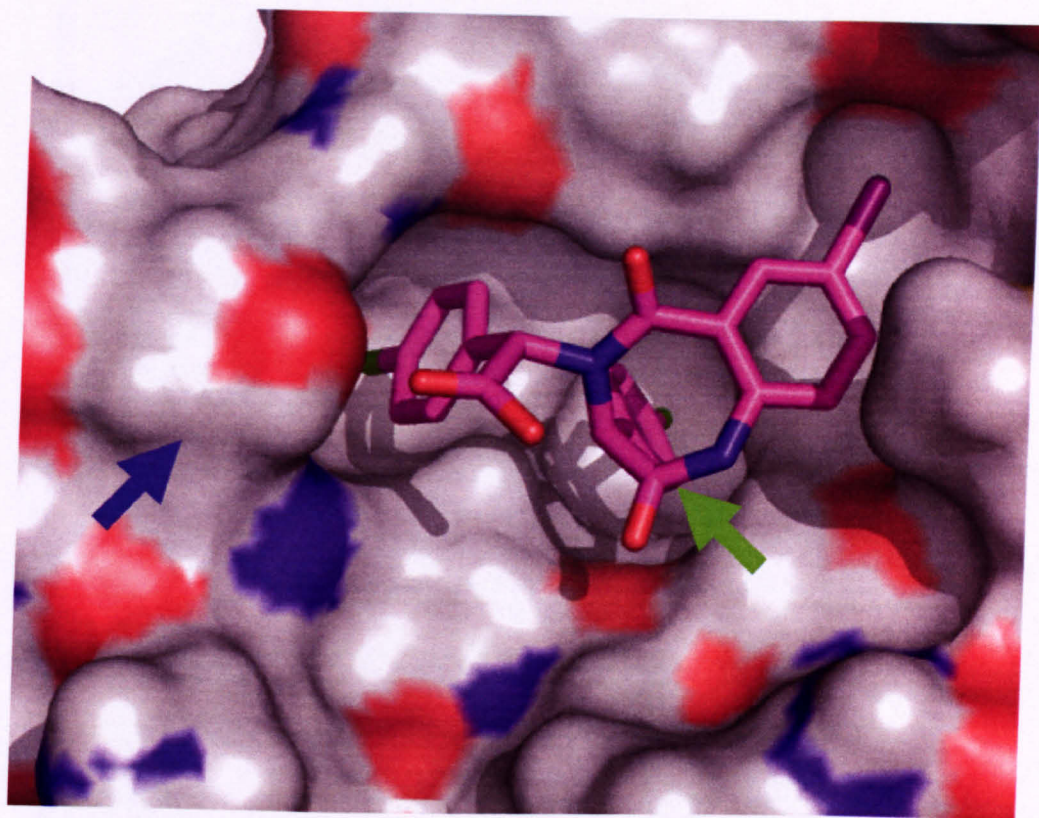


Figure 11 X-ray co-crystal structure of a 1,5-benzodiazepinedione inhibitor (shown as magenta CPK sticks) bound to MDM2 (shown as a grey CPK surface) bound to MDM2 (PDB code: 1T4E). This is the only co-crystal structure in which some of the MDM2 lid region is maintained. This region remains closed over the L26 sub-pocket denoted by the blue arrow. The green arrow denotes the attachment position of solvent exposed groups during subsequent development of this series.

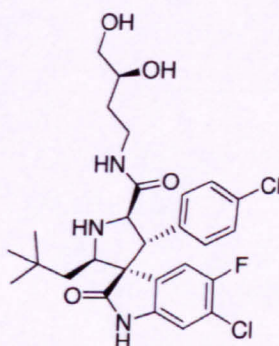
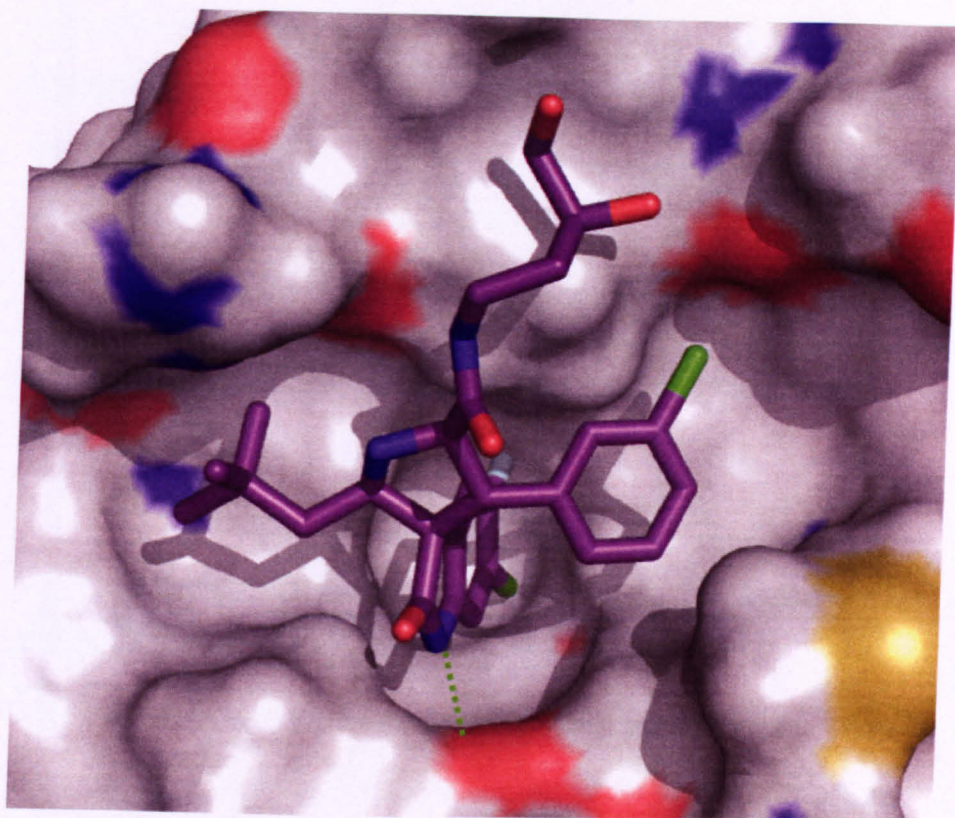


Figure 12 Spiro-oxindole inhibitor MI-219 (shown as purple CPK sticks) docked into MDM2 (PDB code: 1YCR,¹ shown as a grey CPK surface). These compounds mimic all off the features of the peptide and as a result are the most potent known inhibitors. Strategic positioning of the solvent exposed group allows these compounds to simultaneously mimic the hydrophobic interactions of L22 in the wt-p53 the additional polar contacts made by the phosphomethyl phenylalanine and the glutamic acid of the optimized peptide.

Compounds **1-6** (Figure 13) and **MI-219** (Figure 12) were all reported by Shaomeng Wang's group at the University of Michigan.^{128, 132, 133, 141, 143} Compound **1** was discovered through virtual screening for compounds that matched the basic pharmacophore shown in Figure 6 followed by docking into MDM2 from the X-ray structure 1YCR.¹ It inhibits the MDM2-p53 PPI at nM concentrations and induces a non-genotoxic p53 response in cell lines that possess wt-p53.¹²⁸ No further analogues of

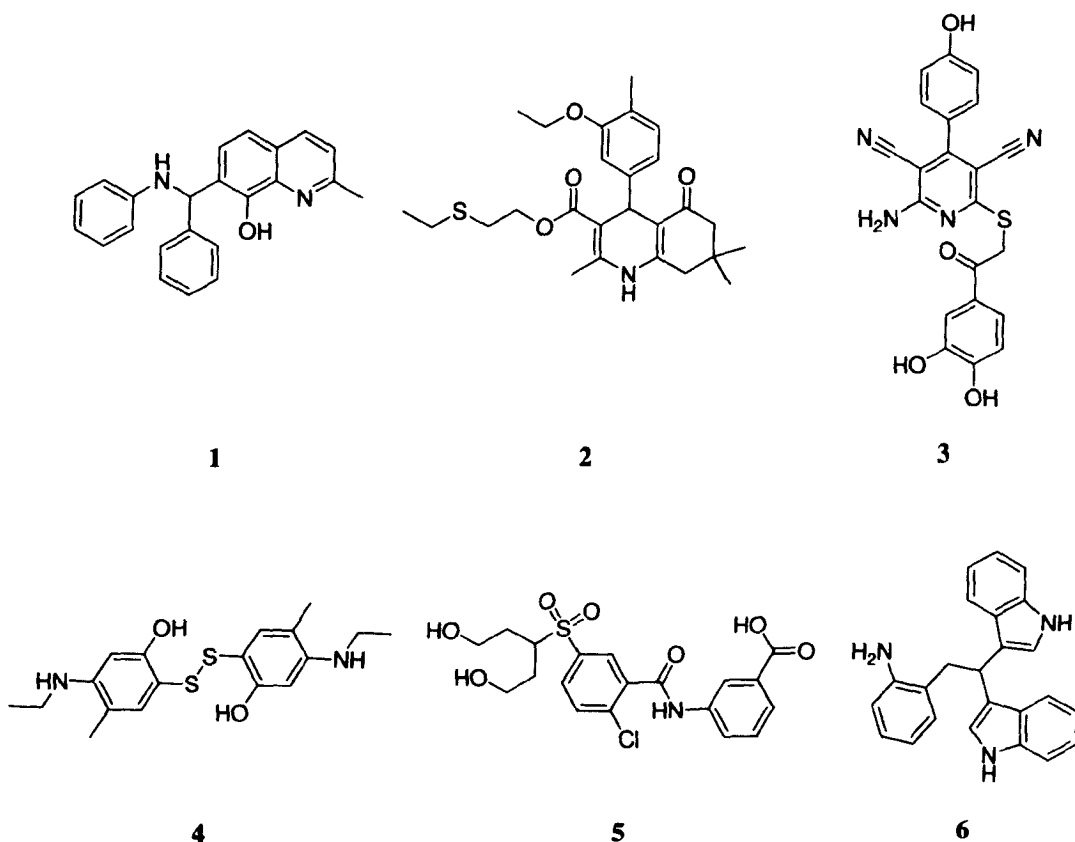


Figure 13 A diverse range of inhibitors of the MDM2-p53 PPI have been discovered by the Wang group using virtual screening.^{128, 143}

1 have been reported. Compounds **2-6** were discovered by virtual screening using an ensemble based receptor model that combined multiple protein structures to better represent flexibility within the binding site. Compound **2** was particularly potent with K_i of 110 nM. The remaining compounds all exhibit low μM activity. Interestingly, only compound **6** from this report possesses three potential binding groups and docking suggests that **2** binds without occupying the L^{26} subpocket.¹⁴³ No further analogues of these compounds have been reported.

A series of isoindolinone based inhibitors, exemplified by compound **7** (Figure 14) were discovered and developed using in silico screening and structure based design in the context of MDM2 from the X-ray structure 1YCR.¹ The most potent of these inhibitors exhibit low μM binding activity but importantly show growth inhibition in the NCI 60 cell-line panel. COMPARE analysis indicated that these represent a novel class of anti-cancer agent.¹⁴⁴ They also induce transcription of p21 and MDM2 consistent with p53 activation.^{145, 146} These inhibitors were suspected to display multiple binding modes as supported by docking. NMR analysis of 12 analogues bound to MDM2 narrowed the possible binding modes down to four possible poses in which either the isoindolinone or chloro phenyl groups occupy the W^{23} sub pocket.¹⁴⁷ This information will be useful to guide further development of these inhibitors.

A pharmacophore derived from the p53 peptide lead to the discovery of a large acylsulfonamide inhibitor (**12**) with low μM binding and cellular activity.¹⁴⁸ However subsequent studies show that this molecule causes precipitation of MDM2.¹³⁴

Compound **10** was discovered using structure-based computational design to design a library of compounds based on a scaffold that projects its side chain functionalities

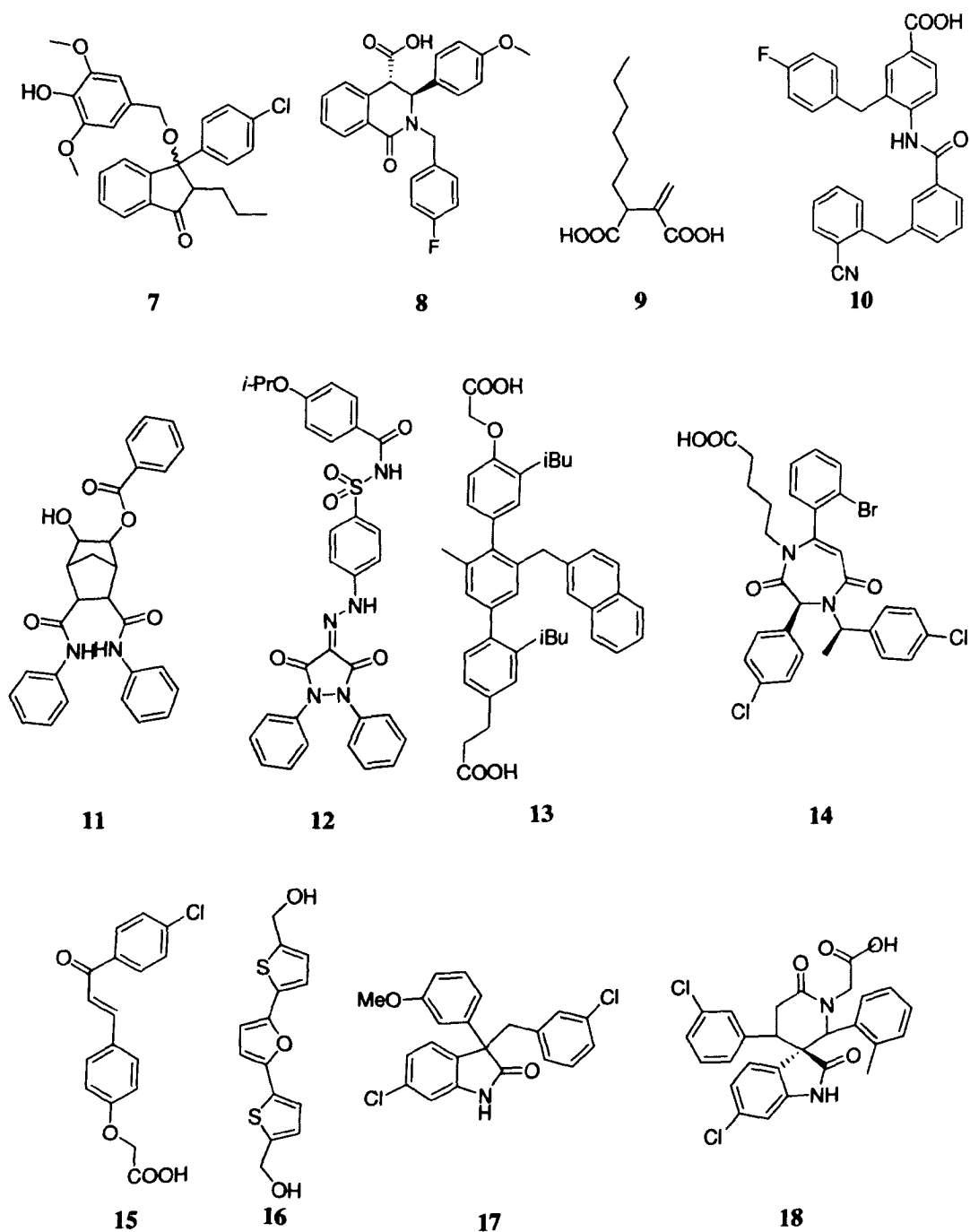


Figure 14 A structurally diverse range of reported inhibitors of the MDM2-p53 PPI

with distance and angular relationships equivalent to those seen in the MDM2 interacting motif of p53. It inhibits the MDM2-p53 PPI at 12 μ M concentrations. Chemical shift perturbation studies confirmed that **10** binds to the p53 binding pocket of MDM2.¹⁴⁹

A series of compounds based on a bicyclic[2.2.1]heptane scaffold (**11**) were discovered using unity and docking into 1YCR. They were reported to inhibit the MDM2-p53 PPI and induce apoptosis in cancer cells. No binding affinity has been reported.¹⁵⁰

The terphenyl scaffold has been used to mimic a number of α -helices and disrupt other important PPI's such as those between the pro-apoptotic protein Bak and the anti-apoptotic proteins Bcl-x_L and Bcl-2.¹⁵¹ The phenyl rings adopt a staggered conformation and the orientation of their substituents mimic the p53 residues involved in binding to MDM2.¹⁵² Compound **13** exhibited high affinity for MDM2 but showed no cellular activity. However a weaker binding analogue showed p53 induced transcription activity at 30 μ M concentration.¹⁵³

A series of diazepine inhibitors similar to compound **14** were designed based on the benzodiazepine-1,4-dione X-ray co-crystal structure 1T4E,¹²² on the basis that this scaffold would mimic the p53 α -helix. Inhibitors with low μ M affinity were prepared but no cellular activity was reported.¹⁵⁴

The chalcones, exemplified by **15**, were the first class of inhibitors to be described. They have been shown, by NMR to bind to MDM2 with the chloro phenyl group occupying the W²³ pocket.¹⁵⁵ The remainder of the molecule makes contacts outside of the binding site and a salt bridge between the acid of the ligand and K⁵¹ of MDM2. However they have been shown to be unable to dissociate the preformed complex.

Replacing the carboxylic acid with boronic acid resulted in molecules that induce apoptosis in p53^{+/+} HCT-116 with 10 fold selectivity over the corresponding isogenic p53^{-/-} cell line.¹⁵⁶

Compound **16**, dubbed RITA (reactivation of p53 and induction of tumour cell apoptosis), was discovered using a cell proliferation assay with HCT p53^{+/+} and p53^{-/-} isogenic cell lines to screen for compounds that could stimulate growth arrest in a p53 dependent manner. This compound is particularly interesting as it binds to p53 rather than MDM2. Although it has been shown not to dissociate the preformed complex, it inhibits the PPI between the two proteins induce p53 accumulation, transcription of its target genes and apoptosis in a non-genotoxic manner.¹⁵⁷

The natural product hexylitaconic acid (**9**) is reported to inhibit the MDM2-p53 PPI at 230 μ M concentrations no cellular data has been published.¹⁵⁸

The oxindole **17**¹⁵⁹ and spiro-oxindole **18**¹⁶⁰ from the patent literature again show the potential of the oxindole to mimic W²³ of p53. **17** is reported to inhibit the MDM2-p53 PPI and induce p53 accumulation and transcription of p21 in cells expressing wt p53. No indication of the potency was given. **18** Is reported to inhibit the MDM2-p53 PPI at 372 nM concentrations.

Most recently a novel class of inhibitor (compound **8**) was discovered¹⁶¹ using a 2D similarity search based on Nutlin-3 followed by shape matching with a negative image of the MDM2 binding site. **8** Is of particular interest in the context of this thesis as it was also a hit in the virtual screening described in Chapter 3. A number of analogues of this compound were prepared that exhibit low μ M binding, and selectively inhibit proliferation of cells expressing wt p53 over those expressing the mutant protein.¹⁶¹

The sulfonamides described in Chapter 2 (compound **19**) were also discovered through structure based screening using LIDEAUS.^{162, 163}

1.9 Therapeutic Window

The key question for any therapeutic strategy that aims to activate the p53 response is whether or not this will result in a selective effect on tumour cells as opposed to the cells of healthy tissues. p53 has been linked to ageing and it has been suggested that p53 activation in normal cells is responsible for some of the side effects of traditional chemotherapy.^{31, 164, 165}

There is evidence that elevating levels of p53 by MDM2 suppression is tolerated. For example, it has been shown that mice with a hypomorphic MDM2 allele produce only about 30% of the normal level of MDM2 and exhibit increased transcriptional and functional activation of p53.¹⁶⁶ Although the animals are small and show p53-dependent apoptosis of lymphoid cells, they are viable, do not age prematurely, and are resistant to tumour formation.¹⁶⁷ Similarly, *in vivo* suppression of MDM2 using antisense oligonucleotides has been demonstrated to result in therapeutic antitumor effects without overt toxicity.¹²² From these and other results¹⁶⁸ it is clear that the p53 pathway differs significantly in normal and p53 wild-type cancer cells and that the latter are selectively sensitive to increases in p53 effector functions.

Extensive pharmacological studies on the effects of inhibiting the MDM2-p53 PPI using both the Nutlin and spiro-oxindole based inhibitors also suggest that cancer cells are more susceptible to the proapoptotic effects of p53 than non-cancerous cells.¹⁶⁹⁻¹⁷³ The p53 response induced by MDM2 inhibitors leads to both cell-cycle arrest and apoptosis in tumor cell lines but only causes cell-cycle arrest in normal cells.^{86, 170, 171, 174}

This selectivity is not only an important indicator of a potential safety margin it also suggests that by inducing cell-cycle arrest in normal cells MDM2 inhibitors can have a chemoprotective effect when used with genotoxic agents. By inducing G1/S and G2/M arrest, Nutlin-3 has been shown to protect non-cancerous cells against the cytotoxic agents gemcitabine and paclitaxel, that kill proliferating cells in S- and M-phase respectively, without reducing their efficacy in cancer cells harbouring mutant p53.^{175, 176} Nutlin-3 was also shown to be lack toxicity towards bone marrow cells both when used alone or in conjunction with the genotoxic agents doxorubicin, chlorambucil and fludarabine against leukaemia cell lines that express wt-p53.^{173, 177, 178} This is significant as bone marrow is very susceptible to the effects of genotoxic agents.

The mode of action of MDM2 inhibitors is consistent with the target rationale. All compounds require cells to possess wt-p53 and a functioning downstream p53 pathway for activity. They cause expression of p53 transcription products such as p21, MDM2, FIG-3 and PUMA among many others (Section 1.4.3). Cells that overexpress the target, MDM2, are considerably more susceptible to apoptosis upon treatment with Nutlin-3 than those that express only low levels.⁸⁶ p53 induction is non-genotoxic as shown by the lack of post translationally modified p53 found in cells treated with MDM2 inhibitors. Furthermore, cells deficient in the enzyme ATM, which acts upstream of p53 and effects its post translational modification in response to genotoxic stress,³³ are also susceptible to apoptosis induced by MDM2 inhibition.¹⁷⁹ These results indicate that the post translational modifications of p53 that occur in response to genotoxic stress are more necessary to prevent it binding to MDM2 than for activating its transcription factor activity.³² That MDM2 inhibitors can induce a complete p53 response without a genotoxic stimulus bodes well for their potential as mono-therapeutic agents.

Both Nutlin-3 and MI-219 are orally bioavailable and show tumor regression in xenograft mouse models of human cancers that express wt, but not mutant, p53.^{86, 135, 171} Both compounds are well tolerated by the animals which show no overt signs of toxicity. Furthermore, neither inhibitor caused apoptosis in small-intestine crypts or thymus tissues that are known to be susceptible to p53 induced apoptosis.^{180, 181}

1.9.1 MDMX: a possible barrier to p53 reactivation?

MDMX is a homologue of MDM2 that also regulates p53¹⁸² and is overexpressed in many cancers,¹⁸³ However its expression is not regulated by p53 so, like MDM2, it is not part of a negative feedback loop. It does not have ubiquitin ligase activity but it is itself a target for MDM2 ubiquitination. It binds p53 at the same site with similar affinity as MDM2 and in doing so blocks its transcriptional activity. A p53 based peptide inhibitor, which binds to both MDM2 and MDMX, has been shown to activate p53 in cells that overexpress both proteins and induce tumor regression in xenograft models.¹⁸⁴

Despite the apparent similarities to MDM2, Nutlin-3 and MI-219 exhibit 260 and >10,000 fold less affinity respectively for MDMX than they do for MDM2.¹⁷¹ MDMX overexpression can prevent p53 reactivation by Nutlin-3.^{185, 186} These results indicate that in cancers where MDMX is overexpressed, it is a potential barrier to successful targeting of MDM2. A recently solved co-crystal structure of MDMX bound to a p53 peptide showed that the L26 pocket is smaller than in MDM2 explaining why MDM2 inhibitors have such low affinity for MDMX (Figure 15).¹⁸⁷ The SAR of MDM2 inhibitors is consistent with this observation. While the affinity of only very few MDM2 inhibitors for MDMX has been reported, it does appear that the more potent and optimized they are for MDM2 the more selective they are for it over MDMX. Increasing

the size of the hydrophobic binding groups results in better occupation of MDM2 and increases potency such that optimized MDM2 inhibitors are probably too big to occupy the binding site of MDMX.

The role of the lid in molecular recognition has previously been implicated for MDM2.¹²¹ A recent computational comparison of MDM2 and MDMX binding suggests that significant differences in the flexible N-terminus lid of the two proteins may affect how each initially recognizes p53 or indeed a small molecule and influences selectivity.¹⁸⁸

The encouraging results observed with MDM2 inhibitors provide precedent that MDMX inhibition may also be achievable. While the development of dual inhibitors of MDM2 and MDMX is desirable it appears that MDM2 potency would be sacrificed in doing so. Ultimately specific inhibitors of each protein that could be used together or separately depending on which protein dominated in a particular cancer may ultimately be required.

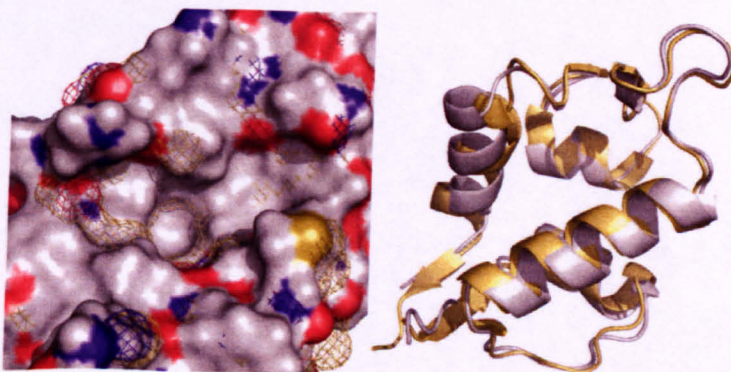


Figure 15 The overlaid co-crystal structure of MDMX (PDB code: 2Z5S) and MDM2 (PDB code: 1YCR) bound to a p53 peptide (not shown). **A:** The L26 pocket of MDMX (gold mesh) is clearly smaller than that of MDM2 (Grey Surface). **B:** While most of the back bone of MDMX (Gold Ribbon) aligns well with MDM2 (Silver Ribbon) the helix that makes up the end of the L26 pocket is less well aligned. Differences in flexibility between the two proteins maybe responsible for the observed selectivity in binding small molecule inhibitors.

1.9.2 Conclusion

The results from the *in vitro* and *in vivo* studies outlined above give a good indication of the safety of MDM2 Inhibitors as mono-therapeutic, orally bio available and non-genotoxic means of p53 reactivation. The selectivity they show for cancer cells underlies the lack of observed on-target toxicity. Furthermore results of these studies indicate the potential scope of this approach as a novel cancer therapy and create a profile of the type of tumors that are likely to respond to it. Profiling of tumors in patients to determine the status of the p53 pathway and its regulatory proteins will facilitate determining the best course of treatment for a given patient.

What has been achieved thus far strongly supports the non-genotoxic activation of p53 in the battle against cancer. With an undisclosed analogue of the Nutlins (R7112) and the E3 ubiquitin ligase inhibitor, JNJ-26854165, now in clinical trials and MI-219 in late stage, pre-clinical development this goal is closer than ever. The ultimate proof of concept will be if the promise shown by MDM2 inhibitors in the laboratory can be translated to the clinic.

1.10 Aims of this project

This project aims to find novel MDM2-p53 PPI inhibitors. In Chapter 2 attempts to develop a known but unoptimised MDM2 inhibitor are described. Chapter 3 uses 3-D shape based virtual screening to look for new inhibitors. Chapter 4 investigates an alternative benzodiazepine based scaffold and the possibility of using the 1,3-dihydrobenzimidazol-2-one ring system as a tryptophan mimic as the basis for developing new inhibitors. The work is guided by what is known about the structural

aspects of the three main classes of inhibitor. Detailed background discussion for each approach is provided at the start of each chapter.

1.11 Fluorescence polarization binding assay.

All assays of the compounds described herein, both in this project and the work that preceded it, were performed at Cyclacel. The binding activity was evaluated using a fluorescence polarization based competitive binding assay. Detecting protein-ligand binding by fluorescence polarisation is based on the principles that when a fluorophore is excited by plane polarized light the emission created is also polarised; that smaller molecules rotate faster than larger molecules in solution and that rotation depolarizes the emission light. Fluorescence polarisation measures the vertical and horizontal components of fluorescence. As the process of fluorescence requires a measurable amount of time, during which rotation occurs, polarisation values are inversely related to the speed of molecular rotation which is related to molecular weight or volume. Therefore a fluorescently labelled ligand will have a higher polarisation value when complexed with any molecule large enough to slow its rate of molecular rotation in comparison to a low polarisation value of the uncomplexed rotating ligand. In an assay an active inhibitor will increase the concentration of uncomplexed fluorophore proportional to its concentration and affinity for the protein, resulting in reduced polarisation which allows the binding activity of the inhibitor to be determined.

For the purposes of screening potential inhibitors of the p53-MDM2 interaction a fluorescently tagged p53 based tracer peptide (fluorescein-MPRFMDYWEGLN) and full length MDM2 were used. The peptide sequence, MPRFMDYWEGLN, is an optimized p53 based peptide (known as the 12/1 peptide) and has been described

previously^{127, 189}. The activity of each compound was determined and reported as the concentration required to displace 50 % of the tracer peptide from the protein (IC_{50} , μM). Throughout the study compound **19**, Nutlin-3 and the optimised 12-1 peptide (non-labelled) are used as positive control compounds. The binding assay is the first step of the screening cascade and the most important for the discussion of this project. Only compounds that were active in it would be considered for functional cell assays.

1.11.1 Loss of assay sensitivity

During the course of this investigation the FP assay became considerably less sensitive. This was thought to be due to degradation of the MDM2 protein. Although attempts to improve the assay were unsuccessful, it was possible to correct the results relative to the positive control inhibitors that were used through out the study and preceding work. Compound **19**, Nutlin-3 and the 12-1 peptide showed IC_{50} values that were on average 3.18 fold higher than previously observed (Table 1). The IC_{50} values of compounds determined under the less sensitive assay conditions were normalised with respect to the previous work by dividing the observed value by 3.18. Compounds that showed measureable inhibition at $500\mu M$ are also noted and where possible the same correction factor is applied to these too. While the assay is insufficiently sensitive to give accurate quantitative data, it is sufficiently sensitive to determine a compounds relative activity and distinguish active compounds from inactive ones.

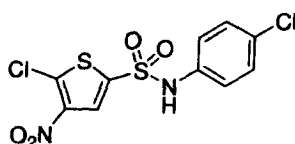
| Entry | Compound | FP | FP | Relative decrease (times) |
|-------|--------------|-------------------------------------|--|---------------------------|
| | | (IC ₅₀ , μM) Original | (IC ₅₀ , μM) low sensitivity | |
| 1 | 19 | 26.4 | 80 | 3.03 |
| 2 | Nutlin | 0.45 | 1.42 | 3.14 |
| 3 | 12-1 peptide | 0.77 | 2.6 | 3.38 |
| 4 | Mean | --- | --- | 3.18 |

Table 1 The loss in sensitivity was consistent for all of the control compounds used throughout the study. An average of this was used to normalise results with respect to previous assays.

2. Bisarylsulfonamides

2.1 Introduction

Bisarylsulfonamides, as exemplified by compound **19**, were investigated as possible inhibitors of the MDM2-p53 PPI. This work was a continuation of a hit-to-lead study initiated at Cyclacel. The aim of this study was to investigate the structural activity relationships (SAR) of these compounds and to determine if they could be developed further as potential non-genotoxic cancer therapies. A series of analogues of **19** were prepared to investigate the importance of various structural features with respect to target affinity. Their ability to bind to MDM2 and inhibit the PPI between it and a fluorescein labelled peptide, based on the MDM2 binding region of p53, was determined using a fluorescence polarisation based competitive binding assay (Section 1.11). In order for this series of compounds to be considered suitable for further development, active analogues would need to exhibit binding activity at low micro or nanomolar concentrations, show clear SAR, not contain the reactive 5-chloro-4-nitrothiophene moiety and induce a non-genotoxic p53 response in cell lines containing wt-p53.



19

The following sections describe the discovery and the results of an initial hit to lead investigation initiated at Cyclacel. The results of this project are then discussed in the context of what was known from the previous work at Cyclacel and about the most important inhibitors described in the literature.

2.2 Discovery

The bis-arylsulfonamide MDM2 inhibitors, exemplified by **19**, were identified by virtual library screening of the Maybridge compound library using LIDAEUS™ (LIgand Discovery At Edinburgh UniverSity).¹⁶² LIDAEUS™ is a structure-based, database mining program used to find potential lead compounds for specific targets.¹⁹⁰ The program automatically docks small-molecule libraries into the target binding site. Hits are generated based on how well the molecule is deemed to dock within the binding site of the target. In this screening campaign the p53/MDM2 crystal structure (1YCR) determined by Kussie et al¹ was used as the target.

This approach yielded 191 hits 7 of which showed binding activity with $IC_{50} < 100 \mu\text{M}$ in a fluorescence polarisation competitive binding assay. These were typically aryl and thienyl-sulfonamides and sulfonate esters. From these, the sulfonamides were selected for further investigation as they show better stability than the sulfonate esters, are easier to prepare and allow more diversity to be achieved in an analogue study as their nitrogen can carry an additional substituent which the oxygen of the sulfonate ester cannot. The latter consideration is of particular importance with respect to this target, as molecules with three groups, that could potentially fill all three sub-pockets of the MDM2 binding site, could be investigated. Through this series of screening and selection the lead compound **19**, which exhibits low μM activity in the FP binding assay, was selected as a starting point for the investigation of bis-aryl sulfonamides as potential MDM2-p53 PPI inhibitors.

Functional assays showed that these compounds did induce a p53 response in cells as would be expected for MDM2-p53 PPI antagonists. Compound **1** and its analogues significantly induced p53 transcriptional activity, measured in a

luciferase-based p53 reporter gene assay (Figure 16). As expected, downstream p53 regulated transcription products, p21 and MDM2, were induced in cancer cells treated with bis-arylsulfonamides (Figure 17). These p53-MDM2 antagonists potently and selectively killed cancer cells by apoptosis. The effects of the compounds was not limited to cells containing wild-type p53, suggesting that either another target of MDM2 is affected or that these compounds also exhibit non-MDM2 specific activity. It is possible that regulation of the E2F-1 transcription factor is also involved in the mode of action of p53-MDM2 antagonists. Compound **19** down regulates E2F-1 levels and transcriptional activity (Figure 17). The *N*-terminus of MDM2 is known to physically and functionally interact with E2F-1¹⁹¹⁻¹⁹³.

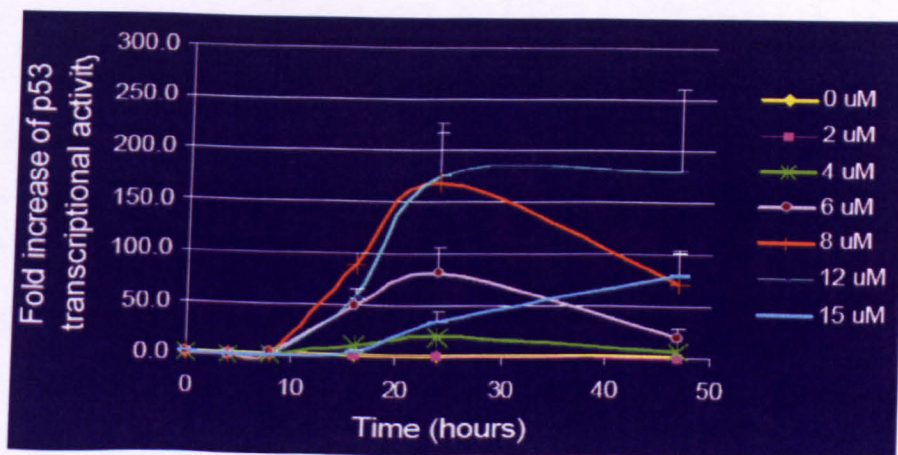


Figure 16 Luciferase-based p53 reporter gene assay shows that compound 19 induces a concentration dependent increase in p53 transcriptional activity.¹⁶²

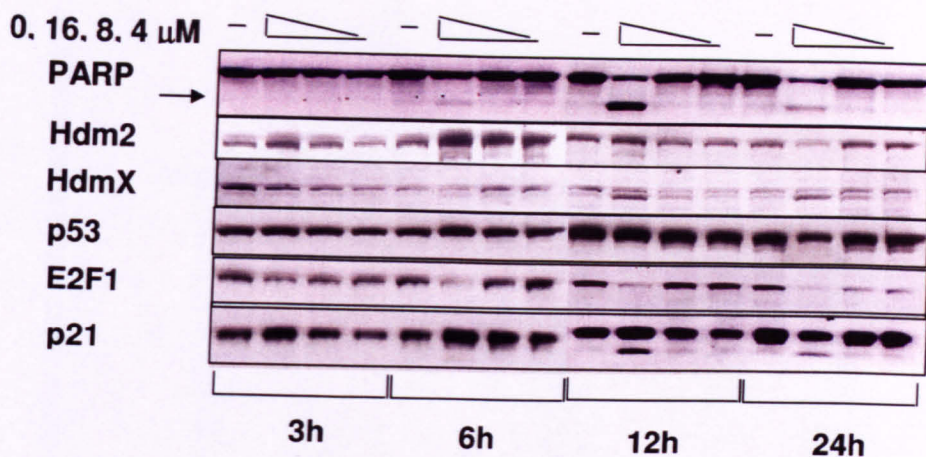
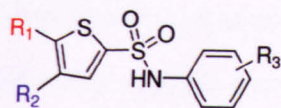


Figure 17 Western blot analysis shows a dose dependant increase in p53 and its transcription products and down-regulation of E2F1 at low μM inhibitor concentrations of **19**.¹⁶² Concentrations of **19** are 0 μM , 16 μM , 8 μM and 4 μM from left to right for each time interval.

2.3 Early development SAR and binding hypothesis

2.3.1 Replacing the 4-nitro and 5-chloro substituents

Prior to the start of this project a number of analogues of **9** were prepared and tested at Cyclacel to investigate the importance of various parts of the molecule with respect to binding activity. Replacing the 5-chloro and 4-nitro substituents of **19** was important for the development of these inhibitors. Such electron deficient thiophene systems are highly activated towards nucleophilic aromatic substitution at the 5-position. In vivo such reactive compounds would be susceptible to attack by nucleophiles such as glutathione, whose function it is to neutralise reactive and potentially toxic compounds.¹⁹⁴ Analogues of **19** bearing the 5-chloro and 4-nitro substituents were indeed found to react with reduced glutathione via nucleophilic aromatic substitution at the 5-position and the resulting compound did not inhibit the PPI.



| Entry | Compound. | R ¹ | R ² | R ³ | FP IC ₅₀ /μM |
|-------|-----------|-----------------|-----------------|---------------------------|-------------------------|
| 1 | 19 | Cl | NO ₂ | <i>p</i> -Cl | 26.41 |
| 2 | 20 | Cl | H | <i>p</i> -Cl | 319.53 |
| 3 | 21 | H | NO ₂ | <i>p</i> -Cl | 123.21 |
| 4 | 22 | NO ₂ | H | <i>p</i> -Cl | 462.38 |
| 5 | 23 | Br | H | <i>p</i> -Cl | 290.22 |
| 6 | 24 | Cl | Br | <i>p</i> -Cl | >500 |
| 7 | 25 | Br | Br | <i>p</i> -Cl | 197.73 |
| 8 | 26 | Me | NO ₂ | <i>p</i> -Cl | >166.67 |
| 9 | 27 | Et | NO ₂ | <i>p</i> -Cl | 237.38 |
| 10 | 28 | | NO ₂ | <i>p</i> -Cl | 16.16 |
| 11 | 29 | | NO ₂ | <i>p</i> -Cl | >500 |
| 12 | 30 | | NO ₂ | <i>p</i> -Cl | 418.66 |
| 13 | 31 | | NO ₂ | <i>p</i> -Cl | 64.38 |
| 14 | 32 | | NO ₂ | <i>p</i> -Cl | 154.48 |
| 15 | 33 | | H | <i>p</i> -Cl | >500 |
| 16 | 34 | | H | <i>p</i> -CF ₃ | 146.49 |
| 17 | 35 | | H | <i>p</i> -CF ₃ | >500 |
| 18 | 36 | | H | <i>p</i> -CF ₃ | 349.86 |
| 19 | 37 | Me | | <i>p</i> -Cl | 122.87 |
| 20 | 38 | Cl | | <i>p</i> -Cl | 134.58 |

Table 2 Initial investigation into replacing the 4- and 5-substituents at Cyclacel.

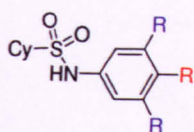
A series of analogues of **19**, investigating alternative 4- and 5-substituents, were prepared (Table 2). Analogue selection was not systematic but looked at a variety of analogues for which there were readily available starting materials. Most of these compounds were considerably less active than **19**. However **28** (Table 2, Entry 10) showed slightly increased activity over **19**. Also of interest was **31** (Table 2, Entry 13) which was only about 2 fold less active than **19**. These compounds are starting points for further investigation and are discussed in detail in Sections 2.6.3 and 2.6.4.

2.3.2 Alternatives to the Thiophene Ring System

A limited number of compounds containing heterocyclic, bicyclic or phenyl ring systems, for which the required starting materials were readily available were prepared and investigated as possible alternatives to thiophene (Table 3). All analogues showed considerably less binding activity than **19**.

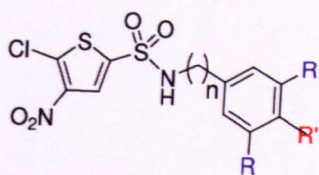
2.3.3 Modifying the *N*-Substituents

Analogues in which the *N*-substituents were varied were prepared (Table 4). Different types and numbers of substituents were well tolerated as were the use of benzyl instead of phenyl *N*-substituents. However all analogues displayed similar activity with only **55** and **59** being slightly less active than **19** (Table 4, entries 2 and 6). These analogues have smaller and larger *p*-substituents respectively than **19**. Further investigation into the nature and pattern of these substituents was required to determine if any SAR existed. This was the initial starting point for the work in this project.



| Entry | Compound | Cy | R | R | FP IC ₅₀ (μM) |
|-------|----------|----|----|-----------------|--------------------------|
| 1 | 39 | | H | CF ₃ | 278.10 |
| 2 | 40 | | H | CF ₃ | 448.41 |
| 3 | 41 | | H | CF ₃ | 106.46 |
| 4 | 42 | | H | CF ₃ | 193.10 |
| 5 | 43 | | H | CF ₃ | 165.39 |
| 6 | 44 | | H | CF ₃ | 308.00 |
| 8 | 45 | | H | CF ₃ | 374.60 |
| 9 | 46 | | H | CF ₃ | 274.99 |
| 10 | 47 | | H | H | >500.00 |
| 11 | 48 | | Cl | H | >500.00 |
| 12 | 49 | | Cl | H | >500.00 |
| 13 | 50 | | Cl | H | 331.38 |
| 14 | 51 | | Cl | H | 418.42 |
| 15 | 52 | | Cl | H | >500.00 |
| 16 | 53 | | H | CF ₃ | 150.83 |
| 17 | 54 | | H | CF ₃ | 128.73 |

Table 3 Initial investigation into alternatives to the thiophene ring system at Cyclacel.

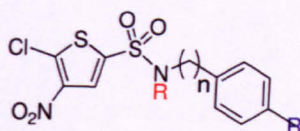


| Entry | Compound | n | R' | R | FP IC ₅₀ (μM) |
|-------|-----------|---|-----------------|----|--------------------------|
| 1 | 19 | 0 | Cl | H | 26.41 |
| 2 | 55 | 0 | F | H | 41.90 |
| 3 | 56 | 0 | CF ₃ | H | 20.39 |
| 4 | 57 | 1 | H | F | 26.98 |
| 5 | 58 | 1 | H | Cl | 24.77 |
| 6 | 59 | 0 | OMe | H | 44.78 |

Table 4 Initial investigation at Cyclacel show that benzyl and phenyl *N*-substituents are tolerated as are various groups on their aryl ring.

Limited investigations were also undertaken to investigate *N,N*-disubstituted analogues (Table 5). The additional *N*-substituent was not just tolerated but in most cases actually improved activity. This led to compound **66**, the most potent inhibitor in the series (Table 5, entry 8). This is consistent with the hypothesis that compounds bearing an additional substituent would potentially have better shape complementarity with the binding site and occupy all three sub-pockets where the bis-aryl analogues, such as **19**, could only occupy two sub-pockets. However the results were not consistent and posed more questions than answers. For example, why would compound **60**, (Table 5, entry 2) show such high activity when the additional group it possesses is too small to occupy an additional sub-pocket yet the intermediate sized *i*-Pr group of compound **61**, (Table 5, entry 3) essentially abolishes activity and some larger benzyl substituents enhance activity (Table 5, entries 4 and 5)? While it could be argued that the total loss of

activity by the larger *o*-substituents of **64** and **65**, (Table 5, entries 6 and 7), was because these groups made the molecule too big to fit in the binding site or, in the case of the nitro group in particular, that they were just chemically unsuitable for the binding site, the total loss of activity was still somewhat surprising.



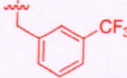
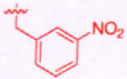
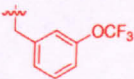
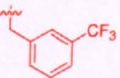
| Entry | Compound. | N | R | R | FP IC ₅₀ / μM |
|-------|-----------|---|-----------------|---|--------------------------|
| 1 | 19 | 0 | Cl | H | 26.41 |
| 2 | 60 | 0 | Cl | Me | 5.87 |
| 3 | 61 | 0 | Cl |  | 249.35 |
| 4 | 62 | 0 | Cl |  | 7.08 |
| 5 | 63 | 0 | Cl |  | 8.45 |
| 6 | 64 | 0 | Cl |  | >500 |
| 7 | 65 | 0 | Cl |  | >500 |
| 8 | 66 | 1 | CF ₃ |  | 3.00 |

Table 5 Initial investigations at Cyclacel showed that additional *N*-substituents may increase binding but there is no clear pattern in how they do so.

2.3.4 SAR Summary

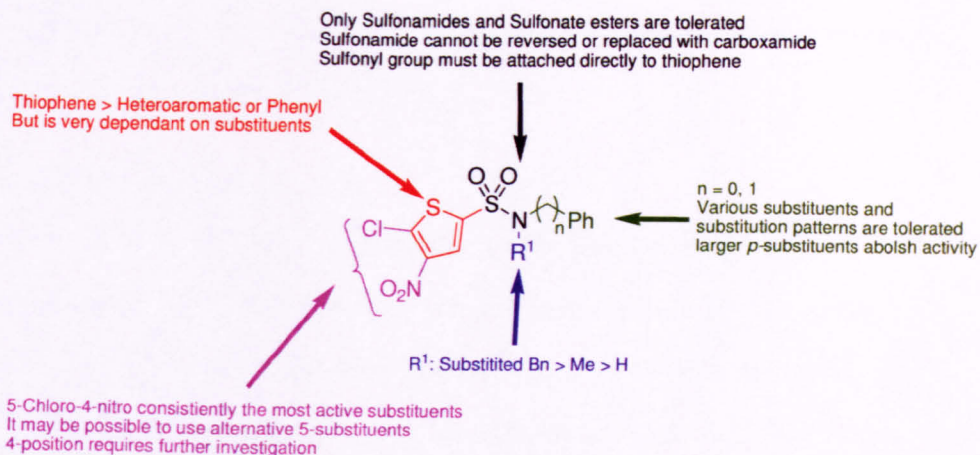


Figure 18 SAR Summary after initial investigation at Cyclacel prior to the start of this project.

Very little SAR emerged from the preliminary investigations. What was known at this stage is summarized in Figure 18. These investigations posed some interesting questions and showed potential starting points for the development of these inhibitors. It was clear that alternative scaffolds to the sulfonamide, with the exception of sulfonate esters were inactive. Increasing the length between the sulfonyl group and thiophene abolished activity as did reversing the sulfonamide such that the thiophene is bound to the sulfonamide nitrogen rather than the sulfur. Yet increasing the length of the *N*-aryl link, in going from phenyl to benzyl was well tolerated and even slightly increased activity. Thiophene based systems still appear to be the best in binding assays and no alternative ring systems were found. But even for the thiophene based systems the 5-chloro-4-nitro substituents appeared to be required for activity. However, some analogues showed that either could be replaced without total loss of activity. On the other hand, a wide range of *N*-substituents were tolerated on the opposite side of the

molecule. However, with the exception of a small number of analogues, which totally abolished activity, and some moderate increases in activity when *N,N*-disubstituted analogues were employed very little SAR was observed.

2.3.5 Binding hypothesis

At this stage the evidence from the analogue study pointed to dominance of SAR by the highly activated thiophene system. The relatively flat SAR could also be as a result of multiple binding modes. Macromolecular NMR studies of the N-terminus domain of MDM2 showed that the largest chemical shift perturbations upon binding these inhibitors were in the vicinity of the p53 binding site. The possible occurrence of multiple binding modes for the bis-arylsulfonamides could be due to their inability to completely fill the binding site as they only possess two potential binding groups. This notion was supported by molecular modelling. Docking studies, where **19** was docked into the binding site of MDM2 from the X-ray structure of the peptide complex (PDB code 1YCR),¹ showed the possibility of multiple binding modes (Figure 19). In the first pose the inhibitor fills two sub-pockets of MDM2 and only one in the second pose. Both of the poses shown suggest that the role of the nitro group may be as an H-bond acceptor with glutamine 72 or glutamine 59 respectively. That the *N,N*-disubstituted analogues could better fill the binding site is also supported by docking (Figure 20). Docking compound **66** into MDM2 (1YCR)¹, suggests it is capable of occupying all three sub-pockets of the binding site and making the H-bond interaction, via its nitro-group, with glutamine 72. The increase in activity observed for the *N,N*-disubstituted analogues is consistent with better filling of the binding site. However, the increase

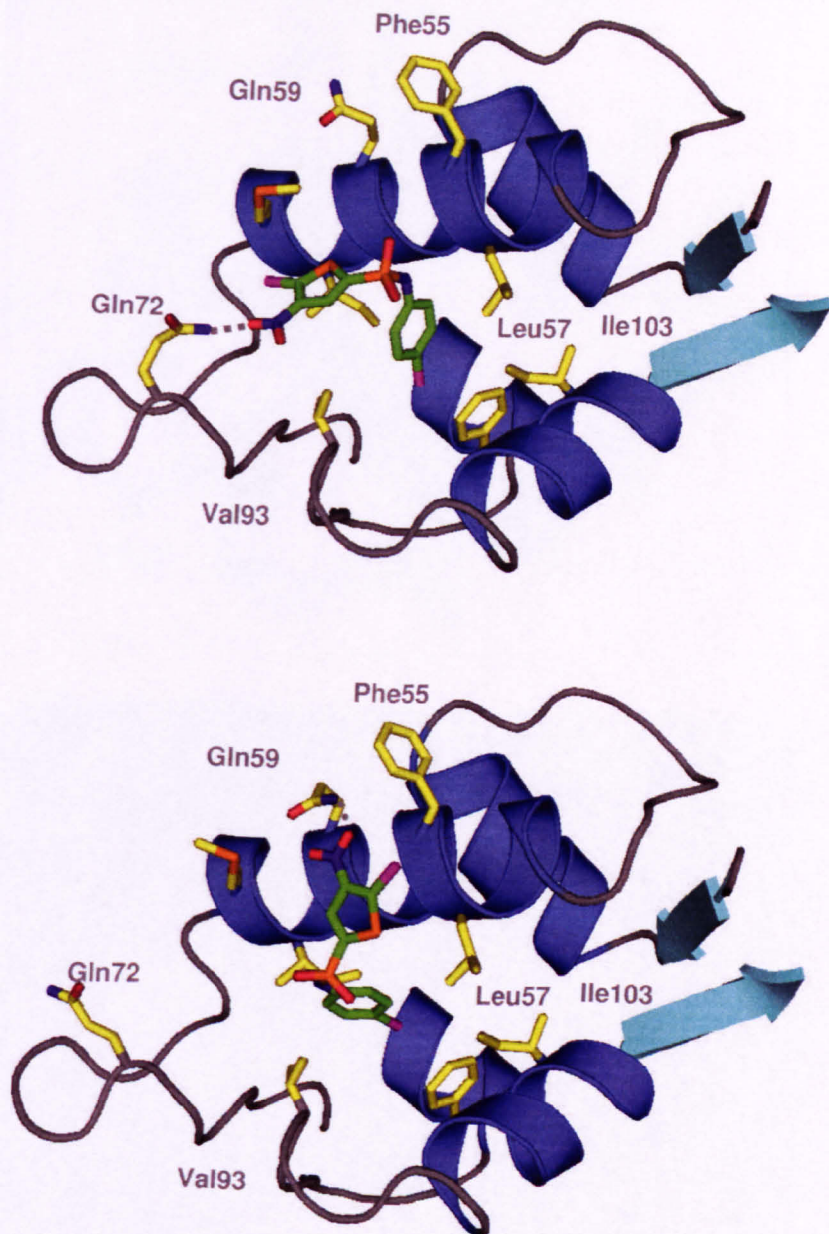


Figure 19 Two proposed poses for target binding. Compound 19 (green CPK sticks) docked in MDM2 (1 YCR)¹ (MDM2 residues, yellow CPK sticks).

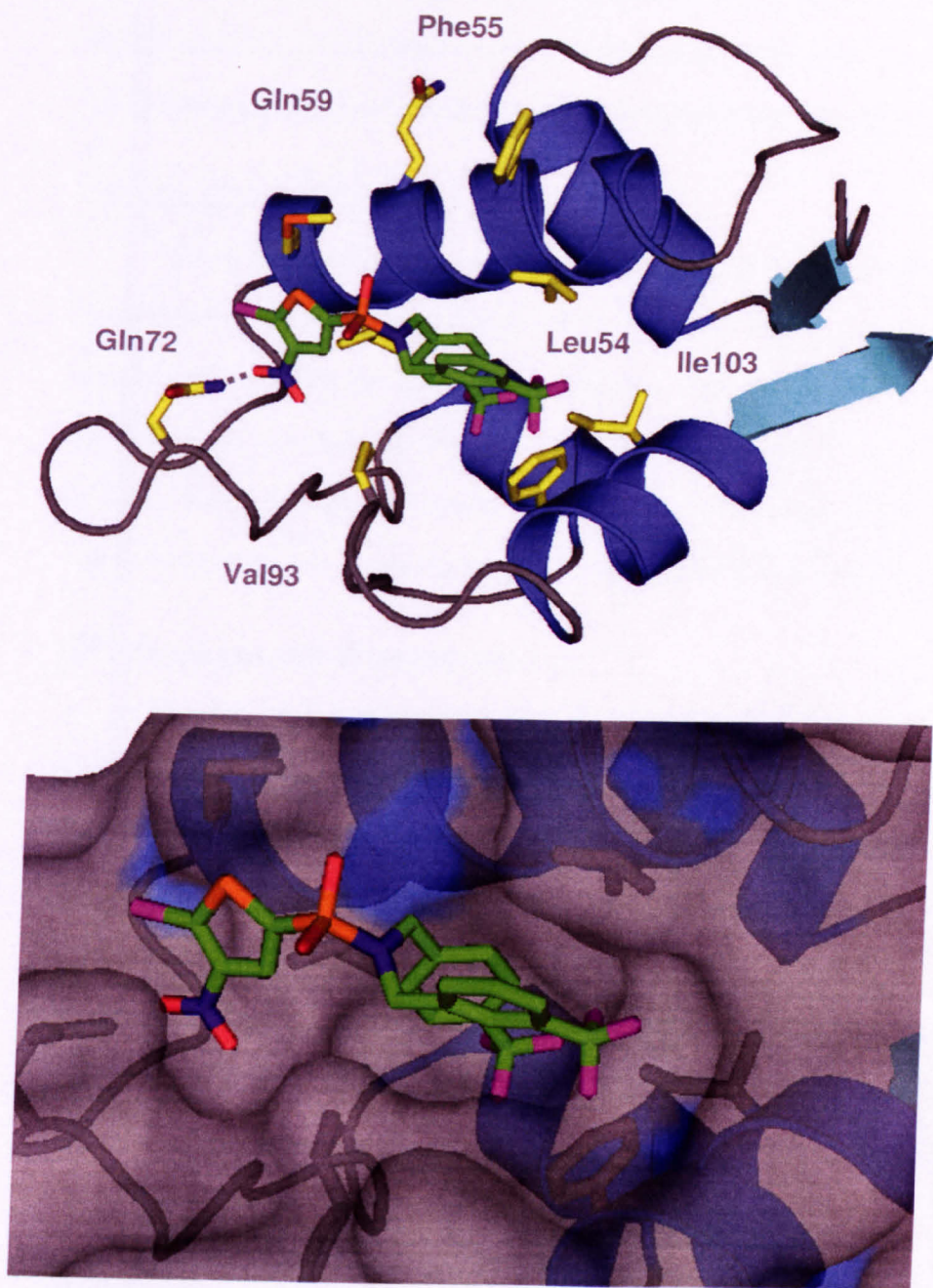


Figure 20 66 (green CPK sticks) docked in MDM2 (1 YCR)¹ Top (MDM2 residues, yellow CPK sticks), bottom (grey surface).

observed in binding activity is more modest than would be expected for filling an additional sub-pocket. The extra hydrophobic contacts could be somewhat offset by an increased entropy penalty that these more flexible molecules might pay upon binding.

2.4 Results and Discussion

The following sections describe the work performed in this project. The aim was to investigate various structural aspects of the molecules and answer some of the questions raised during the initial work at Cyclacel. Some starting points have been identified from the preceding work, here that work is completed by preparing more complete series' of compounds focused on specific parts of the molecule. The aim is to determine if the reactive groups can be replaced and a meaningful SAR established.

2.5 Developing the *N*-substituents

The PPI itself and the three best inhibitor classes rely mostly, or even exclusively, on making hydrophobic contacts with the binding site for their affinity. They maximize this by having excellent shape complementarity with the binding site. In order for the arylsulfonamides to be developed they would have to have their size and shape optimized so they also exhibit excellent shape complementarity with the binding site. To achieve this, a more rigid molecule of the correct size and shape would be required. A more rigid inhibitor of the correct shape, rather than a flexible one which could adopt the correct shape, would reduce the possibility of multiple binding modes and make a much better starting point from which to address the stability issues on the other side of the molecule. Rigid molecules would also pay less of an entropy penalty upon binding than flexible ones. Taking the thienyl moiety as one sub-site binding group and the sulfonamoyl as the scaffold most of this shape would be defined by the nature of

the *N*-substituent(s). The following sections take the previous work as a starting point. The initial investigation focuses on the *N*-substituents to try and determine if any SAR exists and the optimum shape for this part of the molecule can be established. A more complete set of analogues were prepared examining the effects of substitution pattern on binding.

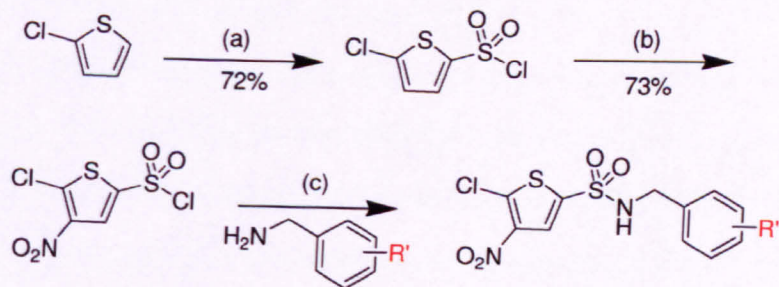
As the only the 5-chloro-4-nitrothiophene based analogues have shown consistent activity this group was maintained throughout the investigation of the *N*-substituents. Although replacing the 5-chloro group is dealt with later (Section 2.6), the methyl group was investigated as the first 5-chloro alternative at the same time as the work on the *N*-substituents was performed. A number of corresponding analogues based on it were prepared too. Although evidence suggested it was not active it is a similar size to chlorine (2 Å vs. 1.8 Å)¹⁹⁵ so sterically should behave similarly if making hydrophobic contacts with MDM2 are the basis for the activity of these inhibitors.

2.5.1 *N*-Aryl Substitution Pattern

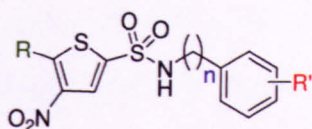
The optimised peptide, Nutlins, spiro-oxindoles and benzodiazepinediones all use aryl halide substituents, a structural feature shared with the sulphonamide inhibitors. The nature and substitution pattern of the *N*-aryl substituents was the first structural feature to be investigated. Whilst a number of analogues with various substituents in different positions had been investigated previously (Table 4) no systematic study of substituent position had been performed. The first set of analogues investigate the *N*-benzyl analogues mono-substituted with trifluoromethyl at each position of the benzene ring. The unsubstituted, *p*-chloro and 3,5-bis-trifluoromethyl analogues were also examined (Table 6).

The analogues were prepared in three steps from 2-chlorothiophene or 2-methylthiophene (Scheme 1). There is considerable difference in the reactivity of the various positions of thiophene towards electrophiles. Performing chlorosulfonation prior to nitration ensured the correct substitution pattern was achieved. Due to the deactivating nature of the substituents being added no di-substitution products were observed for the chloro-analogues. When the same chlorosulfonation conditions were used on 2-methylthiophene however, the methyl group was sufficiently activating to allow significant dichlorosulfonated product to be formed in the first step. This problem was solved by diluting the reactants in chloroform and omitting PCl_5 albeit with a lower yield than obtained for the chloro-analogue. Nitration with fuming nitric acid worked well for both systems.

The final step allowed diversification of the *N*-substituent by the use of different benzyl amines. $\text{S}_\text{N}\text{Ar}$ was found to be a competing reaction because of the highly activated nature of the thiophene ring system and the major contributor to the modest yields in the final step. Slow addition of no more than 1eq of amine and TEA in a DCM solution to the sulfonyl chloride in DCM at 0°C , with the sulfonyl chloride always in excess helped to suppress this.



Scheme 1 (a) ClSO_3H , PCl_5 , 0°C then ambient overnight. (b) 100% fuming HNO_3 , ambient 4 hours. (c) TEA (1eq); benzylamine (1eq) DCM 0°C 5 min warmed to ambient. (R' see Table 6)



| Entry | Compound | n | R | R' | Yield | FP IC ₅₀ (μM) | SD |
|-------|-----------|---|----|---------------------|-------|--------------------------|------|
| 1 | 19 | 0 | Cl | p-Cl | n/a* | 22.22 | 4.86 |
| 2 | 67 | 1 | Cl | H | 48% | 28.88 | 3.58 |
| 3 | 68 | 1 | Cl | p-Cl | 40% | 8.43 | 4.05 |
| 4 | 69 | 1 | Cl | o-CF ₃ | 40% | 11.35 | 3.73 |
| 5 | 70 | 1 | Cl | m-CF ₃ | 48% | 13.6 | 2.61 |
| 6 | 71 | 1 | Cl | p-CF ₃ | 48% | 10.18 | 3.31 |
| 7 | 72 | 1 | Cl | m,m-CF ₃ | 35% | 10.3 | 4.84 |
| 8 | 73 | 0 | Me | p-Cl | n/a* | >250 | --- |
| 9 | 74 | 1 | Me | H | 54% | >250 | --- |
| 10 | 75 | 1 | Me | p-Cl | 29% | >250 | --- |
| 11 | 76 | 1 | Me | o-CF ₃ | 61% | >250 | --- |
| 12 | 77 | 1 | Me | m-CF ₃ | 58% | >250 | --- |
| 13 | 78 | 1 | Me | p-CF ₃ | 69% | >250 | --- |
| 13 | 79 | 1 | Me | m,m-CF ₃ | 68% | >250 | --- |

Table 6 Increasing the size of the *N*-group from phenyl to benzyl and attaching substituents to the aryl ring appears to slightly increase activity but little or no SAR is seen upon changing the type or position of the aryl substituent. Replacing 5-Cl with 5-Me abolishes activity. ***19** Previously prepared at Cyclacel.

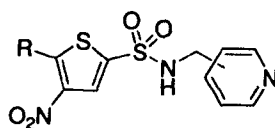
The FP assay shows that there is very little difference in binding activity when either the type or position of the aryl substituent is changed (Table 6). Going from phenyl to benzyl and adding a substituent both slightly increase activity. However the changes in activity are small and not what would be expected for ligands intended to bind to a well defined site relying mainly on hydrophobic interactions. None of the 5-methyl analogues show any activity. Given the similar size of the two substituents this shows that the role of this chlorine is not solely to maximize hydrophobic interactions with the protein. These observations continue to support the two possibilities that (a) the observed activity is dominated by the 5-chloro-4-nitrothienylsulfonyl moiety as a whole

and the *N*-substituents are unimportant or (b) that multiple binding modes occur. More extensive variations to both parts of the molecule were performed to examine this.

2.5.2 *N*-Picoyl groups

All three of the most active literature inhibitors use pendant solubilising groups attached to the scaffold such that they project away from the binding site to improve the pharmacological properties of the compound. The small sulfonamide scaffold offers less possible points of attachment for solubilising groups than any of the most active inhibitors. So the physicochemical properties would need to be an intrinsic property of the core ligand. One possible way to alter the properties would be to use various heterocycles. Another reason to consider heterocyclic groups is that they could potentially make polar contacts with the binding site leading to increased affinity. This has been shown for the benzodiazepinediones. While most benzodiazepine analogues rely solely on hydrophobic interactions, some were able to make polar contacts and exhibited enhanced affinity for MDM2,¹³⁸

As a simple preliminary investigation to see if heterocyclic rings would be tolerated the benzyl of **67** was replaced with 2-, 3- and 4-picoyl groups in compounds **80**, **81** and **82** respectively (Table 7, entries 1, 2 and 3). All three compounds show the same activity and although they show almost two fold decrease in activity over the corresponding benzyl compound, **67**, these groups are somewhat tolerated and indicate that other heterocycles could be used in the future. The corresponding 5-methyl analogues **83**, **84** and **85** were also prepared but found to be inactive (Table 7, entries 4, 5 and 6).



| Entry | Compound | R | Isomer | FP IC ₅₀ (μM) | SD |
|-------|-----------|----|--------|--------------------------|-------|
| 1 | 80 | Cl | 2 | 27.52 | 16.49 |
| 2 | 81 | Cl | 3 | 41.3 | 2 |
| 3 | 82 | Cl | 4 | 38.05 | 7.75 |
| 4 | 83 | Me | 2 | >250 | --- |
| 5 | 84 | Me | 3 | >250 | --- |
| 6 | 85 | Me | 4 | >250 | --- |

Table 7 Replacement of benzene with pyridine rings.

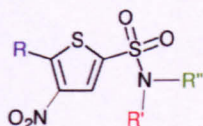
2.5.3 *N,N*-disubstituted sulfonamides

The most active compound at the start of this investigation was **66** (IC₅₀, 3 μM) (Table 5, entry 8). As it incorporated three potential hydrophobic binding groups, it was consistent with the hypothesis that mimicking all three p53 residues would result in better occupancy of the binding site and the resulting increased hydrophobic interactions would lead to increased activity.

Initially the plan was to complete this study by determining the optimum substitution pattern on the *N,N*-bis benzyl rings and to determine if the observation with *N*-alkyl substituents is significant. Synthetically the main challenge here would be to prepare the required secondary amines so the compounds could be prepared by condensation of the desired amine and sulfonyl chloride, as in Scheme 1, or to introduce the second *N*-substituent to the *N*-benzyl analogues, described in section 2.5.1, using the modified Mitsunobu chemistry developed by Tsunoda.^{196, 197}

Some preliminary investigations using commercially available amines were performed and the previously inactive compounds **64** and **65** (Table 5, entries 6 and 7)

were retested and found to have low μM affinity similar to the other bis-benzyl analogues (Table 8, entries 3 and 4). This observation indicates that some of the anomalies shown in Table 5 arose from the original assay. Compared to the corresponding mono benzyl, compound **67** (Table 6, entry 2) the *N,N*-bisbenzyl compound, **86**, showed a 2-fold increase in potency consistent with previous observations (Table 8, entry 1). However addition of the *N*-methyl substituent in compound **87** (Table 8, entry 2) showed the same activity as the corresponding analogue, **67** (Table 6, entry 2). This observation is consistent with the methyl group being too small to make a meaningful contribution to the affinity. Again all of the 5-methyl analogues were inactive (Table 8, entries 5-7).



| Entry | Compound | R | R' | R'' | FP IC ₅₀ | SD |
|-------|-----------|----|-------------|---------------------------|---------------------|------|
| 1 | 86 | Cl | Benzyl | Benzyl | 12.65 | 2.75 |
| 2 | 87 | Cl | Benzyl | Methyl | 24.55 | 0 |
| 3 | 64 | Cl | p-Cl Phenyl | p-NO ₂ Benzyl | 7.54 | --- |
| 4 | 65 | Cl | p-Cl Phenyl | m-OCF ₃ Benzyl | 7.51 | --- |
| 5 | 88 | Me | Benzyl | Benzyl | >250 | --- |
| 6 | 89 | Me | Benzyl | Methyl | >250 | --- |
| 7 | 90 | Me | Benzyl | Phenyl | >250 | --- |

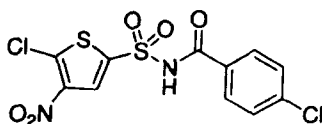
Table 8 Tertiary sulfonamides show increased activity over corresponding secondary ones but show little variation between analogues. 5-methyl analogues show no activity.

The flat SAR observed for a variety of *N*-substituents supported the hypothesis that the 5-chloro-4-nitro-2-sulfonamoyl substituted thiophene ring was dominating the SAR. Because of this synthesis of a series of analogues to investigate the aryl substitution patterns of the *N,N*-bisbenzyl sulfonamides was discontinued until after alternatives to

the chloro and nitro groups were investigated but ultimately abandoned when it became apparent that these groups could not be replaced.

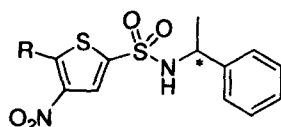
2.5.4 Increasing rigidity; α -branched benzyl substituents

The *N,N*-bis benzyl analogues, like **67**, have two additional single bonds and are less rigid as a result. Although docking suggests they are the correct size and can adopt the correct shape to occupy the binding site, their increased flexibility means they may have to pay too large an entropic penalty to do so and hence only show a modest increase in binding activity over the *N*-benzyl analogues. The Nutlin, benzodiazepinedione and spiro-oxindole series of inhibitors are all based on rigid, cyclic scaffolds that direct their binding groups into the three sub-pockets occupied by the three p53 residues. It has been demonstrated that stabilizing the α -helix of the p53 peptide¹³¹ and using geometric constraints in the benzodiazepines¹³⁸ considerably improves binding. Various ways to prepare more rigid sulfonamide based inhibitors were considered. *N*-acylsulfonamides, such as **91**, where the carbonyl group would help to lock the configuration, were considered. However, a very similar class of compounds were being investigated as anti cancer agents at that time albeit on a different target by another group.¹⁹⁸ Furthermore it was felt that these compounds would not lend themselves well to adding a third binding group at the nitrogen, so no further investigation was performed.



91

It was instead decided to investigate attaching the third binding group to the α -carbon of the N-benzyl group. Given that additional *N*-substituents appeared to enhance binding, it seemed reasonable to investigate whether substituents at the adjacent carbon could do the same. This would lead to a much more rigid and potentially more ligand efficient molecule in which two of the binding groups would be attached to the same sp^3 centre. Firstly both enantiomers of α -methylbenzyl analogues were prepared by the same route shown in Scheme 1 using the optically pure α -methylbenzylamines. This investigated the possibility of using substituents at the methylene carbon of the benzyl group.



| Entry | Compound | R | Enantiomer | FP IC ₅₀ (μM) | SD |
|-------|-----------|----|------------|--------------------------|------|
| 1 | 92 | Cl | S | 18.75 | 5.65 |
| 2 | 93 | Cl | R | 21.4 | 1.1 |
| 3 | 94 | Me | S | >250 | --- |
| 4 | 95 | Me | R | >250 | --- |

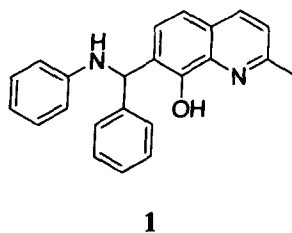
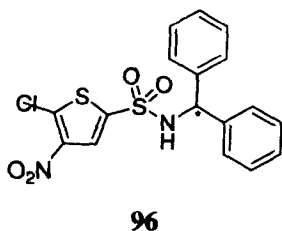
Table 9 C-methyl substituents are tolerated but do not enhance activity over the corresponding des-methyl analogue **67**.

The activity of the 5-chloro compounds **92** and **93** (Table 9, entries 1 and 2) was the same as the corresponding unsubstituted *N*-benzyl and *N*-methyl-*N*-benzyl compounds, **67** (Table 6, entry 2) and **87** (Table 8, entry 2) with no significant difference observed between the enantiomers. This result is expected as the methyl group is too small to act as a binding group in its own right. It did at least show that such modifications were tolerated. In keeping with the previous work the 5-methyl derivatives, **94** and **95** showed no activity (Table 9, entries 3 and 4).

Larger substituents would need to be examined to prove this theory. The obvious choice was to replace the α -methyl with phenyl as in compound **96**. Docking studies showed top ranked poses that occupied the site filling all three subpockets (Figure 21). Further evidence that supported this idea was the discovery of **1**.¹²⁸ This novel class of inhibitor exhibited nM affinity and demonstrated all the correct attributes in functional cell assays. Two of the binding groups on **1** are attached to the same sp^3 carbon supporting the idea that the phenyl groups could be presented in this manner.

To investigate this, compound **96** was prepared in the same way as the sulfonamides already described, by reaction of the required sulfonylchloride with diphenylmethanamine. As the amine was not readily available and was prepared in 2 steps from benzophenone via reduction of the corresponding oxime (Scheme 2).¹⁹⁹

The oxime synthesis was facile and proceeded in high yield. Reduction of the oxime to diphenylmethanamine was performed in the presence of magnesium and ammonium formate.²⁰⁰ In the final coupling step excess base was used to mop up any free acid which could protonate the amine making it into a leaving group driven by the stability of the resulting benzhydryl carbocation. It was noticed that the characteristic deep red colour of the benzhydryl cation formed upon addition of the amine to the reaction mixture and this could account for the modest yield.



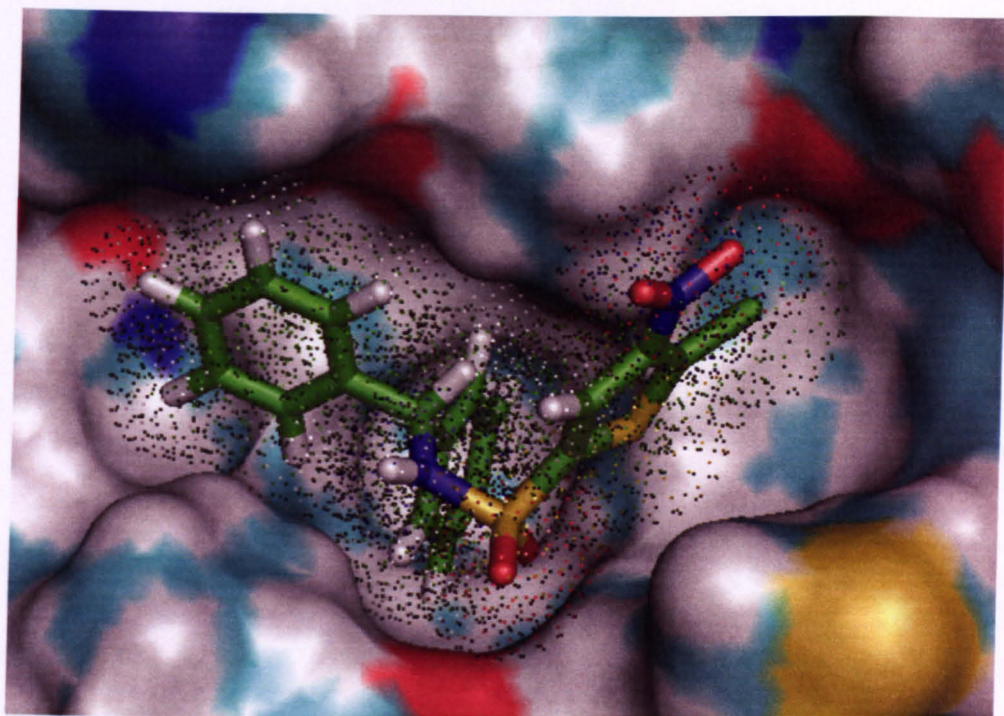
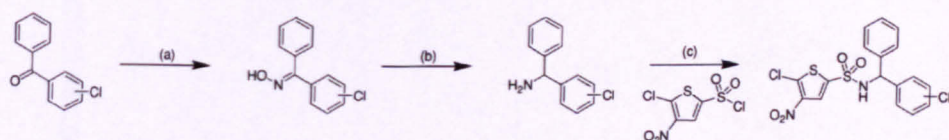


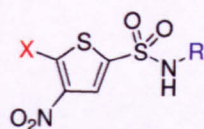
Figure 21 Docking suggests that α -branched sulfonamides could bind to MDM2 filling all three sub-pockets. Compound **96** docked in 1YCR. C, Green; H, White; Cl, pink; N, blue; O, red; S, yellow.



Scheme 2 Synthesis of **96**: (a) $\text{NH}_2\text{OH}\cdot\text{HCl}$, NaOH , EtOH , reflux (b) $\text{CHO}\cdot\text{NH}_4^+$, Mg , MeOH , rt (c) TEA , DCM , rt.

Unfortunately **96** exhibited 2-fold less activity than **19** indicating that this strategy would not work (Table 10, entry 2). This is a modest change in activity upon addition of a substantial group indicating that this side of the molecule plays little part in determining the observed activity. At the same time compound **97** was prepared. It

possessed no *N*-aryl substituent but instead the *n*-butyl group. This small flexible group would not be expected to be able to sufficiently fill one of the sub-pockets so should not show activity. However, it exhibited similar activity to the lead compound, **19** (Table 10, entry 3). This observation conclusively showed that all that was required for activity was the highly activated thiophene ring and unless an alternative to it was found it would not be possible to develop this series further. When the activity of **96** and **97** were determined the assay had become less sensitive, as discussed in Section 1.11.1.



| Entry | Compound | X | R | FP (IC ₅₀ , μM) | Corrected (IC ₅₀ , μM) | SD |
|-------|-----------|----|---|-------------------------------|--------------------------------------|------|
| 1 | 19 | Cl | | 80 | 25.15 | 4.7 |
| 2 | 96 | Cl | | 214.2 | 67.4 | 29.6 |
| 3 | 97 | Cl | | 122.9 | 38.6 | 14.6 |

Table 10 Both α -Branched and linear alkyl *N*-substituents show similar activity to **19**.

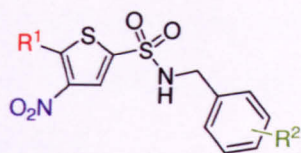
2.6 Replacing the 5-chloro-4-nitrothienylsulfonamoyl group

All the results presented up to this point show a very flat SAR indicating that these inhibitors are not interacting with the binding site mainly through hydrophobic

interactions as is the case for the most potent literature inhibitors. It was becoming clear that the activity of these inhibitors was due to the highly activated thiophene system and that the *N*-substituents were playing little or no role in determining binding affinity. The key question was: could either the 4- or 5-substituents be replaced to give a less reactive species that maintained inhibitory activity? Some alternatives to the 5-chloro and 4-nitro investigated at Cyclacel prior to the start of this project were discussed in Section 2.3.1 (Table 2). Some potential starting points for further investigation were identified and are discussed in the following sections.

2.6.1 5-alkyl substituents

Sterically, a suitable replacement for chlorine is the methyl group. It has considerably different electronic properties but will have a net electron donating effect as opposed to the electron withdrawing effect of chlorine. Most importantly for this investigation it is a much poorer leaving group so analogues based on it will be of a similar size to (Me, 2 Å; Cl, 1.8 Å)¹⁹⁵ but not react like their chloro-counterparts. While previous results indicated that the methyl group was not a suitable chloro-replacement it was thought it might be useful to examine them in the context of other *N*-aryl substituents. The results of this have been presented throughout Section 2.5, and in all cases 5-methyl analogues show no binding activity. If the activity of these compounds was based mainly on them making hydrophobic contacts with the binding site a total loss of activity would not be expected. No activity was observed upon increasing the size of the alkyl substituent to ethyl or *n*-propyl (Table 11).



| Entry | Compound | R ¹ | R ² | FP (IC ₅₀ , μM) |
|-------|------------|----------------|-------------------------------------|----------------------------|
| 1 | 98 | Et | H | >250 |
| 2 | 99 | Et | p-Cl | >250 |
| 3 | 100 | Et | o-CF ₃ | >250 |
| 4 | 101 | Et | m-CF ₃ | >250 |
| 5 | 102 | Et | p-CF ₃ | >250 |
| 6 | 103 | Et | m,m-(CF ₃) ₂ | >250 |
| 7 | 104 | n-Pr | H | >500 |
| 8 | 105 | n-Pr | p-Cl | >500 |
| 9 | 106 | n-Pr | o-CF ₃ | >500 |
| 10 | 107 | n-Pr | m-CF ₃ | >500 |
| 11 | 108 | n-Pr | p-CF ₃ | >500 |
| 12 | 109 | n-Pr | m,m-(CF ₃) ₂ | >500 |

Table 11 Investigation of 5-alkyl substituents

2.6.2 Replacing the 5-chloro group with bromine and hydrogen

Bromine and chlorine are interchangeable within the Nutlin series of inhibitors and both can be used at the *p*-position of the phenyl groups whilst maintaining activity. An obvious omission from the previous work was directly replacing the 5-chloro group with another halogen. Whilst bromine had been tried in positions 4, 5 and 4 and 5 together, compounds **23**, **24** and **25** (Table 2, entries 5, 6 and 7) it had not been used in the context of the 4-nitrogroup. Compound **110** was prepared to test this and found to be of similar activity to all the other 5-chloro-4-nitro-analogues (Table 12, entry 2). As it would also be possible to displace bromine via S_NAr, this was further evidence that the activity of these compounds stemmed from their reactivity.

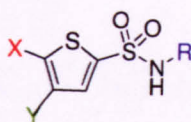
The des-chloro compounds, **111** and **112**, were prepared along with their 5-nitro isomers **113** and **114**. The previous work had identified the corresponding *N-p*-chloro

phenyl analogue **21** as a low activity, non-reactive inhibitor that warranted further investigation (Table 2, entry 3). Neither **111** nor **112** showed any activity in this investigation (Table 12, entries 2 and 3).

The 5-nitro isomer was also formed during the synthesis of these compounds as this position was not blocked by another substituent so was prone to nitration in the second step. Rather than separate the 4- and 5-nitrothiophenesulfonyl chlorides after nitration, the mixture of isomers was carried through the synthesis and the sulfonamides were separated by reverse phase preparative HPLC. The 5-nitro analogue, **114**, showed low activity, (45%) inhibition at 500 μ M (Table 12, entry 6), which, when corrected for the loss of assay sensitivity would mean an IC_{50} of >157. This was not considered sufficiently active to be significant and its des-chloro counterpart, **112**, showed no activity at this level. In the previously investigations the 5-nitro analogue, **22**, (Table 2, entry 4) was found to be inactive too.

2.6.3 5-amino substituents

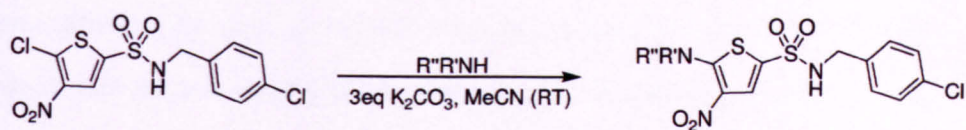
One of the most promising starting points in replacing the 5-chloro substituent was compound **31** (Table 2, entry 13) which bore a 3-hydroxypiperidine in place of chlorine. With activity only 2.5 fold lower than compound **19** it was the second most active compound that did not bear the 5-chloro-4-nitro pair. Structurally, its most similar analogue, **32** (Table 2, entry 14) also showed some activity albeit over 2-fold lower again.



| Entry | Compound | X | Y | R | FP (IC ₅₀ , μM) | Corrected (IC ₅₀ , μM) | SD |
|-------|----------|-----------------|-----------------|---|-------------------------------|--------------------------------------|-----|
| 1 | 19 | Cl | NO ₂ | | 80 | 25.15 | 4.7 |
| 2 | 110 | Br | NO ₂ | | 67.6 | 22.5 | 9.9 |
| 3 | 111 | H | NO ₂ | | >500 | --- | --- |
| 4 | 112 | H | NO ₂ | | >500 | --- | --- |
| 5 | 113 | NO ₂ | H | | >500 | --- | --- |
| 6 | 114 | NO ₂ | H | | >500 | 45% @ 500 μM | --- |

Table 12 Active compounds tested under less sensitive assay conditions showing observed and adjusted IC₅₀ values. All display similar activity to all other active compounds in this study.

A series of analogues investigating a range of structural features including alcohol versus ether, secondary versus tertiary amine, cyclic versus linear and various chain lengths were prepared. Synthesis of the above analogues utilized the reactivity of the highly electron deficient 5-chloro-thiophene system. Compound **68** reacted with the required amine nucleophile in the presence of excess potassium carbonate to give the corresponding 5-amino compound (**Scheme 3**).



Scheme 3 The 5-amino analogues were prepared from **68** by S_NAr with the appropriate amine.

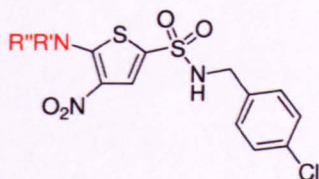
None of these analogues showed the expected activity (Table 13, entries 1-14). Some of the secondary amines showed low activity (20-30 % inhibition at 500 μ M). This was considered too low to be significant. Most surprisingly, **115**, which bore the previously seen to be active 3-hydroxypiperidine showed no activity (Table 13, entry 1).

To further increase structural diversity analogues based on a range of readily available amines were also prepared (Table 14). But again these exhibited little or no activity with the most active being the unsubstituted amino group displaying 40% inhibition at 500 μ M (Table 14, entry 1).

2.6.4 The 5-thioacetate starting point

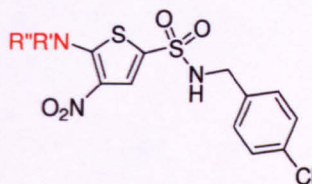
One analogue which had emerged from the previous work, that did not possess the 5-chloro substituent, was the thioester **28**. It actually appeared to be slightly more active than **19** (Table 2, entry 10). The corresponding methyl thioether, **29**, was totally inactive (Table 2, entry 11). Thioesters are not particularly stable so it was quite possible that the activity was due to this. To investigate this it was proposed to prepare the corresponding amide, **137**, and ketone **140**. It was thought that the ester, with such an electron deficient leaving group would be too unstable to be useful. The amide was prepared by acylating the 5-amino analogue with acetic anhydride in the acetic acid (Scheme 4). This extremely electron deficient amine was a poor nucleophile and did not initially react with either acetic anhydride or acetyl chloride. A literature procedure for acylating

electron deficient anilines using catalytic sulfuric acid or acetic acid as solvent^{201, 202} was employed and the latter was found to work well for this substrate too. It was also possible to prepare the diacetylated product **138** by increasing the quantity of acylating agent and using catalytic H₂SO₄. Unfortunately no activity was observed for either **137** or **138** (Table 14 , entries 9 and 10).



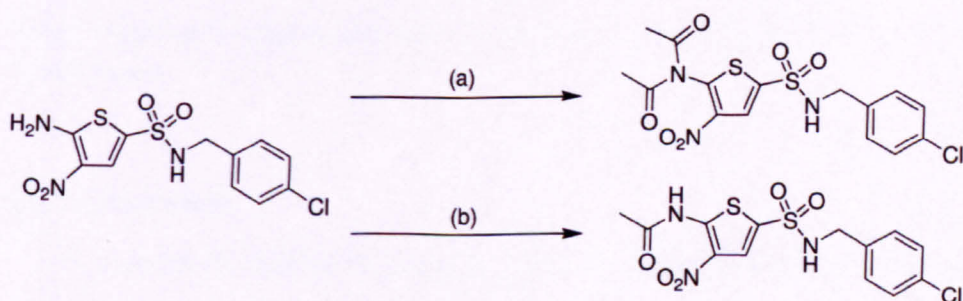
| Entry | Compound | R'R''N | FP IC ₅₀ (μ M) | % Inhibition at 500 μ M |
|-------|------------|--------|-----------------------------------|--------------------------------|
| 1 | 115 | | >500 | --- |
| 2 | 116 | | >500 | --- |
| 3 | 117 | | >500 | --- |
| 4 | 118 | | >500 | --- |
| 5 | 119 | | >500 | 30 |
| 6 | 120 | | >500 | 30 |
| 7 | 121 | | >500 | --- |
| 8 | 122 | | >500 | 20 |
| 9 | 123 | | >500 | --- |
| 10 | 124 | | >500 | 25 |
| 11 | 125 | | >500 | --- |
| 12 | 126 | | >500 | 17 |
| 13 | 127 | | >500 | 20 |
| 14 | 128 | | >500 | 10 |

Table 13 5-Amino analogues prepared to investigate compound 115 as a potential inhibitor.

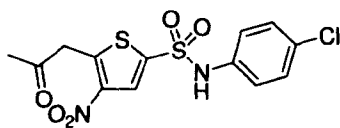


| Entry | Compound | R'R''N | FP IC ₅₀ (μM) | % Inhibition at 500 μM |
|-------|----------|--|-----------------------------|------------------------------|
| 1 | 129 | NH ₂ | >500 | 40 |
| 2 | 130 | NHMe | >500 | 20 |
| 3 | 131 | NMe ₂ | >500 | --- |
| 4 | 132 | NEt ₂ | >500 | --- |
| 5 | 133 | | >500 | --- |
| 6 | 134 | | >500 | 32 |
| 7 | 135 | | >500 | 21 |
| 8 | 136 | MeOOC-CH ₂ -NH ₂ | >500 | 35 |
| 9 | 137 | AcNH ₂ | >500 | --- |
| 10 | 138 | (Ac) ₂ N | >500 | --- |
| 11 | 139 | H ₂ NOOC-CH ₂ -NH ₂ | >500 | --- |

Table 14 Investigation of diversity of 5-amino substituents.

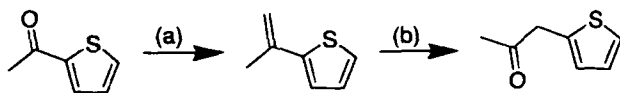


Scheme 4 Acid catalyzed acylation of electron deficient amine; synthesis of 137: (a) Acetic anhydride (excess) H₂SO₄ (catalytic); (b) Acetic acid (solvent), 1 equivalent Acetic anhydride.



140

Unfortunately, **140** was not prepared. It was proposed to install the required ketone on the 2-position of thiophene first then chlorosulfonate, nitrate and condense with the necessary amine as had been done for the chloro and alkyl analogues. The ketone was introduced in two steps starting from 2-acylthiophene which was converted to vinyl thiophene via a Wittig reaction. Vinyl thiophene was reacted with the hypervalent iodine compound, hydroxytosoxyiodobenzene (HTIB or Koser's reagent), in methanol to give the desired ketone²⁰³ (Scheme 5). Unfortunately this compound decomposed rapidly and it was not possible to synthesise beyond this point.



Scheme 5 Synthesis of starting material required for preparation of compound **140** (a) KO^t-Bu, PPh₃, ether; (b) HTIB, MeOH.

2.7 Conclusions

A considerable number of analogues of the bis- and tris-aryl sulfonamides were prepared and their binding activity determined. The work was driven by what is known about the structure of the PPI and how the best literature inhibitors bind and some potential starting points from previous work on this series. The highly activated

thiophene system dominated the SAR and any attempts to modify the shape of the molecule were void as the activity did not stem from making hydrophobic contacts with in the binding site.

That **97**, which posses the *N*-*n*-butyl group has the same activity as the lead compound **19** was strong indication that these compounds were not binding in the expected manner. The fact that the only active chloro replacement was another halogen pointed to the reactivity as the source of activity. Anything that deactivated the thiophene system toward nucleophilic attack also reduced activity. Apart from replacing the chloro leaving group removing either of the electron with drawing groups is also deactivating and appears as lower activity in the binding assay. This would explain why it was not possible to replace, reverse or extend the sulfonyl linker between the sulfur and thiophene, all of which would be less electron with drawing, yet any modification could be performed on the *N*-substituent with very little change in activity. As no non-reactive alternatives to the highly activated 5-chloro-4-nitrothienylsuffonamoyl moiety were found these compounds are no longer been pursued as inhibitors of the MDM2-p53 PPI.

3. Shape based virtual screening for new leads.

3.1 Introduction

3.1.1 Virtual screening

Both the Nutlin and 1,4-benzodiazepine MDM2 inhibitors were discovered by screening their respective companies compound libraries to find compounds that interacted with MDM2.^{135, 139} Although high throughput screening (HTS) of large libraries of compounds for activity against a given target is widely used in industry to find new leads for drug discovery, most of the compounds screened will be inactive against any given target. Whilst this is good from a drug selectivity point of view, it means considerable resources will be used screening a large number of inactive compounds in the hope of finding a few hits that can be developed as drugs.

Another limitation is that even the largest libraries don't sufficiently represent all of druglike molecular space. Large pharmaceutical companies continuously revise and update their compound libraries to improve the quality and diversity of their contents. However, even collectively considering all the largest corporate and commercial libraries would only represent a tiny portion of possible druglike molecular space. An often quoted example that puts the insignificance of any compound library into perspective is that chemical space is an estimated 10^{62} possible molecules, so many that there are not enough atoms in the universe to make one copy of each.²⁰⁴ Therefore the Zinc Database²⁰⁵ (discussed in more detail below), which currently contains about 8.5×10^6 unique, purchasable, drug-like compounds only represents a tiny 8.6×10^{-55} % of this chemical space. The fact that many of these compounds are analogues reduces its diversity further.

Despite its insignificance in chemical space, in the context of a screening campaign this is still a very large number of compounds to accumulate and test. Screening the order

of 10^6 compounds is really only possible for the largest pharmaceutical companies. Small companies or academic investigators, without actual compound libraries, wanting to screen for drugs will not normally have the resources to buy or handle this number of compounds. For example, to purchase one sample of each purchasable compound from the Zinc Database (currently around 8,500,000 compounds), at US\$ 50 per sample, would cost in the region of US\$ 425,000,000.

Virtual screening is an increasingly popular way of selecting compounds from commercial libraries and focusing the actual screening effort.²⁰⁶⁻²⁰⁸ Several rounds of computational screening, each of which removes unwanted compounds from a database for various specified reasons, are performed. The virtual screen culminates in a search and ranking based on a hypothesis that should, hopefully, identify active compounds for a specific target. By collating drug and lead like compounds from various sources and their vendor details the Zinc database²⁰⁵ facilitates the virtual screening and acquisition of compounds suitable for drug discovery.

There are a number of different ways to perform virtual screening but broadly speaking it falls into two classes; ligand based and structure based. Ligand based uses known ligands or pharmacophore models derived from them to search for new ones and structure based, usually docking, uses the target protein or enzyme as a query and selects molecules which are judged, by one or more mathematical scoring functions to, describe and rank the interactions between the screened ligands and the target molecule.

As computational power has increased so too has the ability to handle large amounts of data. Large numbers of molecules can be screened using more complex models to describe them in more detail than ever before. However, all models are approximations

and it is still difficult to dynamically represent a large flexible molecule, such as a protein, and describe its interactions with a large number of ligands in the context of a virtual screen. Some models work better for certain types of target than others as shown in a comparison study of various docking scoring functions.²⁰⁹

Prospective validation of virtual screening is very difficult to perform. It is easier to judge retrospectively and most methods are bench marked against each other using common test sets of known active and decoy molecules.^{210, 211} Most reports on validating virtual screening deal with docking and in particular test the scoring functions used by it.²⁰⁹ In real-world situations the number of unselected active compounds will remain unknown, unless all are tested, which would defeat the purpose of virtual screening in the first place. In benchmarking studies, a screening protocol or scoring function can be considered to work if it is significantly better than random selection, or existing protocols, at reducing a dataset to a smaller number of compounds with an enriched fraction of known actives. However, retrospective validation cannot predict how well a given protocol will work with new targets and datasets. In practice, a virtual screening campaign will ultimately be regarded as successful if it produces novel active hits.

3.1.2 Virtual screening and p53-MDM2

A number of MDM2 inhibitors have been discovered using computational modelling and virtual screening these compounds have been discussed in Section 1.8.

3.2 Shape based virtual screening with ROCS

One way to exploit the information carried within active compounds is to screen compound databases for compounds with similar shape and/or chemistry, the working hypothesis being, that molecules with similar 3D-shape may be active in the same targets.

so known actives could be used as queries to search for new ones. If they have similar chemical groups overlapping they may be even better.

ROCS (Rapid Overlay of Chemical Structures) by Openeye Scientific,²¹² is a 3D shape comparison application, based on the idea that molecules have similar shape if their volumes overlap well and any volume mismatch is a measure of dissimilarity. It uses a smooth Gaussian function to represent the molecular volume so it is possible to routinely minimize to the best global match.²¹² Using a known active molecule as a query, molecules in a database can be compared to it and ranked according to their 3D shape and/or chemical similarity to it. The most similar compounds are regarded as hits. How the hitlist is populated is determined by a number of user defined parameters such as a minimum measure of similarity and/or number of compounds.

Pharmacophore models are derived from a ligand, or more usually several ligands from different series, and based on what structural features and spatial arrangement of them is deemed to be important for activity. Screening based on such models is open to parameterization, subject to how the model is prepared and how much weighting is given to different structural features when scoring how well the database molecules conform to the model. To prepare a good pharmacophore model a considerable amount of prior knowledge will be required so a number of ligands from different classes with a wide range of activity can be used to determine what is and what is not important. The strength of pharmacophore-based screening compared to other ligand similarity screening approaches lies in the ability to detect a diverse set of putative active compounds with totally different chemical scaffolds.²¹³ Pharmacophore models can also bring together activity enhancing features from different molecules that do not necessarily occur together

in the individual ligands. Besides screening, pharmacophore models are very useful in other applications of drug development, like *de novo* design, lead optimization, ADME/toxicology studies, and chemogenomics.^{214, 215}

Shape based screening with ROCS requires only one *bona fide* ligand to use as a query and a database of molecules to compare it to. ROCS takes an holistic approach to ligand based virtual screening in that it considers the query molecule as a whole. A good ligand inherently carries the information as to what is required for binding and much of this information is carried within the 3D shape of the molecule. Good ligands can therefore be used as queries to search for other similarly shaped and hopefully, active molecules.

Given that the best inhibitors of the MDM2-p53 PPI make predominantly hydrophobic interactions with MDM2, that are maximised by the excellent shape complementarity they have with its binding site, it was decided that shape based screening with ROCS would be a suitable approach to finding other inhibitors that do the same. ROCS has been successfully employed to find new leads for the ZipA-FtsZ PPI, which is considered a potential antibacterial drug target.²¹⁶ To date there are no reports of ROCS being used to screen for ligands of the p53-MDM2 PPI. Here a ligand based screen of the ZINC database using ROCS is described.

3.3 Validation of ROCS.

Prospective validation of virtual screening is very difficult to do. Most validation is performed retrospectively on various known test sets of compounds for different targets where a screening strategy is deemed to be successful if it enriches the hitlist with known active compounds. However there are many variables such as diversity, size and nature of

the compounds in the screened database which will all affect the outcome.^{210, 211} Much work has been done to address the issues of validating virtual screening methodology. Most studies are aimed at benchmarking docking programs and scoring functions. ROCS has been compared to various docking programs using some of the same datasets used to retrospectively validate them.²¹⁷⁻²¹⁹ In particular, a study by Hawkins compared the ability of ROCS to that of seven different docking programs at finding known actives from decoy sets for 21 different protein systems. ROCS consistently performed as well as and better than many of the docking programs showing high enrichment of the top ranked compounds with known actives.²¹⁷ This study also showed that very little parameterization is required to perform shape based screening using ROCS. The parameters used by Hawkins were used to perform the screens in this project. The significance of any settings used is dealt with in the appropriate sections below.

3.4 Virtual screening work flow for this project.

3.4.1 Database selection and preparation

The early rounds of a screening campaign generally aim to remove or filter out unsuitable compounds and selection and preparation of the compound database is an extremely important part of this process.²²⁰ What comes out as hits is ultimately a function of what is contained in the search database and the saying “garbage in, garbage out” is often used when discussing database preparation for virtual screening. The easiest way to ensure that undesirable hit compounds do not come out of a screen is not to put them in the first place. This means making sure that the database only contains compounds that are considered suitable for drug development reducing the possibility of obtaining false positives. Furthermore the type of compounds in a database will depend on whether the

goal is to find drugs, leads or fragments^{221, 222} Computationally filtering undesirable compounds from a database is relatively easy and non-CPU intensive. Molecules can be filtered out of a large database on the basis of a small number of simple molecular descriptors such as molecular weight, LogP, number of H-bond donors and acceptors number of rotatable bonds or the presence of certain atoms or functional groups.²²³ It is important to perform filtering early so that computational time is not wasted processing inherently unsuitable molecules during the more CPU intensive phases of a screen.

The Zinc database is a database of commercially available compounds from various vendors for virtual screening.²⁰⁵ It was prepared by Shoichet and Irwin and made freely available to facilitate virtual screening for a wide community of scientists. All compounds that are added to the database are filtered by what is essentially a more lenient rule of six version of Lipinski's rule of five.^{223, 224} Within this are a number of subsets of molecules filtered for different specifications of these properties. It is therefore possible to select a pre-filtered subset based on what one intends to do with the hits. For example, lead-like compounds are generally regarded as smaller than drug like compounds based on the idea that drug molecules tend to get larger as they are developed so it makes sense to start with small compounds to leave some room for this.²²¹ The database is available in a number of commonly used file formats, and each compound contains vendor and purchasing information to facilitate subsequent purchase of hit compounds.

One of the main criteria for this screening campaign was that all compounds should be readily available. So the all purchasable subset was chosen. This would allow the greatest number of available compounds to be examined. It was also desirable that compounds of similar molecular weight to the queries were not excluded. The query

compounds being used in these screens are well optimized and contain a number of halogens, which are important in defining the overall shape and maximizing affinity. As a result the molecular weights of the query molecules are themselves towards the upper end of the range found in the database. Given that ROCS ranks hits based on how well they overlap the query, it was desirable that the database and queries were not mismatched with respect to molecular weight as a result of overly tight filtering criteria. Such a mismatch would lead to larger molecules having better overlap than smaller ones based on size rather than shape similarity.

The database was filtered in the next step using Openeye Filter version 2.0.2²¹² A number of prewritten filter files are included with the program. These include a drug like filter essentially based on Lipinski's rule of five²²⁴ a corresponding lead like filter which only allows smaller "lead-like" molecules through^{221, 222} and a third filter file, known as "filter_blockbuster" which was designed so that it just spans the range of the properties of 141 of the best-selling non-antibiotic prescription drugs from 2005. It was shown that slightly narrowing all the parameters of filter_blockbuster to cover from the 2.5th to the 97.5th percentiles that only 75 of the 141 molecules pass the filter, demonstrating how slight changes to many filters can lead to a significant reduction in the number of compounds that pass all of the filters.²¹² The filter files also allow molecules with certain numbers of particular functional groups to be removed. The filter files can be edited to modify any parameters or allowed functional group.

The Blockbuster filter file was used in this screen. As it allows molecules with a higher molecular weight to pass than either the drug or lead like filters, it would help minimise any size mismatch between the query and database molecules. Being based on

the properties of a relatively small set of molecules this filter file does however have quite a restrictive list of allowed functional groups. The functional group filter of this and the drug-like filter file were combined to make it more lenient.

At the time the screen was performed the all-purchasable subset of the Zinc database contained 2,667,437 molecules. Filtering with the above parameters reduced this slightly to 2,546,386 which were used in the next step. The relatively small number of compounds removed is a positive reflection on the criteria used for inclusion in the ZINC database.

3.4.2 Database preparation; multi-conformer generation

ROCS deals with ligand flexibility by screening multiple conformations of each molecule in the database. The multi-conformer database is generated prior to the screen using Openeye's conformer generation application, OMEGA 2.²¹² This is the most computationally intensive part of the screening process. However, once the multi conformer database has been generated it does not need to be repeated and can be used for all of the queries or for other screening campaigns without further modification.

It is important to ensure that the multi-conformer database supplied to ROCS sufficiently samples conformer space. This database was prepared such that a maximum of 1,000 conformers within 8 kcal mol⁻¹ of the minimum energy conformer, sampled at a rate of 0.5 RMSD for each molecule were generated for each database molecule. Bostrom investigated conformer generation using OMEGA and showed that the bio-active conformation of a number of ligands, would be contained in a multi-conformer dataset prepared using these parameters.²²⁵ It was the case that the bio-active conformation of most ligands in this study was actually within 3.7 kcal mol⁻¹ of the minimum and that by

sampling with a density of 0.5 RMSD the majority of conformers also had a shape Tanimoto co-efficient of greater than 0.9 indicating that they have a very similar overall shape. This result is important, considering that the main measure to be used in this screen is shape similarity and gives confidence that potential hits won't be missed as a result of insufficient sampling density. Sampling with a greater frequency is unnecessary and may result in poorer representation of conformer space within a given energy window if the maximum number of allowed conformers is achieved before a wide range is generated.

496,216,289 conformers of the 2,546,386 compounds were generated which is on average 195 conformers per molecule. They were saved as gz-compressed Openeye binary format. To keep the file size as small as possible Open-eye multi-conformer datasets can be written using "off-set rotor compress". Rather than saving the coordinates for each individual conformer, it uses a reference conformation and implies the others as a function of how they deviate from it. Minimizing the size of the data in this way increases the speed of screening when using parallel processors by reducing traffic on the network as data is sent between the master and slave processors. This database was now ready to be used for screening with either ROCS or Openeye's docking programme FRED.²¹²

3.4.3 Query selection and preparation

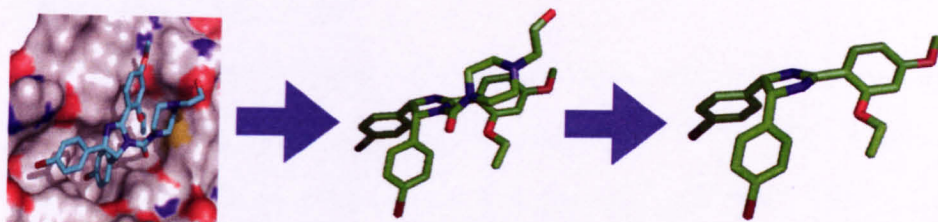
An example of the Nutlins,¹³⁵ 1,4-benzodiazepine-2,5-diones¹²² and spiro-oxindoles^{132, 141} were chosen as queries for this screen. All of these inhibitors bind MDM2 with low to mid nanomolar activity, exhibit clear SAR, and perform as expected in functional assays and in vivo. As a result these compounds carry much information about what is required to be a good ligand for this target and therefore all represent good points from which the search for new ligands can be initiated.

X-ray co-crystal structure data has been published for both the Nutlin¹³⁵ and 1,4-benzodiazepine-2,5-diones¹²² and extensive modelling and SAR investigations provide very strong evidence for the proposed binding pose of the spirooxindoles.^{132, 141} Although it is not necessary to have structural data to perform a ROCS screen, where it was available, the bioactive conformation was used as the query. In the absence of structural data it is suggested that the lowest energy conformer is used and has been shown that this has little effect on the enrichment rates in retrospective validation studies.²¹⁷

Another benefit of having structural information is that it makes it clear which parts of the molecule are pharmacophoric, scaffold or solvent exposed. Given that these molecules are highly optimized and that their molecular weights are towards the upper end of the range of the data base, to minimise any mismatch in size between the query and database molecules the solubilising groups were removed and just the scaffold and three binding groups corresponding to the basic pharmacophore were used as the query. Also because ROCS treats the molecule as a whole it would consider overlap with these groups as good and non-overlap with them as bad thus causing the focus to be taken away from the groups known to be most important for binding. Even in the case of the spiro-oxindoles, where the solubilising group is clearly pharmacophoric and considerably enhances activity, it was thought best to omit it to minimize mismatch between the size of the query and database molecules.

3.4.3.1 Nutlin-2 based query

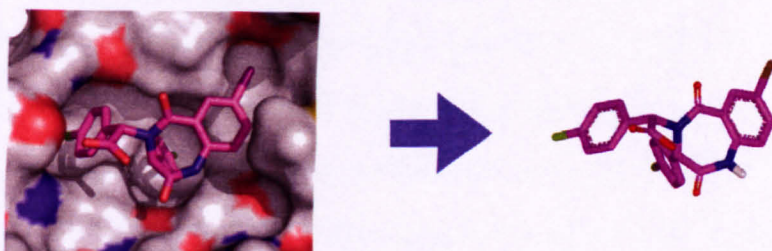
As discussed above, the bioactive conformation from the co-crystal x-ray structure (IRV1)¹³⁵ was used without the solubilising side chain.



Scheme 6 Preparation of the Nutlin based query (Green CPK sticks).¹³⁵ Nutlin-2 was extracted from its crystal structure with MDM2 (grey CPK surface) (1RV1) and its solubilising group removed whilst maintaining the bioactive conformation of the remaining groups. Carbon, green; oxygen, red; nitrogen, blue; bromine, brown.

3.4.3.2 Benzodiazepinedione based query

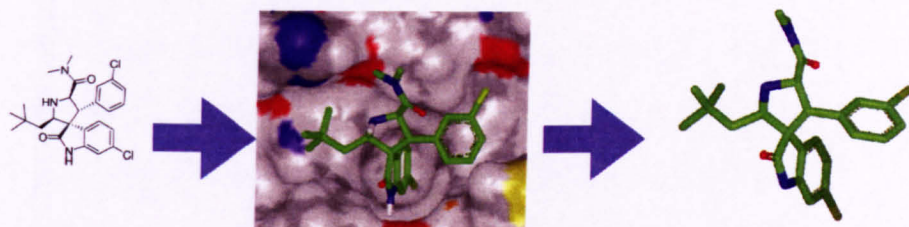
The structure from X-ray co-crystal structure (1T4E)¹²² was used directly as a query. The co-crystallised analogue is one of the simpler analogues in this series and consists mainly of required binding groups and scaffold without the solubilising side chains that are present in the optimized analogues.



Scheme 7 The benzodiazepine query (magenta CPK sticks), was extracted from the crystal structure MDM2 (grey CPK surface) (1T4E) and used without further intervention.

3.4.3.3 Spiro-oxidole query

As no structural data has been published for the spiro-oxindoles, the query was prepared by docking the first generation analogue (MI-43)¹⁴¹ into (1YCR)¹ using FRED.²¹² MI-43 is based on the same core as the most potent analogue MI-219 but does not have solubilising group or a 5-fluoro substituent on the oxindole ring.



Scheme 8 The spirooxindole (MI-43)¹⁴¹ was docked into MDM2 (1YCR)¹ (grey CPK surface) using FRED.²¹² The ligand was then extracted whilst maintaining its docked pose, (Green CPK sticks).

3.4.4 Performing the screen

Using each of the query molecules described above, the multi conformer database was screened using ROCS. The default parameters were used, as recommended by Hawkins to compare ROCS with various docking programs.²¹⁷ In this work it was shown that matching and ranking based on both similar chemistry overlap (which Openeye call Color) and shape similarity was more likely to select known actives from decoy sets than using shape alone.

ROCS overlays and compares every conformer of every compound in the database with the query. Based on the observations of Hawkins,²¹⁷ the program was set to optimize chemistry (Color) overlap and shape alignment. It then scores each between 0 and 1 where a score of 1 is a perfect match. The hits were ranked based on their combo-score which is

simply the sum of the shape Tanimoto and normalized Color score and has a maximum value of 2. Only the top scoring conformer of each database molecule is considered for ranking so that no compound can feature more than once. No minimum shape Tanimoto cut-off was specified. The top 500 hits were produced.

3.4.5 Hit selection for actual screening.

The 1,500 hits obtained from the three queries using ROCS were visually inspected and manually grouped into similar classes. Although clustering applications are available, given the relatively small number of hits to be examined it was decided this was the most efficient way to deal with them. The hits in each group were then inspected overlaid with the query. Hits that were rejected were typically those that only possessed two binding groups or those that despite having a good shape Tanimoto score only did so because they adopted a conformation which would cause it to clash with the binding site rather than fit into it in a shape complimentary manner. In total 200 hit compounds were selected from these groups. However, it was only possible to obtain 155 of them at the time of the screen. The output of the virtual screen is described in the following sections in the context of the queries used and the clusters into which they were divided.

3.4.5.1 Nutlin query

The Nutlin query returned hits which had average shape Tanimoto of 0.73 that ranged between 0.56-0.87 and average combo-score of 1.143 that ranged from 1.117-1.483. The top ranked comboscore hit showed a shape Tanimoto of 0.8350 and the highest Tanimoto at 0.87 is shown by hit 3. The hit compounds have molecular weights between 268.31 and 508.57. Of all the queries this one showed the most diversity with less domination of the hit list by a small number of large clusters. The hit list was divided into

16 different clusters described in the following sections and examples from each are shown in Table 15.

3.4.5.2 Nutlin query, Cluster 1

Compounds in this cluster were typically based on pyrazole and pyrazoline scaffolds bearing substituents in a 2,3,5 pattern (Table 15, Entry 1). They are structurally similar to Nutlins but generally more planar depending on the specific scaffold. The top ranked hit from this cluster is shown overlaid with the query (Figure 22).

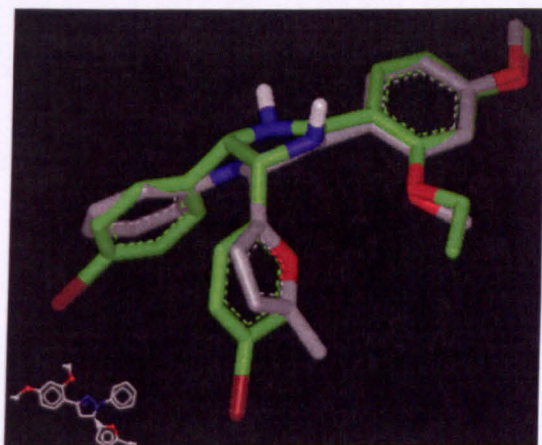


Figure 22 The top ranked hit from Nutlin query cluster 1 (over all rank 6) (Grey CPK sticks) overlaid with the query molecule (Green CPK sticks). This compound is typical of many of the molecules in this class.

3.4.5.3 Nutlin query, Cluster 2

These compounds have two potential binding groups cis to one another on a bicyclic scaffold similar to the known benzodiazepines (Table 15, Entry 2). Also some trans analogues show higher Tanimoto scores but overlap in a manner that would clash with the

protein and were not selected for testing. Examples of both cis- and trans- analogues overlaid with the query molecule are shown in Figure 23.

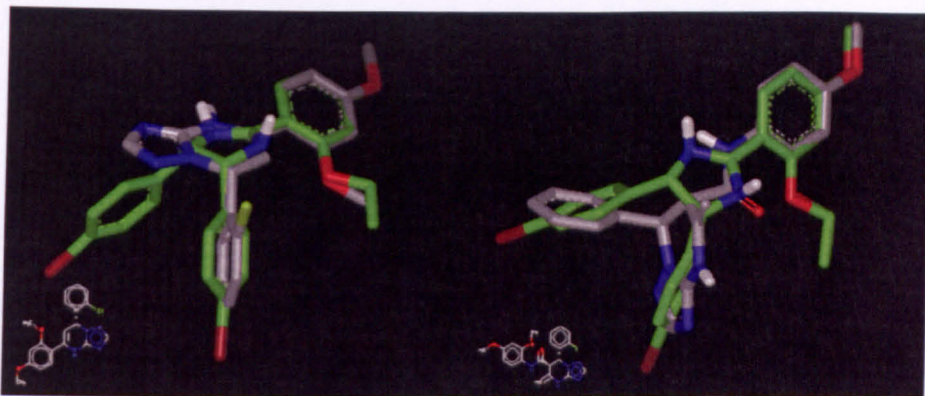


Figure 23 Cis- (left) and trans (right) examples of molecules from cluster 2 (Grey CPK sticks) overlaid with the query molecule (Green CPK sticks).

3.4.5.4 Nutlin query, rejected compounds; clusters 3-7, 11 and 14.

Compounds in these clusters were not selected for testing. They were generally deemed to be too flexible or lacking sufficient groups to occupy all three sub-pockets of the binding site. Cluster 3 consisted of linear amides and ureas. Despite possessing three potential binding groups and making good overlap with the query, high shape Tanimoto coefficients are likely a function of their flexibility. A hit from this cluster overlaid with the query is shown in Figure 24.

Compounds in cluster 4 predominantly possess only two potential binding groups. Some molecules resemble those of cluster 1 but have long flexible linkers between the scaffold and binding group. A typical hit from this cluster is shown overlaid with the query (Figure 25).

Despite high Tanimoto coefficients and some very highly ranked hits, compounds in cluster 5 overlapped the query in a manner likely to clash with the protein (Figure 26).

Cluster 6 consisted of predominantly 1,2,5-substituted imidazoles. At least one of the groups on these molecules is small or attached via too long a flexible linker such that it would not be projected into a sub-pocket (Figure 27).

Cluster 7 consisted mainly flexible, linear molecules similar to clusters 3 and 4 and good Tanimoto coefficients are a function of flexibility. Clusters 11 and 14 consisted of phosphonate esters and flexible tertiary amines respectively.

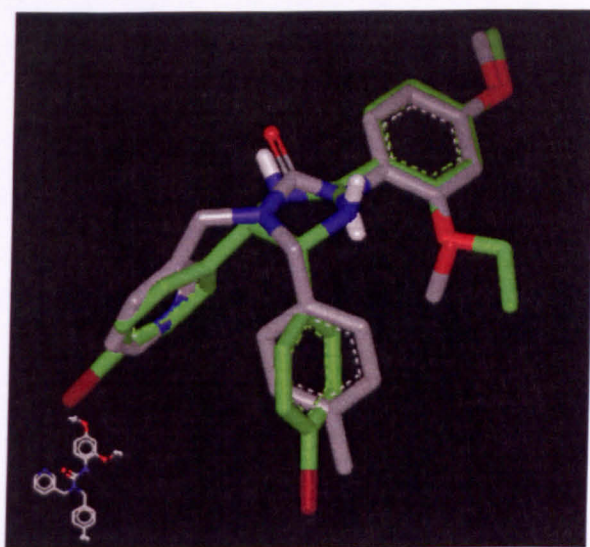


Figure 24 Example of molecules from cluster 3 (Grey CPK sticks) overlaid with the query molecule ((Green CPK sticks).

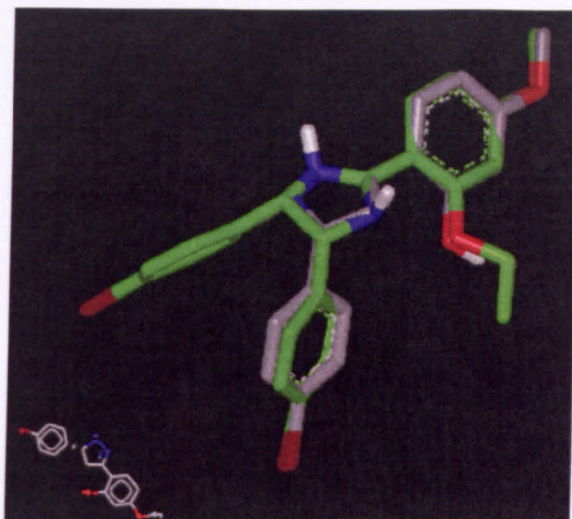


Figure 25 Typical rejected compounds from cluster 4 only possess two potential binding groups (Grey CPK sticks) overlaid with the query molecule (Green CPK sticks).

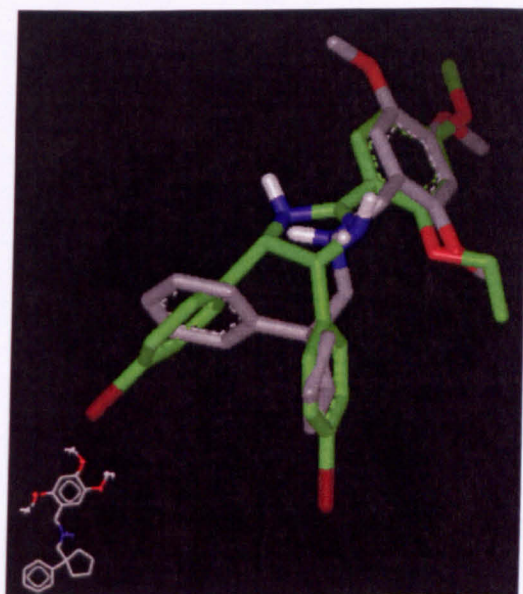


Figure 26 Typical rejected compounds from cluster 5 overlap so that they would clash with the protein (Grey CPK sticks) overlaid with the query molecule (Green CPK sticks).

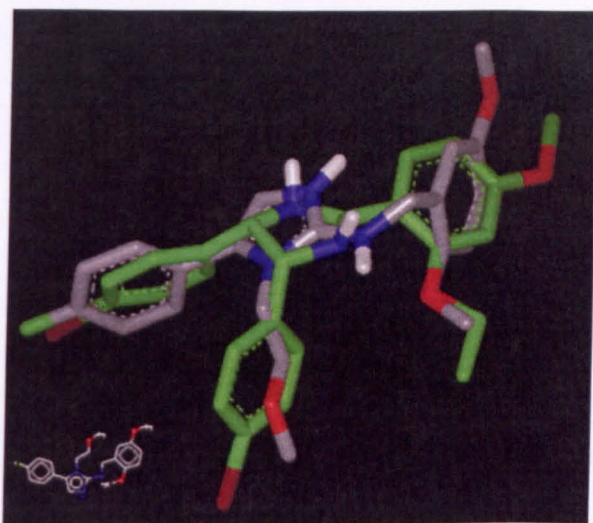


Figure 27 Compounds in cluster 6 typically possessed binding groups that were either to small or flexible or both as shown by this example (Grey CPK sticks) overlaid with the query molecule (Green CPK sticks).

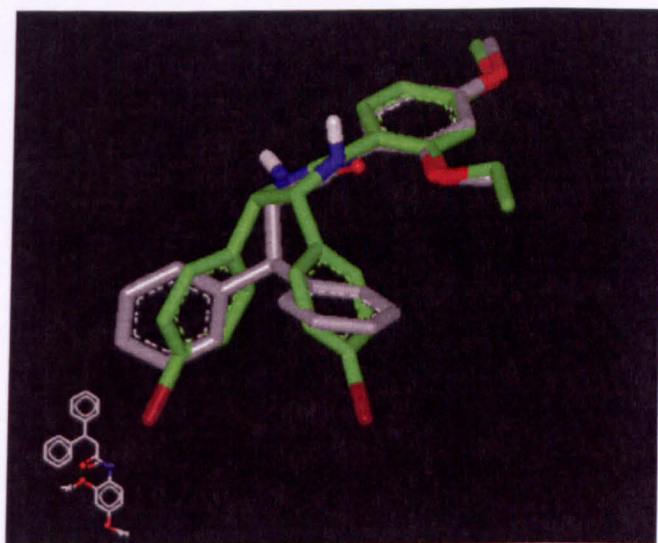


Figure 28 Compound 148, from cluster 8, (Grey CPK sticks) overlaid with the query molecule (Green CPK sticks).ranked 78 over all, and was active in the FP assay.

3.4.5.5 Nutlin query, Cluster 8

Cluster 8 consisted of mainly branched amides. These were smaller and less flexible than the compounds in cluster 3. Some compounds had excellent overlap with Tanimoto coefficients greater than 0.8 (Table 15, entry 8). One of the compounds (148) showed binding activity (Table 18, entry 5) and is shown overlaid with the query (Figure 28).

3.4.5.6 Nutlin query, Cluster 9

Cluster 9 contains both highest ranked and best Tanimoto hits (Table 15, entry 9). It includes imidazoles, some *cis*-2,3,4-substituted imidazolines and imidazolidines very similar to the query. Figure 29 shows two hits from this cluster overlaid with the query.

3.4.5.7 Nutlin query, Cluster 10

Compounds in cluster 10 have three potential binding groups on 2,4,6-substituted 1,2,3,4-tetrahydropyrimidine scaffolds. These compounds overlap well with the query molecule (Figure 30), although the adopted boat conformation with two large groups axially oriented will be energetically unfavourable.

3.4.5.8 Nutlin query, Cluster 12

Compounds in cluster 12 resemble benzodiazepines but have a tricyclic scaffold. These show good overlap with the query and show two possess by which they overlap the query (Figure 31).

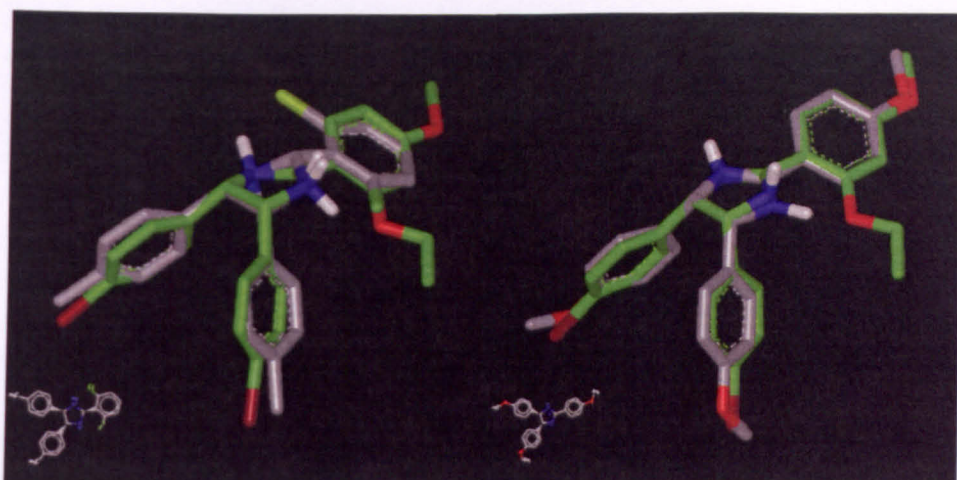


Figure 29 The top ranked hit (left) and the third ranked (right), which has the highest Tanimoto score (Grey CPK sticks) overlaid with the query molecule (Green CPK sticks) were found in cluster 9.

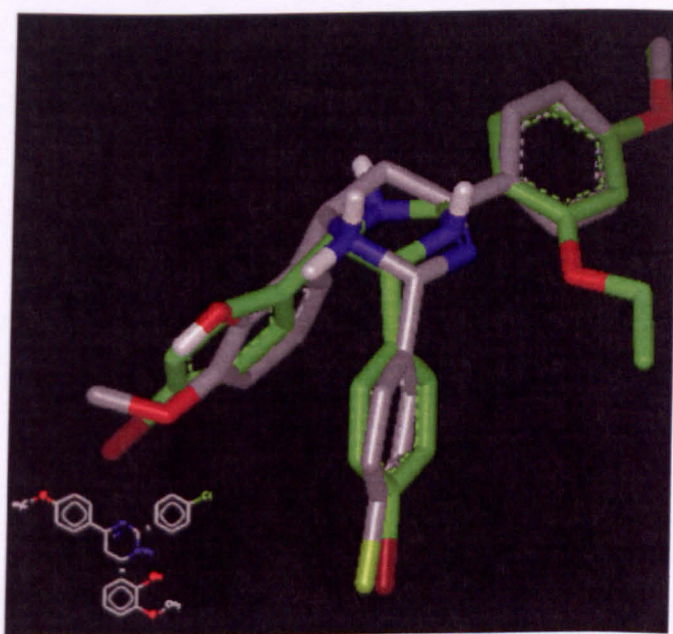


Figure 30 Six membered ring systems like those seen in cluster 10 (Grey CPK sticks) show good potential overlap of the query (Green CPK sticks).

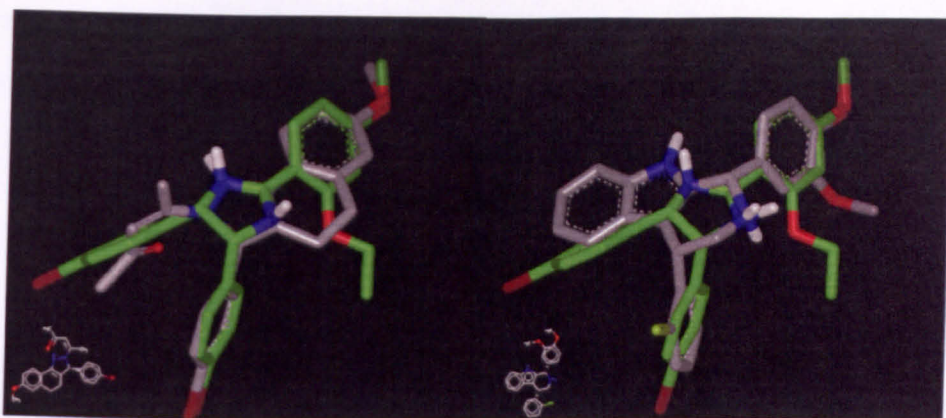


Figure 31 Two hits from cluster 12 (Grey CPK sticks) that have different substitution patterns and adopt different poses when overlaid with the query molecule (Green CPK sticks).

3.4.5.9 Nutlin query, Cluster 13

Compounds in cluster 13 were 3,5-di(furan-2-yl)-2,3,4,5-tetrahydro-6-nitro-2-phenyl-1,2,4-triazines (Table 15, entry 13). Although they possess three potential binding groups and show good overlap with the query they adopt an unfavourable conformation in doing so and bear an unfavourable nitro group. None were selected for testing.

3.4.5.10 Nutlin query, Cluster 15

Cluster 15 contains tri- and tetra-substituted piperidines that overlap the query well and adopt a favourable chair conformation with two of the three large substituents in equatorial orientations.

3.4.5.11 Nutlin query, Cluster 16

Cluster 16 contained whatever compounds remained. It has a variety of compounds most were of little interest and were rejected. However, two were a similar shape to the Nutlin query but based on different heterocyclic scaffolds (Figure 32) and were selected

for testing. One of them (**156**) exhibits activity in the FP binding assay (Table 18, entry 10).

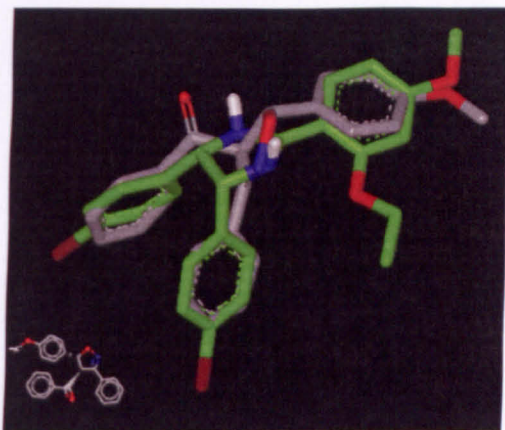
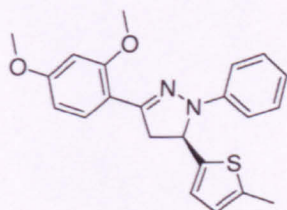


Figure 32 An active compound from cluster 16 (Grey CPK sticks) overlaid with the query molecule (Green CPK sticks).

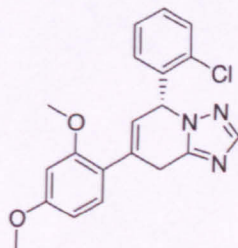
Cluster 1



141

| | |
|--------------|------------|
| Compounds | 120 |
| Tan range | 0.832-0.63 |
| Highest Rank | 6 |
| Lowest Rank | 500 |

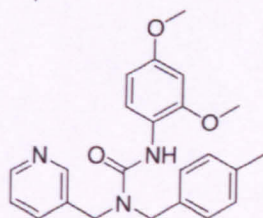
Cluster 2



142

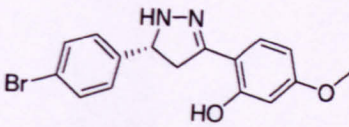
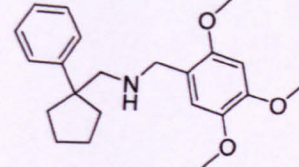
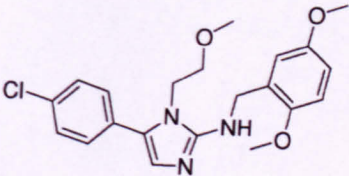
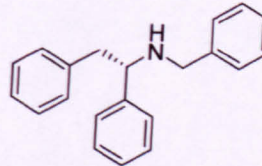
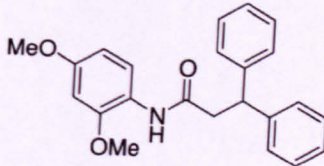
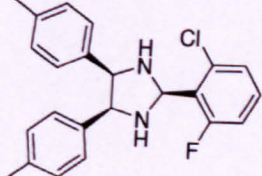
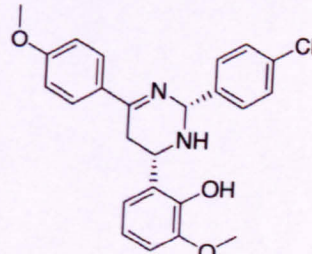
| | |
|--------------|------------|
| Compounds | 47 |
| Tan range | 0.78-0.643 |
| Highest Rank | 33 |
| Lowest Rank | 496 |

Cluster 3



143

| | |
|--------------|-------------|
| Compounds | 20 |
| Tan range | 0.842-0.739 |
| Highest Rank | 21 |
| Lowest Rank | 480 |

| | | | | |
|------------|---|------------|---|---------------------------------|
| Cluster 4 |  | 144 | Compounds Tan range Highest Rank Lowest Rank | 123 0.806-0.604 17 499 |
| Cluster 5 |  | 145 | Compounds Tan range Highest Rank Lowest Rank | 30 0.837-0.692 4 423 |
| Cluster 6 |  | 146 | Compounds Tan range Highest Rank Lowest Rank | 8 0.781-0.702 64 464 |
| Cluster 7 |  | 147 | Compounds Tan range Highest Rank Lowest Rank | 48 0.785-0.617 14 494 |
| Cluster 8 |  | 148 | Compounds Tan range Highest Rank Lowest Rank | 46 0.813-0.685 78 495 |
| Cluster 9 |  | 149 | Compounds Tan range Highest Rank Lowest Rank | 10 0.87-0.626 1 338 |
| Cluster 10 |  | 150 | Compounds Tan range Highest Rank Lowest Rank | 10 0.833-0.609 45 453 |

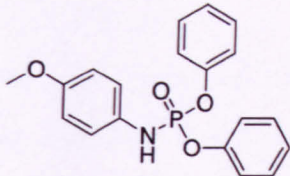
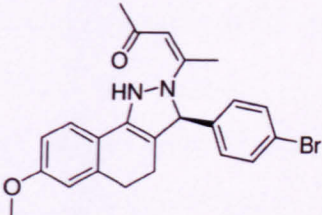
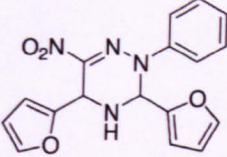
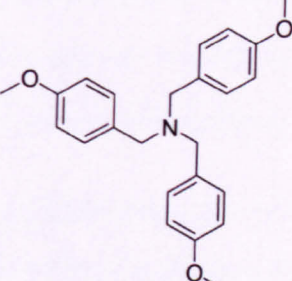
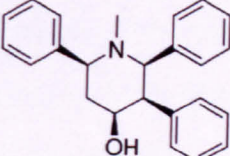
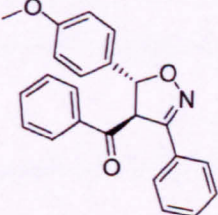
| | | | | |
|------------|---|------------|---|---------------------------------|
| Cluster 11 |  | 151 | Compounds Tan range Highest Rank Lowest Rank | 10 0.806-0.787 206 438 |
| Cluster 12 |  | 152 | Compounds Tan range Highest Rank Lowest Rank | 8 0.772-0.65 295 414 |
| Cluster 13 |  | 153 | Compounds Tan range Highest Rank Lowest Rank | 3 0.649-0.646 28 32 |
| Cluster 14 |  | 154 | Compounds Tan range Highest Rank Lowest Rank | 2 0.75-0.700 167 177 |
| Cluster 15 |  | 155 | Compounds Tan range Highest Rank Lowest Rank | 2 0.682-0.656 173 437 |
| Cluster 16 |  | 156 | Compounds Tan range Highest Rank Lowest Rank | 11 0.816-0.615 173 437 |

Table 15 Representative hits and statistics from each of the 16 clusters found by the Nutlin query.

3.4.5.12 Spiro-oxindole query

The spiro-oxindole query returned hits with an average shape Tanimoto of 0.692, ranging between 0.569-0.799 and comboscore that averaged 1.23 and ranged between 1.194-1.381. The top ranked comboscore hit had a shape Tanimoto of 0.7710 and the highest Tanimoto at 0.799 was shown by the hit ranked 203 overall. The hit compounds have molecular weights between 233.20 and 546.39.

The hit with the highest Tanimoto coefficient scored low overall showing that the Color score was playing a large role in determining these hits. This is not surprising given the number of indole and oxindole based hits that were found which would match aspects of the query chemistry perfectly. This compound has an *N*-methyl group on the indole nitrogen which would make it unable to act as a H-bond donor (Figure 34) showing that minor structural features could drastically alter a compounds overall rank.

3.4.5.13 Spiro-oxindole query, Cluster 1

The largest cluster of compounds for this query are also spiro-oxindoles but with a 4H-pyran as the other ring. There was a considerable variety of substituents. Hit selection focused on compounds with 3 binding groups. Figure 33 shows two of these compounds overlaid with the query. A number of hits from this cluster were selected for testing and two (**179** and **181**) showed binding activity in the FP assay (Table 18, entries 14 and 16).

3.4.5.14 Spiro-oxindole query, Cluster 2

Another large cluster of spiro-oxindoles with a thiazolidine ring were also hits. These compounds only bore two potential binding groups and were not selected for testing. This very uniform group of compounds dominated the top 100 hits.

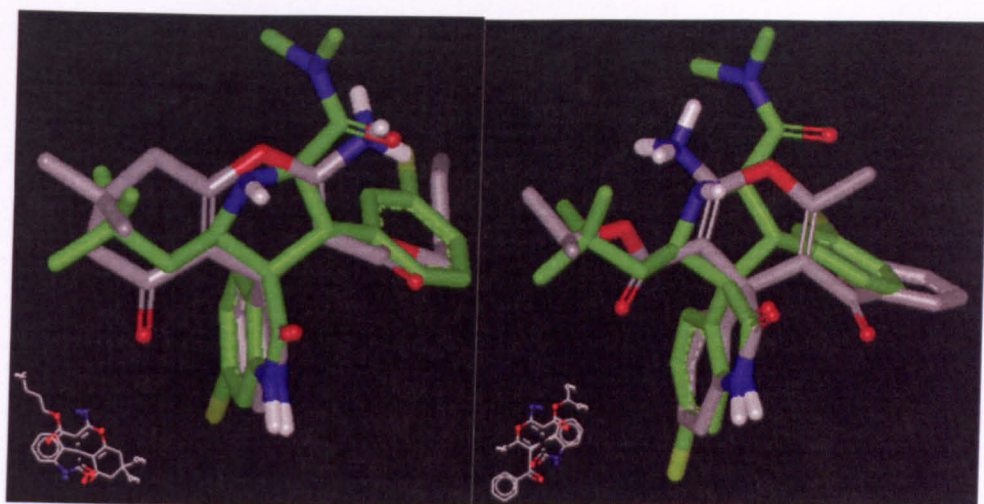


Figure 33 Two examples of compounds from cluster 1 of the spiro-oxindole query screen (Grey CPK sticks) overlaid with the query molecule (Green CPK sticks).

3.4.5.15 Spiro-oxindole query, Cluster 3

These were also spiro-oxindoles. As they only possess two potential binding groups they were not selected for testing (Table 16, entry 3).

3.4.5.16 Spiro-oxindole query, Cluster 4

This cluster consisted of spiro-oxindoles with either pyrazole, isoxazole or pyrazolidinone as the second ring. Many only possess two potential binding groups but some possess three groups and were selected for testing. The molecule with the highest Tanimoto coefficient was found in this cluster however it has an *N*-methyl substituent which would prevent it from mimicking the H-bond interaction made by W²³ of p53 (Figure 34).

3.4.5.17 Spiro-oxindole query, Cluster 5

This cluster did not contain any Spiro cycles. It mainly consisted of 3-substituted indoles attached to five membered nitrogen heterocycles which bore two potential binding groups. A number of these possessed three potential binding groups and showed good overlap with the query (Figure 35).

3.4.5.18 Spiro-oxindole query, Cluster 6

Cluster 6 consisted of tetrazole and triazole pyrimidine based scaffolds with two other potential binding groups bearing some shape similarity to benzodiazepine series and cluster 2 from the Nutlin screen.

3.4.5.19 Spiro-oxindole query, Cluster 7

Cluster 7 is a small group of compounds some of which are similar to Nutlins. Most of these are based on pyrrolidine or imidazoline scaffolds with substituents attached in a 1,2,3-pattern.

3.4.5.20 Spiro-oxindole query, Cluster 8

These compounds do not particularly belong to any group and are linear or possess insufficient groups to completely fill the binding site.

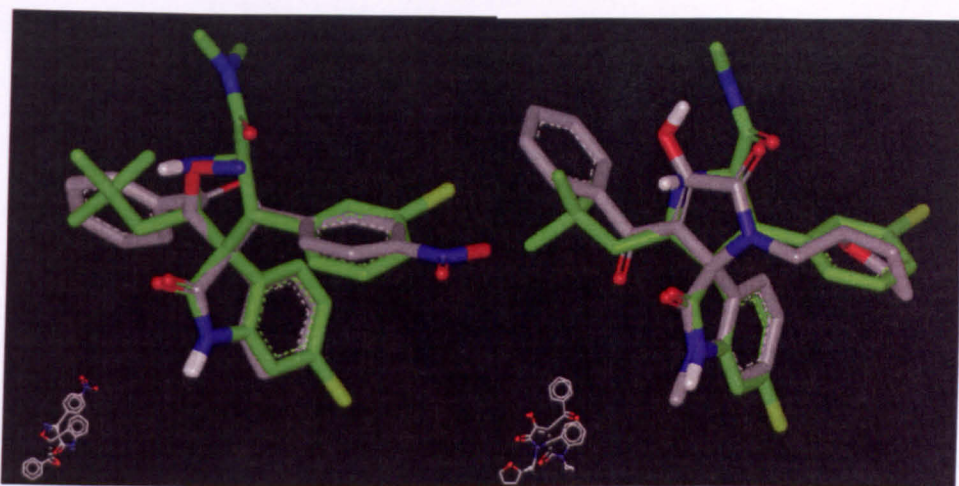


Figure 34 Two hits from cluster 4 (Grey CPK sticks) overlaid with the query molecule (Green CPK sticks). Both show excellent overlap but one contains a nitro substituent (left). The best Tanimoto hit (right) is *N*-methylated and therefore not be able to act as a tryptophan mimic.

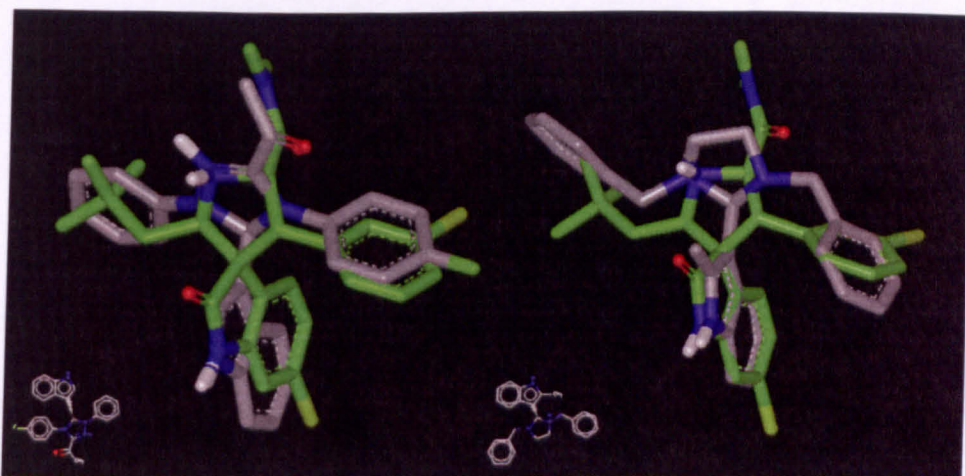


Figure 35 Two non-spirocyclic hits possessing 3 potential binding groups, from cluster 5 (Grey CPK sticks) overlaid with the query molecule (Green CPK sticks).

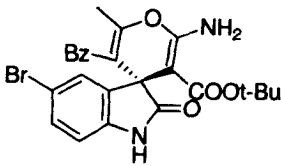
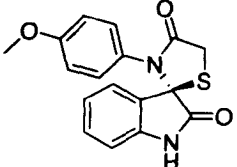
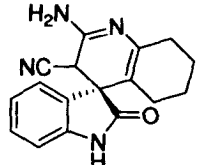
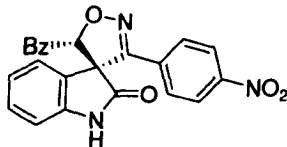
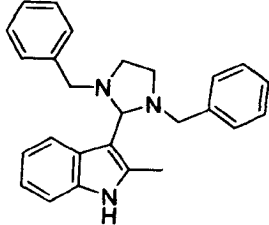
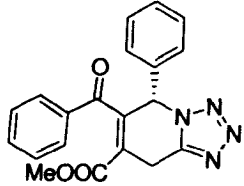
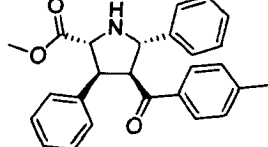
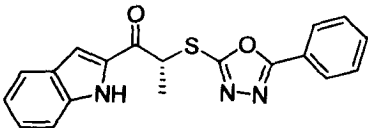
| | | | | |
|-----------|---|------------|---|---------------------------------|
| Cluster 1 |  | 157 | Compounds Tan range Highest Rank Lowest Rank | 221 0.771-0.635 1 500 |
| Cluster 2 |  | 158 | Compounds Tan range Highest Rank Lowest Rank | 91 0.726-0.650 2 137 |
| Cluster 3 |  | 159 | Compounds Tan range Highest Rank Lowest Rank | 58 0.772-0.577 4 496 |
| Cluster 4 |  | 160 | Compounds Tan range Highest Rank Lowest Rank | 123 0.799-0.571 8 499 |
| Cluster 5 |  | 161 | Compounds Tan range Highest Rank Lowest Rank | 34 0.757-0.569 99 494 |
| Cluster 6 |  | 162 | Compounds Tan range Highest Rank Lowest Rank | 17 0.795-0.755 357 497 |
| Cluster 7 |  | 163 | Compounds Tan range Highest Rank Lowest Rank | 5 0.762-0.662 107 478 |
| Cluster 8 |  | 164 | Compounds Tan range Highest Rank Lowest Rank | 28 0.769-0.585 25 483 |

Table 16 The hits from the spiro-oxindole query were grouped into eight clusters.

3.4.5.21 Benzodiazepine query.

The hits obtained using the benzodiazepine query showed shape-Tanimoto coefficients and combo-scores ranging between 0.509-0.791 and 1.1122-1.315 respectively. With the top ranked comboscore hit having a shape Tanimoto of 0.74 and the highest Tanimoto at 0.791 was shown by hit 287. The hit compounds have molecular weights between 266.29 and 546.41.

The benzodiazepine query returned a large number of hits with good chemistry overlap. Many of the hits possess bicyclic-nitrogen heterocycles which show good Color overlap with the benzodiazepine. These included a group of other benzodiazepines and many compounds with bicyclic, nitrogen heterocycles such as quinolines and quinoxilines but little shape similarity to the query (cluster 2). However, some compounds with this type of chemistry that overlap the query well were found (cluster 4). Some of these also show binding activity and are discussed in the following sections.

3.4.5.22 Benzodiazepine query, cluster 1

With 176 compounds, that were relatively close analogues, based on a 1,4-benzodiazepine-2-one scaffold very similar to the query this cluster was very dominant in the hit list. This cluster contained the top ranked hit but hits from it were distributed throughout the hitlist with the lowest being ranked at 476 (Table 17, entry 1). The main difference between the hit compounds and the query was that their phenyl substituent was on the 5 rather than 4-position. This substitution pattern is likely to cause a clash with the protein but as it was the dominant class of compound in the hit list some examples were selected for testing. The top ranking hit, a typical example of the compounds in this cluster, is shown overlaid with the query (Figure 36).

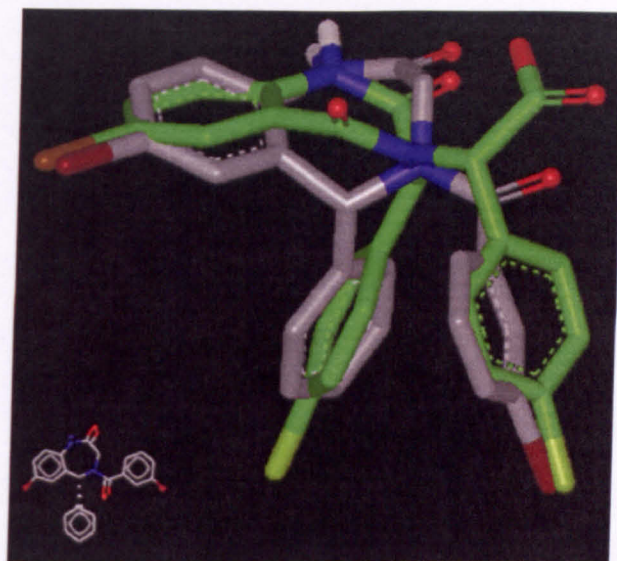


Figure 36 The top hit found using the benzodiazepine query (Grey CPK sticks) overlaid with the query molecule (Green CPK sticks). This was typical of the compounds in this large cluster which dominated this hit list. They exhibit good shape and Color overlap.

3.4.5.23 Benzodiazepine query, cluster 2

With 181 compounds this cluster was also very dominant in the hit list. It is predominantly populated with molecules based on quinoline and quinolinone ring systems that exhibit very good chemistry overlap with the benzodiazepine ring of the query. Apart from this common feature molecules in this cluster are quite varied and less homogeneous than those in cluster 1. Members of this cluster were rejected as they only contain two potential binding groups. The top ranked hit (ranked 11) from this cluster is shown overlaid with the query (Figure 37). It is typical of the molecules in this group. The quinolinone ring system overlaps well with the benzodiazepine of the query but it only contains two potential binding groups and its shape overlap is maximised by a relatively long linker adopting the necessary conformation.

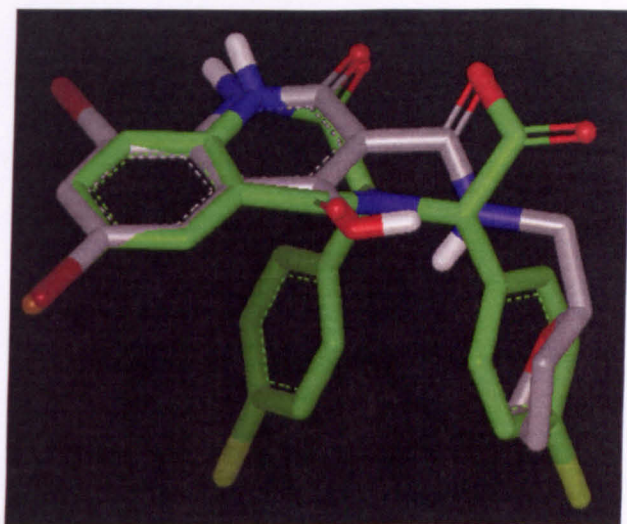


Figure 37 The top ranked compound from cluster 2 (Grey CPK sticks) overlaid with the query molecule (Green CPK sticks). shows good Color overlap but only possesses two potential binding groups.

3.4.5.24 Benzodiazepine query, cluster 3

The compounds in this cluster are predominantly tertiary sulfonamides. Many of these possess quinoline and quinolinone ring systems similar to the compounds in cluster 2. Some possess 3 potential binding groups and are of interest. Testing some of these would also be interesting with respect to Chapter 2. Two of the compounds from this cluster, (**167** and **175**) show binding activity (Table 18, entries 3 and 8). Within this cluster there are examples of hits in which either Color or shape matching are dominant. An example of each is shown in Figure 38. Both compounds are tertiary sulfonamides but overlap the query very differently. The compound on the left possesses a quinazolin-2-one, as seen in the compounds in cluster 2, which is quite similar to the benzodiazepine ring system. As a result it overlaps the query in a manner that matches the similar chemistry at the expense of overall shape overlap and this hit achieves a high colour score. This is clearly not the

optimum shape overlap and it only achieves a low shape Tanimoto score. The similar compound on the right, that does not bear the quinazolin-2-one ring, shows overlap that is clearly dominated by shape matching and its higher Tanimoto coefficient is the main contributor to its overall score. The Color matching in this example is sufficiently strong that the compound on the left, with the lowest Tanimoto score, actually ranks higher overall than the one on the right which has a considerably higher Tanimoto coefficient.

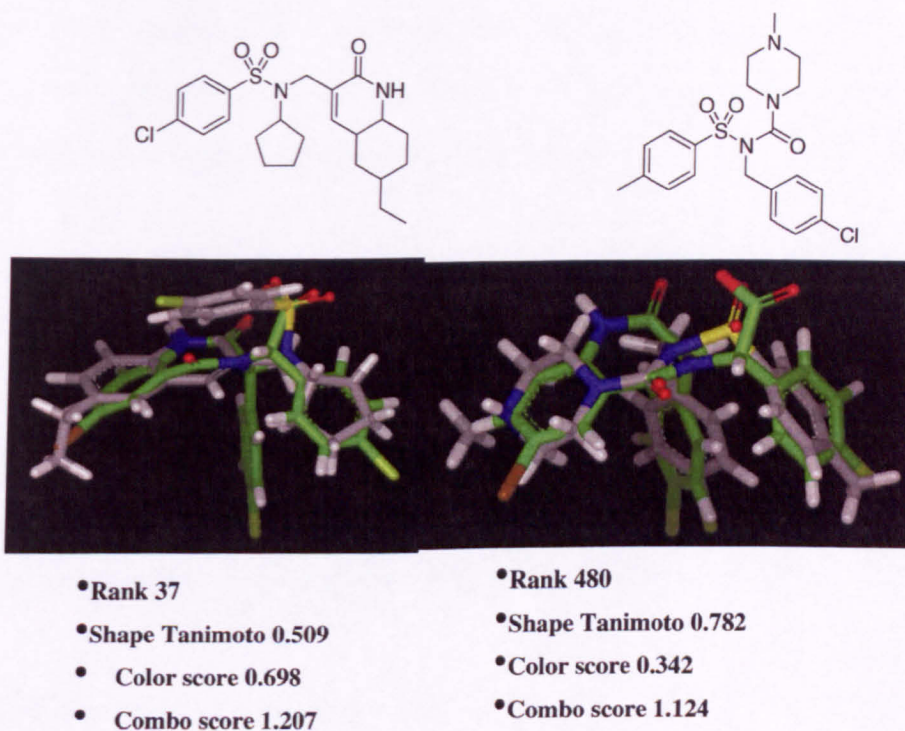


Figure 38 Sulfonamides from cluster 3 are a clear example of dominance of Color score over shape to such an extent that the molecule with the best overlap is the one with the lowest overall rank. (Carbons: grey) overlaid with the query molecule (Carbons: green).

3.4.5.25 Benzodiazepine query, cluster 4

This is the most interesting cluster from this query. It consists of 32 molecules predominantly based on dihydroquinolinone and dihydroquinazolinone ring systems. Like cluster 2, the compounds show good chemistry overlap with the benzodiazepine ring of the query. Unlike cluster 2, a number of compounds possess three potential binding groups and make very good shape and Color overlap with the query. Two such hits (**176** and **168**) show binding activity (Table 18, entries 9 and 12) and a previously described inhibitor, **8**, (Figure 39) was also a hit.¹⁶¹ These compounds show excellent overlap with the query (Figure 40). Furthermore, these hits are small “lead like” compounds that show potential for further investigation and are discussed in Section 3.5.2

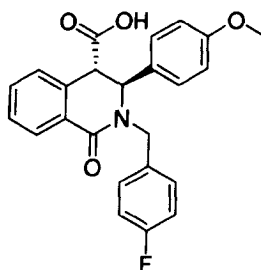


Figure 39 Compound **8** is a previously described inhibitor¹⁶¹ and was a hit in this screen

3.4.5.26 Benzodiazepine query, cluster 5

Compounds in this cluster did not fit into any of the classes discussed above. Most did not show potential as ligands. However some bear three potential binding groups on a rigid scaffold and the imidazoles based compound, **169**, was the most active compound in the FP assay (Table 18, entry 1).

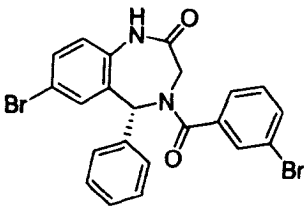
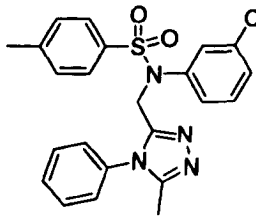
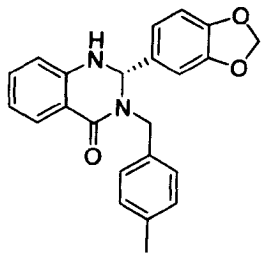
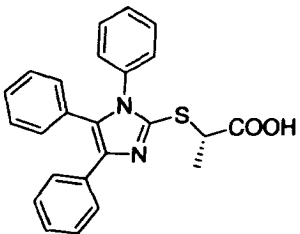
| | | | | |
|-----------|---|-----|--------------|-------------|
| Cluster 1 |  | 165 | Compounds | 176 |
| | | | Tan range | 0.74-0.602 |
| | | | Highest Rank | 1 |
| | | | Lowest Rank | 476 |
| Cluster 2 |  | 166 | Compounds | 181 |
| | | | Tan range | 0.763-0.554 |
| | | | Highest Rank | 11 |
| | | | Lowest Rank | 500 |
| Cluster 3 |  | 167 | Compounds | 74 |
| | | | Tan range | 0.782-0.509 |
| | | | Highest Rank | 37 |
| | | | Lowest Rank | 499 |
| Cluster 4 |  | 168 | Compounds | 32 |
| | | | Tan range | 0.64-0.58 |
| | | | Highest Rank | 7 |
| | | | Lowest Rank | 487 |
| Cluster 5 |  | 169 | Compounds | 37 |
| | | | Tan range | 0.791-0.555 |
| | | | Highest Rank | 8 |
| | | | Lowest Rank | 484 |

Table 17 The hits from the benzodiazepine query were grouped into five clusters.

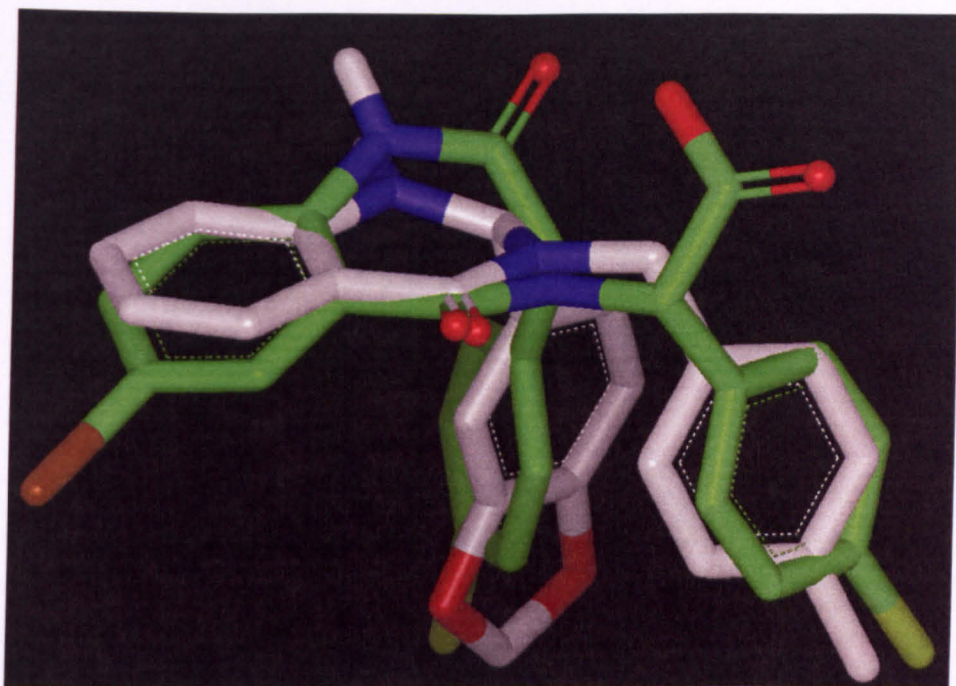
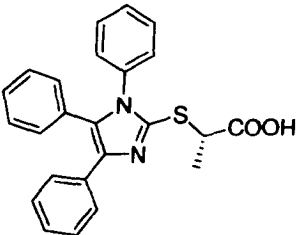
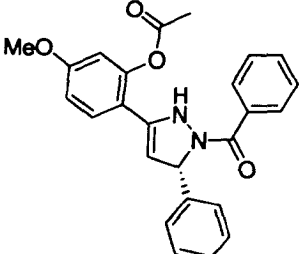
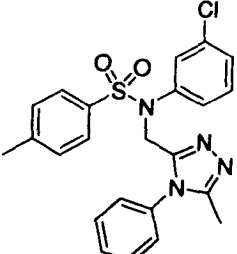
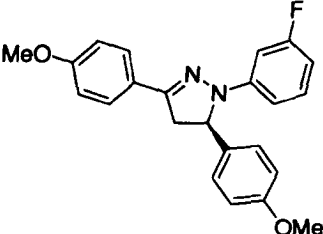
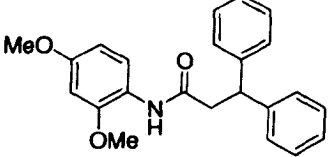
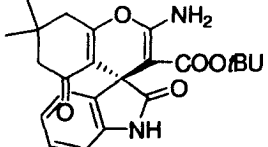
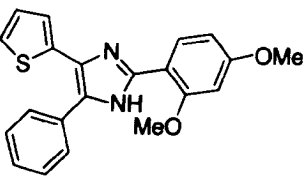
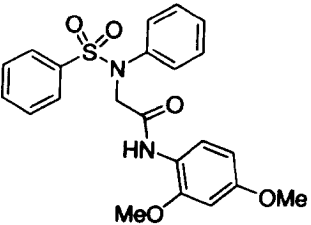
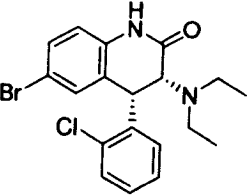
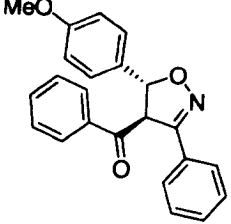
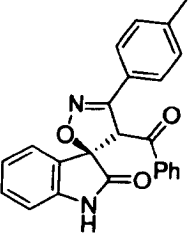
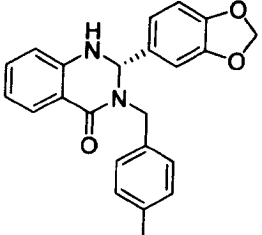


Figure 40 Compound 168 the top ranked hit from cluster 4, (Grey CPK sticks) overlaid with the query molecule (Green CPK sticks).

3.4.6 Screening: binding and cell assays

The 155 purchased compounds were screened at Cyclacel for activity using the FP assay. At the time of the screen the assay was performing with lower sensitivity as discussed in Section 1.11.1. The first round of screening included all compounds and a cut-off point of 50% activity at 500 μ M was set. Using the correction factor of 3.18 this would mean 50% at 157 μ M with the sensitivity of the original assay. Sixteen compounds showed greater than 50% inhibition at 500 μ M. The corrected IC₅₀ values of these compounds were determined. They ranged between 48.22 μ M and 140.42 μ M (Table 18).

| Entry | Structure | Compound | % Inhibition at 500 μ M | IC50 (μ M) | Corrected IC50 (μ M) |
|-------|---|------------|-----------------------------|-----------------|---------------------------|
| 1 |  | 169 | 95.811 | 153.34 | 48.22 |
| 2 |  | 170 | 81.239 | 172.66 | 54.29 |
| 3 |  | 167 | 65.58 | 232.94 | 73.25 |
| 4 |  | 171 | 76.867 | 246.06 | 77.38 |
| 5 |  | 172 | 82.696 | 313.59 | 98.61 |
| 6 |  | 173 | 57.923 | 268.16 | 84.33 |

| | | | | | |
|----|---|------------|--------|--------|--------|
| 7 |  | 174 | 65.938 | 267.80 | 84.21 |
| 8 |  | 175 | 52.095 | 272.01 | 85.54 |
| 9 |  | 176 | 52.095 | 334.40 | 105.16 |
| 10 |  | 156 | 59.058 | 318.20 | 100.06 |
| 11 |  | 177 | 65.938 | 387.09 | 121.73 |
| 12 |  | 168 | 52.095 | 429.39 | 135.03 |

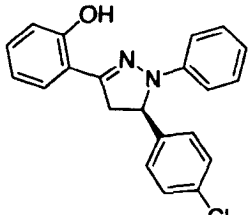
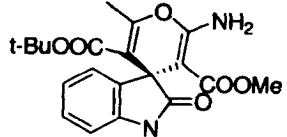
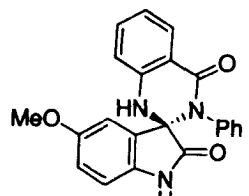
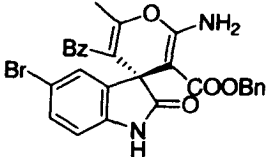
| | | | | | |
|----|---|------------|--------|--------|--------|
| 13 |  | 178 | 55.435 | 373.18 | 117.35 |
| 14 |  | 179 | 61.566 | 379.40 | 119.31 |
| 15 |  | 180 | 61.566 | 446.53 | 140.42 |
| 16 |  | 181 | 52.095 | 436.70 | 137.33 |

Table 18 Binding activity of the active hit compounds.

3.4.7 Functional assays

In order to determine if the hit compounds could induce a p53 response in cells they were assayed using a p53 Luciferase reporter gene assay at Cyclacel. Nutlin-3 was used as a control and showed 9-fold induction of p53 at 10 μ M. This value is very much in agreement with what had been shown previously and demonstrated that the assay was functioning normally. Very little induction was observed for the test compounds. However, three compounds, **156**, **168** and **180**, showed some p53 induction (Figure 41) **156** Showed 2.93 fold induction at 6.58 μ M, **168** showed 2.24 fold at 9.88 μ M and **180**

showed 5.75 fold at 8.89 μ M. **156** and **180** show some indication of dose dependency up to these concentrations.

Nutlin-3 is a highly potent, validated MDM2 inhibitor and the test compounds have already been shown to have a much lower affinity than it for the target. However, that any p53 induction is observed with such low affinity inhibitors is encouraging. If it is possible to prepare any analogues of these compounds that exhibit higher affinity and show increased p53 induction in this assay it will be strong evidence that they are indeed genuine MDM2-p53 PPI inhibitors.

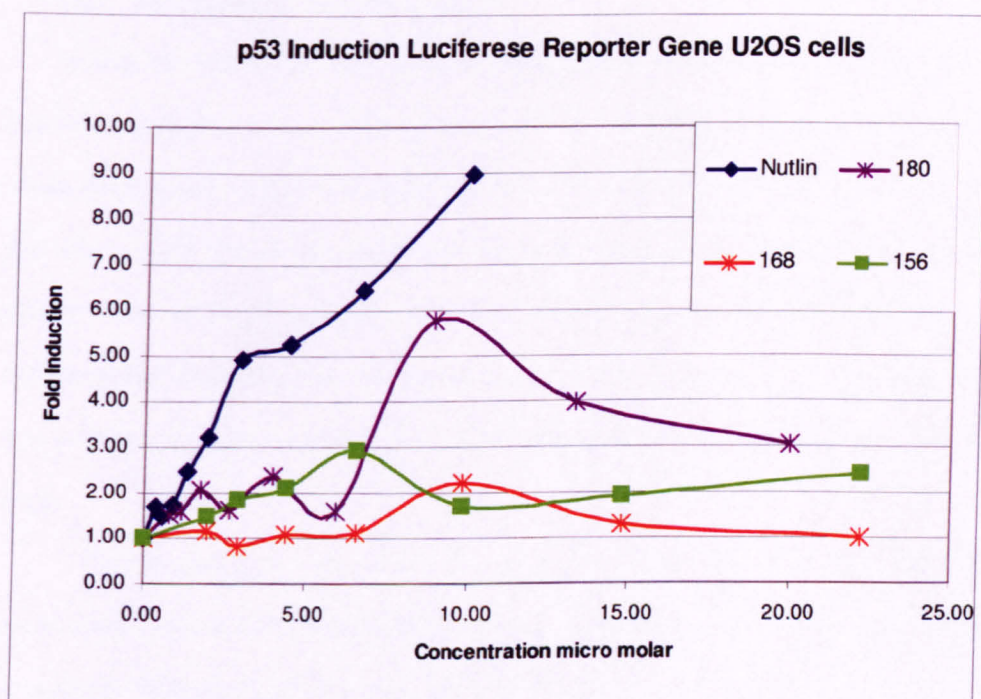


Figure 41 Three of the sixteen hits that show binding activity also show low levels of p53 induction.

3.5 Conclusions and future work

Out of 155 screened compounds 16 that bind the target with moderate to low μM affinity were discovered. These are representative of 9 unique chemo types. Three of these show low to moderate p53 induction in a Luciferase reporter gene assay. Although distinct from them, the hits all bear structural similarities to the known inhibitors that were used as queries to find them. However, they are clearly un-optimised and a number of them are quite small and “lead-like” which leaves considerable scope for further development and are candidates for further hit to lead investigation.

3.5.1 Evaluation of the ROCS screen

Having selected 155 compounds for screening that produced a number of low activity hits that are suitable for drug development and a known inhibitor compound **8**, the ROCS shape based screen can be considered a success. Each of the queries produced some hits that were similar both to themselves and the other queries. The compounds that showed activity were sufficiently different to the known chemo types and ROCS demonstrates a definite ability to scaffold hop. However, having seen how it performs on a large database, it is possible to suggest some ways in which improvements to future screens could be made.

Combo scoring does give better quality hits than shape alone. However there were times when Color scoring clearly dominated the hit selection. This led to high ranking compounds with low shape Tanimoto coefficients and was probably accountable for the domination of the hitlists of the benzodiazepines and spiro-oxindoles by only a few classes of very similar molecules. The example from cluster 3 (section 3.4.5.24) of the benzodiazepine hitlist is a good example of a case where Color score dominated over the

shape score in hit selection (Figure 38). For a hydrophobic target such as MDM2 where shape complementarity is important in determining affinity, shape would need to be prioritised over Color. This could be done by specifying a minimum shape Tanimoto requirement of 0.7 or 0.75 so all compounds would have to have a better measure of shape similarity to be considered as hits.

Another observation was that a considerable number of linear and flexible hits were generated and ultimately discarded during the visual inspection. While some of these were a function of Color-score dominance and would be eliminated by setting a minimum Tanimoto requirement, others may have resulted from the lenient approach to database preparation. Finding rigid molecules that are the correct shape is preferable to finding flexible molecules that may adopt the correct shape. Flexible molecules could be removed by using tighter filter parameters with respect to number of allowed rotatable bonds and reducing the energy window during conformer generation from 8 to 5 kcal mol⁻¹ which would take higher energy conformers out of the database so ROCS would not be able to consider them.

The Zinc database proved to be a very useful tool for this screening campaign. It is often the case that screening libraries that originate from medicinal chemistry campaigns and combinatorial synthesis contain large numbers of very similar compounds. This reduces the diversity of chemical space they represent. This was evident as large clusters of very similar compounds dominated some of the hit lists in this screen. Reducing the size of large clusters before screening or performing subsequent rounds of screening in which clusters that dominate the hitlists have been removed could potentially allow more of chemical space to be represented. The Zinc database has grown considerably since this

screen was performed. The all purchasable dataset is now in excess of 13,500,000 compounds over 8,500,000 of which are unique and available only from a single vendor. As the database grows it will represent more diverse classes of compounds. Performing a similar screen on this larger database using the tighter parameters, outlined above, to reduce the numbers of hits that are either too flexible or do not have sufficient shape similarity to be deemed useful and taking steps to deal with dominant clusters may be a very attractive prospect for finding new leads.

3.5.2 Developing the hits

In order to determine if these are genuine MDM2 inhibitors and if they can be developed further it will be necessary to test more analogues to determine if activity can be improved or any SAR is exhibited. How this might be achieved for the particularly leadlike compound **168** is discussed in the following section.

3.5.2.1 Investigation of 168

Compound **168** was identified in the recent shape based virtual screening using the Johnson and Johnson Benzodiazepine core structure as a query. Although not the most active hit in the FP assay it showed some p53 induction and is structurally very similar to the recently discovered inhibitor, **8**.¹⁶¹ making it very attractive for further development. Furthermore the core structure of this compound is extremely "lead-like" and a range of desirable analogues are synthetically accessible. This section is an overview how this compound could be investigated further as an MDM2 inhibitor.

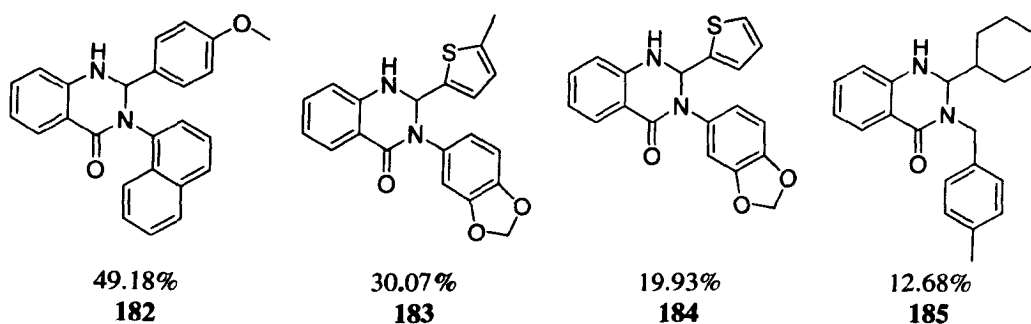


Figure 42 Other analogues of **168** show low binding activity (% inhibition at 500 μ M).

Four similar compounds to **168** were also purchased and tested in the in the initial screen (Figure 42) Only the IC₅₀ of **168** was determined. However one of the other analogues, **182**, was only just outside the threshold for selection for IC₅₀ determination, showing 49.18% inhibition at 500 μ M as opposed to 52.1% shown by **168**. Given the issues with the binding assay this compound may need to be looked at in the SAR study. These compounds also become progressively less active as their substituents become smaller which suggests that the smaller analogues are making less contact with the binding site. Although little more can be gained from this information it does provides some evidence that varying substituent size affects activity as expected.

Variation of the ring substituents R, R' and R'' will allow the overall size and shape of the molecule to be optimised to better fill all three sub-pockets of the binding site. This would allow known SAR features to be investigated. The chemistry assessment below indicates that it should be possible to prepare a number of analogues to facilitate such an investigation (Figure 43). It would be very desirable to investigate substituents on the fused benzene ring. The core molecule is too small to fill the MDM2 site without substitution here. This is clearly evident when overlaid with the benzodiazepine core

structure (Figure 37). Given the emerging importance of MDMX as a target, that it is known to have a similar but smaller binding site than MDM2 and that MDM2 inhibitors show considerably less affinity for it,^{171, 187} small "lead-like" compounds, like **168**, could also be an attractive starting point for the investigation of the requirements of MDMX inhibitors. It would be desirable to simultaneously investigate these compounds with respect to both proteins.

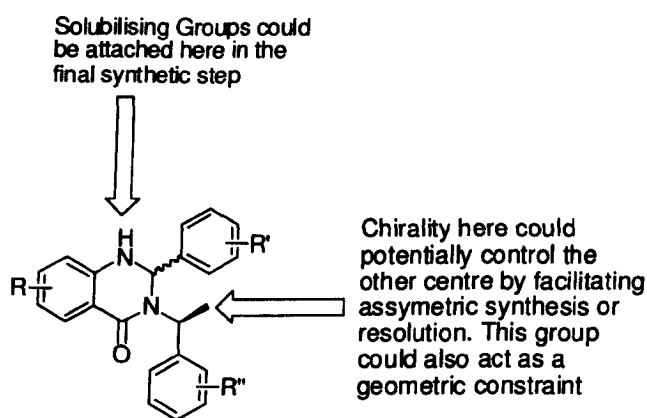


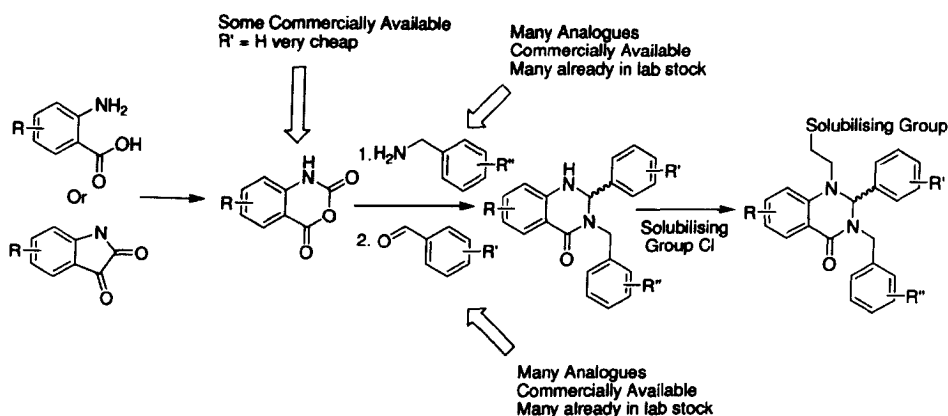
Figure 43 Potential sites for development of these compounds.

The three well developed classes of inhibitors all have solubilising groups attached. From the published SAR of the spiro-oxindoles it is clear that appropriately placed solubilising groups can make additional binding interactions and enhance affinity and should therefore be considered as part of the overall pharmacophore and not just an appendage to improve properties. However, it is convenient to investigate this after the classical pharmacophore has been optimised. There is a free amino group in the ring which would facilitate attachment of pendant solubilising groups. Furthermore, the position of this attachment point coincides with that of the benzodiazepine (see overlay, Figure 37)

which is precedence that it may be well tolerated. This is a positive consequence of using the Color-score chemistry matching in ROCS. The chemistry assessment below shows that this group can be added in the last synthetic step greatly facilitating its investigation.

Compound **168** has one chiral centre. It was tested as the racemate, but it can be expected that only one enantiomer will be responsible for the bulk of the activity and each enantiomer would need to be investigated. The easiest way to do this would be to use α -methyl benzyl amines to prepare diastereomeric compounds which could easily be separated. This substituent could also act as a geometric constraint that helps the compound favour the binding conformation, hence reducing the entropy penalty upon binding. This has been shown to be the case both for the benzodiazepines^{139, 140} and this type of compound for which there is literature precedent for inducing stereochemistry and constraining geometry.²²⁶ If this is successful the methyl group could be replaced and derivatives of phenyl glycine used to (a) mimic the carboxylate group of the benzodiazepines or (b) provide an alternative attachment point for solubilising groups that are chemically and spatially more similar to the activity enhancing ones seen on the spiro-oxindoles.¹³³

It will only be possible to investigate these compounds if a number of analogues can be obtained. While it is possible to purchase analogues with the desired substitution on the benzyl and phenyl groups, suitable analogues substituted on the fused ring are not available. Scheme 9 shows a short route that allows variation in the diversity at all of the main pharmacophore and solubilising groups to be easily investigated.²²⁶ By using readily available chiral benzyl amines or amino acids it should be possible to investigate the role of stereochemistry in the SAR.



Scheme 9 A synthetic route that would give access to a range of analogues.²²⁶

3.5.3 Investigating the other hits

The other hit compounds could be further investigated by testing more analogues of them. The analogues chosen would be based on the known SAR of the literature inhibitors and would mainly be those with halide substituents at various positions of their aryl groups. It would be particularly interesting to investigate **156** and **180** which showed some p53 induction in the Luciferase reporter gene assay and **169**, the most active compound in the FP binding assay. Although **169** does not show any p53 induction it does bear an acid group which would reduce its cell permeability. It would therefore be desirable to test analogues in which the acid is blocked or absent.

4. Scaffold Hopping

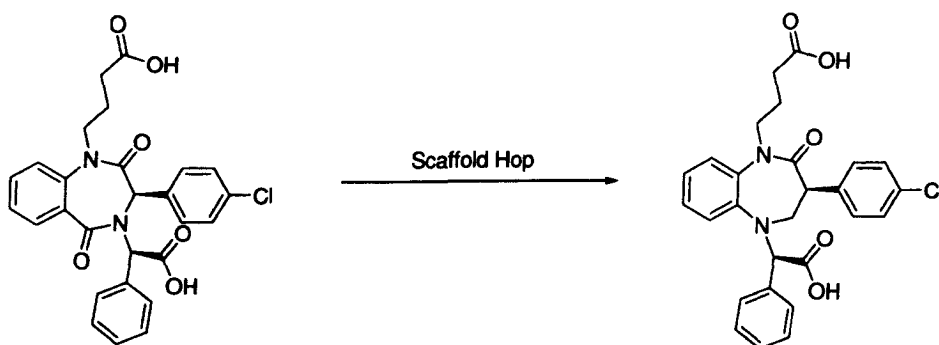
4.1 Introduction

Scaffold hopping is a very important aspect of drug discovery. The goal is generally to find new chemo types of the same pharmacophore. The reasons for this are manifold and may include trying to improve the inherent physico-chemical properties, to move away from toxic or reactive species or from a competitors IP space. There is usually more than one type of ligand for any given target. This is clearly seen in the case of MDM2, where over 20 diverse chemo types have now been described.^{125, 134} Of those for which there is structural or computational evidence that supports them binding in a mode compatible with the accepted pharmacophore model, they utilise different scaffolds to present their binding groups to the sub-pockets of the binding site.^{122, 135} Although, proven as a concept in mouse models with the three most potent inhibitors, the MDM2-p53 PPI is still to be validated in the clinic. Whether or not this can be done may be dependent on the pharmac properties of the inhibitors used, and whether they have any undesirable off-target activity. Therefore, finding and investigating novel classes of inhibitors remains an important area of research.

Scaffold hopping usually involves virtual screening or in-silico de novo design or fragment based drug discovery^{206, 221, 227} which was the subject of Chapter 3. In this chapter, initial investigations on two scaffolds are initiated. One is based on a variation of the known benzodiazepine inhibitors the second is conceptually novel but has sufficient basis to warrant investigation.

4.2 1,5-Benzodiazepine-2-ones

Based on the successful development of the 1,4-benzodiazepine-2,5-diones by Johnson and Johnson and because our collaborators at Cyclacel Ltd were working on a similar chemo type for another target it was suggested that a series of 1,5-benzodiazepine-2-ones be investigated as MDM2 inhibitors (Scheme 10). These compounds were relatively free of IP particularly with respect to use as cancer therapeutics.



Scheme 10 The proposed scaffold hop from the well established 1,4-benzodiazepine-2,5-dione to a novel 1,5-benzodiazepine-2-one scaffold

4.2.1 Computational Docking

This scaffold hop is moving one of the potential binding groups from the 4- to the 5-position of the diazepine ring. In an inhibitor like this where the overall shape of the molecule is likely to be critical to its binding it would be expected that such a change would cause the binding groups to clash with the protein rather than fill its sub pockets and hence be detrimental to activity.

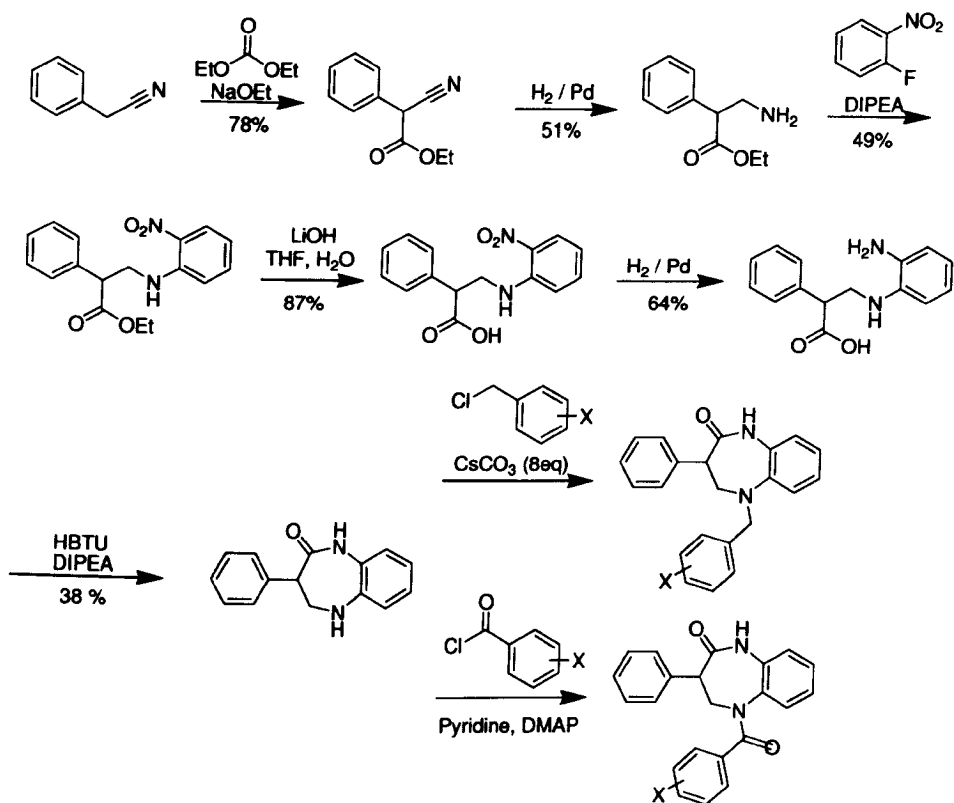
The proposed structure was docked into the binding site of the X-ray co-crystal structure of MDM2 with the p53-peptide (1YCR)¹ using FRED. The 21 top poses, as ranked by Openeye's scoring function, Chemgauss 3,²¹² were examined. The ligand does not occupy the binding site in a shape complimentary manner or even fill the W²³ sub pocket in any of the poses. However it was decided that a small number of simple analogues should be prepared.

4.2.2 Synthesis and testing

Extensive data detailing the medicinal chemistry and SAR development of the 1,4-benzodiazapien-2,5-diones has been published.^{136-140, 154} In this work it has been shown that only one of the two oxo groups on the benzodiazepine ring is required to maintain activity and that the carboxylic acid and solubilising groups can also be removed without total loss of activity.^{139, 140} On this basis some analogues of the core structures, not bearing these features, were prepared (Table 19).

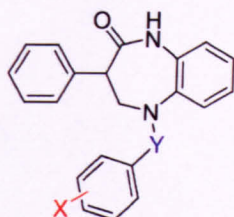
The synthetic route used (Scheme 11) was based on that of Lee et al who prepared a number of similar compounds using solid supported synthesis (SPS) methodology.²²⁸ Direct implementation of the SPS synthesis was not suitable for these compounds as it required an amide group at the 8-position for attachment to the resin which would still be present on the molecule after cleavage. This route was particularly suitable for examining various benzyl/benzoyl substituents where diversity here could be varied in the last step using a common core. Because of this, analogues were based on variations of this group (Table 19). Exploring substituents on other parts of the molecule would however, require that the diversity was introduced earlier such that each analogue would involve multistep synthesis.

The synthesis shown in Scheme 11 worked well. The β -amino ester, ethyl 3-amino-2-phenylpropanoate, was prepared by Claisen condensation between phenylacetonitrile and diethylcarbonate followed by hydrogenation of the nitrile. The β -amino ester was coupled with 2-fluoronitrobenzene by nucleophilic aromatic substitution. It was found that a 3 fold excess of 2-fluoronitrobenzene and DIPEA were required to drive product formation in the third step. Performing the fourth and fifth steps in the order shown in Scheme 11 greatly facilitated isolation of the product. If the nitro group was reduced prior to ester hydrolysis, as was the case in the SPS on which this synthesis was based,²²⁸ the solution phase work up was tedious with emulsion formation and partitioning of the product between both aqueous and organic phases, problems not associated with SPS. However hydrolysis of the ester prior to reduction of the nitro group allowed facile isolation of the product. When the cyclisation step was performed with the peptide coupling reagent, HBTU, the reaction proceeded quicker and products were easier to isolate than when using carbodiimide chemistry. A one-pot reduction-cyclisation using zinc or iron in aqueous acid was unsuccessful although some reduction of the nitro group occurred no cyclisation was observed. Had this been successful it would have merged the three previous steps into one and allowed formation of core cyclised product directly from the nitro ester. Formation of a seven membered ring was probably not sufficient driving force for the cyclisation. The final step of the synthesis worked well using stoichiometric benzyl chloride and excess cesium carbonate base. The use of benzyl bromide leads to formation of the bis-benzyl quaternary ammonium salt. Benzoylation with the necessary benzoylchloride gave the required product but required catalytic DMAP to be added for the reaction to proceed.



Scheme 11 Synthesis of 1,5-benzodiazepine-2-ones.

When tested in the FP assay, all of these compounds were found to be inactive and showed no activity at the highest concentration. This result demonstrated that it was not possible to change the overall shape of the molecule in this way. Had any appreciable activity been shown analogues examining substituents on the phenyl and fused benzene ring would have been investigated.



| Entry | Compound | Y | X | Yield | FPIC ₅₀ (μM) |
|-------|------------|--------------------|--------------|-------|-------------------------|
| 1 | 186 | -CH ₂ - | H | 69% | >500 |
| 2 | 187 | -CH ₂ - | <i>o</i> -Cl | 48% | >500 |
| 3 | 188 | -CH ₂ - | <i>m</i> -Cl | 54% | >500 |
| 4 | 189 | -CH ₂ - | <i>p</i> -Cl | 63% | >500 |
| 5 | 190 | C=O | H | 58% | >500 |
| 6 | 191 | C=O | <i>o</i> -Cl | 48% | >500 |
| 7 | 192 | C=O | <i>m</i> -Cl | 43% | >500 |
| 8 | 193 | C=O | <i>p</i> -Cl | 56% | >500 |

Table 19 All of this series were inactive using the less sensitive assay conditions so much so that it was not possible to apply the correction factor previously used. Yields are of isolated material after purification.

4.2.3 Conclusion

If inhibitors based on a 1,5-benzodiazepine-2-one scaffold were to be developed they would be required to carry their substituents at the same positions as the known active 1,4-benzodiazepine-2,5-diones (Figure 44). This initially appeared to be an attractive proposition that would represent a novel class of inhibitor, based on a privileged structure scaffold,²²⁹ with essentially identical shape to one of the best known inhibitors. Moreover carrying substituents at these positions, 1,5-benzodiazepine-2-diones such as **194**, are almost totally free of any IP. It was therefore, decided to do some preliminary investigations into preparing similar compounds.

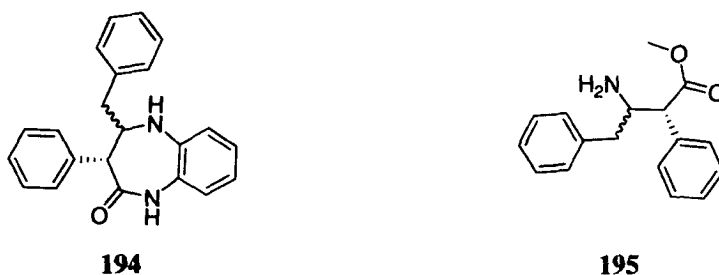


Figure 44 1,5-benzodiazepine-2-diones, **194**, with the same substitution pattern as the known active 1,4-benzodiazepine-2,5-diones would be more likely to be active. α,β -Substituted- β -amino esters, **195**, are the key intermediate required for their preparation.

If analogues of **194** were to be prepared using a similar strategy to that in Scheme 11 the key intermediates would be α,β -substituted- β -amino esters like **195** (Figure 44). It quickly became apparent that these were not subject to IP for a reason. Synthesis of this intermediate would not be as straightforward as it first appeared. There was no literature precedent for the preparation of α,β -substituted- β -amino esters with such large substituents at both α and β positions. Other obstacles to the investigation of these compounds were that all diversity would need to be added at the start of the synthesis so several steps would be required to prepare each analogue and not all of the materials were readily available to investigate the range of analogues required for a comprehensive SAR study. The idea of investigating these compounds was abandoned in favour of a simpler, more drug like and completely novel scaffold as described in the following section.

1,3-Dihydrobenzimidazol-2-one based inhibitors

4.2.4 Background

It is well accepted that drug-like chemical space is limited to molecules with a certain acceptable range of properties.^{223, 224} Privileged structures are molecular scaffolds capable of interacting with a variety of cellular targets.²²⁹ These same structures are repeatedly seen in various bioactive compounds and are therefore excellent starting points from which to initiate drug discovery programs. A number of nitrogen heterocycles are considered privileged structures and occur in a wide spectrum biologically active compounds.

At a presentation by Lipinski²³⁰ and in a recent paper by Ertl,²³¹ that the occurrence of rings in bioactive compounds is concentrated to discreet clusters, based on these privileged structures, was discussed. One such privileged ring system, 1,3-dihydrobenzimidazol-2-one, **196** **197**, (Figure 45). It occurs in many important pharmaceutical compounds. Examples shown in Figure 46 include the H1 receptor antagonist, Oxatomide, **198**,²³² the anti dopaminergic, Domperidone sold as Motilium, **199**,²³³ Filbanserin, the 5-HT1A and 5-HT2A receptor agonist, **200**,²³⁴ the ORL-1 receptor antagonist, J-113,397, **201**,²³⁵ the non-nucleoside HIV inhibitor, **202**,²³⁶ the progesterone receptor antagonist **203**,²³⁷ the p38 MAP kinase inhibitor, **204**,²³⁸ and BIMU8, the 5-HT-4 receptor agonist, **205**.²³⁹

The 1,3-dihydrobenzimidazol-2-one ring system, **196**, could conceivably act as a potential tryptophan mimic and be a good starting point from which to design novel MDM2 inhibitors with the general structure of **197**. Branching at the 3-position, using a minimalistic scaffold (a single sp³ carbon) to project groups into the F¹⁹ and L²⁶ sub-pockets would result in molecules possessing few, if any, superfluous atoms and

potentially be very ligand-efficient,²⁴⁰ which would contribute to their inherent “drug-likeness”.

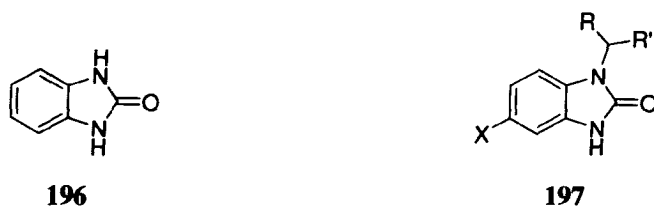


Figure 45 The privileged structure Dihydrobenzimidazol-2-one, 196, could potentially mimic the W²³ residue of p53 and be the basis of potential ligands with the general structure of 197. X: H, Cl or Br; R, R’’: alkyl or aryl.

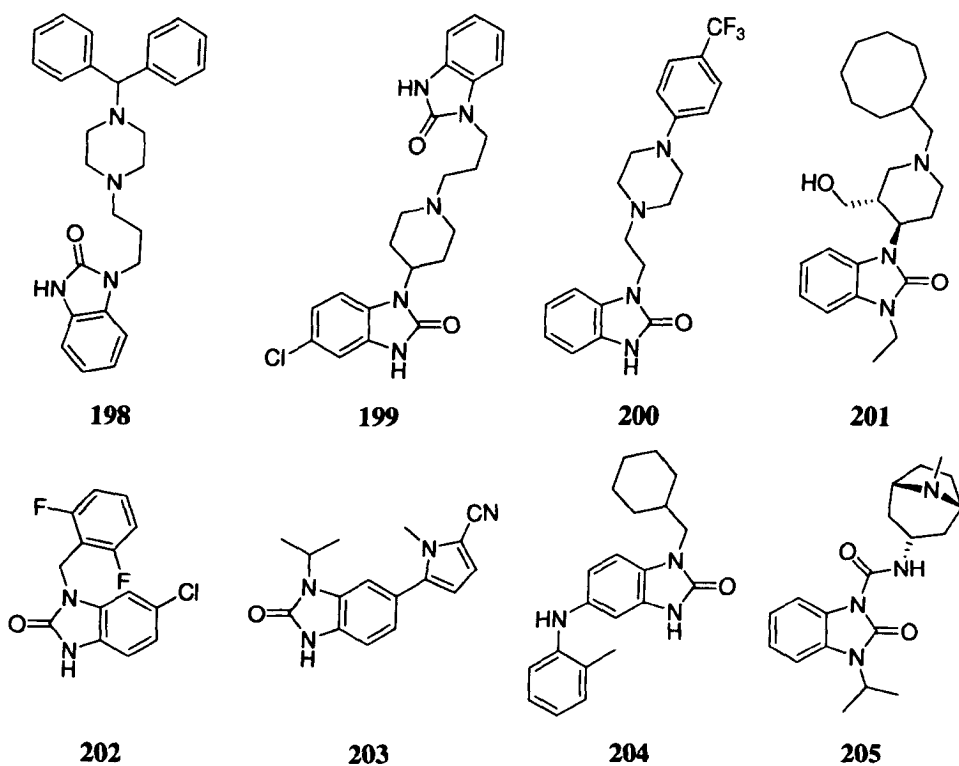


Figure 46 The 1,3-dihydrobenzimidazol-2-one ring system is found in many important pharmaceutical compounds.

There is precedent for 1,3-dihydrobenzimidazol-2-one based inhibitors within the context of what is already known about p-53-MDM2 PPI inhibitors. The 1,3-dihydrobenzimidazol-2-one is very similar to the oxindole ring which is the basis of the most potent spiro-oxindole inhibitors such as MI-291^{132, 141} and a number of inhibitors such as **206** in the patent literature (Figure 47).²⁴¹ The indole based inhibitor, **6**, recently reported by Wang et al,¹⁴³ with the same branching as proposed here that shows low μM affinity and as of yet is totally unoptimised (Figure 47). Probably most convincing was a report, in which the W²³ indole of the p53 peptide is replaced with a 1,3-dihydrobenzimidazol-2-one ring with very little loss of affinity for MDM2.²⁴²

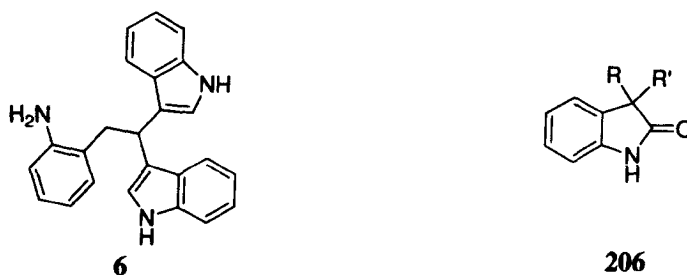


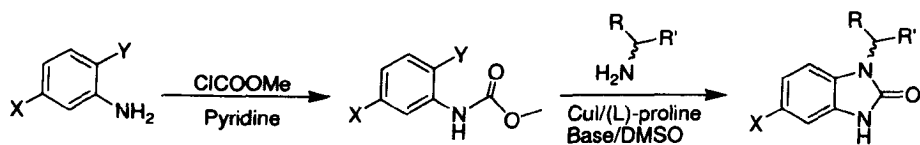
Figure 47 Known inhibitors provide precedent for various aspects of the proposed investigation of 1,3-dihydrobenzimidazol-2-one as the basis for MDM2-p53 PPI inhibitors.^{143,242}

4.2.5 Ligand design and synthesis.

A recent report described a one-pot synthesis of some 3-substituted 1,3-dihydrobenzimidazol-2-ones (Scheme 12).²⁴³ It was decided to use this synthesis as it facilitated varying the molecule in the final step and suitable 2-haloanilines were available from which both the unsubstituted and the all important 6-Cl-substituted analogues could be prepared. Observation of SAR at the 6-position, as observed for the

optimised peptides¹³¹ and spirooxindoles,^{132, 141} would be very indicative of these molecules binding in the predicted manner. The other starting materials that would be required were α -branched primary amines possessing the other two binding groups. The limited availability of amines of this type played a role in deciding what initial analogues would be prepared. Most of the desired amines were not readily available so it was decided to base the analogues on amino acids.

The *L*-enantiomers of tryptophan, phenylalanine and leucine were selected for the first analogues not because of their relationship to this binding site but more so because they would simultaneously represent a small medium and large and aliphatic, aromatic and heteroaromatic binding groups (Table 20).



Scheme 12 X: H, Cl; R, R'': alkyl, aryl

The amino acids were converted to their corresponding *N,N*-dimethyl and pyrrolidyl amides. Amides were chosen as they are the most stable carboxylic acid derivatives and could be modified to vary the size of the third binding group. Also their carbonyl group would reduce the number of rotatable bonds increasing the overall rigidity of these molecules. The *N*-substituents chosen were selected as they are of a similar size to groups used in other inhibitors.

4.2.6 Physico property prediction

Given that this series of molecules were being designed around a privileged structure, it was decided to monitor their pharmaco properties from the outset using the OSIRIS property explorer by Actelion Pharmaceuticals Ltd.²⁴⁴ This is an online property prediction program, available at the Organic Chemistry Portal website.²⁴⁵ For a given structure, this program measures molecular weight and predicts properties associated with drug likeness namely the partition coefficient (cLogP) and aqueous solubility (LogS).²²³ Figure 48 shows how these properties are distributed among commercial drug compounds. The molecular weight, cLogP and LogS values determined for the test compounds (Table 20) are all values shown by the majority of commercial drug compounds.

Drug-likeness, a measure of similarity between a given molecule and commercial drug compounds on the basis of it containing substructure fragments found in 3,300 traded drugs, is also determined. A positive drug-likeness score is indicative that a molecule contains fragments frequently found in commercial drug compounds. With values ranging from 6.09 to 7.48 the compounds in this study are predominantly composed from such fragments. Comparing these values to the distribution of drug-likeness in traded compounds shown in Figure 48, it is clear that they exceed the value normally found. This is good providing that properties such as cLogP are not adversely affected.

The program also recognises and flags functionality associated with toxicity. An overall drug score is also determined. This score is a combination of drug-likeness, cLogP, LogS, molecular weight and toxicity risks and is a measure of compound's overall potential to qualify as a drug. Drug-scores close to 1 indicate a high probability

that a compound will have good drug properties. All of the initial analogues scored very well (Table 20) and did not flag up any toxicity risks. Although the OSIRIS property explorer does not measure all of the Lipinski rule-of-five descriptors of drug likeness such as numbers of H-bond donors and acceptors, rotatable bonds or chiral centres it is clear that all of these compounds comply with these guidelines too.²²³

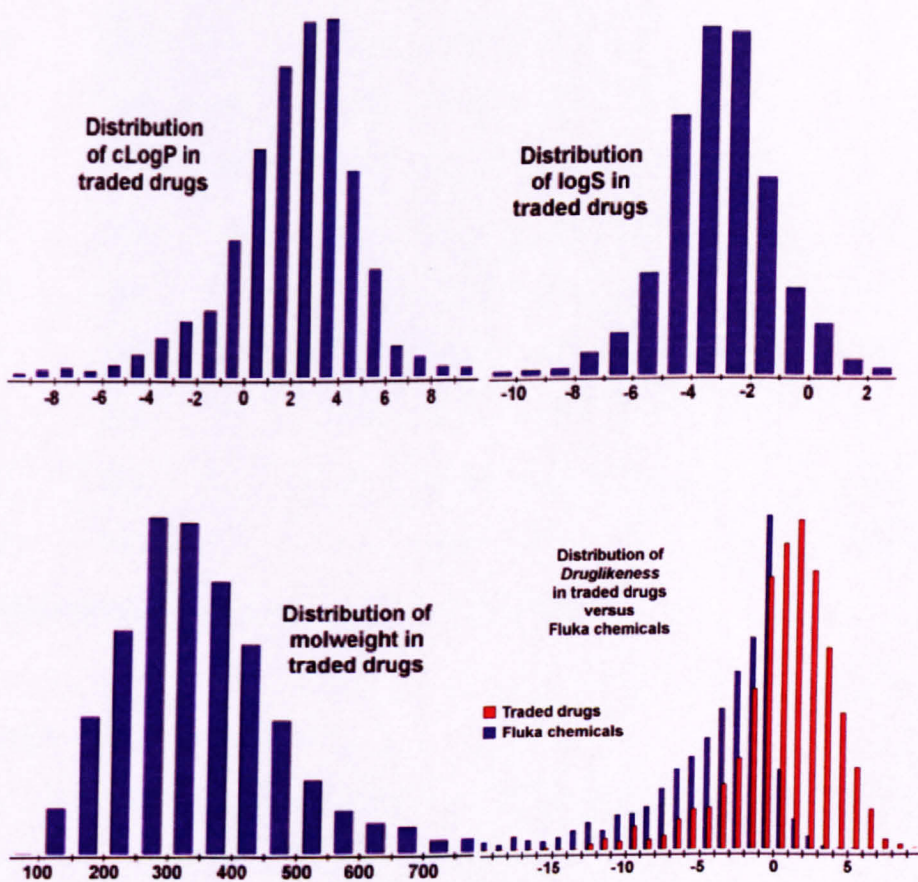
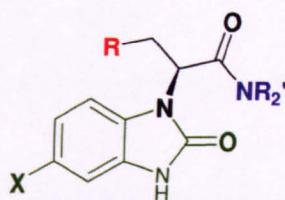


Figure 48 Distribution of properties calculated by OSIRIS property explorer²⁴⁴ among traded drugs.



| Entry | Compound | X | R | NR ₂ ' | Mw | cLogP | LogS | Drug likeness | Drug score |
|-------|----------|----|-----|-------------------|--------|-------|-------|---------------|------------|
| 1 | 207 | H | iPr | NMe ₂ | 275.35 | 2.27 | -3.02 | 6.13 | 0.88 |
| 2 | 208 | H | iPr | Py | 301.38 | 3.08 | -3.7 | 6.09 | 0.8 |
| 3 | 209 | H | Ph | NMe ₂ | 309.36 | 2.28 | -3.45 | 6.83 | 0.84 |
| 4 | 210 | H | Ph | Py | 335.40 | 3.09 | -4.14 | 6.78 | 0.75 |
| 5 | 211 | H | In | Py | 374.44 | 3.15 | -4.66 | 6.75 | 0.67 |
| 6 | 212 | Cl | iPr | NMe ₂ | 309.79 | 2.88 | -3.75 | 6.8 | 0.8 |
| 7 | 213 | Cl | iPr | Py | 335.83 | 3.69 | -4.44 | 6.73 | 0.69 |
| 8 | 214 | Cl | Ph | NMe ₂ | 343.80 | 2.89 | -4.19 | 7.48 | 0.75 |
| 9 | 215 | Cl | Ph | Py | 369.84 | 3.70 | -4.87 | 7.4 | 0.62 |
| 10 | 216 | Cl | In | Py | 408.88 | 3.77 | -5.4 | 7.36 | 0.54 |

Table 20 Predicted drug properties. Key In, indole; Py, pyrrolidine

4.2.7 Docking into MDM2

All of the synthesized ligands and a number of conceptual ones, based on commercially unavailable amines, were docked in MDM2, from the X-ray co-crystal structure with the p53 peptide (1YCR),¹ using FRED.²¹² The top pose for the majority of these ligands was as expected with the 1,3-dihydrobenzimidazol-2-one ring mimicking tryptophan and the other two groups mimicking phenylalanine and leucine. In the case of

compound **216**, where the amino amide was pyrolidyl L-tryptophan the indole is predicted to make an additional H-bond with MDM2 (Figure 49).

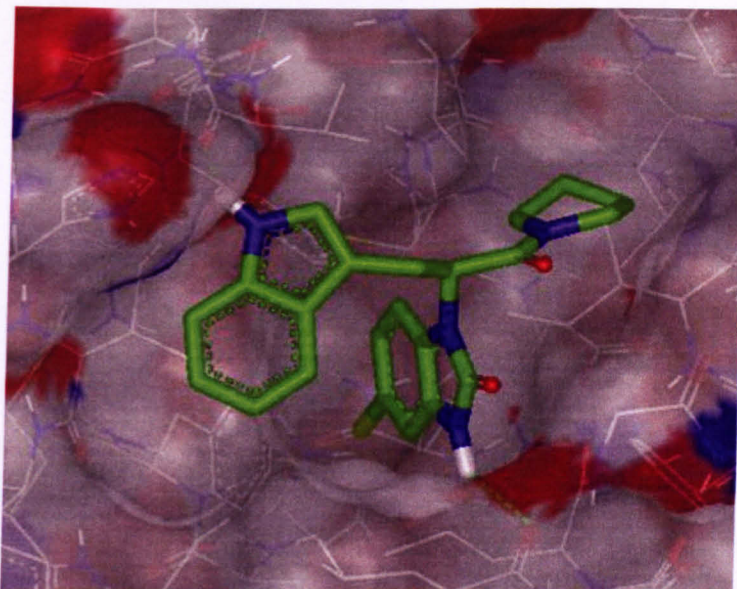
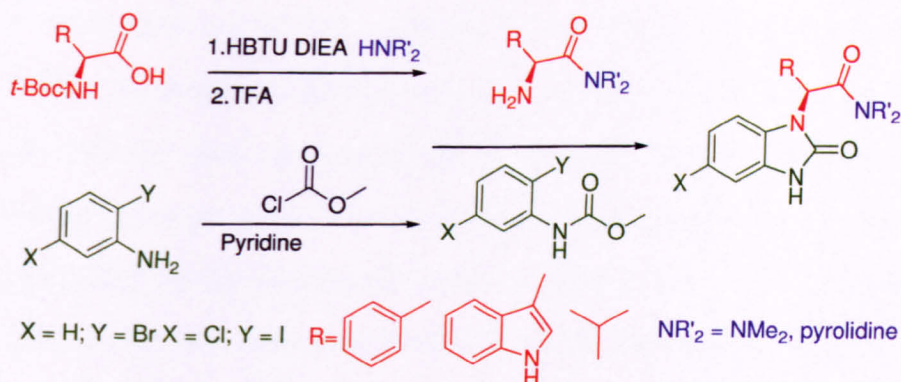


Figure 49 Compound 216 docked into MDM2 from 1YCR¹ using FRED²¹² binds as expected mimicking the H-bond donor ability of W²³ and showing the possibility to make additional H-bonds.

4.2.8 Synthesis

The *t*-*boc*-protected amino acids were coupled with either dimethylamine or pyrrolidine using the peptide coupling reagent HBTU and DIPEA and deprotected in TFA to give the required amino amides.²⁴⁶ The required *o*-halophenylcarbamates were prepared by condensation of the corresponding *o*-haloaniline with methyl chloroformate. The *o*-halophenylcarbamates and amino amides were converted into the desired 3-substituted-1,3-dihydrobenzimidazol-2-ones (Table 21) using the cascade coupling/cyclisation methodology described by Zou et al (Scheme 13).²⁴³



Scheme 13 All compounds were prepared using this convergent synthetic route which is very amenable to analogue synthesis. Coupling/Cyclisation Conditions: 10% CuI / L-proline, K_3PO_4 , DMSO, 70°C then 130°C

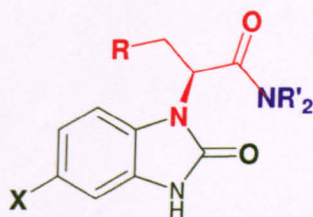
4.2.9 FP Binding Assay and SAR

The results described here are again based on the less sensitive assay and binding affinity is corrected by a factor of 3.18 as previously discussed (Section 1.11.1).

On initial inspection these compounds were all thought to be inactive with uncorrected $\text{IC}_{50} > 500\mu\text{M}$. However, upon closer inspection some analogues showed some, albeit low, dose dependant activity approaching $500\mu\text{M}$. These were mostly the analogues with the 6-chloro substituent which had been shown to greatly enhance the potency of the ultra potent peptides¹³¹ and spiro-oxindoles^{132, 141}. Despite the low activity, this implied that a well established SAR feature was exerting some influence on their affinity for the target. To confirm and quantify this, the assay was performed with a much higher top concentration of 5mM. Interestingly at this high concentration the compounds remained soluble. IC_{50} values were determined and corrected (Table 21).

Once again the 6-chloro analogues showed activity and the corresponding des-chloro counterparts remained mainly inactive with only two slight exceptions, neither of which detract from the possible 6-chloro SAR. Firstly the tryptophan based des-chloro analogue **211**, showed some activity, albeit considerably less than the corresponding 6-chloro analogue **216** (Table 21 entries 5 and 10). Secondly the only 6-chloro analogue that was inactive was **212**, the *N,N*-dimethyl leucine derivative, which is the smallest analogue (Table 21 entry 6).

There also appears to be some SAR based on the size of the side chains. As the size of the molecules **212**, **213** and **214** increases so too does binding activity. Activity is considerably reduced for the next largest analogue, **215**, indicating that the optimum volume may have been exceeded (Table 21 entries 6-9). However, the largest and the second most active compound, **216**, appears to buck this trend and showing the second highest activity of the series (Table 21, entry 10). That **216** is less active than **214** suggests that its increased bulk is reducing its ability to fit into the binding site but its increased activity over **215** indicates that its different functionality is allowing it to make interactions that compounds **212-215** cannot. This is supported by docking that shows its indole making a second H-bond interaction with MDM2 (Figure 49), the fact that its des-chloro counterpart **212** also shows some activity and that it is structurally similar to the previously described inhibitor, **6**, which bears two indole groups.¹⁴³



| Entry | Compound | X | R | NR'2 | Yield | FP IC ₅₀ Adjusted |
|-------|----------|----|--------|------------------|-------|---------------------------------|
| 1 | 207 | H | iPr | NMe ₂ | 55 % | Inactive |
| 2 | 208 | H | iPr | Pyrolidine | 27 % | Inactive |
| 3 | 209 | H | Ph | NMe ₂ | 61 % | Inactive |
| 4 | 210 | H | Ph | Pyrolidine | 69 % | Inactive |
| 5 | 211 | H | Indole | Pyrolidine | 12 % | 753.11 |
| 6 | 212 | Cl | iPr | NMe ₂ | 49% | Inactive |
| 7 | 213 | Cl | iPr | Pyrolidine | 42 % | 588.73 |
| 8 | 214 | Cl | Ph | NMe ₂ | 58 % | 196.18 |
| 9 | 215 | Cl | Ph | Pyrolidine | 41 % | 456.63 |
| 10 | 216 | Cl | Indole | Pyrolidine | 21 % | 239.08 |

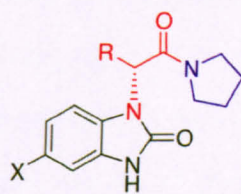
Table 21 Yields and binding activities of the 1,3-dihydrobenzimidazol-2-one compounds as determined by FP competitive binding assay.

4.2.10 Conclusions and Future work

A number of very drug like but low affinity ligands have been found in a very preliminary investigation using a low sensitivity assay. While SAR consistent with known MDM2 inhibitors shown by these analogues is evidence that they may well be bona-fide ligands, they are never the less low affinity ones. However, the analogues that

were investigated were based on a small number of amides derived from natural amino acids there are a number of things to be taken into account when considering these results and planning future work.

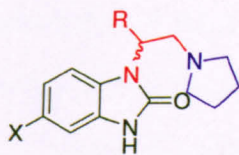
As these compounds are chiral and only one enantiomer was prepared it is likely that the other one will bind with different affinity. So analogues of the general type **217**, based on the corresponding D-amino acids, will need to be tested. The corresponding enantiomers of **213**, **215** and **216** have been prepared but are not yet tested.



217

Although using amino amides as the branched amines for this investigation have some advantages such as stability, ease of variation and rigidity there are also some limitations. In particular, the rigidity provided by the amide carbonyl group will extend to the its nitrogen and be a barrier to rotation. While rigidity is considered a good thing it would probably be beneficial to allow rotation in the bond immediately adjacent to the binding groups so that it could adopt the most favourable conformation and fine tune its interaction with the protein, rather than be locked in to one which may reduce its ability to bind. Given the lack of available α -branched primary amines it would be necessary to prepare these. However this should be possible by addition to sulfonylimines using organometalics such as Grignard reagents, a route that could be employed stereo selectively,²⁴⁷⁻²⁴⁹ or by reduction of the amino amides already used, which would

provide compounds like **218** that would be directly comparable to the work already done.



218

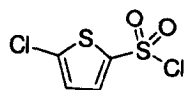
While the compounds discussed here warrant further investigation as outlined new analogues would need to show much enhanced binding activity and SAR. Probably the most important requirement will be to improve the sensitivity of the binding assay so that accurate affinities can be determined. If any better ligands are developed they would need to be tested using functional assays to show that they do indeed induce a non-genotoxic p53 response.

5. Experimental

5.1 Synthesis, General Methods

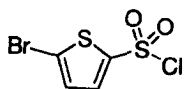
Standard syringe techniques were applied for transfer of air sensitive reagents. Solvents and reagents were purchased from Aldrich, Fisher Scientific, Fluorochem, or Alfa Aesar and were used as received. ^1H and ^{13}C NMR spectra were recorded on a Bruker Avance 400 spectrometer at 400 MHz and 100 MHz respectively at ambient temperature. Chemical shift values are reported in ppm relative to external TMS. High resolution mass spectra (HRMS) were recorded on a Micromass LCT spectrometer, ionization mode: ESI. Optical rotation was measured on a Bellingham and Stanley ADP410 polarimeter. Flash chromatography was performed with the indicated solvent mixture on Fluorochem Silica gel 60 (35-70 μm). Thin layer chromatography was performed using Merck silica gel 60 F₂₅₄ aluminum backed plates visualized by UV irradiation and permanganate staining. All tested compounds show $\geq 95\%$ purity as determined by HPLC. For all compounds except the benzodiazepine series (compounds **186-193**) and the deschloro sulfonamides (compounds **111** and **114**) a Waters, Symmetry column (C18, 3.5 μm , 120 \AA , 4.6 x 50 mm), mobile phase water with 0.1% formic acid and acetonitrile, gradient 5-100 % acetonitrile over 10 min, at a flowrate of 1 mL/min and detection wavelength 254 nm. HPLC of the benzodiazepines was performed using a Phenomenex Onyx monolith column (C18, 4.6 x 100 mm), mobile phase water with 0.1% formic acid and acetonitrile isocratic 45% acetonitrile 3 mL/min and detection wavelength 254 nm

General Procedure A: 5-Chlorothiophene-2-sulfonyl chloride ²⁵⁰



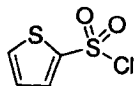
PCl_5 (100 g) was added portionwise to chlorosulfonic acid (80 mL). The mixture was stirred until gas evolution ceased (15 min) and then cooled to 0 °C. 2-Chlorothiophene (11 mL, 120 mmol) was added dropwise with cooling. The reaction mixture was stirred at ambient temperature for 5 h and then carefully added with stirring to ice/ H_2O (2 L). After stirring overnight, the aqueous solution was extracted with ether (3 x 500 mL). The ether extract was washed with H_2O (500 mL) and brine (500 mL), dried (MgSO_4), filtered, and concentrated under reduced pressure to yield 34.14 g (72%) of the desired product: Orange oil; ^1H NMR (400 MHz, CDCl_3) δ 7.66 (d, J = 4.2 Hz, 1H), 7.00 (d, J = 4.2 Hz, 1H).

5-Bromothiophene-2-sulfonyl chloride



2-Bromothiophene (22.53 mL, 23 mmol) was converted to the desired product using the General Procedure A as employed for the analogous chloro compound. The solid that precipitated upon addition to ice and was collected, washed and dried by vacuum filtration to yield 53.38 g (89 %) of the product as a cream crystalline solid: ^1H NMR (400 MHz, CDCl_3) δ 7.66 (d, J = 4.2 Hz, 1H), 7.19 (d, J = 4.2 Hz, 1H).

Thiophene-2-sulfonyl chloride

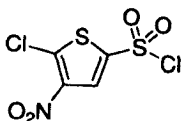


Thiophene (19.1 mL, 230 mmol) was converted to the desired product using the General Procedure A as employed for the analogous chloro compound. The brown oil that separated upon pouring the reaction mixture on to ice was dissolved in ether (250 mL), dried (MgSO₄) and the solvent removed under reduced pressure to yield the desired product as a low melting, brown solid 31.3 g (75%): ¹H NMR (400 MHz, CDCl₃) δ 7.9 (dd, *J*₁ = 4 Hz, *J*₂ = 1.3 Hz, 1H), 7.85 (dd, *J*₁ = 5 Hz, *J*₂ = 1.3 Hz, 1H), 7.21 (dd, *J*₁ = 5 Hz, *J*₂ = 4 Hz, 1H).

General Procedure B: nitration of thienyl sulfonyl chlorides ²⁵⁰

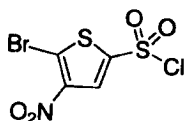
The crude sulfonyl chloride was added dropwise to 100% fuming nitric acid (100 mL) while maintaining the temperature below 60 °C and stirred at ambient temperature for 4 hours. The reaction mixture was added slowly with stirring to ice/H₂O (1 L). Solid products were separated and dried by filtration. Oils were separated, dissolved in diethyl ether and dried (MgSO₄) and the solvent was removed under reduced pressure.

5-chloro-4-nitrothiophene-2-sulfonyl chloride



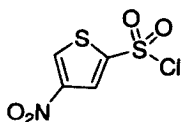
Using General Procedure B, 5-chlorothiophene-2-sulfonyl chloride (17.07 g, 80 mmol) yielded the desired product. Pale yellow solid 15.1 g (73 %). $^1\text{H NMR}$ (400 MHz, CDCl_3) δ 8.31 (s, 1H).

5-Bromo-4-nitrothiophene-2-sulfonyl chloride



Using General Procedure B, 5-bromothiophene-2-sulfonyl chloride (53.38 g, 204 mmol) yielded the desired product. Cream solid (42.5 g, 70 %) $^1\text{H NMR}$ (400 MHz, CDCl_3) δ 8.29 (s, 1H).

4-Nitrothiophene-2-sulfonyl chloride



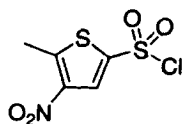
Using General Procedure B, thiophene-2-sulfonyl chloride (31.3 g, 171 mmol) Orange oil 26.88 g (69 %) as a 2:1 mixture of the 4-nitro and 5-nitro isomers in favour of the desired 4-nitro product. The mixture of isomers was used in the next step with out further purification. $^1\text{H NMR}$ (400 MHz, CDCl_3) 4-Nitro isomer (desired) δ 8.77 (d, $J = 1.7$ Hz, 1H), 8.4 (d, $J = 1.7$ Hz, 1H). 5-nitro isomer 7.99 (d, $J = 4.3$ Hz, 1H (0.54 relative to 4-isomer)), 7.88 (d, $J = 4.3$ Hz, 1H (0.54 relative to 4-isomer)).

General Procedure C: 5-Alkyl-4-nitro-2-sulfonyl chlorides²⁵¹

Chlorosulfonic acid (54.5 mL, 816 mmol) in chloroform (500 mL) was cooled a salt / ice bath. A solution of 2-alkylthiophene (267 mmol) in chloroform (200 mL) was added

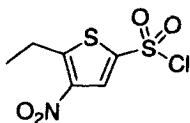
dropwise and the reaction was stirred for 30 min. The solution was poured on to ice and the product was extracted with diethyl ether (3 x 100 mL). The combined organic layers were dried (MgSO_4) and the solvent removed under reduced pressure to yield the crude sulfonyl chloride as brown oil. The crude sulfonyl chloride was added dropwise to 100% fuming nitric acid (100 mL) while maintaining the temperature below $60\text{ }^\circ\text{C}$ and stirred at ambient temperature for 4 h. The reaction mixture was added slowly with stirring to ice/ H_2O (1L). The solid products were separated by filtration and dried under reduced pressure.

5-Methyl-4-nitrothiophene-2-sulfonyl chloride



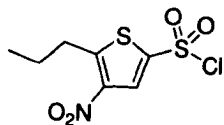
Using General Procedure C, 2-methylsulfonamide (25.7 mL, 267 mmol) yielded 6.6 g (27 %) of the desired product as a cream solid: ^1H NMR (400 MHz, CDCl_3) δ 8.33 (s, 1H), 2.94 (s, 3H).

5-Ethyl-4-nitrothiophene-2-sulfonyl chloride



Using General Procedure C, 2-ethylsulfonamide (25 g, 223 mmol) yielded 18.2 g of the desired product Cream solid (32 %) ^1H NMR (400 MHz, CDCl_3) δ 8.33 (s, 1H), 3.41 (q, $J = 7.38$ Hz, 2H), 1.48 (t, $J = 7.38$ Hz, 3H).

5-*n*-Propyl-4-nitrothiophene-2-sulfonyl chloride

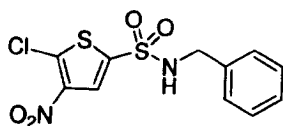


Using General Procedure C, 2-propylsulfonamide (18.69 mL, 223 mmol) yielded 15.6 g (26 %) of the desired product as a cream solid: $^1\text{H NMR}$ (400 MHz, CDCl_3) δ 8.33 (s, 1H), 3.32 (t, $J = 7.4$ Hz, 2H), 1.85 (sx, $J = 7.4$ Hz, 2H), 1.12 (t, $J = 7.4$ Hz, 3H).

General Procedure D: *N*-benzylsulfonamide synthesis

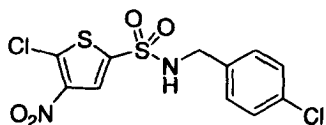
Up to twelve compounds were prepared in parallel using a general sulfonamide synthesis adapted from literature procedures.^{250, 252} The required sulfonylchloride (1.1 eq) and DCM were added to a clean dry reaction tube, ice cooled and stirred. Over 5 minutes, the required benzylamine (1 eq) and TEA (1 eq) in DCM were added. The reaction was stirred on ice for 5 minutes then allowed to warm to room temperature for 1 hour with stirring. 1M aqueous HCl (10 mL) was added followed by DCM (10 mL). The organic layer was separated washed with water (2 x 20 mL), brine (1 x 20 mL), dried (MgSO_4) and the solvent was removed under reduced pressure. The crude material was purified by flash chromatography and/or recrystallisation as detailed below.

N-Benzyl-5-chloro-4-nitrothiophenesulfonamide (67)



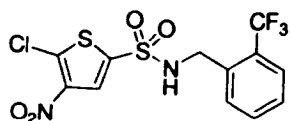
Benzylamine (541 mg, 5 mmol), TEA (505 mg, 5 mmol) in DCM (5 mL) was added to 5-chloro-4-nitrothiophene-2-sulfonyl chloride (1.44 g, 5.5 mmol) in DCM (5 mL) as per General Procedure D. The crude product was purified by flash chromatography (silica gel; hexane/EtOAc, 10:2), recrystallised in hexane, EtOAc and dried under high vacuum at 60 °C overnight yielded 0.8 g (48 %) of **67** as pale yellow crystals: mp 130-131 °C; ¹H NMR (400 MHz, CDCl₃) δ 7.84 (s, 1H), 7.28 (m, 5H), 5.09 (br t, *J* = 6 Hz, 1H), 4.32 (d, *J* = 6.0 Hz, 2H); ¹³C NMR (100 MHz, DMSO-d₆) δ 142.8, 138.6, 137.0, 136.3, 128.7, 128.3, 127.8, 127.0, 46.9; HRMS (ESI) *m/z* calcd for C₁₁H₈ClN₂O₄S₂ [M-H]⁻: 330.9614, found: 330.9579; HPLC T_R: 10.45 min.

***N*-(4-Chlorobenzyl)-5-chloro-4-nitrothiophenesulfonamide (68)**



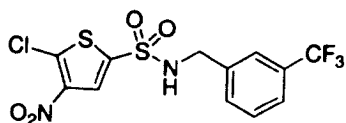
4-Chlorobenzylamine (713 mg, 5 mmol), TEA (505 mg, 5 mmol) in DCM (5 mL) was added to 5-chloro-4-nitrothiophene-2-sulfonyl chloride (1.44 g, 5.5 mmol) in DCM (5 mL) as per General Procedure D. The crude product was purified by flash chromatography (silica gel; hexane/EtOAc, 10:2), recrystallised in hexane, EtOAc and dried under high vacuum at 60°C overnight yielded 0.74 g (40 %) of **68** as pale yellow crystals: mp 98-99 °C; ¹H NMR (400 MHz, CDCl₃) δ 7.91 (s, 1H), 7.3 (dt, *J*_{AB} = 8.5 Hz, 2H), 7.23 (dt, *J*_{AB} = 8.5 Hz, 2H), 5.05 (br t, *J* = 6.0 Hz, 1H), 4.28 (d, *J* = 6.0 Hz, 2H); ¹³C NMR (100 MHz, CDCl₃) δ 137.8, 137.5, 134.9, 128.9, 128.5, 128.1, 127.2, 47.7; HRMS (ESI) *m/z* calcd for C₁₁H₇Cl₂N₂O₄S₂ [M-H]⁻: 364.9224, found: 364.9216; HPLC T_R: 10.96 min.

***N*-(2-Trifluoromethylbenzyl)-5-chloro-4-nitrothiophenesulfonamide (69)**



2-Trifluoromethylbenzylamine (881 mg, 5 mmol), TEA (505 mg, 5 mmol) in DCM (5 mL) was added to 5-chloro-4-nitrothiophene-2-sulfonyl chloride (1.44 g, 5.5 mmol) in DCM (5 mL) as per General Procedure D. The crude product was purified by flash chromatography (silica gel; hexane/EtOAc, 10:2), recrystallised in hexane, EtOAc and dried under high vacuum at 60 °C overnight yielded 0.8 g (40 %) of **69** as pale yellow crystals: mp 98-99 °C; ¹H NMR (400 MHz, CDCl₃) δ 7.88 (s, 1H), 7.66 (m, 1H), 7.57 (m, 2H), 7.46 (m, 1H), 5.21 (t, *J* = 6.2 Hz, 1H), 4.48 (d, *J* = 6.2 Hz, 2H); HRMS (ESI) *m/z* calcd for C₁₂H₇ClF₃N₂O₄S₂ [M-H]⁻: 398.9488, found: 398.9483; HPLC T_R: 11 min.

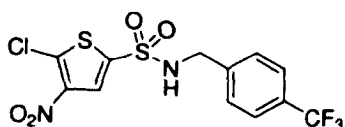
***N*-(3-Trifluoromethylbenzyl)-5-chloro-4-nitrothiophenesulfonamide (70)**



3-Trifluoromethylbenzylamine (881 mg, 5 mmol), TEA (505 mg, 5 mmol) in DCM (5 mL) was added to 5-chloro-4-nitrothiophene-2-sulfonyl chloride (1.44 g, 5.5 mmol) in DCM (5 mL) as per General Procedure D. The crude product was purified by flash chromatography (silica gel; hexane/EtOAc, 10:2), recrystallised in hexane, EtOAc and dried under high vacuum at 60 °C overnight yielded 1.1 g (55 %) of **70** as pale yellow crystals: mp 130-131 °C; ¹H NMR (400 MHz, DMSO-*d*₆) δ 9.04 (t, *J* = 6 Hz, 1H), 7.83 (s, 1H), 7.60-7.51 (m, 4H), 4.33 (d, *J* = 6 Hz, 2H); ¹³C NMR (100 MHz, DMSO-*d*₆) δ

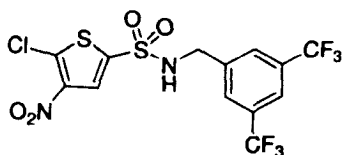
142.7, 138.7, 138.5, 136.5, 132.6, 129.9, 129.5 (q, $J = 32.7$ Hz), 127.0, 124.6 (q, $J = 4.1$ Hz), 124.6 (q, $J = 272.5$ Hz), 124.5 (q, $J = 3.8$ Hz), 46.2; HRMS (ESI) m/z calcd for $C_{12}H_7ClF_3N_2O_4S_2$ [M-H]⁻: 398.9488, found: 398.9482; HPLC T_R : 11.03 min.

***N*-(4-Trifluoromethylbenzyl)-5-chloro-4-nitrothiophenesulfonamide (71)**



4-Trifluoromethylbenzylamine (881 mg, 5 mmol), TEA (505 mg, 5 mmol) in DCM (5 mL) was added to 5-chloro-4-nitrothiophene-2-sulfonyl chloride (1.44 g, 5.5 mmol) in DCM (5 mL) as per General Procedure D. The crude product was purified by flash chromatography (silica gel; hexane/EtOAc, 10:2), recrystallised in hexane, EtOAc and dried under high vacuum at 60 °C overnight yielded 1.1 g (55 %) of **71** as pale yellow crystals: mp 123-124 °C; ¹H NMR (400 MHz, CDCl₃) δ 7.94 (s, 1H), 7.65 (d, $J = 8.1$ Hz, 2H), 7.42 (d, $J = 8.1$ 2H), 5.14 (t, $J = 6.0$ Hz, 1H), 4.38 (d, $J = 6.0$ Hz, 2H); HRMS (ESI) m/z calcd for $C_{12}H_7ClF_3N_2O_4S_2$ [M-H]⁻: 398.9488, found: 398.9488; HPLC T_R : 11.05 min.

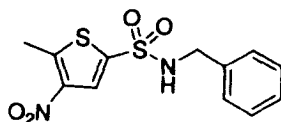
***N*-(3,5-Bistrifluoromethylbenzyl)-5-chloro-4-nitrothiophenesulfonamide (72)**



3,5-Bistrifluoromethylbenzylamine (1.22 g, 5 mmol), TEA (505 mg, 5 mmol) in DCM (5 mL) was added to 5-chloro-4-nitrothiophene-2-sulfonyl chloride (1.44 g, 5.5 mmol) in

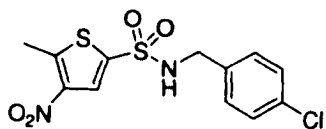
DCM (5 mL) as per General Procedure D. The crude product was purified by flash chromatography (silica gel; hexane/EtOAc, 10:2), recrystallised in hexane, EtOAc and dried under high vacuum at 60 °C overnight yielded 0.65 g (35 %) of **72** as pale yellow crystals: mp 169–170 °C; ¹H NMR (400 MHz, CDCl₃) δ 7.93 (s, 1H), 7.84 (s, 1H), 7.75 (s, 2H), 4.46 (s, *J* = 6.0 Hz, 1H), 4.38 (d, *J* = 6.1 Hz, 2H); ¹³C NMR (100 MHz, DMSO-*d*₆) δ 142.7, 140.9, 138.5, 136.7, 130.6 (q, *J_F* = 33 Hz), 129.1, 127.2, 123.7 (q, *J_F* = 272.3 Hz), 121.5, 45.6; HRMS (ESI) *m/z* calcd for C₁₃H₆ClF₆N₂O₄S₂ [M-H]⁻: 466.9462, found: 466.9369; HPLC T_R: 11.55 min.

***N*-Benzyl-5-methyl-4-nitrothiophenesulfonamide (74)**



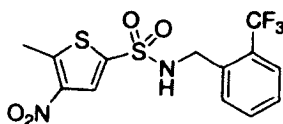
Benzylamine (541 mg, 5 mmol), TEA (505 mg, 5 mmol) in DCM (5 mL) was added to 5-methyl-4-nitrothiophene-2-sulfonyl chloride (1.33 g, 5.5 mmol) in DCM (5 mL) as per General Procedure D. The crude product was purified by flash chromatography (silica gel; hexane/EtOAc, 10:6), recrystallised from chloroform and dried under high vacuum at 60 °C overnight yielded 0.85g (54 %) of **74** as a cream crystalline solid: mp 109-110 °C; ¹H NMR (400 MHz, CDCl₃) δ 7.94 (s, 1H), 7.3-7.23 (m, 5H), 4.9 (br t, *J* = 6 Hz, 1H), 4.29 (d, *J* = 6.0 Hz, 2H), 2.83 (s, 3H); ¹³C NMR (100 MHz, CDCl₃) δ 149.3, 136.7, 135.4, 128.8, 128.2, 128.2, 128.0, 47.7, 15.9; HRMS (ESI) *m/z* calcd for C₁₂H₁₁N₂O₄S₂ [M-H]⁻: 311.0160, found: 311.0418; HPLC T_R: 10.14 min.

***N*-(4-Chlorobenzyl)-5-methyl-4-nitrothiophenesulfonamide (75)**



4-Chlorobenzylamine (713 mg, 5 mmol), TEA (505 mg, 5 mmol) in DCM (5 mL) was added to 5-methyl-4-nitrothiophene-2-sulfonyl chloride (1.33 g, 5.5 mmol) in DCM (5 mL) as per General Procedure D. The crude product was crystallised from chloroform and dried under high vacuum at 60 °C overnight yielded 0.5 g (29 %) of **75** as a cream crystalline solid: mp 130-131 °C; ¹H NMR (400 MHz, DMSO-d₆) δ 8.77 (t, 6 Hz, 1H), 7.82 (s, 1H) 7.35 (dt, *J*_{AB} = 8.5 Hz, 2H), 7.28 (dt, *J*_{AB} = 8.5 Hz, 2H), 4.15 (d, *J* = 6.0 Hz, 2H), 2.78 (s, 3H); ¹³C NMR (100 MHz, DMSO-d₆) δ 149.8, 143.2, 137.6, 136.4, 132.5, 130.0, 128.9, 128.6, 127.3, 46.1, 15.9; HRMS (ESI) *m/z* calcd for C₁₂H₁₀ClN₂O₄S₂ [M-H]⁻: 344.9771, found: 344.9771; HPLC T_R: 10.58 min..

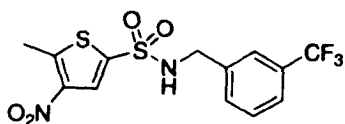
***N*-(2-Trifluoromethylbenzyl)-5-methyl-4-nitrothiophenesulfonamide (76)**



2-Trifluoromethylbenzylamine (441 mg, 2.5 mmol), TEA (253 mg, 2.5 mmol) in DCM (2.5 mL) was added to 5-methyl-4-nitrothiophene-2-sulfonyl chloride (665 mg, 2.75 mmol) in DCM (2.5 mL) as per General Procedure D. The crude product was purified by flash chromatography (silica gel; hexane/EtOAc, 8:3), recrystallised in hexane, EtOAc and dried under high vacuum at 60 °C overnight yielded 0.58 g (61 %) of **76** as a cream solid: mp 118-119 °C; ¹H NMR (400 MHz, CDCl₃) δ 7.95 (s, 1H), 7.65 (m, 1H), 7.58 (m, 2H), 7.44 (m, 1H), 5.05 (t, *J* = 6.1 Hz, 1H), 4.45 (d, *J* = 6.1 Hz, 2H),

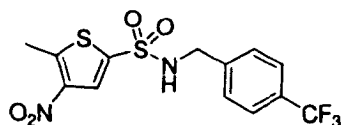
2.84 (s, 3H); ^{13}C NMR (100 MHz, CDCl_3) δ 149.6, 143.2, 136.5, 136.5, 131.4, 131.1 (q, $J_F = 3.7$ Hz), 129.4, 128.3, 127.8, 125.0 (q, $J_F = 3.7$ Hz), 124.5 (q, $J_F = 3.8$ Hz), 123.8 (q, $J_F = 272.3$ Hz), 47.0, 15.8; HRMS (ESI) m/z calcd for $\text{C}_{13}\text{H}_{10}\text{F}_3\text{N}_2\text{O}_4\text{S}_2$ $[\text{M}-\text{H}]^-$: 379.0034, found:379.0039; HPLC T_R : 10.72 min.

***N*-(3-Trifluoromethylbenzyl)-5-methyl-4-nitrothiophenesulfonamide (77)**



3-Trifluoromethylbenzylamine (441 mg, 2.5 mmol), TEA (253 mg, 2.5 mmol) in DCM (2.5 mL) was added to 5-methyl-4-nitrothiophene-2-sulfonyl chloride (665 mg, 2.75 mmol) in DCM (2.5 mL) as per General Procedure D. The crude product was purified by flash chromatography (silica gel; hexane/EtOAc, 8:3), recrystallised in hexane, EtOAc and dried under high vacuum at 60 °C overnight yielded 0.55 g (58 %) of **77** as a cream crystalline solid: mp 109-110 °C; ^1H NMR (400 MHz, CDCl_3) δ 7.90 (s, 1H), 7.55-7.45 (m, 4H), 5.31 (t, $J = 6$ Hz, 1H), 4.36 (d, $J = 6$ Hz, 2H), 2.81 (s, 3H); HRMS (ESI) m/z calcd for $\text{C}_{13}\text{H}_{10}\text{F}_3\text{N}_2\text{O}_4\text{S}_2$ $[\text{M}-\text{H}]^-$: 379.0034, found:379.0046; HPLC T_R : 10.14 min.

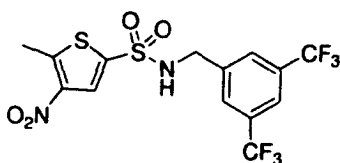
***N*-(4-Trifluoromethylbenzyl)-5-methyl-4-nitrothiophenesulfonamide (78)**



4-Trifluoromethylbenzylamine (441 mg, 2.5 mmol), TEA (253 mg, 2.5 mmol) in DCM (2.5 mL) was added to 5-methyl-4-nitrothiophene-2-sulfonyl chloride (665 mg,

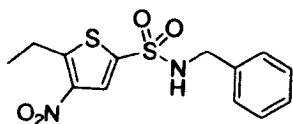
2.75 mmol) in DCM (2.5 mL) as per General Procedure D. The crude product was purified by flash chromatography (silica gel; hexane/EtOAc, 8:3), recrystallised in hexane, EtOAc and dried under high vacuum at 60 °C overnight yielded 0.66 g (69 %) of **78** as a cream crystalline solid: mp: 125-130 °C; ¹H NMR (400 MHz, CDCl₃) δ 7.98 (s, 1H), 7.59 (d, *J* = 8.2 Hz, 2H), 7.41 (d, *J* = 8.2 Hz, 2H), 5.15 (t, *J* = 6.0 Hz, 1H), 4.35 (d, *J* = 6.0 Hz, 2H) 2.83 (s, 3H); HRMS (ESI) *m/z* calcd for C₁₃H₁₀F₃N₂O₄S₂ [M-H]⁻: 379.0034, found: 379.041; HPLC T_R: 10.72 min.

***N*-(3,5-Bistrifluoromethylbenzyl)-5-methyl-4-nitrothiophenesulfonamide (79)**



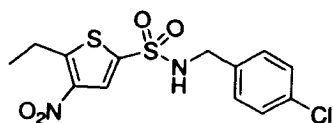
3,5-Bistrifluoromethylbenzylamine (610 mg, 2.5 mmol), TEA (253 mg, 2.5 mmol) in DCM (2.5 mL) was added to 5-methyl-4-nitrothiophene-2-sulfonyl chloride (665 mg, 2.75 mmol) in DCM (2.5 mL) as per General Procedure D. The crude product was purified by recrystallisation from chloroform and dried under high vacuum at 60 °C overnight yielded 0.75g (68 %) of **79** as a cream crystalline solid: mp 170.8–171.5 °C; ¹H NMR (400 MHz, CDCl₃) δ 7.95 (s, 1H), 7.82 (m, 1H), 7.73 (m, 2H), 5.12 (br t, *J* = 6.5 Hz, 1H), 4.45 (d, *J* = 6.5 Hz, 2H), 2.86 (s, 3H); HRMS (ESI) *m/z* calcd for C₁₄H₉F₆N₂O₄S₂ [M-H]⁻: 446.9908, found: 446.9926; HPLC T_R: 11.26 min.

***N*-Benzyl-5-ethyl-4-nitrothiophenesulfonamide (98)**



Benzylamine (261 mg, 2.5 mmol), TEA (253 mg, 2.5 mmol) in DCM (2.5 mL) was added to 5-ethyl-4-nitrothiophene-2-sulfonyl chloride (665 mg, 2.75 mmol) in DCM (2.5 mL) as per General Procedure D. The crude product was purified by flash chromatography (silica gel; hexane/EtOAc, 7:3), recrystallised from chloroform and dried under high vacuum at 60 °C overnight yielded 0.63 g (77 %) of **98** as a cream solid: mp 88.5-89.6 °C; ¹H NMR (400 MHz, CDCl₃) δ 7.95 (s, 1H), 7.31-7.19 (m, 5H), 4.9 (br t, *J* = 6 Hz, 1H), 4.29 (d, *J* = 6.0 Hz, 2H), 3.29 (q, *J* = 7.4 Hz, 2H), 1.36 (t, *J* = 7.4 Hz, 3H); ¹³C NMR (100 MHz, CDCl₃) δ 157.0, 142.4, 136.8, 135.4, 128.8, 128.4, 128.2, 128.0, 128.0, 47.6, 23.7, 14.2; HRMS (ESI) *m/z* calcd for C₁₃H₁₃N₂O₄S₂ [M-H]⁻: 325.0317, found: 325.0334; HPLC T_R: 10.91 min.

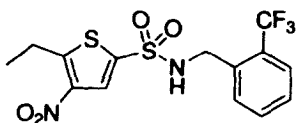
***N*-(4-Chlorobenzyl)-5-ethyl-4-nitrothiophenesulfonamide (99)**



4-Chlorobenzylamine (357 mg, 2.5 mmol), TEA (253 mg, 2.5 mmol) in DCM (2.5 mL) was added to 5-ethyl-4-nitrothiophene-2-sulfonyl chloride (665 mg, 2.75 mmol) in DCM (2.5 mL) as per General Procedure D. The crude product was purified by flash chromatography (silica gel; hexane/EtOAc, 7:3), recrystallised from chloroform yielded 0.71 g (79 %) of **99** cream crystalline solid mp: 130.7-133 °C; ¹H NMR (400 MHz, CDCl₃) δ 7.95 (s, 1H), 7.32-7.23 (m, 5H), 4.93 (t, 5.9 Hz, 1H) 4.30 (d, *J* = 5.9 Hz, 2H),

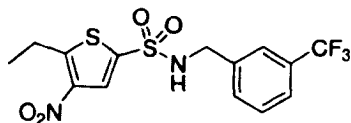
3.30 (q, $J = 7.4$ Hz, 2H), 1.39 (t, 7.4 Hz, 3H); ^{13}C NMR (100 MHz, CDCl_3) δ 157.1, 142.4, 136.7, 134.3, 133.9, 129.4, 129.0, 128.5, 46.9, 23.7, 14.2; HRMS (ESI) m/z calcd for $\text{C}_{13}\text{H}_{12}\text{ClN}_2\text{O}_4\text{S}_2$ [M-H] $^-$: 358.9917, found: 358.9917; HPLC T_R : 10.54 min.

***N*-(2-Trifluoromethylbenzyl)-5-ethyl-4-nitrothiophenesulfonamide (100)**



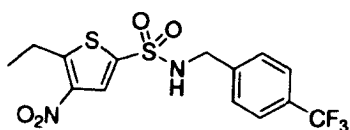
2-Trifluoromethylbenzylamine (441 mg, 2.5 mmol), TEA (253 mg, 2.5 mmol) in DCM (2.5 mL) was added to 5-ethyl-4-nitrothiophene-2-sulfonyl chloride (665 mg, 2.75 mmol) in DCM (2.5 mL) as per General Procedure D. The crude product was purified by flash chromatography (silica gel; hexane/EtOAc, 7:3), recrystallised in hexane, EtOAc and dried under high vacuum at 60 °C overnight yielded 0.58 g (59 %) of **100** as a cream solid: mp 95-95.8 °C; ^1H NMR (400 MHz, CDCl_3) δ 7.94 (s, 1H), 7.64-7.40 (m, 4H), 5.39 (t, $J = 6.1$ Hz, 1H), 4.45 (d, $J = 6.1$ Hz, 2H), 3.29 (q, $J = 7.6$ Hz, 2H), 1.38 (t, $J = 7.6$ Hz, 3H); ^{13}C NMR (100 MHz, CDCl_3) δ 157.1, 142.4, 136.6, 133.9, 132.5, 131.1, 128.5, 128.4, 128.3 (q, $J_F = 30.3$ Hz), 126.3 (q, $J_F = 5.6$ Hz), 124.2 (q, $J_F = 273.8$ Hz), 44.3, 23.7, 14.2; HRMS (ESI) m/z calcd for $\text{C}_{14}\text{H}_{12}\text{F}_3\text{N}_2\text{O}_4\text{S}_2$ [M-H] $^-$: 393.0191, found: 393.0224; HPLC T_R : 11.06 min.

***N*-(3-Trifluoromethylbenzyl)-5-ethyl-4-nitrothiophenesulfonamide (101)**



3-Trifluoromethylbenzylamine (441 mg, 2.5 mmol), TEA (253 mg, 2.5 mmol) in DCM (2.5 mL) was added to 5-ethyl-4-nitrothiophene-2-sulfonyl chloride (665 mg, 2.75 mmol) in DCM (2.5 mL) as per General Procedure D. The crude product was purified by flash chromatography (silica gel; hexane/EtOAc, 7:3), recrystallised in hexane, EtOAc and dried under high vacuum at 60 °C overnight yielded 0.55 g (56 %) of **101** as a cream solid: mp 86-88.5 °C; ¹H NMR (400 MHz, CDCl₃) δ 7.89 (s, 1H), 7.52-7.42 (m, 4H), 5.77 (t, *J* = 6.2 Hz, 1H), 4.37 (d, *J* = 6.2 Hz, 2H), 3.25 (q, *J* = 7.5 Hz 2H), 1.36 (t, *J* = 7.5 Hz, 3H); ¹³C NMR (100 MHz, CDCl₃) δ 157.3, 142.4, 136.6, 131.4, 131.1 (q, *J_F* = 32.9 Hz), 129.4, 128.6, 125.0 (q, *J_F* = 3.7 Hz), 124.5 (q, *J_F* = 3.7 Hz), 123.8 (q, *J_F* = 272.8 Hz), 47.0, 23.7, 14.0; HRMS (ESI) *m/z* calcd for C₁₄H₁₂F₃N₂O₄S₂ [M-H]⁻: 393.0191, found: 393.0160; HPLC T_R: 11.05 min.

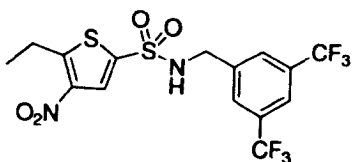
***N*-(4-Trifluoromethylbenzyl)-5-ethyl-4-nitrothiophenesulfonamide (102)**



4-Trifluoromethylbenzylamine (441 mg, 2.5 mmol), TEA (253 mg, 2.5 mmol) in DCM (2.5 mL) was added to 5-ethyl-4-nitrothiophene-2-sulfonyl chloride (665 mg, 2.75 mmol) in DCM (2.5 mL) as per General Procedure D. The crude product was purified by flash chromatography (silica gel; hexane/EtOAc, 7:3), recrystallised in hexane, EtOAc and dried under high vacuum at 60 °C overnight yielded 0.66 g (67 %) of **102** as cream solid: mp 92.4-94.6 °C; ¹H NMR (400 MHz, CDCl₃) δ 7.94 (s, 1H), 7.53 (d, *J* = 8.2 Hz, 2H), 7.40 (d, *J* = 8.2 Hz, 2H), 6.01 (t, *J* = 6.2 Hz, 1H), 4.34 (d, *J* = 6.2 Hz, 2H), 3.25 (q, *J* = 7.5 Hz, 2H), 1.36 (t, *J* = 7.5 Hz, 3H); ¹³C NMR (100 MHz, CDCl₃)

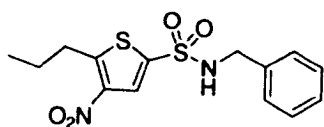
δ 157.3, 142.4, 139.6, 136.4, 130.4 (q, $J_F = 31.8$ Hz), 128.6, 128.2, 125.7 (q, $J_F = 3.8$ Hz), 123.8 (q, $J_F = 271$ Hz), 46.9, 23.6, 14.1; HRMS (ESI) m/z calcd for $C_{14}H_{12}F_3N_2O_4S_2$ [M-H]⁻: 393.0191, found: 393.2028; HPLC T_R : 11.04 min.

***N*-(3,5-Bistrifluoromethylbenzyl)-5-ethyl-4-nitrothiophenesulfonamide (103)**



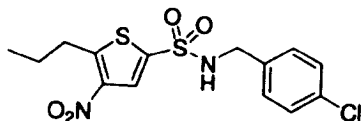
3,5-Bistrifluoromethylbenzylamine (610 mg, 2.5 mmol), TEA (253 mg, 2.5 mmol) in DCM (2.5 mL) was added to 5-ethyl-4-nitrothiophene-2-sulfonyl chloride (665 mg, 2.75 mmol) in DCM (2.5 mL) as per General Procedure D. The crude product was purified by flash chromatography (silica gel; hexane/EtOAc, 7:3), recrystallised in hexane, EtOAc and dried under high vacuum at 60 °C overnight yielded 0.75 g (65 %) of **103** as a cream solid: mp 152.9-155.9 °C; ¹H NMR (400 MHz, CDCl₃) δ 7.98 (s, 1H), 7.82 (s, 1H), 7.74 (s, 2H), 5.17 (br t, $J = 6.2$ Hz, 1H), 4.46 (d, $J = 6.2$ Hz, 2H), 3.30 (q, $J = 7.5$ Hz, 2H), 1.39 (t, $J = 7.5$ Hz, 3H); ¹³C NMR (100 MHz, CDCl₃) δ 157.5, 138.4, 136.4, 132.4, 132.1, 128.7, 128.0, 123.0 (q, $J_F = 272.2$ Hz), 122.2 (q, $J_F = 3.8$ Hz), 46.5, 23.7, 14.0; HRMS (ESI) m/z calcd for $C_{15}H_{11}F_6N_2O_4S_2$ [M-H]⁻: 461.0064, found: 461.0096; HPLC T_R : 11.57 min.

***N*-Benzyl-5-propyl-4-nitrothiophenesulfonamide (104)**



Benzylamine (261 mg, 2.5 mmol), TEA (253 mg, 2.5 mmol) in DCM (2.5 mL) was added to 5-*n*-propyl-4-nitrothiophene-2-sulfonyl chloride (742 mg, 2.75 mmol) in DCM (2.5 mL) as per General Procedure D. The crude product was purified by flash chromatography (silica gel; hexane/EtOAc, 10:2) and dried under high vacuum at 60 °C overnight yielded 0.25 g (29 %) of **104** as a cream solid: mp 104.2-106.5 °C; ¹H NMR (400 MHz, CDCl₃) δ 7.94 (s, 1H), 7.33-7.24 (m, 5H), 4.94 (br t, *J* = 6 Hz, 1H), 4.29 (d, *J* = 6.0 Hz, 2H), 3.21 (t, 7.7 Hz, 2H), 1.78 (m, 2H), 1.07 (t, *J* = 7.3 Hz, 3H); ¹³C NMR (100 MHz, CDCl₃) δ 155.0, 142.6, 136.9, 135.4, 128.8, 128.4, 128.2, 128.0, 47.6, 31.6, 23.5, 13.8; HRMS (ESI) *m/z* calcd for C₁₄H₁₅N₂O₄S₂ [M-H]⁻: 339.4120, found: 339.0441; HPLC T_R: 10.94 min.

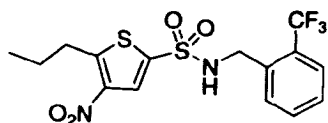
N-(4-Chlorobenzyl)-5-propyl-4-nitrothiophenesulfonamide (105)



4-Chlorobenzylamine (357 mg, 2.5 mmol), TEA (253 mg, 2.5 mmol) in DCM (2.5 mL) was added to 5-*n*-propyl-4-nitrothiophene-2-sulfonyl chloride (742 mg, 2.75 mmol) in DCM (2.5 mL) as per General Procedure D. The crude product was purified by flash chromatography (silica gel; hexane/EtOAc, 10:2) and dried under high vacuum at 60 °C overnight yielded 0.32 g (34 %) of **105** as a cream crystalline solid: mp 92.1-94.8 °C; ¹H NMR (400 MHz, CDCl₃) δ 7.97 (s, 1H), 7.29 (dt, *J*_{AB} = 8.4 Hz, 2H), 7.20 (dt, *J*_{AB} = 8.4 Hz, 2H), 4.98 (t, *J* = 6 Hz, 1H), 4.26 (d, *J* = 6.0 Hz, 2H), 3.22 (m, 2H), 1.79 (m, 2H), 1.07 (t, *J* = 7.3, 3H); ¹³C NMR (100 MHz, CDCl₃) δ 155.3, 142.6, 136.7, 134.2, 134.0,

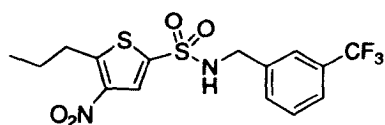
129.4, 128.9, 128.4, 46.8, 31.6, 23.5, 13.8; HRMS (ESI) m/z calcd for $C_{14}H_{14}ClN_2O_4S_2$ [M-H]: 373.0084, found: 373.0102; HPLC T_R : 11.27 min.

***N*-(2-Trifluoromethylbenzyl)-5-propyl-4-nitrothiophenesulfonamide (106)**



2-Trifluoromethylbenzylamine (441 mg, 2.5 mmol), TEA (253 mg, 2.5 mmol) in DCM (2.5 mL) was added to 5-*n*-propyl-4-nitrothiophene-2-sulfonyl chloride (742 mg, 2.75 mmol) in DCM (2.5 mL) as per General Procedure D. The crude product was purified by flash chromatography (silica gel; hexane/EtOAc, 10:2) and dried under high vacuum at 60 °C overnight yielded 0.25 g (25 %) of **106** as a cream microcrystalline solid: mp 97.8-99.5 °C; 1H NMR (400 MHz, $CDCl_3$) δ 7.95 (s, 1H), 7.64 (m, 1H), 7.57 (m, 2H), 7.43 (m, 1H), 5.01 (t, $J = 6.4$ Hz, 1H), 4.6 (d, $J = 6.4$ Hz, 2H), 3.22 (m, 2H), 1.78 (m, 2H), 1.07 (t, $J = 7.3$ Hz, 3H); ^{13}C NMR (100 MHz, $CDCl_3$) δ 155.2, 142.6, 136.6, 133.9, 132.4, 130.9, 128.6, 128.4, 128.2 (q, $J_F = 30.2$ Hz), 126.2 (q, $J_F = 4.7$ Hz), 124.1 (q, $J_F = 273.8$ Hz), 44.1, 31.6, 23.5, 13.7; HRMS (ESI) m/z calcd for $C_{15}H_{14}F_3N_2O_4S_2$ [M-H]: 407.4100, found: 407.0307; HPLC T_R : 11.45 min.

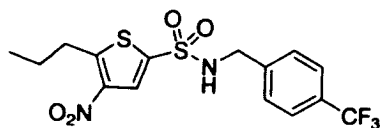
***N*-(3-Trifluoromethylbenzyl)-5-propyl-4-nitrothiophenesulfonamide (107)**



3-Trifluoromethylbenzylamine (441 mg, 2.5 mmol), TEA (253 mg, 2.5 mmol) in DCM (2.5 mL) was added to 5-*n*-propyl-4-nitrothiophene-2-sulfonyl chloride (742 mg,

2.75 mmol) in DCM (2.5 mL) as per General Procedure D. The crude product was purified by flash chromatography (silica gel; hexane/EtOAc, 10:2) and dried under high vacuum at 60 °C overnight yielded 0.20 g (20 %) of **107** as cream needles: mp 76.4-77.5 °C; ¹H NMR (400 MHz, CDCl₃) δ 7.93 (s, 1H), 7.55-7.45 (m, 4H), 5.08 (t, *J* = 6.2 Hz, 1H), 4.37 (d, *J* = 6.2 Hz, 2H), 3.21 (m, 2H), 1.77 (m, 2H), 1.07 (t, *J* = 7.3, 3H); ¹³C NMR (100 MHz, CDCl₃) δ 155.4, 142.5, 136.6, 136.6, 131.4, 131.2 (q, *J_F* = 31.7 Hz), 129.4, 128.5, 125.0 (q, *J_F* = 3.7 Hz), 124.5 (q, *J_F* = 3.7 Hz), 122.4 (q, *J_F* = 272.4 Hz), 47.0, 31.6, 23.4, 13.8; HRMS (ESI) *m/z* calcd for C₁₅H₁₄F₃N₂O₄S₂ [M-H]: 407.4100, found: 407.0300; HPLC T_R: 11.41 min.

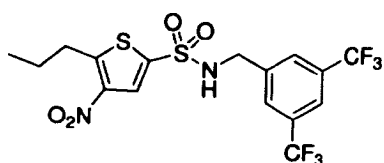
***N*-(4-Trifluoromethylbenzyl)-5-propyl-4-nitrothiophenesulfonamide (108)**



4-Trifluoromethylbenzylamine (441 mg, 2.5 mmol), TEA (253 mg, 2.5 mmol) in DCM (2.5 mL) was added to 5-*n*-propyl-4-nitrothiophene-2-sulfonyl chloride (742 mg, 2.75 mmol) in DCM (2.5 mL) as per General Procedure D. The crude product was purified by flash chromatography (silica gel; hexane/EtOAc, 10:2) and dried under high vacuum at 60 °C overnight yielded 0.19 g (19 %) of **108** as a cream microcrystalline solid: mp 92.2-93.8 °C; ¹H NMR (400 MHz, CDCl₃) δ 7.99 (s, 1H), 7.59 (d, 2H), 7.42 (d, 2H), 5.02 (t, *J* = 6.2 Hz, 1H), 4.36 (d, *J* = 6.2 Hz, 2H), 3.21 (t, *J* = 7.3 Hz, 2H), 1.77 (s, *J* = 7.3 Hz, 2H), 1.07 (t, *J* = 7.3, 3H); ¹³C NMR (100 MHz, DMSO-*d*₆) δ 155.3, 142.6, 139.6, 136.6, 130.7 (q, *J_F* = 32.9 Hz), 128.5, 128.2, 125.8 (q, *J_F* = 3.9 Hz), 123.8

(q, $J_F = 271.6$ Hz), 46.9, 31.6, 23.5, 13.8; HRMS (ESI) m/z calcd for $C_{15}H_{14}F_3N_2O_4S_2$ [M-H]: 407.4100, found: 407.0307; HPLC T_R : 11.4 min.

***N*-(3,5-Bistrifluoromethylbenzyl)-5-propyl-4-nitrothiophenesulfonamide (109)**



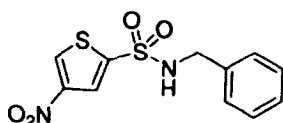
3,5-Bistrifluoromethylbenzylamine (610 mg, 2.5 mmol), TEA (253 mg, 2.5 mmol) in DCM (2.5 mL) was added to 5-*n*-propyl-4-nitrothiophene-2-sulfonyl chloride (742 mg, 2.75 mmol) in DCM (2.5 mL) as per General Procedure D. The crude product was purified by flash chromatography (silica gel; hexane/EtOAc, 10:2) and dried under high vacuum at 60 °C overnight yielded 0.65 g (55 %) of **109** as a cream solid: mp 150-153.5 °C; 1H NMR (400 MHz, $CDCl_3$) δ 7.96 (s, 1H), 7.59 (s, 1H), 7.73 (s, 2H), 5.33 (t, $J = 6.2$ Hz, 1H), 4.44 (d, $J = 6.2$ Hz, 2H), 3.21 (t, $J = 7.3$ Hz, 2H), 1.76 (s, $J = 7.3$ Hz, 2H), 1.0 (t, $J = 7.3$, 3H); ^{13}C NMR (100 MHz, $DMSO-d_6$) δ HRMS (ESI) m/z calcd for $C_{16}H_{13}F_6N_2O_4S_2$ [M-H]: 475.0221, found: 475.0035; HPLC T_R : 11.92 min.

General procedure 4-nitro and 5-nitrothiophenesulfonamides

To a solution of the mixture of 4- and 5-nitro thienylsulfonyl chlorides (455 mg, 2 mmol) in DCM (2 mL) benzyl amine (216 mg) or 4-chlorobenzyl amine (285 mg, 2 mmol) and triethylamine (202, 1eq) in DCM (2ml) as per the General Procedure D. The products were purified by flash chromatography (silica gel; hexane/EtOAc, 10:2) to yield 0.20 g (33 %) of a 5:4 mixture of the 4-nitro (**111**):5-nitro (**113**) regioisomers (1H NMR) and 0.20 g (30 %) of a 5:4 mixture of the 4-nitro (**112**):5-nitro (**114**) regioisomers

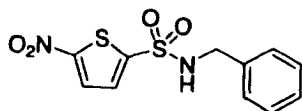
(¹H NMR). The isomers were resolved using reverse phase preparative hplc (Phenomenex Onyx C₁₈ monolithic column 100mm x 10mm; isocratic 40% MeCN/60%H₂O, 23.5 ml min⁻¹).

***N*-Benzyl-4-nitrothiophenesulfonamide (111)**



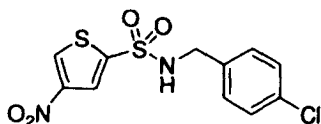
Colourless crystalline solid; ¹H NMR (400 MHz, CDCl₃) δ 8.43 (d, *J* = 1.6 Hz, 1H), 7.97 (d, *J* = 1.6 Hz, 1H), 7.32-7.22 (m, 5H), 4.95 (t, *J* = 6.0 Hz, 1H), 4.95 (d, *J* = 6 Hz, 2H); HRMS (ESI) *m/z* calcd for C₁₁H₉N₂O₄S₂ [M-H]⁻: 297.0004, found: 297.0012; HPLC T_R: 5.39 min.

***N*-Benzyl-5-nitrothiophenesulfonamide (113)**



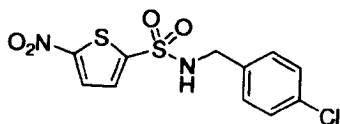
Colourless crystalline solid; ¹H NMR (400 MHz, CDCl₃) δ 7.81 (d, *J* = 4.3 Hz, 1H), 7.43 (d, *J* = 4.3 Hz, 1H), 7.35-7.2 (m, 5H), 5.07 (brs, 1H), 4.31 (d, *J* = 3.3 Hz, 2H); HRMS (ESI) *m/z* calcd for C₁₁H₉N₂O₄S₂ [M-H]⁻: 297.0004, found: 296.9908; HPLC T_R: 3.72 min.

***N*-(4-Chlorobenzyl)-4-nitrothiophenesulfonamide (112)**



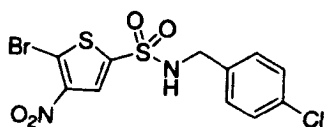
Colourless crystalline solid; $^1\text{H NMR}$ (400 MHz, CDCl_3) δ 8.47 (d, $J = 1.6$ Hz, 1H), 8.02 (d, $J = 1.6$ Hz, 1H), 7.33-7.29 (m, 2H), 7.22-7.18 (m, 2H), 4.98 (brs, 1H), 4.28 (brs, 2H); HRMS (ESI) m/z calcd for $\text{C}_{11}\text{H}_8\text{ClN}_2\text{O}_4\text{S}_2$ [M-H] $^-$: 330.9614, found: 330.9602; HPLC T_R : 7.18 min.

***N*-(4-Chlorobenzyl)-5-nitrothiophenesulfonamide (114)**



Colourless crystalline solid; $^1\text{H NMR}$ (400 MHz, CDCl_3) δ 7.85 (d, $J = 4.2$ Hz, 1H), 7.47 (d, $J = 4.2$ Hz, 1H), 7.32 (m, 2H), 7.20 (m, 2H), 4.99 (brs, 1H), 4.28 (brs, 2H). HRMS (ESI) m/z calcd for $\text{C}_{11}\text{H}_8\text{ClN}_2\text{O}_4\text{S}_2$ [M-H] $^-$: 330.9614, found: 330.9620; HPLC T_R : 3.98 min.

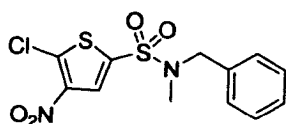
***N*-(4-Chlorobenzyl)-5-bromo-4-nitrothiophenesulfonamide (110)**



4-Chlorobenzylamine (357 mg, 2.5 mmol), TEA (253 mg, 2.5 mmol) in DCM (2.5 mL) was added to 5-bromo-4-nitrothiophene-2-sulfonyl chloride (766 mg, 2.75 mmol) in DCM (2.5 mL) as per General Procedure D. The crude product was purified by flash chromatography (silica gel; hexane/EtOAc, 10:2) yielded 0.48 g (47 %) of **110** as a pale yellow microcrystalline solid: mp 134-137 °C; $^1\text{H NMR}$ (400 MHz, CDCl_3) δ 7.84 (s, 1H), 7.28 (m, 5H), 5.09 (br t, $J = 6$ Hz, 1H), 4.32 (d, $J = 6.0$ Hz, 2H); $^{13}\text{C NMR}$ (100 MHz, DMSO-d_6) δ 145.1, 141.9, 136.2, 132.6, 130.2, 128.7, 127.5, 121.4, 46.1; HRMS

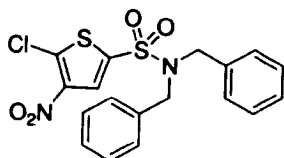
(ESI) m/z calcd for $C_{11}H_7BrN_2O_4S_2$ [M-H]⁻: 408.8719, found: 408.8625; HPLC T_R : 12.4 min.

***N*-Benzyl-*N*-methyl-5-chloro-4-nitrothiophenesulfonamide (87)**



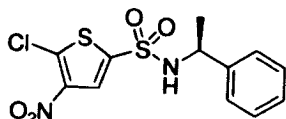
A solution of *N*-methyl-benzylamine (0.31 g, 2.5 mmol) and TEA (253 mg, 2.5 mmol) in DCM (3 mL) was added dropwise to a solution of 5-chloro-4-nitrothiophene-2-sulfonyl chloride (0.72 g, 2.75 mmol) in DCM (2 mL) as per General Procedure D. Crystallisation from hexane and EtOAc yielded 0.29 g (33 %) of **87** as off white crystals: mp 96.5-98.5 °C; ¹H NMR (400 MHz, CDCl₃) δ 7.93 (s, 1H), 7.40-7.31 (m, 5H), 4.27 (s, 2H), 2.76 (s, 3H); HPLC T_R : 11.03 min.

***N,N*-Dibenzyl-5-chloro-4-nitrothiophenesulfonamide (86)**



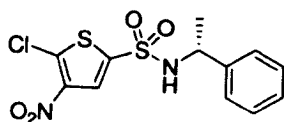
A solution of dibenzylamine (0.986 g, 2.5 mmol) and TEA (253 mg, 2.5 mmol) in DCM (3 mL) was added to to a solution of 5-chloro-4-nitrothiophene-2-sulfonyl chloride (0.72 g, 2.75 mmol) in DCM (2 mL) as per General Procedure D. Crystallisation twice from hexane/EtOAc yielded 0.25 g (24 %) of **86** as a yellow solid: mp 116-118.5 °C; ¹H NMR (400 MHz, CDCl₃) δ 8.17 (s, 1H), 7.60-7.19 (m, 10H), 4.41 (s, 4H); HPLC T_R : 14.4 min.

(S)-N-(1-Phenylethyl)-5-chloro-4-nitrothiophenesulfonamide (92)



A solution of (S)- α -methylbenzylamine (305 mg, 2.5 mmol) and TEA (253 mg, 2.5 mmol) in DCM (3 mL) was added to a solution of 5-chloro-4-nitrothiophene-2-sulfonyl chloride (0.72 g, 2.75 mmol) in DCM (2 mL) as per General Procedure D. Crystallisation from DCM yielded 0.79 g (79 %) of **92** as cream crystals: mp 159.1-160.7 °C; ^1H NMR (400 MHz, DMSO- d_6) δ 8.98 (brs, 1H), 7.50 (s, 1H), 7.25-7.11 (m, 5H), 4.52 (q, $J = 7.2$ Hz, 1H), 1.37 (d, $J = 7.2$ Hz, 3H); ^{13}C NMR (100 MHz, CDCl_3) δ 140.6, 138.2, 137.2, 128.8, 128.2, 127.3, 126.3, 54.7, 23.6; HRMS (ESI) m/z calcd for $\text{C}_{12}\text{H}_{10}\text{ClN}_2\text{O}_4\text{S}_2$ [M-H] $^-$: 344.9771, found: 344.9741; $[\alpha]_D^{20} = -50$ (c 0.52, MeOH); HPLC T_R : 10.02 min.

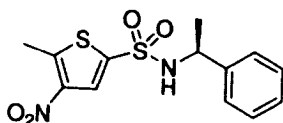
(R)-N-(1-Phenylethyl)-5-chloro-4-nitrothiophenesulfonamide (93)



A solution of (R)- α -methylbenzylamine (305 mg, 2.5 mmol) and TEA (253 mg, 2.5 mmol) in DCM (3 mL) was added to a solution of 5-chloro-4-nitrothiophene-2-sulfonyl chloride (0.72 g, 2.75 mmol) in DCM (2 mL) as per General Procedure D. Crystallisation from DCM yielded 0.71 g (82 %) of **93** cream crystals: mp 159-160 °C; ^1H NMR (400 MHz, DMSO- d_6) δ 8.97 (brs, 1H), 7.50 (s, 1H), 7.25-7.11 (m, 5H), 4.52 (q, $J = 7.2$ Hz, 1H), 1.37 (d, $J = 7.2$ Hz, 3H); ^{13}C NMR (100 MHz, CDCl_3) δ 140.6,

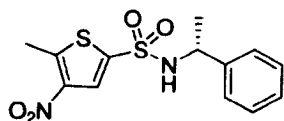
138.2, 137.2, 128.8, 128.2, 127.3, 126.3, 54.7, 23.6; HRMS (ESI) m/z calcd for $C_{12}H_{10}ClN_2O_4S_2$ [M-H]⁻: 344.9771, found: 344.9773; $[\alpha]_D^{20} = +42.6^\circ$ (c 0.47, MeOH); HPLC T_R : 10.66 min.

(S)-N-(1-Phenylethyl)-5-methyl-4-nitrothiophenesulfonamide (94)



A solution of (S)- α -methylbenzylamine (305 mg, 2.5 mmol) and TEA (253 mg, 2.5 mmol) in DCM (3 mL) was added to a solution of 5-methyl-4-nitrothiophene-2-sulfonyl chloride (665 mg, 2.75 mmol) in DCM (2 mL) as per General Procedure D. Crystallisation from DCM yielded 0.68 g (83 %) of **94** as cream crystals: mp 101.6-104 °C; ¹H NMR (400 MHz, CDCl₃) δ 7.62 (s, 1H), 7.25-7.12 (m, 5H), 4.97 (d $J = 7$, 1H), 4.63 (qn, $J = 7.0$ Hz, 1H), 1.37 (d, $J = 7.0$ Hz, 3H); ¹³C NMR (100 MHz, CDCl₃) δ 148.9, 142.9, 141.0, 137.2, 128.6, 128.8, 127.8, 126.2, 54.5, 23.6, 15.8; HRMS (ESI) m/z calcd for $C_{13}H_{13}N_2O_4S_2$ [M-H]⁻: 325.0317, found: 324.3018; $[\alpha]_D^{20} = -51.63^\circ$ (c 0.47, DCM); HPLC T_R : 10.33 min.

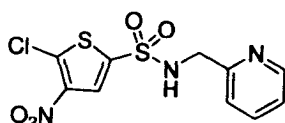
(R)-N-(1-Phenylethyl)-5-methyl-4-nitrothiophenesulfonamide (95)



A solution of (R)- α -methylbenzylamine (305 mg, 2.5 mmol) and TEA (253 mg, 2.5 mmol) in DCM (3 mL) was added to a solution of 5-methyl-4-nitrothiophene-2-

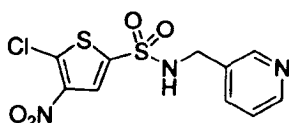
sulfonyl chloride (665 mg, 2.75 mmol) in DCM (2 mL) as per General Procedure D. Crystallisation from DCM yielded 0.66 g (81 %) of **95** as cream crystals: mp 101.6-104.2 °C; ¹H NMR (400 MHz, CDCl₃) δ 7.62 (s, 1H), 7.25-7.12 (m, 5H), 4.97 (d, *J* = 7.0 Hz, 1H), 4.63 (qn, *J* = 7.0 Hz, 1H), 1.37 (d, *J* = 7.0 Hz, 3H); HRMS (ESI) *m/z* calcd for C₁₃H₁₃N₂O₄S₂ [M-H]⁻: 325.0317, found: 324.2574; [α]_D²⁰ = +53.6° (c 0.47, DCM)

***N*-(2-Picolyl)-5-chloro-4-nitrothiophenesulfonamide (80)**



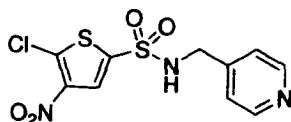
2-Picolylamine (273 mg, 2.5 mmol) and TEA (253 mg, 2.5 mmol) in DCM (3 mL) was added to a solution of 5-chloro-4-nitrothiophene-2-sulfonyl chloride (0.72 g, 2.75 mmol) in DCM (2 mL) as per General Procedure D. Crystallisation from ethanol yielded 0.71 g (85 %) of **80** as a brown solid: mp 170-172 °C; ¹H NMR (400 MHz, DMSO-d₆) δ 9.10 (t, *J* = 5.8 Hz, 1H), 8.44 (ddd, *J*₁ = 4.8 Hz, *J*₂ = 1.7 Hz, *J*₃ = 0.7 Hz, 1H), 7.91 (s, 1H), 7.76 (td, *J*₁ = 7.8 Hz, *J*₂ = 1.8 Hz, 1H), 7.39 (d, *J* = 7.7 Hz, 1H), 7.26 (qd, *J*₁ = 4.8 Hz, *J*₂ = 1 Hz, 1H), 4.30 (d, *J* = 6.1 Hz, 2H); ¹³C NMR (100 MHz, DMSO-d₆) δ 156.6, 149.3, 142.8, 138.6, 137.3, 136.3, 127.0, 123.0, 122.5, 48.5; HRMS (ESI) *m/z* calcd for C₁₀H₇ClN₃O₄S₂ [M-H]⁻: 331.9566, found: 331.9468; HPLC T_R: 10.32 min.

***N*-(3-Picolyl)-5-chloro-4-nitrothiophenesulfonamide (81)**



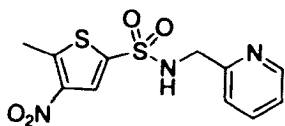
3-Picolylamine (273 mg, 2.5 mmol) and TEA (253 mg, 2.5 mmol) in DCM (3 mL) was added to a solution of 5-chloro-4-nitrothiophene-2-sulfonyl chloride (0.72 g, 2.75 mmol) in DCM (2 mL) as per General Procedure D. Crystallisation from ethanol yielded 0.65 g (78 %) of **81** as a beige solid: mp 180-184 °C; ¹H NMR (400 MHz, DMSO-d₆) δ 9.19 (brs, 1H), 8.48 (d, *J* = 1.7 Hz, 1H), 8.44 (dd, *J*₁ = 4.8 Hz, *J*₂ = 1.7 Hz, 1H), 7.96 (s, 1H), 7.71 (dt, *J*₁ = 7.8 Hz, *J*₂ = 1.8 Hz, 1H), 7.32 (dd, *J*₁ = 4.8 Hz, *J*₂ = 1 Hz, 1H), 4.23 (s, 2H); ¹³C NMR (100 MHz, DMSO-d₆) δ 194.3, 148.8, 142.9, 138.3, 136.5, 136.4, 133.1, 127.2, 123.9, 44.3; HRMS (ESI) *m/z* calcd for C₁₀H₇ClN₃O₄S₂ [M-H]⁻: 331.9566, found: 331.9541; HPLC T_R: 8.97 min.

***N*-(4-Picolyl)-5-chloro-4-nitrothiophenesulfonamide (82)**



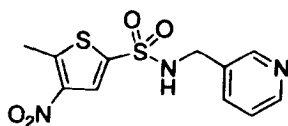
4-Picolylamine (273 mg, 2.5 mmol) and TEA (253 mg, 2.5 mmol) in DCM (3 mL) was added to a solution of 5-chloro-4-nitrothiophene-2-sulfonyl chloride (0.72 g, 2.75 mmol) in DCM (2 mL) as per General Procedure D. Crystallisation from ethanol yielded 0.66 g (79 %) of **82** as a dark brown solid: mp 148-150 °C; ¹H NMR (400 MHz, DMSO-d₆) δ 9.06 (t, *J* = 6 Hz, 1H), 8.50 (d, *J* = 4.3 Hz, 2H), 7.96 (s, 1H), 7.31 (d, *J*₁ = 6.3 Hz, 2H), 4.25 (d, *J* = 6 Hz, 2H); ¹³C NMR (100 MHz, DMSO-d₆) δ 152.7, 145.9, 143.0, 137.8, 136.7, 127.4, 124.3, 45.5; HRMS (ESI) *m/z* calcd for C₁₀H₇ClN₃O₄S₂ [M-H]⁻: 331.9566, found: 331.9554; HPLC T_R: 8.03 min.

***N*-(2-Picolyl)-5-methyl-4-nitrothiophenesulfonamide (83)**



2-Picolylamine (273 mg, 2.5 mmol) and TEA (253 mg, 2.5 mmol) in DCM (3 mL) was added to a solution of 5-methyl-4-nitrothiophene-2-sulfonyl chloride (665 mg, 2.75 mmol) in DCM (2 mL) as per General Procedure D. Crystallisation from ethanol yielded 0.70 g (89 %) of **83** as a beige solid: mp 125.4-126.4 °C; ¹H NMR (400 MHz, DMSO-*d*₆) δ 8.87 (brs, 1H), 8.44 (ddd, *J*₁ = 4.8 Hz, *J*₂ = 1.8 Hz, *J*₃ = 1 Hz, 1H) 7.83 (s, 1H), 7.73 (td, *J*₁ = 7.8 Hz, *J*₂ = 1.8 Hz, 1H), 7.36 (d, *J* = 7.8 Hz, 1H) 7.24 (qd, *J*₁ = 4.8 Hz, *J*₂ = 1 Hz, 1H), 4.25 (s, 2H), 2.76 (s, 3H); ¹³C NMR (100 MHz, DMSO-*d*₆) δ 156.9, 149.8, 149.3, 143.2, 137.6, 137.2, 127.3, 123.0, 122.4, 48.5, 15.9; HRMS (ESI) *m/z* calcd for C₁₁H₁₀N₃O₄S₂ [M-H]⁻: 312.0113, found: 312.0110; HPLC T_R: 7.4 min.

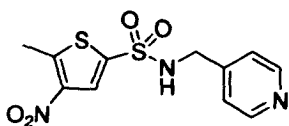
***N*-(3-Picolyl)-5-methyl-4-nitrothiophenesulfonamide (84)**



3-Picolylamine (273 mg, 2.5 mmol) and TEA (253 mg, 2.5 mmol) in DCM (3 mL) was added to a solution of 5-methyl-4-nitrothiophene-2-sulfonyl chloride (665 mg, 2.75 mmol) in DCM (2 mL) as per General Procedure D. Crystallisation from ethanol yielded 0.65 g (83 %) **84** as a beige solid: mp 160-162.5 °C; ¹H NMR (400 MHz, DMSO-*d*₆) δ 8.80 (brs, 1H), 8.46 (d, *J* = 1.7 Hz, 1H), 8.44 (dd, *J*₁ = 4.8 Hz, *J*₂ = 1.7 Hz, 1H), 7.88 (s, 1H), 7.67 (dt, *J*₁ = 7.8 Hz, *J*₂ = 1.7 Hz, 1H), 7.32 (dd, *J*₁ = 4.8 Hz, *J*₂ = 1 Hz, 1H), 4.18 (s, 2H), 2.77 (s, 3H); ¹³C NMR (100 MHz, DMSO-*d*₆) δ 149.9, 149.5,

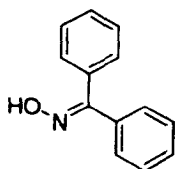
149.0, 143.3, 137.4, 136.0, 133.1, 127.4, 123.8, 44.4, 15.9; HRMS (ESI) m/z calcd for $C_{11}H_{10}N_3O_4S_2$ [M-H]⁻: 312.0113, found: 312.0105; HPLC T_R : 7.51 min.

***N*-(4-Picolyl)-5-methyl-4-nitrothiophenesulfonamide (85)**



4-Picolylamine (273 mg, 2.5 mmol) and TEA (253 mg, 2.5 mmol) in DCM (3 mL) was added to a solution of 5-methyl-4-nitrothiophene-2-sulfonyl chloride (665 mg, 2.75 mmol) in DCM (2 mL) as per General Procedure D. Crystallisation from ethanol yielded 0.68 g (87 %) of **85** as a beige solid: mp 177-179 °C; ¹H NMR (400 MHz, DMSO-*d*₆) δ 8.88 (brs, 1H), 8.48 (d, *J* = 5.5 Hz, 2H), 7.91 (s, 1H), 7.29 (d, *J*₁ = 5.5 Hz, 2H), 4.20 (s, 2H), 2.78 (s, 3H); ¹³C NMR (100 MHz, DMSO-*d*₆) δ 150.0, 146.7, 143.3, 137.2, 127.5, 122.9, 45.5, 15.9; HRMS (ESI) m/z calcd for $C_{11}H_{10}N_3O_4S_2$ [M-H]⁻: 312.0113, found: 312.0111; HPLC T_R : 7.44 min.

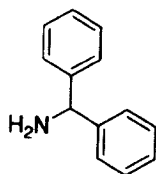
Benzophenone oxime ¹⁹⁹



A mixture of benzophenone (100 g, 550 mmol), hydroxylamine hydrochloride (60 g, 860 mmol) 95 per cent ethyl alcohol (200 mL) and water (40 mL) was added to a 2-L round-bottomed flask. Powdered sodium hydroxide (110 g, 2.75 moles) was added in portions, with stirring. The vigorous reaction was cooled in a water bath. After all the

sodium hydroxide addition the mixture was refluxed for five minutes. After cooling, the contents were poured into a solution of concentrated hydrochloric acid (300 mL) in H₂O (2 L). The precipitate was filtered with suction, thoroughly washed with water, and dried to yield 106g (98 %) of benzophenone oxime as a white solid: mp 140-142 °C, 141-142 °C (lit). ¹H NMR (400 MHz, DMSO-d₆) δ 11.36 (s, 1H), 7.49-7.27 (m, 10H). HRMS (ESI) m/z calcd for C₁₃H₁₂NO [M+H]⁺: 198.0919, found:198.0932.

Diphenylmethanamine ²⁰⁰



Ammonium formate (9.46 g 200 mmol) and magnesium powder (5 g, 41 mmol) were added to a solution of benzophenone oxime (9.65 g, 50 mmol) in methanol (50 mL). The mixture was stirred under a nitrogen atmosphere at room temperature. After the completion of reaction (monitored by TLC), the reaction mixture was filtered through celite. The solvent was evaporated under reduced pressure and the residue dissolved in DCM (200 mL) and washed with brine (2 x 100 mL). The organic layer was dried (MgSO₄) and the solvent removed under reduced pressure. The residue was dissolved in ether (100 mL) and poured into a solution of HCl in ether (100 mL). The precipitate was filtered, washed with ether, dissolved in 2M NaOH and extracted with DCM (3 x 50 mL). The organic layer was dried (MgSO₄) and the solvent removed under reduced pressure to yield 2.1 g (23 %) of the desired product as a colourless oil ¹H NMR

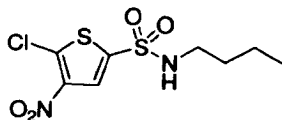
(DMSO-d₆) δ 8.44 (s, 1H), 7.43-7.27 (m, 10H). ¹³C NMR (400 MHz, CDCl₃) δ 145.05, 128.55, 127.09, 126.91, 59.65.

***N*-(Diphenylamine)-5-chloro-4-nitrothiophenesulfonamide (96)**



Diphenylmethanamine (458 mg, 2.5 mmol) and TEA (253 mg, 2.5 mmol) in DCM (3 mL) were added to a solution of the sulfoyl chloride (0.72 g, 2.75 mmol) in DCM (2 mL) as in General Procedure D. The crude product was purified by flash chromatography (silica gel; hexane/EtOAc, 9:1), recrystallised in hexane/EtOAc and dried under high vacuum at 60 °C overnight to yield 200 mg (20 %) of **96** as a white crystalline solid: mp 191.8-193.1 °C; ¹H NMR (400 MHz, CDCl₃) 7.49 (s, 1H), 7.33-7.25 (m, 6H), 7.22-7.18 (m, 4H), 5.76 (d, *J* = 7.8 Hz, 1H), 5.42 (d, *J* = 7.8 Hz, 1H); ¹³C NMR (100 MHz, CDCl₃) δ 141.8, 139.6, 139.1, 136.1, 128.3, 127.7, 127.5, 126.5, 61.9; HRMS (ESI) *m/z* calcd for C₁₇H₁₂ClN₂O₄S₂ [M-H]⁻: 406.9927, found: 406.9926; HPLC T_R: 11.31 min.

***N*-*n*-Butyl-5-chloro-4-nitrothiophenesulfonamide (97)**

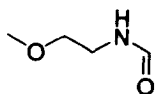


n-Butylamine (185 mg, 2.5 mmol) and TEA (253 mg, 2.5 mmol) in DCM (3 mL) were added to a solution of the sulfonyl chloride (0.72 g, 2.75 mmol) in DCM (2 mL) as in

General Procedure D. The crude product was purified by flash chromatography (silica gel; hexane/EtOAc, 9:1), recrystallised in hexane/EtOAc and dried under high vacuum at 60 °C overnight to yield 0.65 g (87 %) of **97** as a cream crystalline solid: mp 81-82.3 °C; ¹H NMR (400 MHz, CDCl₃) δ 8.02 (s, 1H), 4.65 (t, *J* = 5.7 Hz, 1H), 3.14 (q, *J* = 7.1 Hz, 2H), 1.57 (m, 2H), 1.39 (s, *J* = 7.5 Hz, 2H), 0.95 (t, *J* = 7.5 Hz, 3H); ¹³C NMR (100 MHz, CDCl₃) δ 142.6, 137.7, 137.4, 126.8, 43.4, 31.5, 19.7, 13.5; HRMS (ESI) *m/z* calcd for C₈H₁₀ClN₂O₄S₂ [M-H]⁻: 296.9771, found: 296.9746; HPLC T_R: 10.48 min.

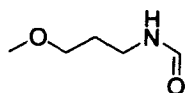
N-Methylamines

N-(2-Methoxy)ethyl-1-formamide ²⁵³



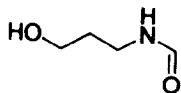
2-Methoxyethyl-1-amine (35 mL, 400 mmol) was refluxed in ethylformate (80 mL, 1 mole) overnight. Excess ethylformate was removed by rotary evaporation to give the desired product as a colourless oil in quantitative yield (41.25 g). ¹H NMR (400 MHz, CDCl₃) δ 8.17 (s, 1H), 6.72 (brs, 1H), 3.50-3.44 (m, 4H), 3.37 (s, 3H).

N-(2-methoxy)propyl-1-formamide ²⁵³



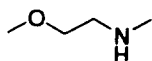
3-Methoxypropyl-1-amine (41 mL, 400 mmol) was refluxed in ethylformate (80 mL, 1 mole) overnight. Excess ethylformate was removed by rotary evaporation to give the desired product as a colourless oil in quantitative yield (46.9 g). ¹H NMR (400 MHz, CDCl₃) δ 8.15 (s, 1H), 6.21 (brs, 1H), 3.52-3.39 (m, 4H), 3.35 (s, 3H), 1.8 (m, 2H).

***N*-(3-hydroxy)propyl-1-formamide** ²⁵³



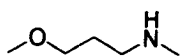
3-Amino-1-propanol (31 mL, 400 mmol) was refluxed in ethylformate (80.5 mL, 1 mole) overnight. Excess ethylformate was removed by rotary evaporation to give the desired product as a colourless oil in quantitative yield (41.24 g). ¹H NMR (400 MHz, CDCl₃) δ 8.13 (s, 1H), 6.67 (brs, 1H), 3.68-3.60 (m, 2H), 3.43-3.32 (m, 2H), 1.75-1.66 (m, 2H).

2-methoxy-*N*-methylethan-1-amine



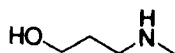
N-(2-Methoxyethyl)formamide (5.16 g, 50 mmol) and LiAlH₄ (2.1 g, 55 mmol) were refluxed in anhydrous THF (25 mL). The reaction was quenched by careful addition of water (5 mL). The solvent was removed under reduced pressure 1M NaOH (20 mL was added and the aqueous layer washed with DCM (3 x 20 mL). The combined organic layers were dried (MgSO₄) and the solvent was removed under reduced pressure to yield the product as a colourless oil 3.52 g (79%): ¹H NMR (400 MHz, CDCl₃) δ 3.50 (t, *J* = 5.1 HZ, 2H), 3.36 (s, 3H), 2.74 (t, *J* = 5.1 Hz, 2H), 2.44 (s, 3H).

3-Methoxy-*N*-methylpropan-1-amine



N-(3-Methoxypropyl)formamide (5.85 g, 50 mmol) and LiAlH₄ (2.1 g, 55 mmol) were refluxed in anhydrous THF (25 mL). The reaction was quenched by careful addition of water (5 mL). The solvent was removed under reduced pressure 1M NaOH (20 mL was added and the aqueous layer washed with DCM (3 x 20 mL). The combined organic layers were dried (MgSO₄) and the solvent was removed under reduced pressure to yield the product as a colourless oil 3.3 g (64%): ¹H NMR (400 MHz, CDCl₃) δ 3.80 (t, *J* = 6.2 Hz, 2H), 3.28 (s, 3H), 2.60 (t, *J* = 6.8 Hz, 2H), 2.37 (s, 3H), 1.71 (qn, *J* = 6.8 Hz; 2H); HRMS (ESI) *m/z* calcd for C₅H₁₄NO [M+H]⁺: 104.1075, found: 104.1089.

***N*-Methylpropan-3-ol-1-amine**



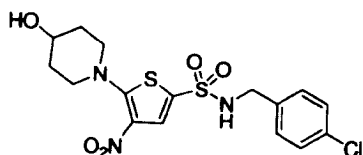
N-(3-hydroxy)propyl-1-formamide (5.16 g, 50 mmol) and LiAlH₄ (2.1 g, 55 mmol) were refluxed in anhydrous THF (25 mL). The reaction was quenched by careful addition of water (5 mL). The solvent was removed under reduced pressure 1M NaOH (20 mL was added and the aqueous layer washed with DCM (3 x 20 mL). The combined organic layers were dried (MgSO₄) and the solvent was removed under reduced pressure to yield the product as a colourless oil 3.2 g (72%): ¹H NMR (400 MHz, CDCl₃) δ 3.76 (t, *J* = 5.5 Hz, 2H), 2.80 (t, *J* = 5.9 Hz, 2H), 2.39 (s, 3H), 1.67 (qn, *J* = 5.5 Hz, 2H).

General Procedure E: 5-amination of *N*-(4-chlorobenzyl)-5-chloro-4-nitrothiophenesulfonamide (68)

The required amine nucleophile (2.2 mmol) was added to a solution of *N*-(4-chlorobenzyl)-5-chloro-4-nitrothiophenesulfonamide (68) (734 mg, 2 mmol) in

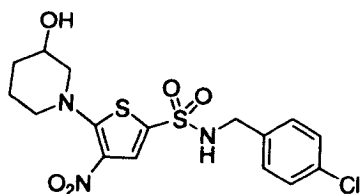
MeCN (5 mL) and K_2CO_3 (829 mg, 6 mmol). The reaction was stirred at room temperature and monitored by TLC until **68** was consumed. The solids were removed by filtration and the solvent removed under reduced pressure. The crude products were purified by dry flash chromatography on a plug of silica gel.

***N*-(4-Chlorobenzyl)-5-(4-hydroxypiperidin-1-yl)-4-nitrothiophenesulfonamide (116)**



4-Hydroxypiperidine (220 mg, 2.2 mmol) was used as in General Procedure E. The crude material was purified by dry flash chromatography (silica gel; hexane/EtOAc/MeOH, 10:2:1) to yield 600 mg (70 %) of **116** as a bright yellow solid: mp 167.5-169.4 °C; 1H NMR (400 MHz, DMSO- d_6) δ 8.6 (t, J = 6 Hz, 1H), 7.62 (s, 1H), 7.34-7.27 (m, 4H), 4.90 (d, J = 4.1 Hz, 1H), 4.13 (d, J = 6 Hz, 2H), 3.79 (m, 1H), 3.48 (m, 2H), 3.20 (m, 2H), 1.9 (m, 2H), 1.61 (m, 2H); ^{13}C NMR (100 MHz, DMSO- d_6) 163.3, 136.6, 132.4, 130.1, 129.2, 128.7, 128.5, 123.7, 64.4, 51.3, 46.0, 33.6; HRMS (ESI) m/z calcd for $C_{16}H_{17}ClN_3O_5S_2$ [M-H]: 430.0298, found: 430.0280; HPLC T_R : 9.55 min.

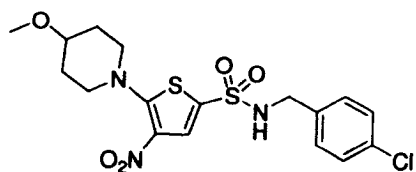
***N*-(4-Chlorobenzyl)-5-(3-hydroxypiperidin-1-yl)-4-nitrothiophenesulfonamide (115)**



3-Hydroxypiperidine (220 mg, 2.2 mmol) was used as in General Procedure E. The crude material was purified by dry flash chromatography (silica gel; hexane/EtOAc/MeOH, 10:2:1) to yield 530 mg (62 %) of **115** as a bright yellow crystalline solid: mp 133.5-136.8 °C; ^1H NMR (400 MHz, CDCl_3) δ 7.89 (s, 1H), 7.30-7.20 (m, 4H), 4.93 (t, $J = 6.4$ Hz, 1H), 4.23 (d, $J = 6.4$ Hz, 2H), 4.09 (m, 1H), 3.49 (dd, $J_1 = 12.4$ Hz, $J_2 = 3.5$ Hz, 1H), 3.29 (m, 2H), 2.10 (m, 2H), 1.95 (m, 1H), 1.76 (m, 2H); ^{13}C NMR (100 MHz, DMSO-d_6) δ 163.4, 136.6, 132.4, 130.1, 129.2, 128.5, 128.4, 123.2, 65.2, 60.4, 54.1, 46.0, 31.8, 21.9; HRMS (ESI) m/z calcd for $\text{C}_{16}\text{H}_{17}\text{ClN}_3\text{O}_5\text{S}_2$ [M-H]: 430.0298, found: 430.0309; HPLC T_R : 9.75 min

***N*-(4-Chlorobenzyl)-5-(4-methoxypiperidin-1-yl)-4-nitrothiophenesulfonamide**

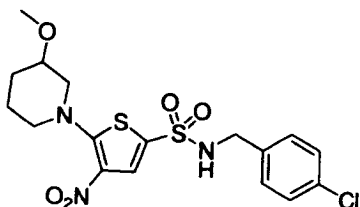
(**118**)



4-Methoxypiperidine (253 mg, 2.2 mmol) was used as in General Procedure E. The crude material was purified by dry flash chromatography (silica gel; hexane/EtOAc, 10:2) to yield 350 mg (39 %) of **118** as a bright yellow crystalline solid: mp 167-169 °C; ^1H NMR (400 MHz, CDCl_3) δ 7.93 (s, 1H), 7.33-7.22 (m, 4H), 4.85 (t, $J = 6.4$ Hz, 1H), 4.25 (d, $J = 6.4$ Hz, 2H), 3.61-3.50 (m, 3H), 3.41 (s, 3H), 3.33-3.26 (m, 2H), 2.13-2.04 (m, 2H), 1.99-1.90 (m, 2H); ^{13}C NMR (100 MHz, CDCl_3) δ 172.2, 134.3, 134.2, 130.6, 130.4, 129.4, 128.9, 122.6, 56.0, 50.5, 46.8, 29.6; HRMS (ESI) m/z calcd for $\text{C}_{17}\text{H}_{19}\text{ClN}_3\text{O}_5\text{S}_2$ [M-H]: 444.0455, found: 444.0477; HPLC T_R : 10.62 min

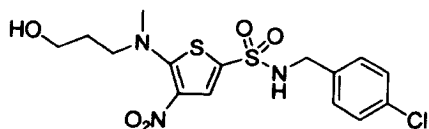
***N*-(4-Chlorobenzyl)-5-(3-methoxypiperidin-1-yl)-4-nitrothiophenesulfonamide**

(117)



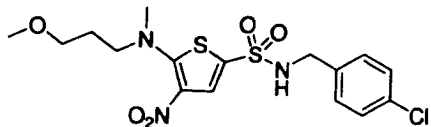
3-Methoxypiperidine (253 mg, 2.2 mmol) was used as in General Procedure E. The crude material was purified by dry flash chromatography (silica gel; hexane/EtOAc, 10:2) to yield 450 mg (50 %) of **117** as a bright yellow crystalline solid: mp 80.6-82.5 °C; ¹H NMR (400 MHz, CDCl₃) δ 7.89 (s, 1H), 7.33-7.18 (m, 4H), 4.85 (t, *J* = 6.5 Hz, 1H), 4.25 (d, *J* = 6.5 Hz, 2H), 3.70-3.64 (m, 1H), 3.58-3.51 (m, 1H), 3.47-3.40 (m, 1H), 3.39 (s, 3H), 3.23-3.16 (m, 1H), 3.13-2.07 (m, 1H), 2.11-1.95 (m, 2H), 1.81-1.70 (m, 1H), 1.66-1.57 (m, 1H); ¹³C NMR (100 MHz, CDCl₃) δ 163.6, 134.3, 134.0, 130.5, 129.4, 129.3, 128.9, 122.6, 57.4, 56.6, 54.3, 46.8, 28.7, 21.9; HRMS (ESI) *m/z* calcd for C₁₇H₁₉ClN₃O₅S₂ [M-H]⁻: 444.0455, found: 444.0471; HPLC T_R: 10.65 min.

***N*-(4-Chlorobenzyl)-5-(*N*-methyl-*N*-propan-1-ol-3-amino)-4-nitrothiophenesulfonamide (125)**



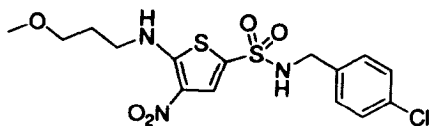
N-Methyl-*N*-propan-1-ol-3-amine (194 mg, 2.2 mmol) was used as in General Procedure E. The crude material was purified by dry flash chromatography (silica gel; hexane/EtOAc/MeOH, 10:2:1) to yield 460 mg (55 %) of **125** as a bright yellow crystalline solid: mp 84.2-86.9 °C; ¹H NMR (400 MHz, CDCl₃) δ 7.84 (s, 1H), 7.31-7.27 (m, 4H), 4.94 (t, *J* = 6.3 Hz, 1H), 4.23 (d, *J* = 6.3 Hz, 2H), 3.73 (m, 2H), 3.56 (m, 2H), 3.12 (s, 3H), 1.97 (m, 2H), 1.49 (t, *J* = 4.9 Hz, 1H); ¹³C NMR (100 MHz, CDCl₃) δ 163.2, 134.5, 133.9, 130.8, 129.4, 128.8, 128.1, 121.2, 59.5, 55.3, 46.7, 43.9, 29.6; HRMS (ESI) *m/z* calcd for C₁₅H₁₇ClN₃O₅S₂ [M-H]⁻: 418.0298, found: 418.0290; HPLC T_R: 9.53 min.

***N*-(4-Chlorobenzyl)-5-(*N*-3-methoxypropyl-*N*-methylamino)-4-nitrothiophenesulfonamide (126)**



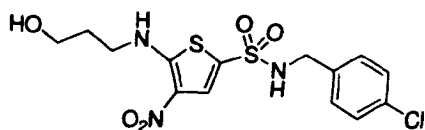
N-3-Methoxypropyl-*N*-methylamine (227 mg, 2.2 mmol) was used as in General Procedure E. The crude material was purified by dry flash chromatography (silica gel; hexane/EtOAc, 10:2) to yield 430 mg (50 %) of **126** as a bright yellow crystalline solid: mp 65.4-67.3 °C; ¹H NMR (400 MHz, CDCl₃) δ 7.85 (s, 1H), 7.31-7.19 (m, 4H), 4.84 (t, *J* = 6.7 Hz, 1H), 4.23 (d, *J* = 6.7 Hz, 2H), 3.55 (m, 2H), 3.41 (m, 2H), 3.31 (s, 3H), 3.11 (s, 3H), 1.97 (m, 2H); ¹³C NMR (100 MHz, CDCl₃) δ 162.9, 134.4, 134.0, 130.9, 129.4, 128.9, 128.1, 121.0, 69.1, 58.8, 55.5, 46.8, 44.0, 27.2; HRMS (ESI) *m/z* calcd for C₁₆H₁₉ClN₃O₅S₂ [M-H]⁻: 432.0455, found: 432.0456; HPLC T_R: 10.49 min.

***N*-(4-Chlorobenzyl)-5-(*N*-3-methoxypropylamino)-4-nitrothiophenesulfonamide (124)**



N-3-Methoxypropylamine (196 mg, 2.2 mmol) was used as in General Procedure E. The crude material was purified by dry flash chromatography (silica gel; hexane/EtOAc, 10:2) to yield 720mg (86 %) of **124** as a bright yellow crystalline solid: mp 126-127.3 °C; ¹H NMR (400 MHz, CDCl₃) δ 7.85 (s, 1H), 7.31-7.19 (m, 4H), 4.84 (t, *J* = 6.7 Hz, 1H), 4.23 (d, *J* = 6.7 Hz, 2H), 3.55 (m, 2H), 3.41 (m, 2H), 3.31 (s, 3H), 1.97 (m, 2H); ¹³C NMR (100 MHz, CDCl₃) δ 162.4, 134.4 134.0 129.4, 128.9, 128.7, 124.6, 119.0, 71.1, 59.0, 47.3, 46.8, 28.0; HRMS (ESI) *m/z* calcd for C₁₅H₁₇ClN₃O₅S₂ [M-H]⁻: 418.0298, found: 418.0309; HPLC T_R: 10.39 min.

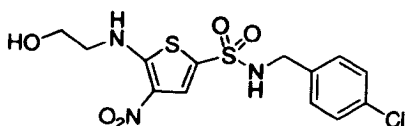
***N*-(4-Chlorobenzyl)-5-(*N*-propan-1-ol-3-amino)-4-nitrothiophenesulfonamide (123)**



N-Propan-1-ol-3-amine (163 mg, 2.2 mmol) was used as in General Procedure E. The crude material was purified by dry flash chromatography (silica gel; hexane/EtOAc, 10:2) to yield 740 mg (91 %) of **123** as a bright yellow crystalline solid: mp 133.2-135.9 °C; ¹H NMR (400 MHz, CDCl₃) δ 7.82 (s, 1H), 7.32-7.19 (m, 4H), 4.22 (s, 2H), 3.91 (t, *J* = 5.4 Hz, 2H), 3.49 (t, *J* = 6.3 Hz, 2H), 2.04 (m, 2H); ¹³C NMR (100 MHz, DMSO-*d*₆) 162.5, 136.7, 132.4, 130.1, 128.5, 127.4, 123.9, 120.1, 59.0, 46.9, 46.0,

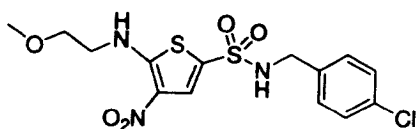
30.7; HRMS (ESI) m/z calcd for $C_{14}H_{15}ClN_3O_5S_2$ $[M-H]^-$: 404.0142, found: 404.0074;
HPLC T_R : 11.38 min.

***N*-(4-Chlorobenzyl)-5-(*N*-ethan-1-ol-2-amino)-4-nitrothiophenesulfonamide (119)**



N-Propan-1-ol-3-amine (134 mg, 2.2 mmol) was used as in General Procedure E. The crude material was purified by dry flash chromatography (silica gel; hexane/EtOAc/MeOH, 10:2:1) to yield 740 mg (94 %) **119** as a bright yellow crystalline solid: mp 170.7-172 °C; 1H NMR (400 MHz, $CDCl_3$) δ 7.52 (s, 1H), 7.39-7.29 (m, 4H), 5.08 (t, $J = 6$, 1H), 4.11 (s, 2H), 3.39 (m, 2H); ^{13}C NMR (100 MHz, DMSO- d_6) 163.3, 136.7, 132.4, 130.0, 128.6, 127.1, 124.2, 120.0, 59.3, 51.7, 46.0; HRMS (ESI) m/z calcd for $C_{13}H_{13}ClN_3O_5S_2$ $[M-H]^-$: 389.9985, found: 389.9984; HPLC T_R : 9.36 min.

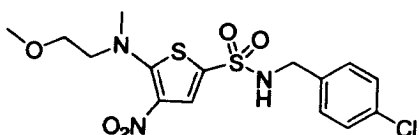
***N*-(4-chlorobenzyl)-5-(*N*-2-methoxyethylamino)-4-nitrothiophenesulfonamide (120)**



N-2-Methoxyethylamine (165 mg, 2.2 mmol) was used as in General Procedure E. The crude material was purified by dry flash chromatography (silica gel; hexane/EtOAc, 10:2) to yield 720 mg (91 %) of **120** as a bright yellow crystalline solid: mp 153-155.2 °C; 1H NMR (400 MHz, $CDCl_3$) δ 8.57 (brs, 1H), 7.82 (s, 1H), 7.33-7.21 (m, 4H), 5.08 (t, $J = 6.2$ Hz, 1H), 4.22 (d, $J = 6.2$ Hz, 2H), 3.68 (q, $J = 5.3$ Hz, 2H), 3.49 (t, $J = 5.3$ Hz, 2H), 3.49 (s, 3H); ^{13}C NMR (100 MHz, $CDCl_3$) δ 162.6, 134.3, 134.1, 129.4, 129.0,

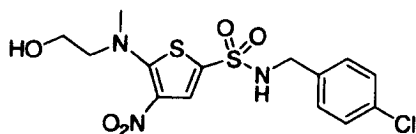
128.6, 125.0, 119.4, 69.4, 59.2, 48.0, 46.8; HRMS (ESI) m/z calcd for $C_{14}H_{15}ClN_3O_5S_2$ [M-H]: 404.0142, found: 404.0120; HPLC T_R : 10.84 min.

***N*-(4-Chlorobenzyl)-5-(*N*-3-methoxyethyl-*N*-methylamino)-4-nitrothiophenesulfonamide (122)**



N-3-Methoxyethyl-*N*-methylamine (196 mg, 2.2 mmol) was used as in General Procedure E. The crude material was purified by dry flash chromatography (silica gel; hexane/EtOAc, 10:2) to yield 510 mg (61 %) of **122** as a bright yellow crystalline solid: mp 100-101.7 °C; 1H NMR (400 MHz, $CDCl_3$) δ 7.87 (s, 1H), 7.34-7.21 (m, 4H), 4.86 (t, $J = 6.1$ Hz, 1H), 4.23 (d, $J = 6.1$ Hz, 2H), 3.65 (m, 4H), 3.34 (s, 3H), 3.18 (s, 3H), ^{13}C NMR (100 MHz, $CDCl_3$) δ 163.5, 134.4, 133.9, 130.8, 129.4, 128.9, 128.2, 121.4, 70.1, 59.0, 57.6, 46.7, 44.2; HRMS (ESI) m/z calcd for $C_{15}H_{17}ClN_3O_5S_2$ [M-H]: 418.0298, found: 418.0265; HPLC T_R : 10.39 min.

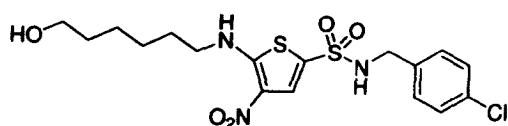
***N*-(4-Chlorobenzyl)-5-(*N*-methyl-*N*-ethan-1-ol-2-amino)-4-nitrothiophenesulfonamide (121)**



N-Methyl-*N*-ethan-1-ol-2-amine (196 mg, 2.2 mmol) was used as in General Procedure E. The crude material was purified by dry flash chromatography (silica gel; hexane/EtOAc/MeOH, 10:2:1) to yield 480 mg (59 %) of **121** as a bright yellow

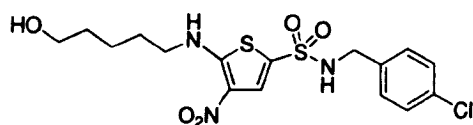
crystalline solid: mp 76-79 °C; ^1H NMR (400 MHz, CDCl_3) δ 7.85 (s, 1H), 7.32-7.19 (m, 4H), 4.86 (t, $J = 6$ Hz, 1H), 4.26 (d, $J = 6$ Hz, 2H), 3.97 (q, $J = 5.3$ Hz, 2H), 3.65 (t, $J = 5.3$ Hz, 2H), 3.22 (s, 3H); ^{13}C NMR (100 MHz, DMSO-d_6) δ 163.5, 136.7, 132.4, 130.0, 129.4, 128.6, 127.4, 122.0, 60.1, 58.5, 46.0, 44.0; HRMS (ESI) m/z calcd for $\text{C}_{14}\text{H}_{15}\text{ClN}_3\text{O}_5\text{S}_2$ [M-H]: 404.0142, found: 403.9974; HPLC T_R : 9.56 min.

***N*-(4-Chlorobenzyl)-5-(*N*-hexan-1-ol-6-amino)-4-nitrothiophenesulfonamide (128)**



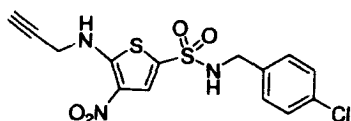
N-Hexan-1-ol-6-amine (256 mg, 2.2 mmol) was used as in General Procedure E. The crude material was purified by dry flash chromatography (silica gel; hexane/EtOAc/MeOH, 10:2:1) to yield 302 mg (34 %) of **128** as a bright yellow crystalline solid: mp 102-104.2 °C; ^1H NMR (400 MHz, CDCl_3) δ 8.43 (t, $J = 6$ Hz, 1H), 7.82 (s, 1H), 7.53-7.22 (m, 4H), 4.88 (t, $J = 6.5$ Hz, 1H), 4.22 (d, $J = 6.5$ Hz, 2H), 3.68 (m, 2H), 3.34 (m, 2H), 1.81 (m, 2H), 1.61 (m, 2H), 1.48 (m, 4H); ^{13}C NMR (100 MHz, DMSO-d_6) δ 162.4, 136.7, 132.4, 130.1, 128.5, 127.4, 123.9, 120.0, 61.1, 49.0, 46.0, 32.8, 27.9, 26.6, 25.6; HRMS (ESI) m/z calcd for $\text{C}_{17}\text{H}_{21}\text{ClN}_3\text{O}_5\text{S}_2$ [M-H]: 446.0611, found: 446.0619; HPLC T_R : 10.01 min.

***N*-(4-Chlorobenzyl)-5-(*N*-2-methoxypentanol-5-amino)-4-nitrothiophenesulfonamide (127)**



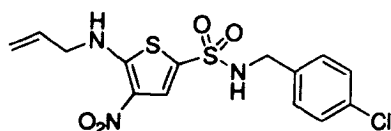
N-2-Methoxypentanol-5-amine (225 mg, 2.2 mmol) was used as in General Procedure E. The crude material was purified by dry flash chromatography (silica gel; hexane/EtOAc/MeOH, 10:2:1) to yield 480 mg (55 %) of **127** as a bright yellow crystalline solid: mp 123.2-125.8 °C; ¹H NMR (400 MHz, DMSO-*d*₆) δ 9.32 (brs, 1H), 8.58 (brs, 1H), 7.49 (s, 1H), 7.34-7.28 (m, 4H), 4.41 (t, *J* = 4.5 Hz, 1H), 4.12 (s, 2H), 3.41 (m, 2H), 3.32 (m, 2H), 1.65 (m, 2H), 1.46 (m, 2H), 1.35 (m, 2H); ¹³C NMR (100 MHz, DMSO-*d*₆) δ 162.5, 136.7, 132.4, 130.1, 128.5, 127.4, 123.9, 120.0, 61.0, 49.0, 46.0, 32.5, 27.7, 23.3; HRMS (ESI) *m/z* calcd for C₁₆H₁₉ClN₃O₅S₂ [M-H]⁻: 432.0455, found: 432.0438; HPLC T_R: 9.74 min.

***N*-(4-Chlorobenzyl)-5-(*N*-propargylamino)-4-nitrothiophenesulfonamide (134)**



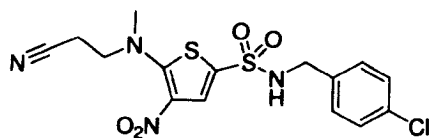
Propargylamine (121 mg, 2.2 mmol) was used as in General Procedure E. The crude material was purified by dry flash chromatography (silica gel; hexane/EtOAc, 10:2) to yield 450 mg (58 %) of **134** as a bright yellow crystalline solid: mp 150-152.1 °C; ¹H NMR (400 MHz, DMSO-*d*₆) δ 9.55 (brs, 1H), 8.59 (brs, 1H), 7.53 (s, 1H), 7.37-7.28 (m, 4H), 4.23 (d, *J* = 2.5 Hz, 2H), 4.13 (s, 2H), 3.50 (t, 1H); HRMS (ESI) *m/z* calcd for C₁₄H₁₁ClN₃O₄S₂ [M-H]⁻: 383.9879, found: 383.9859; HPLC T_R: 9.44 min.

***N*-(4-Chlorobenzyl)-5-(*N*-allylamino)-4-nitrothiophenesulfonamide (133)**



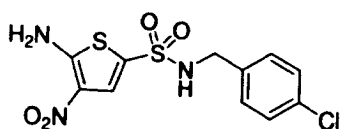
Allylamine (125 mg, 2.2 mmol) was used as in General Procedure E. The crude material was purified by dry flash chromatography (silica gel; hexane/EtOAc, 10:2) to yield 493 mg (64 %) of **133** as a bright yellow crystalline solid: mp 141.5-144.9 °C; ¹H NMR (400 MHz, DMSO-d₆) δ 9.51 (brs, 1H), 8.54 (brs, 1H), 7.51 (s, 1H), 7.34-7.27 (m, 4H), 5.86-5.77 (m, 1H), 5.32-5.27 (m, 2H), 4.11 (d, *J* = 4.8 Hz, 2H), 4.00 (s, 2H); ¹³C NMR (100 MHz, CDCl₃) δ 162.2, 134.2, 134.1, 129.9, 129.4, 129.0, 128.4, 125.1, 120.1, 120.0, 50.2, 46.8; HRMS (ESI) *m/z* calcd for C₁₄H₁₃ClN₃O₄S₂ [M-H]⁻: 386.0036, found: 385.9993; HPLC T_R: 10.49 min.

***N*-(4-Chlorobenzyl)-5-(*N*-methyl-*N*-(2-cyano)ethan-1-amino)-4-nitrothiophenesulfonamide (135)**



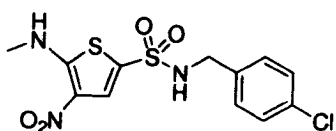
N-(2-Cyano)ethan-*N*-methyl-1-amine (183 mg, 2.2 mmol) was used as in General Procedure E. The crude material was purified by dry flash chromatography (silica gel; hexane/EtOAc, 10:2) to yield 484 mg (58 %) of **135** as a bright yellow crystalline solid: mp 145.7-147.3 °C; ¹H NMR (400 MHz, CDCl₃) δ 7.85 (s, 1H), 7.32-7.19 (m, 4H), 4.86 (t, *J* = 6 Hz, 1H), 4.26 (d, *J* = 6 Hz, 2H), 3.97 (q, *J* = 5.3 Hz, 2H), 3.65 (t, *J* = 5.3 Hz, 2H), 3.22 (s, 3H); 162.8, 136.6, 132.4, 130.1, 129.3, 128.6, 128.5, 123.7, 119.0, 53.1, 46.0, 43.0, 16.0; HRMS (ESI) *m/z* calcd for C₁₅H₁₄ClN₄O₄S₂ [M-H]⁻: 413.0145, found: 412.9505; HPLC T_R: 10.13 min.

***N*-(4-Chlorobenzyl)-5-amino-4-nitrothiophenesulfonamide (129)**



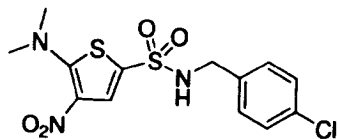
Ammonia was bubbled through a solution of *N*-(4-chlorobenzyl)-5-chloro-4-nitrothiophenesulfonamide (**68**) (734 mg, 2 mmol) in MeCN (5 mL) and K₂CO₃ (829 mg, 6 mmol). The reaction was stirred at room temperature and monitored by TLC until **68** was consumed. Nitrogen was bubbled through the solution, the solids were removed by filtration and the solvent removed under reduced pressure. The crude products were purified by dry flash chromatography on a plug of silica gel to yield 696 mg (80 %) of **129** as a yellow solid: mp: 179-182.1 °C; ¹H NMR (400 MHz, DMSO-d₆) δ 8.84 (brs 3H), 7.43 (s, 1H), 7.33 (m, 4H), 4.1 (s, 2H); ¹³C NMR (100 MHz, DMSO-d₆) δ 162.6, 136.8, 132.3, 130.0, 128.6, 126.5, 124.6, 119.9, 45.9; HRMS (ESI) *m/z* calcd for C₁₁H₉ClN₃O₄S₂ [M-H]⁻: 345.9723, found: 345.9730; HPLC T_R: 7.82 min.

***N*-(4-Chlorobenzyl)-5-methylamino-4-nitrothiophenesulfonamide (130)**



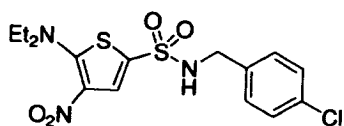
Methylammonium hydrochloride (146 mg, 2.2 mmol) was used as in General Procedure E. The crude material was purified by dry flash chromatography (silica gel; hexane/EtOAc, 10:2) to yield 424 mg (59 %) of **130** as a bright yellow crystalline solid; ¹H NMR (400 MHz, DMSO-d₆) δ 9.36 (q, *J* = 4.8 Hz, 1H), 8.54 (t, *J* = 6.3 Hz, 1H), 7.53 (s, 1H), 7.36-7.29 (m, 4H), 4.11 (d, *J* = 6.3 Hz, 2H), 3.01 (d, *J* = 4.8 Hz, 3H); HRMS (ESI) *m/z* calcd for C₁₂H₁₁ClN₃O₄S₂ [M-H]⁻: 359.9879, found: 359.9939 HPLC T_R: 9.97 min.

***N*-(4-Chlorobenzyl)-5-dimethylamino-4-nitrothiophenesulfonamide (131)**



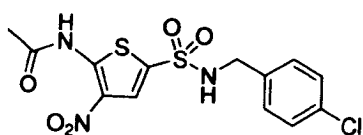
Dimethylammonium hydrochloride (179 mg, 2.2 mmol) was used as in General Procedure E. The crude material was purified by dry flash chromatography (silica gel; hexane/EtOAc, 10:2) to yield 442 mg (59 %) of **131** as a bright yellow crystalline solid: mp 130.7-133 °C; ¹H NMR (400 MHz, CDCl₃) δ 7.87 (s, 1H), 7.31-7.20 (m, 4H), 4.84 (t, *J* = 6.5 Hz, 1H), 4.22 (d, *J* = 6.5 Hz, 2H), 3.16 (s, 6H); HRMS (ESI) *m/z* calcd for C₁₃H₁₄ClN₃O₄S₂ [M-H]⁻: 374.0036, found: 374.0029; HPLC T_R: 10.86 min.

***N*-(4-Chlorobenzyl)-5-diethylamino-4-nitrothiophenesulfonamide (132)**



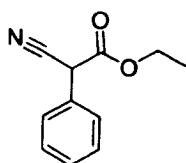
Diethylammonium chloride (242 mg, 2.2 mmol) was used as in General Procedure E. The crude material was purified by dry flash chromatography (silica gel; hexane/EtOAc, 10:2) to yield 44 mg (55 %) of **132** as a bright yellow crystalline solid: ¹H NMR (400 MHz, CDCl₃) δ 8.57 (s, 1H), 7.55 (s, 1H), 7.32-7.26 (m, 4H), 4.14 (s, 2H), 3.44 (q, *J* = 7.1 Hz, 4H), 1.12 (t, *J* = 7.1 Hz, 6H); HRMS (ESI) *m/z* calcd for C₁₅H₁₇ClN₃O₄S₂ [M-H]⁻: 402.0349, found: 402.0323; HPLC T_R: 10.88 min.

***N*-(4-Chlorobenzyl)-5-(*N*-acetyl)-4-nitrothiophenesulfonamide (137)^{201, 202}**



129 (70 mg, 0.2 mmol) and acetic anhydride (22 mg, 0.22 mmol) were refluxed in glacial acetic acid until no more **129** was observed by tlc. The reaction was cooled and water added (2 mL). The pale yellow precipitate was separated by filtration washed with water and dried to yield 50 mg (64 %) pale yellow crystals: $^1\text{H NMR}$ (400 MHz, DMSO- d_6) δ 11.60 (s, 1H), 8.64 (t, $J = 6.5$ Hz, 1H), 7.70 (s, 1H), 7.35-7.27 (m, 4H), 4.12 (d, $J = 6.5$ Hz, 2H), 2.42 (s, 3H); HRMS (ESI) m/z calcd for $\text{C}_{13}\text{H}_{11}\text{ClN}_3\text{O}_5\text{S}_2$ $[\text{M}-\text{H}]^-$: 387.9827, found: 387.9838; HPLC T_R : 10.16 min.

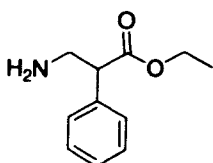
Ethyl Phenylcyanoacetate ²⁵⁴



Sodium ethoxide (15.1 mL, 25 wt% in ethanol, 66 mmol, 2.0 equiv.) was added slowly by syringe to a solution of benzyl cyanide (3.80 mL, 33 mmol) and diethyl carbonate (31.99 mL, 264 mmol, 8.0 equiv.) in toluene at 0 °C. The resulting solution was stirred at 0 °C for 10 minutes, then heated to 80 °C and stirred for 12 hours. After quenching with 1M aqueous hydrochloric acid (75 mL), the mixture was extracted with diethyl ether (2 x 200 mL). The combined organic extracts were washed with brine (100 mL), dried (Mg_2SO_4), and concentrated under reduced pressure. The residue was purified by flash chromatography (silica gel, pet ether/EtOAc 9:1), to yield a colorless oil 4.77g,

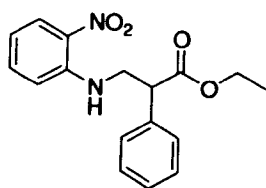
(76%). $^1\text{H NMR}$ (400 MHz, CDCl_3) δ 7.48-7.4 (m, 5H), 4.71 (s, 1H), 4.25 (qd, $J_1 = 7.2$ Hz, $J_2 = 1.5$ Hz, 2H), 1.29 (t, $J = 7.2$ Hz, 3H).

Ethyl 3-amino-2-phenylpropanoate



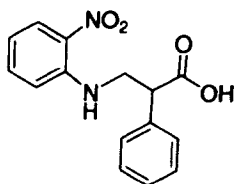
A solution of ethyl phenylcyanoacetate (4.77 g, 25.24 mmol) in ethanol (30 mL) was degassed by sonication under aspirator vacuum for 5 minutes and backfilled with nitrogen. 10% palladium on charcoal was carefully added under a blanket of nitrogen. A septum was fitted and 3.5ml conc HCl injected. The flask was evacuated under aspirator vacuum for 5 minutes. A H₂ balloon and needle was inserted into the septum. The reaction was stirred vigorously at room temperature and the balloon was refilled until no further consumption of hydrogen was apparent. The reaction mixture filtered through celite. The solvent was evaporated to yield a yellow waxy solid which was washed with EtOAc to give 2.96g (51 %) of the desired product as a white crystalline solid: mp 158-159 °C, literature: 160-161 °C; $^1\text{H NMR}$ (400 MHz, CD_3OD) δ 7.46-7.28 (m, 5H), 4.71 (s, 1H), 4.21 (qd, $J_1 = 6.9$ Hz, $J_2 = 2.8$ Hz, 2H), 4.01 (m, 1H), 3.6 (m, 1H), 3.25 (m, 1H), 1.21 (t, $J = 6.9$ Hz, 3H); HRMS (ESI) m/z calcd for $\text{C}_{11}\text{H}_{16}\text{NO}_2$ $[\text{M}+\text{H}]^+$: 194.1181, found: 194.1193.

Ethyl 3-(2-nitrophenylamino)-2-phenylpropanoate



Ethyl 3-amino-2-phenylpropanoate (2.28 g, 11 mmol), 2-fluoronitrobenzene (25 mL, 22 mmol) and DIPEA (39.8 mL, 22 mmol) in THF (150ml) were refluxed until no more was Ethyl 3-amino-2-phenylpropanoate detected by TLC. The solvent was removed under reduced pressure and the orange residue purified by flash chromatography (silica gel; DCM/Pet ether, 4:6). Two orange bands were observed on the column the second contained the product as a yellow oil (1.7 g, 49 %): $^1\text{H NMR}$ (400 MHz, CDCl_3) δ 8.16 (m, 2H), 7.42-7.31 (m, 5H), 6.86 (dd, $J_1 = 8.6$ Hz, $J_2 = 6.3$ Hz, 1H), 6.66 (m, 1H), 4.26-4.12 (m, 2H), 4.04-3.93 (m, 2H), 3.68-3.62 (m, 1H), 1.23 (t, $J = 7.1$ Hz, 3H); HRMS (ESI) m/z calcd for $\text{C}_{17}\text{H}_{19}\text{N}_2\text{O}_4$ $[\text{M}+\text{H}]^+$: 315.1345, found: 315.1303.

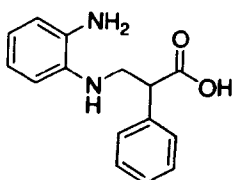
3-(2-Nitrophenylamino)-2-phenylpropanoic acid



Ethyl 3-(2-nitrophenylamino)-2-phenylpropanoate (2 g, 6 mmol) and lithium hydroxide (1.1 g, 24 mmol) was refluxed in 1:1 THF and water (60 ml) until no more starting material was detected by TLC. THF was removed under reduced pressure the solution was neutralised with 2M HCl and extracted with DCM (2 x 50 mL). The organic layer was dried (MgSO_4) and evaporated under reduced pressure to yield 1.5 g (87 %) of the product as an orange solid: $^1\text{H NMR}$ (400 MHz, CDCl_3) δ 8.17 (m, 2H), 7.49-7.33 (m,

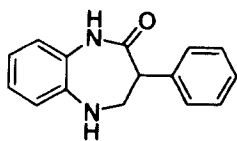
5H), 6.89 (dd, $J_1 = 8.6$ Hz, $J_2 = 6.3$ Hz, 1H), 6.69 (m, 1H), 4.02 (m, 1H), 3.74-3.68 (m, 2H); HRMS (ESI) m/z calcd for $C_{15}H_{15}N_2O_4$ $[M+H]^+$: 287.1032, found: 287.1027.

3-(2-Aminophenylamino)-2-phenylpropanoic acid



A solution of 3-(2-Nitrophenylamino)-2-phenylpropanoic acid (1.5 g, 5.24 mmol) in THF (30 mL) was degassed by sonication under aspirator vacuum for 5 minutes and backfilled with nitrogen. 10% palladium on charcoal was carefully added under a blanket of nitrogen. A septum was fitted and conc HCl (1 mL) was injected. The flask was evacuated under aspirator vacuum for 5 minutes. A H_2 balloon and needle were as inserted into the septum. The reaction was stirred vigorously at room temperature and the balloon was refilled until no further consumption of hydrogen was apparent. The reaction mixture was filtered through celite. Removal of the solvent under reduced pressure yielded 0.86 g (64 %) of the the product as a white solid: 1H NMR (400 MHz, $CDCl_3$) δ 7.42-7.19 (m, 7H), 6.89 (d, $J = 7.8$ Hz, 1H), 6.73 (m, 1H), 4.02 (m, 1H), 3.94 (m, 1H), 3.78 (m, 1H), 3.61 (m, 1H) 3.29 (m, 1H); HRMS (ESI) m/z calcd for $C_{15}H_{16}N_2O_2$ $[M+H]^+$: 257.1290, found: 257.1239.

4,5-Dihydro-3-phenyl-1H-benzo[b][1,4]diazepin-2(3H)-one



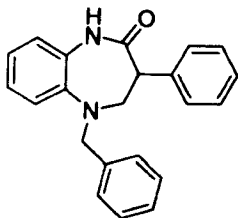
3-(2-Aminophenylamino)-2-phenylpropanoic acid (450 mg, 1.75 mmol), DIPEA (0.68 mL, 4.0 mmol) and HBTU (759 mg, 2.0 mmol) were stirred in THF (5 mL) at room temperature until no more starting material was observed by TLC and MS. The solvent was removed under reduced pressure. The residue was dissolved in DCM (50 mL) washed with saturated sodium bicarbonate (50 mL) and brine (50 mL), dried (MgSO_4) and concentrated under reduced pressure. Purification by flash chromatography (silica gel; pet ether/EtOAc, 1:1) yielded 160 mg (38 %) of the desired product as a beige solid: $^1\text{H NMR}$ (400 MHz, CDCl_3) δ 7.38-7.35 (m, 12H), 7.10 (td, $J_1 = 7.6$ Hz, $J_2 = 1.5$ Hz, 1H), 7.02 (td, $J_1 = 7.6$ Hz, $J_2 = 1.5$ Hz, 1H), 6.90 (dd, $J_1 = 7.6$ Hz, $J_2 = 1.5$ Hz, 1H), 5.15 (d, $J = 15.6$ Hz, 1H), 5.04 (d, $J = 15.6$ Hz, 1H), 4.08 (s, 1H), 3.79 (d, $J = 3.8$ Hz, 1H), 3.78 (m, 1H), 3.48 (brs, 1H); HRMS (ESI) m/z calcd for $\text{C}_{15}\text{H}_{16}\text{N}_2\text{O}_2$ $[\text{M}+\text{H}]^+$: 239.1184, found: 239.1254.

5-Benzyl-4,5-dihydro-3-phenyl-1H-benzo[b][1,4]diazepin-2(3H)-ones

General Procedure F

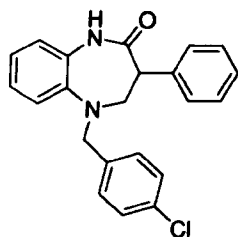
4,5-Dihydro-3-phenyl-1H-benzo[b][1,4]diazepin-2(3H)-one (50 mg, 0.2 mmol), the appropriate benzylchloride (0.2 mmol) and cesium carbonate (520 mg, 1.6 mmol) were refluxed in acetonitrile until no starting material was observed by TLC and MS. The reaction mixture was filtered and the solvent removed under reduced pressure. The crude products were purified by flash chromatography.

5-Benzyl-4,5-dihydro-3-phenyl-1H-benzo[b][1,4]diazepin-2(3H)-one (186)



Using benzylamine (25 mg, 0.2 mmol) as per General Procedure F yielded 45 mg of **186** (69 %) as a cream solid: mp 223-224 °C; ¹H NMR (400 MHz, CDCl₃) δ 7.38-7.35 (m, 12H), 7.10 (td, *J*₁ = 7.6 Hz, *J*₂ = 1.5 Hz, 1H), 7.02 (td, *J*₁ = 7.6 Hz, *J*₂ = 1.5 Hz, 1H), 6.90 (dd, *J*₁ = 7.6 Hz, *J*₂ = 1.5 Hz, 1H), 5.15 (d, *J* = 15.6 Hz, 1H), 5.04 (d, 15.6 Hz, 1H), 4.08 (m, 2H), 3.79 (d, *J* = 3.8 Hz, 2H), 3.78 (m, 1H), 3.48 (brs, 1H); ¹³C NMR (100 MHz, CDCl₃) δ 172.8, 140.9, 137.9, 136.2, 135.8, 129.6, 128.3, 128.2, 127.5, 127.2, 126.9, 126.8, 123.3, 123.1, 122.1, 57.9, 52.2, 47.5; ¹³C NMR (100 MHz, CDCl₃) δ HRMS (ESI) *m/z* calcd for C₂₂H₂₁N₂O [M+H]⁺: 329.1654, found: 329.1664; HPLC T_R: 2.52 min.

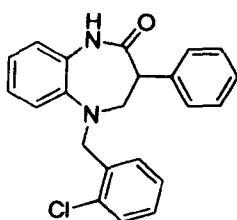
5-(4-Chlorobenzyl)-4,5-dihydro-3-phenyl-1H-benzo[b][1,4]diazepin-2(3H)-one (189)



Using 4-chlorobenzylamine (32 mg, 0.2 mmol) as per General Procedure F yielded 46 mg of **189** (63 %) as a cream solid: mp 172-174.8 °C; ¹H NMR (400 MHz, CDCl₃) δ 7.51 (m, 1H), 7.38-7.09 (m, 10H), 7.10 (td, *J*₁ = 7.6 Hz, *J*₂ = 1.5 Hz, 1H), 6.93 (dd, *J*₁ =

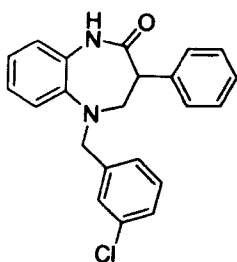
7.6 Hz, $J_2 = 1.5$ Hz, 1H), 5.30 (d, $J = 16.9$ Hz, 1H), 5.17 (d, $J = 16.9$ Hz, 1H), 4.12 (m, 2H), 3.82 (m, 1H), 3.62 (brs, 1H); ^{13}C NMR (100 MHz, CDCl_3) δ 172.9, 141.0, 136.3, 136.0, 135.4, 132.7, 129.6, 128.7, 128.5, 128.3, 127.6, 127.0, 123.3, 123.2, 122.2, 57.9, 51.5, 47.4; HRMS (ESI) m/z calcd for $\text{C}_{22}\text{H}_{20}\text{ClN}_2\text{O}$ $[\text{M}+\text{H}]^+$: 363.1264, found: 363.1120; HPLC T_R : 3.99 min.

5-(2-Chlorobenzyl)-4,5-dihydro-3-phenyl-1H-benzo[b][1,4]diazepin-2(3H)-one (187)



Using 2-chlorobenzylamine (32 mg, 0.2 mmol) as per General Procedure F yielded 35 mg of **187** (48 %) as a cream solid: mp: 148-150 °C; ^1H NMR (400 MHz, CDCl_3) δ 7.38-7.09 (m, 11H), 7.10 (td, $J_1 = 7.8$ Hz, $J_2 = 1.6$ Hz, 1H), 6.93 (dd, $J_1 = 7.8$ Hz, $J_2 = 1.6$ Hz, 1H), 5.30 (d, $J = 15.6$ Hz, 1H), 5.17 (d, $J = 15.6$ Hz, 1H), 4.06 (m, 2H), 3.78 (m, 1H), 3.47 (brs, 1H); ^{13}C NMR (100 MHz, CDCl_3) δ 172.9, 141.0, 139.9, 136.0, 135.4, 134.2, 129.6, 128.3, 127.6, 127.2, 127.1, 127.0, 125.3, 123.3, 123.2, 122.3, 58.0, 51.7, 47.4; HRMS (ESI) m/z calcd for $\text{C}_{22}\text{H}_{20}\text{ClN}_2\text{O}$ $[\text{M}+\text{H}]^+$: 363.1264, found: 363.1117; HPLC T_R : 4.12 min.

5-(3-Chlorobenzyl)-4,5-dihydro-3-phenyl-1H-benzo[b][1,4]diazepin-2(3H)-one (188)

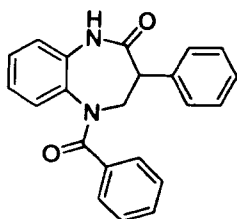


Using 4-chlorobenzylamine (32 mg, 0.2 mmol) as per General Procedure F yielded 39 mg of **188** (54 %) as a cream solid: mp 129-131 °C; ¹H NMR (400 MHz, CDCl₃) δ 7.38-7.09 (m, 11H), 7.10 (td, *J*₁ = 7.8 Hz, *J*₂ = 1.6 Hz, 1H), 6.93 (dd, *J*₁ = 7.8 Hz, *J*₂ = 1.6 Hz, 1H), 5.30 (d, *J* = 15.8 Hz, 1H), 5.17 (d, 15.8 Hz, 1H), 4.08 (m, 2H), 3.80 (m, 1H), 3.53 (brs, 1H); ¹³C NMR (100 MHz, CDCl₃) δ 172.8, 140.8, 136.0, 135.5, 134.9, 132.4, 129.6, 129.2, 128.2, 128.0, 127.6, 127.0, 123.3, 123.0, 122.2, 58.1, 50.1, 47.5; HRMS (ESI) *m/z* calcd for C₂₂H₂₀ClN₂O [M+H]⁺: 363.1264, found: 363.1130; HPLC T_R: 4.17 min.

General Procedure G synthesis of 5-benzoyl-4,5-dihydro-3-phenyl-1H-benzo[b][1,4]diazepin-2(3H)-ones

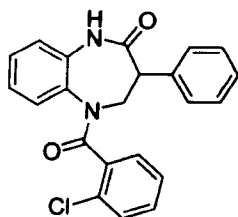
4,5-Dihydro-3-phenyl-1H-benzo[b][1,4]diazepin-2(3H)-one (50 mg, 0.2 mmol), the appropriate benzoylchloride (0.2 mmol) and DMAP (catalytic) were refluxed in pyridine until no starting material was observed by TLC and MS. The reaction mixture was filtered and the solvent removed under reduced pressure. The crude products were purified by flash chromatography.

5-Benzoyl-4,5-dihydro-3-phenyl-1H-benzo[b][1,4]diazepin-2(3H)-one (190)



Using benzoylchloride (28 mg, 0.2 mmol) as per General Procedure G yielded 40 mg (58 %) of **190** as a cream solid: mp 214-217.5 °C; ¹H NMR (400 MHz, CDCl₃) δ 8.7 (brs, 1H), 7.44-6.72 (m, 14H), 5.09 (t, *J* = 11.6 Hz, 1H), 4.01 (m, 2H); ¹³C NMR (100 MHz, CDCl₃) δ 173.5, 171.3, 135.2, 135.2, 135.1, 134.6, 130.3, 129.8, 128.7, 128.5, 128.3, 128.0, 126.3, 122.7, 56.0, 46.8; HRMS (ESI) *m/z* calcd for C₂₂H₁₉N₂O₂ [M+H]⁺: 343.1447, found: 343.1463; HPLC T_R: 1.06 min.

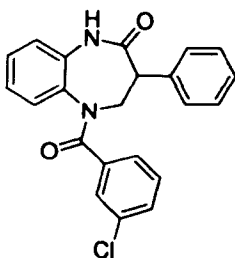
5-(2-Chlorobenzyl)-4,5-dihydro-3-phenyl-1H-benzo[b][1,4]diazepin-2(3H)-one (191)



Using 2-chlorobenzoylchloride (35 mg, 0.2 mmol) as per General Procedure G yielded 36 mg (48 %) of **191** as a cream solid: mp 210.5-212.3 °C; ¹H NMR (400 MHz, CDCl₃) δ 8.08 (brs, 1H), 7.49-6.88 (m, 13H), 5.30 (t, *J* = 12.3 Hz, 1H), 3.97 (m, 2H); ¹³C NMR (100 MHz, CDCl₃) δ 173.1, 168.3, 135.7, 135.3, 134.4, 133.5, 131.2, 130.9, 130.24, 129.8, 129.6, 129.4, 129.2, 128.5, 128.0, 126.5, 126.2, 122.9, 54.7, 46.7; HRMS (ESI) *m/z* calcd for C₂₂H₁₈ClN₂O₂ [M+H]⁺: 377.1057, found: 377.1092; HPLC T_R: 1.25 min.

5-(3-Chlorobenzoyl)-4,5-dihydro-3-phenyl-1H-benzo[b][1,4]diazepin-2(3H)-one

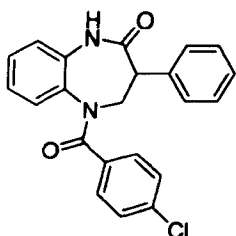
(192)



Using 3-chlorobenzoylchloride (35 mg, 0.2 mmol) as per General Procedure G yielded 32 mg (43 %) of **192** as a cream solid: mp: 204.6-206.5 °C; ¹H NMR (400 MHz, CDCl₃) δ 8.57 (brs, 1H), 7.43-6.72 (m, 13H), 5.06 (t, *J* = 12.6 Hz, 1H), 3.99 (m, 2H); ¹³C NMR (100 MHz, CDCl₃) δ 173.3, 169.7, 136.8, 135.1, 134.7, 134.4, 134.2, 130.4, 130.2, 129.8, 129.2, 129.1, 128.6, 128.5, 128.1, 126.5, 126.1, 122.8, 55.9, 46.8; HRMS (ESI) *m/z* calcd for C₂₂H₁₈ClN₂O₂ [M+H]⁺: 377.1057, found: 377.0894; HPLC T_R: 1.49 min.

5-(4-Chlorobenzoyl)-4,5-dihydro-3-phenyl-1H-benzo[b][1,4]diazepin-2(3H)-one

(193)



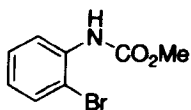
Using 4-chlorobenzoylchloride (35 mg, 0.2 mmol) as per General Procedure G yielded 42 mg (56 %) of **193** as a cream solid: mp: 230.7-233 °C; ¹H NMR (400 MHz, CDCl₃) δ 8.53 (brs, 1H), 7.43-6.72 (m, 13H), 5.05 (t, *J* = 12.5 Hz, 1H), 3.99 (m, 2H), ¹³C NMR (100 MHz, CDCl₃) δ 173.4, 170.1, 136.5, 135.0, 135.0, 134.4, 130.2, 129.8, 129.8,

129.0, 128.5, 128.3, 128.1, 126.6, 122.8, 56.0, 46.8; HRMS (ESI) m/z calcd for $C_{22}H_{18}ClN_2O_2$ $[M+H]^+$: 377.1057, found: 377.0964; HPLC T_R : 1.48 min.

Synthesis of methyl -2-halophenylcarbamates

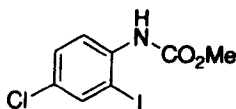
A 50ml round bottomed flask equipped with magnetic stirrer was charged with 20ml of chloroform ($CHCl_3$), 5-chloro-2-iodoaniline (2.53g, 14.8mmol) 1.03g of pyridine (1.05ml, 13mmol) and a catalytic amount of DMAP. The mixture was stirred in an ice bath while 1.13g of methyl chloroformate (0.93ml, 12mmol) was added dropwise over 1 hour maintaining the temperature at $10^\circ C$. The reaction was monitored by tlc (7:3 40-60 petroleum ether: EtOAc) developed in ninhydrin. After that, the mixture was poured onto a large amount of crushed ice and H_2O . The organic phase was washed three times with H_2O (20 mL), saturated NaCl and dried over anhydrous $MgSO_4$. The solvent was removed under reduced pressure. The crude was recrystallised from hexanes.

Methyl 2-bromophenylcarbamate



Pale brown oil that crystallised from a small amount of hexane to give beige needles in the freezer which were filtered washed with light petroleum and dried under vacuum at room temperature 2.55g (74%): 1H NMR (400 MHz, $CDCl_3$) δ 8.14 (d, $J = 8.1$ Hz, 1H), 7.51 (dd, $J_1 = 8$ Hz $J_2 = 1.4$ Hz 1H), 7.31 (td, $J_1 = 8$ Hz $J_2 = 1.4$, 1H), 7.14 (brs 1H), 3.81 (s, 3H).

Methyl 4-chloro-2-iodophenylcarbamate



Beige needles 2.64g (85%): ¹H NMR (400 MHz, CDCl₃) δ 8.15 (s, 1H), 7.65 (d, *J* = 8.5 Hz, 1H), 6.97 (brs, 1H), 5.41 (dd, *J*₁ = 8.5 Hz, *J*₂ = 2.48 Hz, 1H), 3.82 (s, 3H).

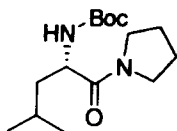
General Procedure H: Syntheses of aminoamides²⁴⁶

(tert-butoxycarbonyl)-protected L-leucine (2.0 g, 8.0 mmol), L-phenylalanine (2.12 g, 8.0 mmol) or L-tryptophan (2.44 mg, 8.0 mmol) were dissolved in dimethylformamide (DMF) (5 mL) under a nitrogen atmosphere. HBTU (4.55 g, 12.0 mmol) and DIEA (2.7 mL, 16 mmol) were successfully added. The reaction mixture was stirred for 1 hour. Pyrrolidine (0.74 mL, 9.0 mmol) or 2M dimethylamine in THF (4.5 mL, 9.0 mmol) was then added and the reaction was allowed to stir for 1 hour. The reaction was acidified with 2N HCl to pH 3, the mixture was diluted with water and extracted with EtOAc. The organic phase was washed with brine and dried (MgSO₄). The solvent was evaporated under reduced pressure. The crude product was purified by flash chromatography on silica gel eluting with petroleum/EtOAc.

General Procedure I: *t*-Boc Deprotection of amino amides.

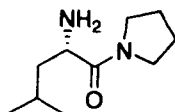
The amino amides were stirred in TFA for 1 hour at room temperature. The volatiles were removed under reduced pressure.

(S)- ϵ -Butyl-4-methyl-1-oxo-1-(pyrrolidin-1-yl)pentan-2-ylcarbamate



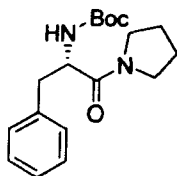
Using General Procedure H, 1.72 g (67 %) of the desired compound was prepared as a colourless oil: $^1\text{H NMR}$ (400 MHz, CDCl_3) δ 5.23 (d, $J = 9.59$ Hz, 1H), 4.45 (td, $J = 9.59$ Hz, 3.83 Hz, 1H), 3.67 (m, 1H), 3.51 (m, 1H), 3.41 (m, 2H), 1.97 (m, 2H), 1.87 (m, 2H), 1.72 (m, 1H), 1.55-1.45 (m, 1H) 1.42 (s, 9H), 1.40-1.31 (m, 1H), 0.98 (d, $J = 6.6$ Hz, 3H). 0.92 (d, $J = 6.6$ Hz, 3H); HRMS (ESI) m/z calcd for $\text{C}_{15}\text{H}_{29}\text{N}_2\text{O}_3$ $[\text{M}+\text{H}]^+$: 285.2178, found: 285.3654.

(S)-2-Amino-4-methyl-1-(pyrrolidin-1-yl)pentan-1-one



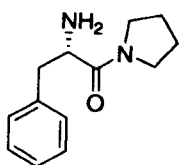
Using General Procedure I, 0.73g (65 %) of the title compound was obtained as a colourless oil: $^1\text{H NMR}$ (400 MHz, CDCl_3) δ 3.55-3.33 (m, 4H), 3.02 (s, 1H), 3.96 (s, 1H), 2.03-1.76 (m, 4H), 1.41-1.30 (m, 2H) 0.93 (m, 6H); HRMS (ESI) m/z calcd for $\text{C}_{10}\text{H}_{21}\text{N}_2\text{O}$ $[\text{M}+\text{H}]^+$ required: 185.1654, found 185.1671.

(S)- ϵ -Butyl-1-oxo-3-phenyl-1-(pyrrolidin-1-yl)propan-2-ylcarbamate



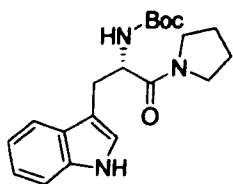
Using General Procedure H, 1.82 g (64 %) of the title compound was prepared as a colourless oil: $^1\text{H NMR}$ (400 MHz, CDCl_3) δ 7.31-7.15 (m, 5H), 5.40 (d, $J = 8.9$ Hz, 1H), 4.57 (dd, $J_1 = 8.9$ Hz, $J_2 = 6.0$ Hz, 1H), 3.38 (m, 3H), 2.96 (m, 2H), 2.54 (m, 1H), 1.88-1.47 (m, 4H), 1.43 (s, 9H); HRMS (ESI) m/z calcd for $\text{C}_{18}\text{H}_{27}\text{N}_2\text{O}_3$ $[\text{M}+\text{H}]^+$ required 319.2022, found: 319.1843.

(S)-2-Amino-3-phenyl-1-(pyrrolidin-1-yl)propan-1-one



Using General Procedure I, 1.08g (87 %) of the title compound was obtained as a colourless oil: $^1\text{H NMR}$ (400 MHz, CDCl_3) δ 7.35-7.19 (m, 5H), 3.73 (t, $J = 6.9$ Hz, 1H), 3.46 (m, 1H), 3.33 (m, 4H), 2.94 (m, 2H), 2.70 (m, 1H) 1.82-1.57 (m, 4H); HRMS (ESI) m/z calcd for $\text{C}_{13}\text{H}_{19}\text{N}_2\text{O}$ $[\text{M}+\text{H}]^+$ required: 219.1497, found 219.1329.

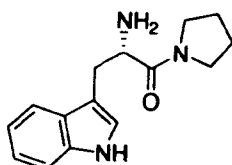
(S)-4-Butyl-3-(1H-indol-3-yl)-1-oxo-1-(pyrrolidin-1-yl)propan-2-ylcarbamate



Using General Procedure H, 1.06 g (85 %) of the title compound was prepared as a colourless oil: $^1\text{H NMR}$ (400 MHz, CDCl_3) δ 8.15 (brs, 1H), 7.62 (d, $J = 7.6$ Hz, 1H), 7.33 (d, $J = 7.6$ Hz, 1H), 7.16 (t, $J = 7.6$ Hz, 1H), 7.13-7.05 (m, 2H), 5.51 (d, $J = 9$ Hz, 1H), 4.66 (dd, $J_1 = 9$ Hz, $J_2 = 6.0$ Hz 1H), 3.48-3.05 (m, 5H), 2.50 (m, 1H), 1.61 (m,

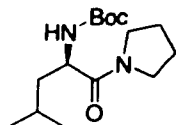
2H), 1.44 (s, 9H), 1.38-1.19 (m, 3H); HRMS (ESI) m/z calcd for $C_{20}H_{28}N_3O_3$ $[M+H]^+$ required: 358.2131, found: 358.2130.

(S)-2-Amino-3-(1H-indol-3-yl)-1-(pyrrolidin-1-yl)propan-1-one



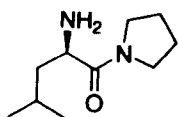
Using General Procedure I, 0.72g (94 %) of the title compound was obtained as a pale brown oil: 1H NMR (400 MHz, $CDCl_3$) δ 8.24 (s, 1H), 7.59 (d, $J = 8.5$ Hz, 1H), 7.36 (d, $J = 8.5$ Hz, 1H), 7.19 (t, $J = 7.5$ Hz, 1H) 7.14-7.06 (m, 2H), 3.83 (t, $J = 7.3$ Hz, 1H), 3.49-3.42 (m, 1H), 3.40-3.31 (m, 2H), 3.19-3.11 (m, 1H), 2.99-2.87 (m, 2H), 1.79-1.49 (m, 6H); HRMS (ESI) m/z calcd for $C_{15}H_{20}N_3O$ $[M+H]^+$ required: 258.1606, found: 258.1574.

(R)- *t*-Butyl-4-methyl-1-oxo-1-(pyrrolidin-1-yl)pentan-2-ylcarbamate



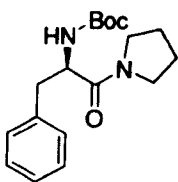
Using General Procedure H, 0.71 g (28 %) of the desired compound was prepared as a colourless oil: 1H NMR (400 MHz, $CDCl_3$) δ 5.23 (d, $J = 9.59$ Hz, 1H), 4.45 (td, $J_1 = 9.59$ Hz, $J_2 = 3.83$ Hz, 1H), 3.67 (m, 1H), 3.51 (m, 1H), 3.41 (m, 2H) 1.97 (m, 2H), 1.87 (m, 2H), 1.72 (m, 1H), 1.55-1.45 (m, 1H), 1.42 (s, 9H), 1.40-1.31 (m, 1H), 0.98 (d, $J = 6.6$ Hz, 3H). 0.92 (d, $J = 6.6$ Hz, 3H); HRMS (ESI) m/z calcd for $C_{15}H_{29}N_2O_3$ $[M+H]^+$ required: 285.2178, found: 285.1938.

(R)-2-Amino-4-methyl-1-(pyrrolidin-1-yl)pentan-1-one



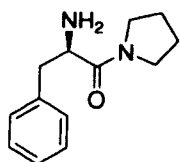
Using General Procedure I, 430 g (94 %) Colourless oil, $^1\text{H NMR}$ (400 MHz, CDCl_3) δ 3.60 (brs, 1H), 3.55-3.33 (m, 4H), 3.17 (brs, 2H), 1.96-1.76 (m, 4H), 1.45-1.30 (m, 2H), 0.89 (s, 3H), 0.88 (s, 3H); HRMS (ESI) m/z calcd for $\text{C}_{10}\text{H}_{21}\text{N}_2\text{O}$ $[\text{M}+\text{H}]^+$ required: 185.1654, found: 185.1342.

(R)-*t*-Butyl-1-oxo-3-phenyl-1-(pyrrolidin-1-yl)propan-2-ylcarbamate



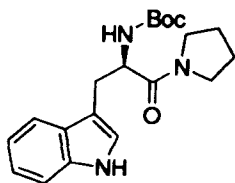
Using General Procedure H, 1.02 g (36 %) of the desired compound was prepared as a colourless oil: $^1\text{H NMR}$ (400 MHz, CDCl_3) δ 7.28-7.17 (m, 5H), 5.40 (d, $J = 8.8$ Hz, 1H), 4.57 (m, 1H), 3.38 (m, 3H), 2.96 (m, 2H), 2.57 (m, 1H), 1.88-1.47 (m, 4H), 1.43 (s, 9H); HRMS (ESI) m/z calcd for $\text{C}_{18}\text{H}_{27}\text{N}_2\text{O}_3$ $[\text{M}+\text{H}]^+$ required 319.2022, found 319.1941.

(R)-2-Amino-3-phenyl-1-(pyrrolidin-1-yl)propan-1-one



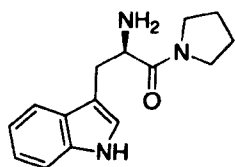
Using General Procedure I, 0.62 g (89 %) Colourless oil, $^1\text{H NMR}$ (400 MHz, CDCl_3) δ 7.35-7.19 (m, 5H), 3.73 (t, $J = 6.9$ Hz, 1H), 3.46 (m, 1H), 3.33 (m, 4H), 2.94 (m, 2H), 2.70 (m, 1H), 1.82-1.57 (m, 4H); HRMS (ESI) m/z calcd for $\text{C}_{13}\text{H}_{19}\text{N}_2\text{O}$ $[\text{M}+\text{H}]^+$ required: 219.1497, found 219.1212.

(R)-*t*-Butyl-3-(1H-indol-3-yl)-1-oxo-1-(pyrrolidin-1-yl)propan-2-ylcarbamate



Using General Procedure H, 1.02 g (32 %) of the desired compound was prepared as a white solid: $^1\text{H NMR}$ (400 MHz, CDCl_3) δ 8.16 (brs, 1H), 7.62 (d, $J = 7.6$ Hz, 1H), 7.33 (d, $J = 7.6$ Hz, 1H), 7.16 (t, $J = 7.6$ Hz, 1H), 7.13-7.05 (m, 2H), 5.50 (d, $J = 9$ Hz, 1H), 4.67 (m, 1H), 3.48-3.05 (m, 5H), 2.51 (m, 1H), 1.61 (m, 2H), 1.44 (s, 9H), 1.38-1.19 (m, 3H); HRMS (ESI) m/z calcd for $\text{C}_{20}\text{H}_{28}\text{N}_3\text{O}_3$ $[\text{M}+\text{H}]^+$ required: 358.2131, found: 358.2057.

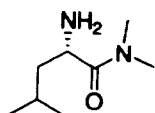
(R)-2-Amino-3-(1H-indol-3-yl)-1-(pyrrolidin-1-yl)propan-1-one



Using General Procedure I, 715 mg (97 %) of the title compound was obtained as a cream solid, $^1\text{H NMR}$ (400 MHz, CDCl_3) δ 8.24 (s, 1H), 7.59 (d, $J = 8.5$ Hz, 1H), 7.36 (d, $J = 8.5$ Hz, 1H), 7.19 (t, $J = 7.5$ Hz, 1H), 7.14-7.06 (m, 2H), 3.83 (t, $J = 7.3$ Hz, 1H),

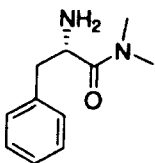
3.49-3.42 (m, 1H), 3.40-3.31 (m, 2H), 3.19-3.11 (m, 1H), 2.99-2.87 (m, 2H), 1.79-1.49 (m, 6H); HRMS (ESI) m/z calcd for $C_{15}H_{20}N_3O$ $[M+H]^+$ required 258.1606, found: 258.1580.

(S)-2-Amino-N,N,4-trimethylpentanamide



Using General Procedure I: 1H NMR (400 MHz, $CDCl_3$) δ 3.68–3.76 (m, 1H), 3.02 (s, 3H), 2.96 (s, 3H), 1.75–1.93 (m, 1H), 1.62 (s, 2H), 1.29–1.39 (m, 2H), 0.94 (d, $J = 6.6$ Hz, 3H), 0.93 (d, $J = 6.7$ Hz, 3H); HRMS (ESI) m/z calcd for $C_8H_{19}N_2O$ $[M+H]^+$: 159.1497, found: 159.1597.

(S)-2-Amino-N,N-dimethyl-3-phenylpropanamide

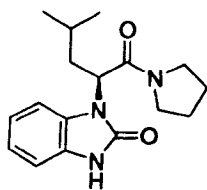


Using General Procedure I: 1H NMR (400 MHz, $CDCl_3$) δ 7.15–7.34 (m, 5H), 3.94 (t, $J = 7.2$ Hz, 1H), 2.94 (dd, $J_1 = 13.2$, $J_2 = 6.8$ Hz, 1H), 2.91 (s, 3H), 2.77 (dd, $J_1 = 13.2$, $J_2 = 7.4$ Hz, 1H), 2.73 (s, 3H), 1.80 (s, 2H), HRMS (ESI) m/z calcd for $C_{11}H_{17}N_2O$ $[M+H]^+$: 193.1341, found: 193.1347.

General Procedure J: syntheses of benzoimidazolones

A Schlenk tube was charged with the appropriate methyl-2-halophenylcarbamate, (1.0mmol), CuI (38mg, 0.2mmol), L-proline (46mg, 0.4mmol), and K₃PO₄ (424mg, 2.0mmol), evacuated and backfilled with nitrogen (3 cycles). Aminoamide (1.0mmol) and DMSO (2ml) were added. The reaction mixture was stirred at 70 °C until the coupling was completed detected by TLC. The solution was then heated at 130 °C until the coupling product disappeared, monitored by TLC and mass spec. The cooled mixture was then partitioned between EtOAc and saturated NH₄Cl. The organic layer was washed with saturated NaCl, dried over anhydrous MgSO₄ and concentrated under vacuum. The residue was then purified by normal phase flash column chromatography on silica gel with the appropriate ration of EtOAc and petroleum ether mobile phase to provide the desired product.

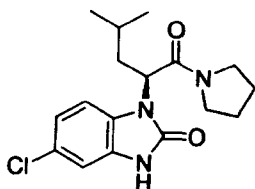
(S)-1-(4-Methyl-1-oxo-1-(pyrrolidin-1-yl)pentan-2-yl)-1H-benzo[d]imidazol-2(3H)-one (208)



Using General Procedure J 81 mg, (27%) of **208** was obtained: mp 170.3-173 °C; ¹H NMR (400 MHz, CDCl₃) δ 9.49 (s, 1H), 7.46 (m, 1H), 7.07 (m, 3H), 5.33 (dd, *J*₁ = 9.73 Hz, *J*₂ = 5.05 Hz, 1H), 3.65 (m, 1H), 3.53 (m, 1H), 3.42 (m, 1H), 3.29 (m, 1H), 2.15 (m, 1H), 2.02-1.78 (m, 4H), 1.73 (m, 1H), 1.01 (d, *J* = 6.84 Hz, 3H), 0.09 (d, *J* = 6.84 Hz, 3H); ¹³C NMR (100 MHz, CDCl₃) δ 167.6, 155.2, 128.7, 127.9, 121.7, 121.7, 111.3,

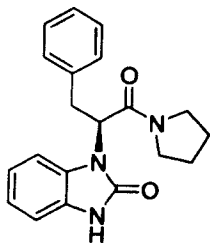
109.4, 52.1, 46.4, 46.4, 37.9, 26.3, 24.6, 23.9, 23.2, 22.0; HRMS (ESI) m/z calcd for $C_{17}H_{24}N_3O_2$ $[M+H]^+$ required: 302.1869, found 302.1727; $[\alpha]_D^{20} = -112^\circ$ (c 0.75, DCM); HPLC T_R : 8.73 min..

(S)-5-Chloro-1-(4-methyl-1-oxo-1-(pyrrolidin-1-yl)pentan-2-yl)-1H-benzo[d]imidazol-2(3H)-one (213)



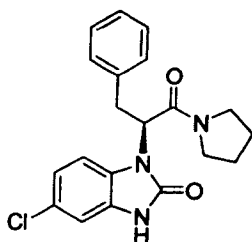
Using General Procedure J, 141 mg, (42%) of **213** was obtained: mp 153-155 °C; 1H NMR (400 MHz, $CDCl_3$) δ 9.49 (s, 1H), 7.56 (d, $J = 8.48$ Hz, 1H), 7.07 (d, $J = 2.01$ Hz, 1H), 7.03 (dd, $J_1 = 8.48$ Hz, $J_2 = 2.01$ Hz, 1H), 5.33 (dd, $J_1 = 9.9$ Hz, $J_2 = 5.80$ Hz, 1H), 3.64 (m, 1H), 3.35 (m, 1H), 3.39 (m, 2H), 2.12 (m, 1H), 2.02-1.71 (m, 5H), 1.42 (m, 1H), 1.01 (d, $J = 6.62$ Hz, 3H), 0.9 (d, $J = 6.62$ Hz, 3H); ^{13}C NMR (100 MHz, $CDCl_3$) δ 167.6, 155.4, 129.0, 127.4, 127.3, 121.6, 112.2, 109.9, 52.2, 46.6, 46.4, 37.8, 26.22, 24.6, 24.0, 23.1, 21.9; HRMS (ESI) m/z calcd for $C_{17}H_{23}ClN_3O_2$ $[M+H]^+$: 336.1479, found 336.1434; $[\alpha]_D^{20} = -67.4^\circ$ (c 1.84, DCM); HPLC T_R : 10.02 min.

(S)-1-(1-Oxo-3-phenyl-1-(pyrrolidin-1-yl)propan-2-yl)-1H-benzo[d]imidazol-2(3H)-one (210)



Using General Procedure J, 231 mg, (69%) of **210** was obtained: mp 162-165 °C; ¹H NMR (400 MHz, CDCl₃) δ 8.73 (s, 1H), 7.56 (m, 1H), 7.21-6.97 (m, 4H), 5.41 (m, 1H), 3.58-3.28 (m, 5H), 3.15 (m, 1H), 1.80 (m, 3H), 1.70 (m, 1H); ¹³C NMR (100 MHz, CDCl₃) δ 166.8, 155.0, 137.1, 129.3, 128.6, 128.3, 127.7, 126.7, 121.8, 121.8, 121.8, 111.0, 109.7, 55.3, 46.4, 46.4, 35.3, 26.2, 23.9; HRMS (ESI) m/z calcd for C₂₀H₂₂N₃O₂ [M+H]⁺ 336.1712, found 336.1597; [α]_D²⁰ = -97.2° (c 0.91, DCM) HPLC T_R: 8.83 min.

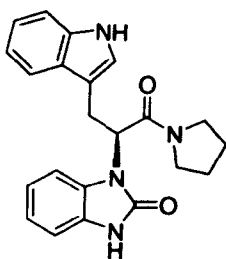
(S)-5-Chloro-1-(1-oxo-3-phenyl-1-(pyrrolidin-1-yl)propan-2-yl)-1H-benzo[d]imidazol-2(3H)-one (215)



Using General Procedure J, 152 mg, (41 %) of **215** was obtained: mp 91-93 °C; ¹H NMR (400 MHz, CDCl₃) δ 9.24 (s, 1H), 7.32 (d, *J* = 8.75 Hz, 1H), 7.21-6.98 (m, 4H), 5.41 (m, 1H), 3.51 (m, 2H), 3.42 (m, 2H), 3.31 (m, 1H), 3.20 (m, 1H), 1.89-1.68 (m, 4H); ¹³C NMR (100 MHz, CDCl₃) δ 166.6, 155.0, 136.7, 129.2, 128.6, 128.4, 127.5, 127.3,

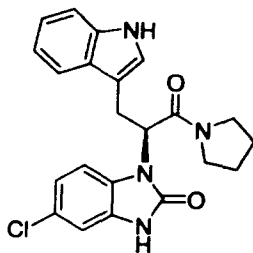
126.9, 121.8, 112.1, 110.1, 55.4, 46.5, 46.4, 35.3, 26.1, 23.9; HRMS (ESI) m/z calcd for $C_{20}H_{21}ClN_3O_2$ $[M+H]^+$: 370.1322, found 370.1314; $[\alpha]_D^{20} = -41.7^\circ$ (c 1.49, DCM). HPLC T_R : 9.93 min

(S)-1-(3-(Indol-3-yl)-1-7oxo-1-(pyrrolidin-1-yl)propan-2-yl)-1H-benzo[d]imidazol-2(3H)-one (211)



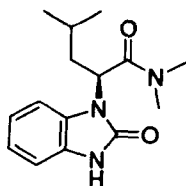
Using General Procedure J, 45 mg, (12 %) of **211** was obtained: 1H NMR (400 MHz, $CDCl_3$) δ 9.76 (s, 1H), 8.08 (s, 1H), 7.61 (d, 7.1 Hz, 1H), 7.53 (d, 7.1 Hz, 1H), 7.20-7.21 (m, 5H), 7.21 (d, $J = 8.41$ Hz, 1H), 6.93 (m, 1H), 6.81 (d, $J = 2.28$ Hz, 1H), 5.53 (m, 1H), 3.74 (m, 1H), 3.55-3.36 (m, 4H), 3.14 (m, 1H), 1.79-1.61 (m, 4H); ^{13}C NMR (100 MHz, $CDCl_3$) δ 167.3, 155.2, 136.0, 128.7, 128.0, 127.5, 123.2, 121.8, 121.8, 121.7, 119.3, 118.4, 111.2, 111.1, 110.8, 109.7, 54.5, 46.4, 46.4, 26.1, 25.1, 23.8; HRMS (ESI) m/z calcd for $C_{22}H_{23}N_4O_2$ $[M+H]^+$: 375.1821, found 375.1798; $[\alpha]_D^{20} = -68.2^\circ$ (c 2.2, DCM); HPLC T_R : 8.83 min.

(S)-5-Chloro-1-(3-(indol-3-yl)-1-oxo-1-(pyrrolidin-1-yl)propan-2-yl)-1H-benzo[d]imidazol-2(3H)-one (216)



Using General Procedure J, 86 mg, (21 %) of **216** was obtained: ^1H NMR (400 MHz, CDCl_3) δ 9.10 (s, 1H), 7.88 (brs, 1H), 7.57 (d, $J = 8.4$ Hz, 1H), 7.53 (d, $J = 7.3$ Hz, 1H), 7.21 (d, $J = 8.41$ Hz, 1H), 7.14 (dt, $J_1 = 7.5$ Hz, $J_2 = 1.2$ Hz, 1H), 7.11-7.06 (m, 2H), 6.93 (d, $J = 2.03$ Hz, 1H), 6.84 (d, $J = 2.35$ Hz, 1H), 5.51 (m, 1H), 3.70 (m, 1H), 3.56-3.33 (m, 4H), 3.20 (m, 1H), 1.88-1.67 (m, 4H); ^{13}C NMR (100 MHz, CDCl_3) δ 167.0, 155.1, 136.0, 128.7, 127.4, 127.4, 127.3, 123.0, 122.0, 121.8, 119.5, 118.4, 112.1, 111.2, 110.7, 110.0, 54.5, 46.5, 46.3, 26.1, 25.1, 23.9; HRMS (ESI) m/z calcd for $\text{C}_{22}\text{H}_{22}\text{ClN}_4\text{O}_2$ [$\text{M}+\text{H}$] $^+$ required: 409.1431, found 409.1603; $[\alpha]_D^{20} = -40^\circ$ (c 0.5, DCM); HPLC T_R : 8.83 min.

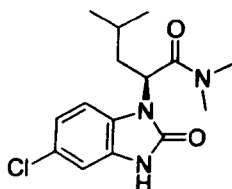
(S)-2-(1,2-Dihydro-2-oxobenzo[d]imidazol-3-yl)-N,N,4-trimethylpentanamide (207)



Using General Procedure J, 151 mg, (55 %) of **207** was obtained: mp 198-200 $^\circ\text{C}$; ^1H NMR (400 MHz, CDCl_3) δ 8.86 (s, 1H), 7.41 (m, 1H), 7.05 (m, 3H), 5.45 (dd, $J_1 = 9.3$

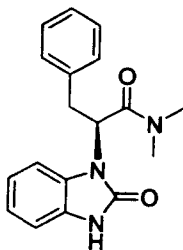
Hz, $J_2 = 5.4$ Hz, 1H), 3.06 (s, 3H), 2.94 (s, 3H), 2.10 (m, 1H), 1.94 (m, 1H), 1.44 (m, 1H), 1.01 (d, $J = 6.5$ Hz, 3H), 0.89 (d, $J = 6.5$ Hz, 3H); ^{13}C NMR (100 MHz, CDCl_3) δ 169.1, 155.2, 128.6, 128.1, 121.7, 121.6, 111.1, 109.6, 50.3, 38.2, 37.0, 36.2, 24.5, 23.1, 22.0; HRMS (ESI) m/z calcd for $\text{C}_{15}\text{H}_{22}\text{N}_3\text{O}_2$ $[\text{M}+\text{H}]^+$ required 276.1712, found 276.1649; $[\alpha]_D^{20} = -193.4^\circ$ (c 1.82, DCM); HPLC T_R : 8.52 min.

(S)-2-(6-Chloro-1,2-dihydro-2-oxobenzo[d]imidazol-3-yl)-N,N,4-trimethylpentanamide (212)



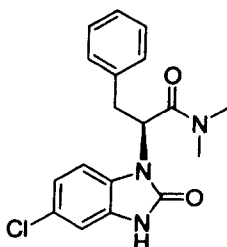
Using General Procedure J, 152 mg, (49 %) of **212** was obtained: mp 149-152 °C; ^1H NMR (400 MHz, CDCl_3) δ 9.22 (s, 1H), 7.37 (d, $J = 8.9$ Hz, 1H), 7.07-7.01 (m, 2H), 5.45 (dd, $J_1 = 9.9$ Hz, $J_2 = 5.8$ Hz, 1H), 3.08 (s, 3H), 2.95 (s, 3H), 2.08 (m, 1H), 1.94 (m, 1H), 1.41 (m, 1H), 1.00 (d, $J = 6.6$ Hz, 3H), 0.89 (d, $J = 6.6$ Hz, 3H); ^{13}C NMR (100 MHz, CDCl_3) δ 168.0, 155.2, 128.9, 127.4, 127.3, 121.7, 112.2, 110.0, 50.3, 38.1, 37.1, 36.1, 24.6, 23.0, 22.0; HRMS (ESI) m/z calcd for $\text{C}_{15}\text{H}_{21}\text{ClN}_3\text{O}_2$ $[\text{M}+\text{H}]^+$ required 310.1322, found 310.1245; $[\alpha]_D^{20} = -110.4^\circ$ (c 1.19, DCM); HPLC T_R : 9.69 min.

(S)-2-(1,2-Dihydro-2-oxobenzo[d]imidazol-3-yl)-N,N-dimethyl-3-phenylpropanamide (209)



Using General Procedure J, 189 mg, (61 %) of **209** was obtained: mp 166-168 °C; ^1H NMR (400 MHz, CDCl_3) δ 8.33 (s, 1H), 7.52 (m, 1H), 7.20-6.99 (m, 8H), 5.54 (dd, $J_1 = 9$ Hz, $J_2 = 6.4$ Hz, 1H), 3.49 (m, 1H), 3.35 (m, 1H), 2.95 (s, 3H), 2.94 (s, 3H); ^{13}C NMR (100 MHz, CDCl_3) δ 168.3, 154.8, 137.1, 129.3, 128.5, 128.3, 127.8, 126.7, 121.8, 121.9, 110.9, 109.8, 53.7, 36.9, 36.2, 35.6; HRMS (ESI) m/z calcd for $\text{C}_{18}\text{H}_{20}\text{N}_3\text{O}_2$ $[\text{M}+\text{H}]^+$ 310.1556, found 310.1440; $[\alpha]_D^{20} = -182.9^\circ$ (c 1.05, DCM); HPLC T_R : 8.29 min

(S)-2-(6-Chloro-1,2-dihydro-2-oxobenzo[d]imidazol-3-yl)-N,N-dimethyl-3-phenylpropanamide (214)



Using General Procedure J, 308 mg, (58 %) of **214** was obtained: mp 141-143 °C; ^1H NMR (400 MHz, CDCl_3) δ 9.62 (m, 1H), 7.46 (d, $J = 8.6$ Hz, 1H), 7.19-7.01 (m, 7H), 5.53 (m, 1H), 3.45 (m, 1H), 3.33 (m, 1H), 2.95 (m, 6H); ^{13}C NMR (100 MHz, CDCl_3) δ

168.2, 154.9, 136.7, 129.2, 128.9, 128.4, 127.5, 127.1, 126.9, 121.8, 111.9, 110.3, 53.7, 37.0, 36.2, 35.6; HRMS (ESI) m/z calcd for $C_{18}H_{19}ClN_3O_2$ $[M+H]^+$ 344.1166, found 344.1173; $[\alpha]_D^{20} = -64.9^\circ$ (c 2.25, DCM); HPLC T_R : 9.93 min.

5.2 Computational Methods

5.2.1 General methods

2D structures were prepared using Chemdraw Ultra Version 8.0 (Cambridge Soft) and saved in .skc format. The remaining programs used are by Openeye²¹² and the following versions were used throughout. Babel 3 Version 2.1 was used to convert file formats. Vida Version 2.1.1 was used for preparing the query molecules, visualisation of results from ROCS and FRED and creating images. The Zinc database was filtered with Filter Version 2.0.1. Multi-conformer dataset generation was performed using Omega Version 2.1.0. ROCS Version 2.2 was used to perform the shape based screen and all docking was performed with FRED Version 2.2 and scored with the default scoring function, Chemgauss 3.

5.2.2 Command lines, parameter files and prefixes.

The above versions of all of the Openeye programs, with the exception of Vida, are run from the command line. Unless specifically flagged on the command line all parameters run at their default settings. Examples of command lines used to perform the tasks as outlined are given. Each time the programmes are run a .param file is created which lists all of the parameters and their settings used. Examples of parameter files from Omega and ROCS showing all of the settings used during conformer generation and screening in this project are given Sections 5.2.6-5.2.9. It is possible to use the

.param file generated during a run to perform subsequent runs with the same parameters by flagging `-param <filename>.param` on the command line. Any parameter flagged on the command line will take precedence over the corresponding setting in the .param file. The `-prefix` flag on the command line is used to prefix all output files produced by a run with the same name.

5.2.3 Spiro-oxindole query preparation

The 2D structure of MI-43 was prepared using Chemdraw Ultra Version 8.0 saved in .skc format and converted to .ism (isomeric SMILES) using Babel 3.

```
prompt> babel3 -in MI43.skc -out MI43.ism
```

All stereoisomers were enumerated using Flipper (a component of Omega) the output was saved in .sdf format.

```
prompt> flipper -in MI43.ism -out MI43.sdf
```

The desired stereoisomer was visually selected using Vida2 saved as .oeb.gz format and a multi conformer database of it was generated using Omega2 and also saved in .oeb.gz format. Conformers were enumerated up to a maximum energy of 8 kcal mol⁻¹ above that global minimum sampled at a density such that conformers had a minimum RMSD of 0.5 as defined by the `-ewindow` and `-rms` flags respectively.

```
prompt> omega -in MI43.oeb.gz -out MI43_multi.oeb.gz -ewindow 8 -rms  
0.5 -prefix MI219_multi
```

The multi conformer database was docked into MDM2 1YCR¹ using FRED and the top 20 poses as ranked by the default scoring function, Chemgauss 3, were output.

```
prompt> fred -dbase MI43_multi.oeb.gz -rec 1YCR_rec.oeb.gz -prefix MI43  
-num alt poses 20
```

The docked poses were visualised in Vida2. The top ranked pose bound in the predicted manner¹³² and was selected and saved in .oeb.gz format to be used as the ROCS query.

5.2.4 Nutlin and Benzodiazepiene query preparation

Using Vida 2 Nutlin-2 and the benzodiazepiene were extracted from their respective X-ray co-crystal structures, 1RV1 and 1T4E downloaded from the PDB database. The atoms of the solubilising groups of Nutlin-2 were deleted and both structures were saved as .oeb.gz format to be used as ROCS queries.

5.2.5 Database preparation

The the “all purchasable subset” of the Zinc database with protonation states enumerated between pH 5.75 to 8.25 was downloaded in .mol2 format. The filter file, blockbuster_drug.txt, was prepared by taking the most lenient combination of allowed physical properties and chemistry/functional groups from the supplied filter_blockbuster.txt and filter_drug.txt files. Blockbuster_drug.txt Section 5.2.8 was used as the basis for filtering the database with Filter Version 2.0.1. The filtered dataset was saved in .oeb.gz format.

```
prompt> filter -in zinc_purchaseable.mol2 -out  
zinc_purchaseable_blockbusterdrug.oeb.gz -filter blockbuster_drug.txt
```

The multi conformer database was generated using Omega Version 2.1.0 and written in .oeb.gz format with offset rotor compression. Conformers were enumerated up to a maximum energy of 8 kcal mol⁻¹ above the global minimum sampled at a density such that conformers had a minimum RMSD of 0.5 as defined by the -ewindow and -rms flags respectively. The task was distributed to X processors in Y work stations as defined in the file pvm.conf. An example of a pvm.conf file is shown in Section 5.2.9

```
prompt> omega -in zinc_purchaseable_blockbusterdrug.oeb.gz -out
zinc_purchasable_blockbusterdrug_multi.oeb.gz.oeb.gz -ewindow 8 -rms 0.5
-prefix zinc_purchasable_blockbusterdrug_multi -rotorOffsetCompress true -
pvmconf pvm.conf
```

ROCS, Version 2.2, was used to screen the multiconformer database. Chemistry overlap was optimised using the Implicit Mills Dean forcefield supplied with ROCS. The top 500 hits as ranked by combo score were output in .sdf format. The task was distributed to X processors in Y work stations as defined in the file pvm.conf (Section 5.2.9

```
prompt> ROCS -query benzodiazepiene_pdb.oeb.gz -dbase
zinc_purchasable_blockbusterdrug_multi.oeb.gz -besthits 500 -rankby combo -
optchem true -chemff ImplicitMillsDean -prefix
zinc_purchasable_blockbusterdrug_benzodiazepiene -pvmconf pvm.conf
```

The hits were visually inspected and manually clustered in Vida 2.

5.2.6 Omega .param file examples

The Omega .param file used in this project to generate the multi conformer dataset of the Zinc all purchasable database.

```
#Interface settings
```

```
#File Options :
```

```
-commentEnergy false (default)
-in zinc_purchaseable_blockbusterdrug.oeb.gz
-includeInput false (default)
#-log (Not set, no default)
-out zinc_purchaseable_blockbusterdrug_multi.oeb.gz
#-param (Not set, no default)
-prefix zinc_purchaseable_blockbusterdrug_multi
-rotorOffsetCompress true
-sdEnergy false (default)
#-status (Not set, no default)
-verbose false (default)
-warts false (default)
```

```
#3D Construction Parameters :
```

```
#-addfraglib (Not set, no default)
-buildff mmff94s_NoEstat (default)
-canonOrder true (default)
-deleteFixHydrogens true (default)
-dielectric 1.000000 (default)
-exponent 1.000000 (default)
#-fixfile (Not set, no default)
-fixrms 0.150000 (default)
-fromCT true (default)
-maxmatch 10 (default)
#-setfraglib (Not set, no default)
-umatch true (default)
```

```
#Structure Enumeration :
```

```
-enumNitrogen true (default)
-enumRing true (default)
```

```
#Torsion Driving Parameters :
  #-erange (Not set, no default)
  -ewindow 8.000000
  #-maxConfRange (Not set, no default)
  -maxconfgen 50000 (default)
  -maxconfs 400 (default)
  -maxrot -1 (default)
  -maxtime 120.000000 (default)
  -rangeIncrement 5 (default)
  -rms 0.500000
  #-rmsrange (Not set, no default)
  -searchff mmff94s_NoEstat (default)
  -tordrive true (default)
  #-torlib (Not set, no default)
```

```
#PVM :
  #-pvmconf pvm.conf
  -pvmdebug false (default)
  #-pvmlog (Not set, no default)
  -pvmpass 10 (default)
```

5.2.7 Example of the ROCS Parameter file used in this screen

```
#Interface settings
```

```
#InputOptions :
  -query benzodiazepiene_pdb.oeb.gz
  -mcquery false (default)
  -dbase zinc_purchasable_blockbusterdrug_multi.oeb.gz
  -scdbase false (default)
  #-param (Not set, no default)
```

```
#OutputOptions :
  -prefix zinc_purchasable_blockbusterdrug_benzodiazepiene
  -besthits 500 (default)
  -cutoff 0.000000 (default)
  -rankby combo
  -maxconfs 1 (default)
  -maxhits 0 (default)
```

```

#HitsOutputOptions :
-conflabel title (default)
-outputquery true (default)
-nostructs false (default)
#-hitsfile (Not set, no default)
-oformat sdf (default)

#ReportOutputOptions :
-report each (default)
#-reportfile (Not set, no default)
-stats hits (default)

#LogOutputOptions :
#-logfile (Not set, no default)
-verbose false (default)

#ShapeOptions :
-tanimoto_cutoff 0.000000 (default)
-subtan false (default)
#-randomstarts (Not set, no default)
-opt true (default)
-scoreonly false (default)

#ColorOptions :
-allcolor false (default)
-chemff ImplicitMillsDean
-optchem true

#PVM :
-pvmconf pvm.conf
-pvmdebug false (default)
-pvmpass 5 (default)

```

5.2.8 The Filter file used in this project, blockbuster_drug.txt.

```

#/*
#Copyright (C) 2000-2005 by OpenEye Scientific Software, Inc.
#*/
#This file defines the rules for filtering multi-structure files based on
#properties and substructure patterns.
MIN_MOLWT      130          "Minimum molecular weight"

```

| | | |
|--|------|---|
| MAX_MOLWT | 781 | "Maximum molecular weight" |
| MIN_NUM_HVY | 9 | "Minimum number of heavy atoms" |
| MAX_NUM_HVY | 55 | "Maximum number of heavy atoms" |
| MIN_RING_SYS | 0 | "Minimum number of ring systems" |
| MAX_RING_SYS | 5 | "Maximum number of ring systems" |
| MIN_RING_SIZE | 0 | "Minimum atoms in any ring system" |
| MAX_RING_SIZE | 20 | "Maximum atoms in any ring system" |
| MIN_CON_NON_RING | 0 | "Minimum number of connected non-ring atoms" |
| MAX_CON_NON_RING | 19 | "Maximum number of connected non-ring atoms" |
| MIN_FCNGRP | 0 | "Minimum number of functional groups" |
| MAX_FCNGRP | 7 | "Maximum number of functional groups" |
| MIN_UNBRANCHED | 1 | "Minimum number of connected unbranched non-ring atoms" |
| MAX_UNBRANCHED | 13 | "Maximum number of connected unbranched non-ring atoms" |
| MIN_CARBONS | 3 | "Minimum number of carbons" |
| MAX_CARBONS | 41 | "Maximum number of carbons" |
| MIN_HETEROATOMS | 1 | "Minimum number of heteroatoms" |
| MAX_HETEROATOMS | 14 | "Maximum number of heteroatoms" |
| MIN_Het_C_Ratio | 0.04 | "Minimum heteroatom to carbon ratio" |
| MAX_Het_C_Ratio | 4.0 | "Maximum heteroatom to carbon ratio" |
| MIN_HALIDE_FRACTION | 0.0 | "Minimum Halide Fraction" |
| MAX_HALIDE_FRACTION | 0.66 | "Maximum Halide Fraction" |
| <p>#count ring degrees of freedom = (#BondsInRing) - 4 - (RigidBondsInRing) - (BondsSharedWithOtherRings)</p> <p>#must be >= 0, from JCAMD 14:251-265,2000.</p> | | |
| ADJUST_ROT_FOR_RING | true | "BOOLEAN for whether to estimate degrees of freedom in rings" |
| MIN_ROT_BONDS | 0 | "Minimum number of rotatable bonds" |
| MAX_ROT_BONDS | 16 | "Maximum number of rotatable bonds" |
| MIN_RIGID_BONDS | 4 | "Minimum number of rigid bonds" |

| | | |
|--|-----------|---|
| MAX_RIGID_BONDS | 55 | "Maximum number of rigid bonds" |
| MIN_HBOND_DONORS | 0 | "Minimum number of hydrogen-bond donors" |
| MAX_HBOND_DONORS | 9 | "Maximum number of hydrogen-bond donors" |
| MIN_HBOND_ACCEPTORS | 0 | "Minimum number of hydrogen-bond acceptors" |
| MAX_HBOND_ACCEPTORS | 13 | "Maximum number of hydrogen-bond acceptors" |
| MIN_LIPINSKI_DONORS | 0 | "Minimum number of hydrogens on O & N atoms" |
| MAX_LIPINSKI_DONORS | 6 | "Maximum number of hydrogens on O & N atoms" |
| MIN_LIPINSKI_ACCEPTORS | 1 | "Minimum number of oxygen & nitrogen atoms" |
| MAX_LIPINSKI_ACCEPTORS | 14 | "Maximum number of oxygen & nitrogen atoms" |
| MIN_COUNT_FORMAL_CRG | 0 | "Minimum number formal charges" |
| MAX_COUNT_FORMAL_CRG | 4 | "Maximum number of formal charges" |
| MIN_SUM_FORMAL_CRG | -2 | "Minimum sum of formal charges" |
| MAX_SUM_FORMAL_CRG | 2 | "Maximum sum of formal charges" |
| MIN_CHIRAL_CENTERS | 0 | "Minimum chiral centers" |
| MAX_CHIRAL_CENTERS | 21 | "Maximum chiral centers" |
| MIN_XLOGP | -3.0 | "Minimum XLogP" |
| MAX_XLOGP | 6.85 | "Maximum XLogP" |
| #choices are insoluble<poorly<moderately<soluble<very<highly | | |
| MIN_SOLUBILITY | insoluble | "Minimum solubility" |
| PSA_USE_SandP | false | "Count S and P as polar atoms" |
| MIN_2D_PSA | 0.0 | "Minimum 2-Dimensional (SMILES) Polar Surface Area" |
| MAX_2D_PSA | 205.0 | "Maximum 2-Dimensional (SMILES) Polar Surface Area" |
| AGGREGATORS | true | "Eliminate known aggregators" |
| PRED_AGG | false | "Eliminate predicted aggregators" |
| #secondary filters (based on multiple primary filters) | | |
| GSK_VEBER | false | "PSA>140 or >10 rot bonds" |
| MAX_LIPINSKI | 3 | "Maximum number of Lipinski violations" |
| MIN_ABS | 0.11 | "Minimum probability F>10% in rats" |
| PHARMACOPIA | false | "LogP > 5.88 or PSA > 131.6" |

ALLOWED_ELEMENTS H,C,N,O,F,P,S,Cl,Br,I

ELIMINATE_METALS Sc,Ti,V,Cr,Mn,Fe,Co,Ni,Cu,Zn,Y,Zr,Nb,Mo,Tc,Ru,Rh,Pd,Ag,Cd

#acceptable molecules must have <= instances of each of the patterns below

#specific, undesirable functional groups

RULE 0 quinone
RULE 0 pentafluorophenyl_esters
RULE 0 paranitrophenyl_esters
RULE 0 HOBT_esters
RULE 0 triflates
RULE 0 lawesson_s_reagent
RULE 0 phosphoramides
RULE 1 beta_carbonyl_quat_nitrogen
RULE 0 acylhydrazide
RULE 0 cation_C_Cl_I_P_or_S
RULE 0 phosphoryl
RULE 0 alkyl_phosphate
RULE 1 phosphinic_acid
RULE 0 phosphanes
RULE 0 phosphoranes
RULE 0 imidoyl_chlorides
RULE 0 nitroso
RULE 0 N_P_S_Halides
RULE 0 carbodiimide
RULE 0 isonitrile
RULE 0 triacyloxime
RULE 0 cyanohydrins
RULE 0 acyl_cyanides
RULE 0 sulfonylnitrile
RULE 0 phosphorylnitrile
RULE 0 azocyanamides
RULE 0 beta_azo_carbonyl
RULE 2 polyenes
RULE 0 saponin_derivatives
RULE 1 cytochalasin_derivatives
RULE 4 cycloheximide_derivatives
RULE 1 monensin_derivatives
RULE 1 squalestatin_derivatives

#functional groups which often eliminate compounds from consideration

RULE 0 acid_halide
RULE 0 aldehyde
RULE 3 alkyl_halide
RULE 0 anhydride
RULE 0 azide
RULE 0 azo
RULE 2 di_peptide
RULE 1 michael_acceptor
RULE 0 beta_halo_carbonyl
RULE 3 nitro
RULE 0 oxygen_cation
RULE 0 peroxide
RULE 0 phosphonic_acid
RULE 0 phosphonic_ester
RULE 0 phosphoric_acid
RULE 0 phosphoric_ester
RULE 1 sulfonic_acid
RULE 0 sulfonic_ester
RULE 0 tricarbo_phosphene
RULE 0 epoxide
RULE 0 sulfonyl_halide
RULE 0 halopyrimidine
RULE 0 perhalo_ketone
RULE 0 aziridine
RULE 1 oxalyl
RULE 0 alphahalo_amine
RULE 0 halo_amine
RULE 1 halo_alkene
RULE 0 acyclic_NCN
RULE 0 acyclic_NS
RULE 0 SCN2
RULE 0 terminal_vinyl
RULE 0 hetero_hetero
RULE 0 hydrazine
RULE 0 N_methoyl
RULE 2 NS_beta_haloethyl
RULE 0 propiolactones
RULE 0 nitroso
RULE 0 iodoso
RULE 0 iodoxy
RULE 0 noxide

```
#groups of molecules

RULE 2 dye

#functional groups which are allowed, but may not be wanted in high quantities
#common functional groups

RULE 6 alcohol
RULE 5 alkene
RULE 4 amide
RULE 4 amino_acid
RULE 3 amine
RULE 4 primary_amine
RULE 4 secondary_amine
RULE 4 tertiary_amine
RULE 2 carboxylic_acid
RULE 6 halide
RULE 4 iodine
RULE 3 ketone
RULE 4 phenol
RULE 2 imine
RULE 1 methyl_ketone
RULE 1 alkylaniline
RULE 4 sulfonamide
RULE 1 sulfonylurea
RULE 0 phosphonamide
RULE 1 alphahalo_ketone
RULE 0 oxaziridine
RULE 1 cyclopropyl
RULE 2 guanidine
RULE 0 sulfonimine
RULE 0 sulfinimine
RULE 1 hydroxamic_acid
RULE 0 phosphoryl
RULE 0 sulfinylthio
RULE 0 disulfide
RULE 0 enol_ether
RULE 2 enamine
RULE 0 organometallic
RULE 0 dithioacetal
RULE 1 oxime
```

RULE 0 isothiocyanate
RULE 0 isocyanate
RULE 3 lactone
RULE 3 lactam
RULE 1 thioester
RULE 1 carbonate
RULE 0 carbamic_acid
RULE 1 thiocarbamate
RULE 0 triazine
RULE 1 malonic

#other functional groups

RULE 2 alkyne
RULE 4 aniline
RULE 4 aryl_halide
RULE 2 carbamate
RULE 3 ester
RULE 6 ether
RULE 1 hydrazone
RULE 0 nonacylhydrazone
RULE 1 hydroxylamine
RULE 2 nitrile
RULE 2 sulfide
RULE 2 sulfone
RULE 2 sulfoxide
RULE 0 thiourea
RULE 1 thioamide
RULE 1 thiol
RULE 2 urea

RULE 0 hemiketal
RULE 0 hemiacetal
RULE 0 ketal
RULE 3 acetal
RULE 0 aminal
RULE 0 hemiaminal

#protecting groups

RULE 0 benzyloxycarbonyl_CBZ
RULE 0 t_butoxycarbonyl_tBOC

```
RULE 0 fluorenylmethoxycarbonyl_Fmoc
RULE 1 dioxolane_5MR
RULE 1 dioxane_6MR
RULE 1 tetrahydropyran_THP
RULE 1 methoxyethoxymethyl_MEM
RULE 2 benzyl_ether
RULE 2 t_butyl_ether
RULE 0 trimethylsilyl_TMS
RULE 0 t_butyltrimethylsilyl_TBDMS
RULE 0 triisopropylsilyl_TIPS
RULE 0 t_butylsilyl_TBDPS
RULE 1 phthalimides_PHT
RULE 2 arenesulfonyl
```

5.2.9 Example PVM.conf.

This is an example of the format of a PVM.conf file used to distribute Omega and ROCS jobs to 14 processors across 10 workstations. The number 1 or 2 denotes the number of CPUs to be used in that host.

```
host <host name> 2
host <host name> 2
host <host name> 2
host <host name> 1
host <host name> 2
```

6. Bibliography

1. Kussie, P. H.; Gorina, S.; Marechal, V.; Elenbaas, B.; Moreau, J.; Levine, A. J.; Pavletich, N. P., Structure of the MDM2 Oncoprotein Bound to the p53 Tumor Suppressor Transactivation Domain. *Science* **1996**, *274*, (5289), 948-953.
2. WHO, Fight Against Cancer. In 2007.
3. Lengauer, C.; Diaz, L. A.; Saha, S., Cancer drug discovery through collaboration. *Nature Reviews Drug Discovery* **2005**, *4*, (5), 375-380.
4. Pevarello, P., Recent drug approvals from the US FDA and EMEA: what the future holds. *Future Medicinal Chemistry* **2009**, *1*, (1), 35-48.
5. Hanahan, D.; Weinberg, R. A., The Hallmarks of Cancer. *Cell* **2000**, *100*, (1), 57-70.
6. Thomson, A. B.; Critchley, H. O. D.; Wallace, W. H. B., Fertility and progeny. *European Journal of Cancer* **2002**, *38*, (12), 1634-1644.
7. Hawkins, M. M., Commentary. *European Journal of Cancer* **2001**, *37*, (16), 2074-2081.
8. Capdeville, R.; Buchdunger, E.; Zimmermann, J.; Matter, A., Glivec (STI571, imatinib), a rationally developed, targeted anticancer drug. *Nature Reviews Drug Discovery* **2002**, *1*, (7), 493-502.
9. Lynch, T. J., Activating Mutations in the Epidermal Growth Factor Receptor Underlying Responsiveness of Non-Small-Cell Lung Cancer to Gefitinib. *New England Journal of Medicine* **2004**, *350*, (21), 2129-2139.
10. Baselga, J.; Swain, S. M., Novel anticancer targets: revisiting ERBB2 and discovering ERBB3. *Nature Reviews Cancer* **2009**, *9*, (7), 463-475.
11. Zhelleva, D. I.; Lane, D. P.; M., F. P., The p53-Mdm2 Pathway: Targets for the Development of New Anticancer Therapeutics. *Mini Reviews in Medicinal Chemistry* **2003**, (3), 257-270.
12. Wang, Z.; Sun, Y., Targeting p53 for Novel Anticancer Therapy. *Translational Oncology* **2010**, *3*, (1), 1 - 12.
13. Chen, F.; Wang, W.; El-Deiry, W. S., Current strategies to target p53 in cancer. *Biochemical Pharmacology* **2010**, *80*, (5), 724-730.
14. Lane, D. P., p53, guardian of the genome. *Nature* **1992**, *358*, (6381), 15-16.
15. Vogelstein, B.; Lane, D.; Levine, A. J., Surfing the p53 network. *Nature* **2000**, *408*, (6810), 307-310.

16. Lane, D. P.; Crawford, L. V., T antigen is bound to a host protein in SV40-transformed cells. *Nature* **1979**, 278, (5701), 261-263.
17. Linzer, D. I. H.; Levine, A. J., Characterization of a 54K Dalton cellular SV40 tumor antigen present in SV40-transformed cells and uninfected embryonal carcinoma cells. *Cell* **1979**, 17, (1), 43-52.
18. Michalovitz, D.; Halevy, O.; Oren, M., Conditional inhibition of transformation and of cell proliferation by a temperature-sensitive mutant of p53. *Cell* **1990**, 62, (4), 671-680.
19. Hollstein, M.; Sidransky, D.; Vogelstein, B.; Harris, C. C., p53 mutations in human cancers. *Science* **1991**, 253, (5015), 49-53.
20. Nigro, J. M.; Baker, S. J.; Preisinger, A. C.; Jessup, J. M.; Hosteller, R.; Cleary, K.; Signer, S. H.; Davidson, N.; Baylin, S.; Devilee, P.; Glover, T.; Collins, F. S.; Weslon, A.; Modali, R.; Harris, C. C.; Vogelstein, B., Mutations in the p53 gene occur in diverse human tumour types. *Nature* **1989**, 342, (6250), 705-708.
21. Finlay, C. A.; Hinds, P. W.; Levine, A. J., The p53 proto-oncogene can act as a suppressor of transformation. *Cell* **1989**, 57, (7), 1083-1093.
22. Finlay, C. A.; Hinds, P. W.; Tan, T. H.; Eliyahu, D.; Oren, M.; Levine, A. J., Activating mutations for transformation by p53 produce a gene product that forms an hsc70-p53 complex with an altered half-life. *Mol. Cell. Biol.* **1988**, 8, (2), 531-539.
23. Lane, D. P.; Benchimol, S., p53: oncogene or anti-oncogene? *Genes & Development* **1990**, 4, (1), 1-8.
24. Levine, A. J.; Momand, J., Tumor suppressor genes: the p53 and retinoblastoma sensitivity genes and gene products. *Biochimica et Biophysica Acta (BBA) - Reviews on Cancer* **1990**, 1032,(1), 119-136.
25. Bargonetti, J.; Friedman, P. N.; Kern, S. E.; Vogelstein, B.; Prives, C., Wild-type but not mutant p53 immunopurified proteins bind to sequences adjacent to the SV40 origin of replication. *Cell* **1991**, 65, (6), 1083-1091.
26. Soussi, T.; May, P., Structural Aspects of the p53 Protein in Relation to Gene Evolution: A Second Look. *Journal of Molecular Biology* **1996**, 260, (5), 623-637.
27. Soussi, T., Structural aspects of the p53 protein in relation to gene evolution evolution. *Journal of Molecular Biology* **1990**, 5, (7), 945-952.
28. Lane, D. P.; Cheok, C. F.; Brown, C. J.; Madhumalar, A.; Ghadessy, F. J.; Verma, C., The Mdm2 and p53 genes are conserved in the Arachnids. *Cell Cycle* **2010**, 9, (4), 748 - 754.

29. Ziemer, M. A.; Mason, A.; Carlson, D. M., Cell-free translations of proline-rich protein mRNAs. *Journal of Biological Chemistry* **1982**, 257, (18), 11176-11180.
30. Chan, W. M.; Siu, W. Y.; Lau, A.; Poon, R. Y. C., How Many Mutant p53 Molecules Are Needed To Inactivate a Tetramer? *Molecular and Cellular Biology* **2004**, 24, (8), 3536-3551.
31. Vousden, K. H.; Lane, D. P., p53 in health and disease. *Nature Reviews Molecular Cell Biology* **2007**, 8, (4), 275-283.
32. Olsson, A.; Manzl, C.; Strasser, A.; Villunger, A., How important are post-translational modifications in p53 for selectivity in target-gene transcription and tumour suppression? *Cell Death Differ* **2007**, 14, (9), 1561-1575.
33. Appella, E.; Anderson, C. W., Post-translational modifications and activation of p53 by genotoxic stresses. *European Journal of Biochemistry* **2001**, 268, (10), 2764-2772.
34. Bode, A. M.; Dong, Z., Post-translational modification of p53 in tumorigenesis. *Nature Reviews Cancer* **2004**, 4, (10), 793-805.
35. Agarwal, M. L.; Agarwal, A.; Taylor, W. R.; Stark, G. R., p53 controls both the G2/M and the G1 cell cycle checkpoints and mediates reversible growth arrest in human fibroblasts. *Proceedings of the National Academy of Sciences of the United States of America* **1995**, 92, (18), 8493-8497.
36. Stewart, N.; Hicks, G. G.; Paraskevas, F.; Mowat, M., Evidence for a second cell cycle block at G2/M by p53. *Oncogene* **1995**, 10, (1), 109-15.
37. Waldman, T.; Kinzler, K. W.; Vogelstein, B., p21 Is Necessary for the p53-mediated G1 Arrest in Human Cancer Cells. *Cancer Research* **1995**, 55, (22), 5187-5190.
38. Doumont, G.; Martoriati, A.; Beekman, C.; Bogaerts, S.; Mee, P. J.; Bureau, F.; Colombo, E.; Alcalay, M.; Bellefroid, E.; Marchesi, F.; Scanziani, E.; Pelicci, P. G.; Marine, J.-C., G1 checkpoint failure and increased tumor susceptibility in mice lacking the novel p53 target Ptp^{rv}. *EMBO J* **2005**, 24, (17), 3093-3103.
39. Wang, X. W.; Zhan, Q.; Coursen, J. D.; Khan, M. A.; Kontny, H. U.; Yu, L.; Hollander, M. C.; O' Connor, P. M.; Fornace, A. J.; Harris, C. C., GADD45 induction of a G2/M cell cycle checkpoint. *Proceedings of the National Academy of Sciences of the United States of America* **1999**, 96, (7), 3706-3711.
40. Hermeking, H.; Lengauer, C.; Polyak, K.; He, T.-C.; Zhang, L.; Thiagalingam, S.; Kinzler, K. W.; Vogelstein, B., 14-3-3 σ Is a p53-Regulated Inhibitor of G2/M Progression. *Molecular cell* **1997**, 1, (1), 3-11.

41. Collavin, L.; Monte, M.; Verardo, R.; Pflieger, C.; Schneider, C., Cell-cycle regulation of the p53-inducible gene B99. *FEBS Letters* **2000**, 481, (1), 57-62.
42. Fridman, J. S.; Lowe, S. W., Control of apoptosis by p53. *Oncogene* **22**, (56), 9030-9040.
43. Pietsch, E. C.; Sykes, S. M.; McMahon, S. B.; Murphy, M. E., The p53 family and programmed cell death. *Oncogene* **27**, (50), 6507-6521.
44. Toshiyuki, M.; Reed, J. C., Tumor suppressor p53 is a direct transcriptional activator of the human bax gene. *Cell* **1995**, 80, (2), 293-299.
45. Sax, J. K.; Fei, P.; Murphy, M. E.; Bernhard, E.; Korsmeyer, S. J.; El-Deiry, W. S., BID regulation by p53 contributes to chemosensitivity. *Nature Cell Biology* **2002**, 4, (11), 842-849.
46. Mitchell, A., Death by PUMA. *Nature Reviews Molecular Cell Biology* **2001**, 2, (5), 319-319.
47. Shibue, T.; Takeda, K.; Oda, E.; Tanaka, H.; Murasawa, H.; Takaoka, A.; Morishita, Y.; Akira, S.; Taniguchi, T.; Tanaka, N., Integral role of Noxa in p53-mediated apoptotic response. *Genes & Development* **2003**, 17, (18), 2233-2238.
48. Moroni, M. C.; Hickman, E. S.; Denchi, E. L.; Caprara, G.; Colli, E.; Cecconi, F.; Muller, H.; Helin, K., Apaf-1 is a transcriptional target for E2F and p53. *Nature Cell Biology* **2001**, 3, (6), 552-558.
49. Li, Y.; Raffo, A. J.; Drew, L.; Mao, Y.; Tran, A.; Petrylak, D. P.; Fine, R. L., Fas-Mediated Apoptosis Is Dependent on Wild-Type p53 Status in Human Cancer Cells Expressing a Temperature-Sensitive p53 Mutant Alanine-143. *Cancer Research* **2003**, 63, (7), 1527-1533.
50. Wu, G. S.; Burns, T. F.; McDonald, E. R.; Jiang, W.; Meng, R.; Krantz, I. D.; Kao, G.; Gan, D.-D.; Zhou, J.-Y.; Muschel, R.; Hamilton, S. R.; Spinner, N. B.; Markowitz, S.; Wu, G.; El-Deiry, W. S., KILLER/DR5 is a DNA damage-inducible p53-regulated death receptor gene. *Nature Genetics* **1997**, 17, (2), 141-143.
51. Chipuk, J. E.; Green, D. R., p53's Believe It or Not: Lessons on Transcription-Independent Death. *Journal of Clinical Immunology* **2003**, 23, (5), 355-361.
52. Bonini, P.; Cicconi, S.; Cardinale, A.; Vitale, C.; Serafino, A. L.; Ciotti, M. T.; Marlier, L. N. J. L., Oxidative stress induces p53-mediated apoptosis in glia: p53 transcription-independent way to die. *Journal of Neuroscience Research* **2004**, 75, (1), 83-95.
53. Moll, U. M.; Wolff, S.; Speidel, D.; Deppert, W., Transcription-independent pro-apoptotic functions of p53. *Current Opinion in Cell Biology* **2005**, 17, (6), 631-636.

54. Speidel, D., Transcription-independent p53 apoptosis: an alternative route to death. *Trends in Cell Biology* 20, (1), 14-24.
55. Slee, E. A.; O'Connor, D. J.; Lu, X., To die or not to die: how does p53 decide? *Oncogene* 23, (16), 2809-2818.
56. Allan, L. A.; Fried, M., p53-dependent apoptosis or growth arrest induced by different forms of radiation in U2OS cells: p21WAF1/CIP1 repression in UV induced apoptosis. *Oncogene* 1999, 18, (39), 5403-5412.
57. Itahana, K.; Dimri, G.; Campisi, J., Regulation of cellular senescence by p53. *European Journal of Biochemistry* 2001, 268, (10), 2784-2791.
58. Wynford-Thomas, D., p53: Guardian of Cellular Senescence. *The Journal of Pathology* 1996, 180, (2), 118-121.
59. Radford, I. R., P53 Status, DNA Double-strand Break Repair Proficiency, and Radiation Response of Mouse Lymphoid and Myeloid Cell Lines. *International Journal of Radiation Biology* 1994, 66, (5), 557-560.
60. Ford, J. M.; Hanawalt, P. C., Li-Fraumeni syndrome fibroblasts homozygous for p53 mutations are deficient in global DNA repair but exhibit normal transcription-coupled repair and enhanced UV resistance. *Proceedings of the National Academy of Sciences of the United States of America* 1995, 92, (19), 8876-8880.
61. Coates, P. J.; Save, V.; Ansari, B.; Hall, P. A., Demonstration of DNA damage/repair in individual cells using in situ end labelling: Association of p53 with sites of DNA damage. *The Journal of Pathology* 1995, 176, (1), 19-26.
62. Adimoolam, S.; Ford, J. M., p53 and regulation of DNA damage recognition during nucleotide excision repair. *DNA Repair* 2003, 2, (9), 947-954.
63. Lawler, J.; Miao, W.-M.; Duquette, M.; Bouck, N.; Bronson, R. T.; Hynes, R. O., Thrombospondin-1 Gene Expression Affects Survival and Tumor Spectrum of p53-Deficient Mice. *American Journal of Pathology* 2001, 159, (5), 1949-1956.
64. Dameron, K. M.; Volpert, O. V.; Tainsky, M. A.; Bouck, N., Control of angiogenesis in fibroblasts by p53 regulation of thrombospondin-1. *Science* 1994, 265, (5178), 1582-1584.
65. Strohmeyer, D.; Rössing, C.; Bauerfeind, A.; Kaufmann, O.; Schlechte, H.; Bartsch, G.; Loening, S., Vascular endothelial growth factor and its correlation with angiogenesis and p53 expression in prostate cancer. *The Prostate* 2000, 45, (3), 216-224.
66. Fontanini, G.; Boldrini, L.; Vignati, S.; Chiné, S.; Basolo, F.; Silvestri, V.; Lucchi, M.; Mussi, A.; Angeletti, C. A.; Bevilacqua, G., Bcl2 and p53 regulate vascular endothelial growth factor (VEGF)-mediated angiogenesis in non-small cell lung carcinoma. *European Journal of Cancer* 1998, 34, (5), 718-723.

67. Lane, D., Cancer How cells choose to die. *Nature* **2001**, 414, (6859), 25-27.
68. Lowe, S. W.; Bodis, S.; McClatchey, A.; Remington, L.; Ruley, H. E.; Fisher, D. E.; Housman, D. E.; Jacks, T., p53 status and the efficacy of cancer therapy in vivo. *Science* **1994**, 266, (5186), 807-810.
69. Levine, A. J., p53, the Cellular Gatekeeper for Growth and Division. *Cell* **1997**, 88, (3), 323-331.
70. El-Deiry, W. S., The role of p53 in chemosensitivity and radiosensitivity. *Oncogene* **22**, (47), 7486-7495.
71. O'Connor, P. M.; Jackman, J.; Bae, I.; Myers, T. G.; Fan, S.; Mutoh, M.; Scudiero, D. A.; Monks, A.; Sausville, E. A.; Weinstein, J. N.; Friend, S.; Fornace, A. J.; Kohn, K. W., Characterization of the p53 Tumor Suppressor Pathway in Cell Lines of the National Cancer Institute Anticancer Drug Screen and Correlations with the Growth-Inhibitory Potency of 123 Anticancer Agents. *Cancer Research* **1997**, 57, (19), 4285-4300.
72. Lane, D. P.; Lain, S., Therapeutic exploitation of the p53 pathway. *Trends in Molecular Medicine* **2002**, 8, (4), S38-S42.
73. Lain, S.; Lane, D., Improving cancer therapy by non-genotoxic activation of p53. *European Journal of Cancer* **2003**, 39, (8), 1053-1060.
74. Harris, A. L., Mutant p53—the commonest genetic abnormality in human cancer? *The Journal of Pathology* **1990**, 162, (1), 5-6.
75. Hollstein, M.; Hergenhahn, M.; Yang, Q.; Bartsch, H.; Wang, Z.-Q.; Hainaut, P., New approaches to understanding p53 gene tumor mutation spectra. *Mutation Research/Fundamental and Molecular Mechanisms of Mutagenesis* **1999**, 431, (2), 199-209.
76. Hainaut, P.; Hollstein, M., p53 and human cancer: the first ten thousand mutations. *Advanced Cancer Research* **1999**, 77, 81.
77. Joerger, A. C.; Fersht, A. R., Structural Biology of the Tumor Suppressor p53. *Annual Review of Biochemistry* **2008**, 77, (1), 557-582.
78. Peng, Z., Current Status of Gendicine in China: Recombinant Human Ad-p53 Agent for Treatment of Cancers. *Human Gene Therapy* **2005**, 16, (9), 1016-1027.
79. Pearson, S.; Jia, H., China Approves First Gene Therapy. *Nature Biotechnology* **2004**, (1), 3.
80. McCormick, Cancer Specific Viruses and the Development of ONYX-015. *Cancer Biology and Therapy* **2003**, 2, (0), S157-S160

81. Khuri, F. R.; Nemunaitis, J.; Ganly, I.; Arseneau, J.; Tannock, I. F.; Romel, L.; Gore, M.; Ironside, J.; MacDougall, R. H.; Heise, C.; Randlev, B.; Gillenwater, A. M.; Brusco, P.; Kaye, S. B.; Hong, W. K.; Kim, D. H., A controlled trial of intratumoral ONYX-015, a selectively-replicating adenovirus, in combination with cisplatin and 5-fluorouracil in patients with recurrent head and neck cancer. *Nat Med* **2000**, *6*, (8), 879-885.
82. Kim, D. H.; Thorne, S. H., Targeted and armed oncolytic poxviruses: a novel multi-mechanistic therapeutic class for cancer. *Nat Rev Cancer* **2009**, *9*, (1), 64-71.
83. Liu, T. C.; Galanis, E.; Kim, D., Clinical trial results with oncolytic virotherapy: a century of promise, a decade of progress. *Nature clinical practice. Oncology* **2007**, *4*, (2), 101-17.
84. Lain, S.; Hollick, J. J.; Campbell, J.; Staples, O. D.; Higgins, M.; Aoubala, M.; McCarthy, A.; Appleyard, V.; Murray, K. E.; Baker, L.; Thompson, A.; Mathers, J.; Holland, S. J.; Stark, M. J. R.; Pass, G.; Woods, J.; Lane, D. P.; Westwood, N. J., Discovery, In Vivo Activity, and Mechanism of Action of a Small-Molecule p53 Activator. *Cancer cell* **2008**, *13*, (5), 454-463.
85. Jin, S.; Levine, A. J., The p53 functional circuit. *Journal of Cell Science* **2001**, *114*, (23), 4139-4140.
86. Tovar, C.; Rosinski, J.; Filipovic, Z.; Higgins, B.; Kolinsky, K.; Hilton, H.; Zhao, X. L.; Vu, B. T.; Qing, W. G.; Packman, K.; Myklebost, O.; Heimbrook, D. C.; Vassilev, L. T., Small-molecule MDM2 antagonists reveal aberrant p53 signaling in cancer: Implications for therapy. *Proceedings of the National Academy of Sciences of the United States of America* **2006**, *103*, (6), 1888-1893.
87. Dancey, J.; Sausville, E. A., Issues and progress with protein kinase inhibitors for cancer treatment. *Nature Reviews Drug Discovery* **2003**, *2*, (4), 296-313.
88. Ferreira, C. G.; Epping, M.; Kruyt, F. A. E.; Giaccone, G., Apoptosis: Target of Cancer Therapy. *Clinical Cancer Research* **2002**, *8*, (7), 2024-2034.
89. Hinds, M. G.; Day, C. L., Regulation of apoptosis: uncovering the binding determinants. *Current Opinion in Structural Biology* **2005**, *15*, (6), 690-699.
90. Oltsersdorf, T.; Elmore, S. W.; Shoemaker, A. R.; Armstrong, R. C.; Augeri, D. J.; Belli, B. A.; Bruncko, M.; Deckwerth, T. L.; Dinges, J.; Hajduk, P. J.; Joseph, M. K.; Kitada, S.; Korsmeyer, S. J.; Kunzer, A. R.; Letai, A.; Li, C.; Mitten, M. J.; Nettesheim, D. G.; Ng, S.; Nimmer, P. M.; O'Connor, J. M.; Oleksijew, A.; Petros, A. M.; Reed, J. C.; Shen, W.; Tahir, S. K.; Thompson, C. B.; Tomaselli, K. J.; Wang, B. L.; Wendt, M. D.; Zhang, H. C.; Fesik, S. W.; Rosenberg, S. H., An inhibitor of Bcl-2 family proteins induces regression of solid tumours. *Nature* **2005**, *435*, (7042), 677-681.

91. Li, L.; Thomas, R. M.; Suzuki, H.; De Brabander, J. K.; Wang, X.; Harran, P. G., A Small Molecule Smac Mimic Potentiates TRAIL- and TNF α -Mediated Cell Death. *Science* **2004**, 305, (5689), 1471-1474.
92. Bockbrader, K. M.; Tan, M.; Sun, Y., A small molecule Smac-mimic compound induces apoptosis and sensitizes TRAIL- and etoposide-induced apoptosis in breast cancer cells. *Oncogene* **2005**, 24, (49), 7381-7388.
93. Iwakuma, T.; Lozano, G., MDM2, An Introduction. *Molecular Cancer Research* **2003**, 1, (14), 993-1000.
94. Cahilly-Snyder, L.; Yang-Feng, T.; Francke, U.; George, D. L., Molecular analysis and chromosomal mapping of amplified genes isolated from a transformed mouse 3T3 cell line. *Somatic Cell and Molecular Genetics* **1987**, 13, (3), 235-244.
95. Fakharzadeh, S. S.; Trusko, S. P.; George, D. L., Tumorigenic potential associated with enhanced expression of a gene that is amplified in a mouse tumor cell line. *Embo Journal* **1991**, 10, (6), 1565-1569.
96. de Oca Luna, R. M.; Wagner, D. S.; Lozano, G., Rescue of early embryonic lethality in mdm2-deficient mice by deletion of p53. *Nature* **1995**, 378, (6553), 203-206.
97. Jones, S. N.; Roe, A. E.; Donehower, L. A.; Bradley, A., Rescue of embryonic lethality in Mdm2-deficient mice by absence of p53. *Nature* **1995**, 378, (6553), 206-208.
98. Wu, X.; Bayle, J. H.; Olson, D.; Levine, A. J., The p53-mdm-2 autoregulatory feedback loop. *Genes & Development*. **1993**, 7, (7), 1126-1132.
99. Barak, Y.; Juven, T.; Haffner, R.; Oren, M., Mdm2 Expression Is Induced by Wild Type-P53 Activity. *Embo Journal* **1993**, 12, (2), 461-468.
100. Momand, J.; Zambetti, G. P.; Olson, D. C.; George, D.; Levine, A. J., The mdm-2 oncogene product forms a complex with the p53 protein and inhibits p53-mediated transactivation. *Cell* **1992**, 69, (7), 1237-1245.
101. Haupt, Y.; Maya, R.; Kazaz, A.; Oren, M., Mdm2 promotes the rapid degradation of p53. *Nature* **1997**, 387, (6630), 296-299.
102. Tao, W. K.; Levine, A. J., Nucleocytoplasmic shuttling of oncoprotein Hdm2 is required for Hdm2-mediated degradation of p53. *Proceedings of the National Academy of Sciences of the United States of America* **1999**, 96, (6), 3077-3080.
103. Matheu, A.; Maraver, A.; Serrano, M., The Arf/p53 Pathway in Cancer and Aging. *Cancer Res* **2008**, 68, (15), 6031-6034.
104. Dai, M. S.; Shi, D. D.; Jin, Y. T.; Sun, X. X.; Zhang, Y. P.; Grossman, S. R.; Lu, H., Regulation of the MDM2-p53 pathway by ribosomal protein L11 involves a post-

- ubiquitination mechanism. *Journal of Biological Chemistry* **2006**, 281, (34), 24304-24313.
105. Jin, A.; Itahana, K.; O'Keefe, K.; Zhang, Y., Inhibition of HDM2 and activation of p53 by ribosomal protein L23. *Molecular and Cellular Biology* **2004**, 24, (17), 7669-7680.
106. Fang, S. Y.; Jensen, J. P.; Ludwig, R. L.; Vousden, K. H.; Weissman, A. M., Mdm2 is a RING finger-dependent ubiquitin protein ligase for itself and p53. *Journal of Biological Chemistry* **2000**, 275, (12), 8945-8951.
107. Meek, D. W.; Knippschild, U., Posttranslational modification of MDM2. *Molecular Cancer Research* **2003**, 1, (14), 1017-1026.
108. Momand, J.; Jung, D.; Wilczynski, S.; Niland, J., The MDM2 gene amplification database. *Nucleic Acids Research* **1998**, 26, (15), 3453-3459.
109. Frank, B.; Axel, M.; Peter, W.; Matthias, K.; Matthias, B.; Christine, L.; Ulrich, G.; Hannelore, S.; Helge, T., Amplification of the mdm2 gene, but not expression of splice variants of mdm2 mRNA, is associated with prognosis in soft tissue sarcoma. *International Journal of Cancer* **2001**, 95, (3), 168-175.
110. Vousden, K. H.; Lu, X., Live or Let Die: The Cell's Response to p53. *Nature Reviews Cancer* **2002**, 2, (8), 594-604.
111. Fry, D. C.; Graves, B.; Vassilev, L. T., Development of E3-substrate (MDM2-p53)-binding inhibitors: Structural aspects. In *Ubiquitin and Protein Degradation, Pt B*, Elsevier Academic Press Inc: San Diego, 2005; Vol. 399, pp 622-633.
112. Stuhmer, T.; Arts, J.; King, P.; Page, M.; Bommert, K.; Leo, E.; Bargou, R. C. A first-in-class HDM2-inhibitor (JNJ-26854165) in phase I development shows potent activity against multiple myeloma (MM) cells in vitro and ex vivo. May 20, 2008.
113. Kojima, K.; Burks, J. K.; Arts, J.; Andreeff, M., The Novel Tryptamine Derivative JNJ-26854165 Induces Wild-Type p53- and E2F1-Mediated Apoptosis in Acute Myeloid and Lymphoid Leukemias. *Molecular Cancer Therapeutics* **2010**.
114. Tabernero, J.; Dirix, L.; Schoffski, P.; Cervantes, A.; Capdevila, J.; Baselga, J.; van Beijsterveldt, L.; Winkler, H.; Kraljevic, S.; Zhuang, S. H., Phase I pharmacokinetic (PK) and pharmacodynamic (PD) study of HDM-2 antagonist JNJ-26854165 in patients with advanced refractory solid tumors. In *Journal of Clinical Oncology (Meeting Abstracts)*, 2009; Vol. 27, p 3514.
115. Dickens, M. P.; Fitzgerald, R.; Fischer, P. M., Small-molecule inhibitors of MDM2 as new anticancer therapeutics. *Seminars in Cancer Biology* **2010**, 20, (1), 10-18.

116. Liang, S.-H.; Clarke, M. F., Regulation of p53 localization. *European Journal of Biochemistry* **2001**, 268, (10), 2779-2783.
117. LaIn, S.; Midgley, C.; Sparks, A.; Lane, E. B.; Lane, D. P., An Inhibitor of Nuclear Export Activates the p53 Response and Induces the Localization of HDM2 and p53 to U1A-Positive Nuclear Bodies Associated with the PODs. *Experimental Cell Research* **1999**, 248, (2), 457-472.
118. Bogan, A. A.; Thorn, K. S., Anatomy of hot spots in protein interfaces. *Journal of Molecular Biology* **1998**, 280, (1), 1-9.
119. Myers, M. C.; Wang, Jera, J. A.; Bang, J.-k.; Hara, T.; Saito, S. i.; Zambetti, G. P.; Appella, D. H., A New Family of Small Molecules To Probe the Reactivation of Mutant p53. *Journal of the American Chemical Society* **2005**, 127, (17), 6152-6153.
120. Uhrinova, S.; Uhrin, D.; Powers, H.; Watt, K.; Zheleva, D.; Fischer, P.; McInnes, C.; Barlow, P. N., Structure of Free MDM2 N-terminal Domain Reveals Conformational Adjustments that Accompany p53-binding. *Journal of Molecular Biology* **2005**, 350, (3), 587-598.
121. Showalter, S. A.; Brüscheweiler-Li, L.; Johnson, E.; Zhang, F.; Brüscheweiler, R., Quantitative Lid Dynamics of MDM2 Reveals Differential Ligand Binding Modes of the p53-Binding Cleft. *Journal of the American Chemical Society* **2008**, 130, (20), 6472-6478.
122. Grasberger, B. L.; Lu, T. B.; Schubert, C.; Parks, D. J.; Carver, T. E.; Koblisch, H. K.; Cummings, M. D.; LaFrance, L. V.; Milkiewicz, K. L.; Calvo, R. R.; Maguire, D.; Lattanze, J.; Franks, C. F.; Zhao, S. Y.; Ramachandren, K.; Bylebyl, G. R.; Zhang, M.; Manthey, C. L.; Petrella, E. C.; Pantoliano, M. W.; Deckman, I. C.; Spurlino, J. C.; Maroney, A. C.; Tomczuk, B. E.; Molloy, C. J.; Bone, R. F., Discovery and cocystal structure of benzodiazepinedione HDM2 antagonists that activate p53 in cells. *Journal of Medicinal Chemistry* **2005**, 48, (4), 909-912.
123. Espinoza-Fonseca, L. M.; García-Machorro, J., Aromatic-aromatic interactions in the formation of the MDM2-p53 complex. *Biochemical and Biophysical Research Communications* **2008**, 370, (4), 547-551.
124. Fischer, P., Peptide, Peptidomimetic, and Small-molecule Antagonists of the p53-HDM2 Protein-Protein Interaction. *International Journal of Peptide Research and Therapeutics* **2006**, 12, (1), 3-19.
125. Hardcastle, I. R., Inhibitors of the MDM2-p53 interaction as anticancer drugs. *Drugs of the Future* **2007**, 32, 883-896.
126. Justin K. Murray, S. H. G., Targeting protein-protein interactions: Lessons from p53/MDM2. *Peptide Science* **2007**, 88, (5), 657-686.

127. Bottger, V.; Bottger, A.; Howard, S. F.; Picksley, S. M.; Chene, P.; GarciaEcheverria, C.; Hochkeppel, H. K.; Lane, D. P., Identification of novel mdm2 binding peptides by phage display. *Oncogene* **1996**, 13, (10), 2141-2147.
128. Lu, Y. P.; Nikolovska-Coleska, Z.; Fang, X. L.; Gao, W.; Shangary, S.; Qiu, S.; Qin, D. G.; Wang, S. M., Discovery of a nanomolar inhibitor of the human murine double minute 2 (MDM2)-p53 interaction through an integrated, virtual database screening strategy. *Journal Of Medicinal Chemistry* **2006**, 49, (13), 3759-3762.
129. Garcia-Echeverria, C.; Chene, P.; Blommers, M. J. J.; Furet, P., Discovery of Potent Antagonists of the Interaction between Human Double Minute 2 and Tumor Suppressor p53. *Journal of Medicinal Chemistry* **2000**, 43, (17), 3205-3208.
130. Sakurai, K.; Schubert, C.; Kahne, D., Crystallographic Analysis of an 8-mer p53 Peptide Analogue Complexed with MDM2. *Journal of the American Chemical Society* **2006**, 128, (34), 11000-11001.
131. Chène, P.; Fuchs, J.; Bohn, J.; García-Echeverría, C.; Furet, P.; Fabbro, D., A small synthetic peptide, which inhibits the p53-hdm2 interaction, stimulates the p53 pathway in tumour cell lines. *Journal of Molecular Biology* **2000**, 299, (1), 245-253.
132. Ding, K.; Lu, Y.; Nikolovska-Coleska, Z.; Wang, G.; Qiu, S.; Shangary, S.; Gao, W.; Qin, D.; Stuckey, J.; Krajewski, K.; Roller, P. P.; Wang, S., Structure-Based Design of Spiro-oxindoles as Potent, Specific Small-Molecule Inhibitors of the MDM2-p53 Interaction. *Journal of Medicinal Chemistry* **2006**, 49, (12), 3432-3435.
133. Wang, S.; Shangary, S.; Ding, K.; Wang, G.; Qin, D.; Lu, Y.; Nikolovska-Coleska, Z.; Qiu, S.; McEachern, D.; Miller, R.; Yang, D., Design of Ultrapotent Non-Peptide Small-Molecule Inhibitors of the MDM2-p53 Interaction and Evaluation of Their Therapeutic Potential and Mechanism of Action in vitro and in vivo. In *AACR Annual Meeting*, AACR: Washington D.C., 2006.
134. Dömling, A., Small molecular weight protein-protein interaction antagonists--an insurmountable challenge? *Current Opinion in Chemical Biology* **2008**, 12, (3), 281-291.
135. Vassilev, L. T.; Vu, B. T.; Graves, B.; Carvajal, D.; Podlaski, F.; Filipovic, Z.; Kong, N.; Kammlott, U.; Lukacs, C.; Klein, C.; Fotouhi, N.; Liu, E. A., In vivo activation of the p53 pathway by small-molecule antagonists of MDM2. *Science* **2004**, 303, (5659), 844-848.
136. Koblisch, H. K.; Zhao, S. Y.; Franks, C. F.; Donatelli, R. R.; Tominovich, R. M.; LaFrance, L. V.; Leonard, K. A.; Gushue, J. M.; Parks, D. J.; Calvo, R. R.; Milkiewicz, K. L.; Marugan, J. J.; Raboisson, P.; Cummings, M. D.; Grasberger, B. L.; Johnson, D. L.; Lu, T. B.; Molloy, C. J.; Maroney, A. C., Benzodiazepinedione inhibitors of the Hdm2 : p53 complex suppress human tumor cell proliferation in vitro and sensitize tumors to doxorubicin in vivo. *Molecular Cancer Therapeutics* **2006**, 5, (1), 160-169.

137. Leonard, K.; Marugan, J. J.; Raboisson, P.; Calvo, R.; Gushue, J. M.; Koblisch, H. K.; Lattanze, J.; Zhao, S.; Cummings, M. D.; Player, M. R., Novel 1,4-benzodiazepine-2,5-diones as Hdm2 antagonists with improved cellular activity. *Bioorganic & Medicinal Chemistry Letters* **2006**, *16*, (13), 3463-3468.
138. Marugan, J. J.; Leonard, K.; Raboisson, P.; Gushue, J. M.; Calvo, R.; Koblisch, H. K.; Lattanze, J.; Zhao, S.; Cummings, M. D.; Player, M. R., Enantiomerically pure 1,4-benzodiazepine-2,5-diones as Hdm2 antagonists. *Bioorganic & Medicinal Chemistry Letters* **2006**, *16*, (12), 3115-3120.
139. Parks, D. J.; LaFrance, L. V.; Calvo, R. R.; Milkiewicz, K. L.; Gupta, V.; Lattanze, J.; Ramachandren, K.; Carver, T. E.; Petrella, E. C.; Cummings, M. D., 1,4-Benzodiazepine-2,5-diones as small molecule antagonists of the HDM2-p53 interaction: discovery and SAR. *Bioorganic & Medicinal Chemistry Letters* **2005**, *15*, (3), 765-770.
140. Parks, D. J.; LaFrance, L. V.; Calvo, R. R.; Milkiewicz, K. L.; Jose Marugan, J.; Raboisson, P.; Schubert, C.; Koblisch, H. K.; Zhao, S.; Franks, C. F., Enhanced pharmacokinetic properties of 1,4-benzodiazepine-2,5-dione antagonists of the HDM2-p53 protein-protein interaction through structure-based drug design. *Bioorganic & Medicinal Chemistry Letters* **2006**, *16*, (12), 3310-3314.
141. Ding, K.; Lu, Y.; Nikolovska-Coleska, Z.; Qiu, S.; Ding, Y.; Gao, W.; Stuckey, J.; Krajewski, K.; Roller, P. P.; Tomita, Y.; Parrish, D. A.; Deschamps, J. R.; Wang, S., Structure-Based Design of Potent Non-Peptide MDM2 Inhibitors. *Journal of the American Chemical Society* **2005**, *127*, (29), 10130-10131.
142. Deng, J. X.; Dayam, R.; Neamati, N., Patented small molecule inhibitors of p53-MDM2 interaction. *Expert Opinion on Therapeutic Patents* **2006**, *16*, (2), 165-188.
143. Bowman, A. L.; Nikolovska-Coleska, Z.; Zhong, H. Z.; Wang, S. M.; Carlson, H. A., Small molecule inhibitors of the MDM2-p53 interaction discovered by ensemble-based receptor models. *Journal of the American Chemical Society* **2007**, *129*, 12809-12814.
144. Shoemaker, R. H., The NCI60 human tumour cell line anticancer drug screen. *Nature Reviews Cancer* **2006**, *6*, (10), 813-823.
145. Hardcastle, I. R.; Ahmed, S. U.; Atkins, H.; Calvert, A. H.; Curtin, N. J.; Farnie, G.; Golding, B. T.; Griffin, R. J.; Guyenne, S.; Hutton, C.; Kallbad, P.; Kemp, S. J.; Kitching, M. S.; Newell, D. R.; Norbedo, S.; Northen, J. S.; Reid, R. J.; Saravanan, K.; Willems, H. M. G.; Lunec, J., Isoindolinone-based inhibitors of the MDM2-p53 protein-protein interaction. *Bioorganic & Medicinal Chemistry Letters* **2005**, *15*, (5), 1515-1520.
146. Hardcastle, I. R.; Ahmed, S. U.; Atkins, H.; Farnie, G.; Golding, B. T.; Griffin, R. J.; Guyenne, S.; Hutton, C.; Kallbad, P.; Kemp, S. J.; Kitching, M. S.; Newell, D. R.; Norbedo, S.; Northen, J. S.; Reid, R. J.; Saravanan, K.; Willems, H. t. M. G.; Lunec, J., Small-Molecule Inhibitors of the MDM2-p53 Protein-Protein Interaction Based on an Isoindolinone Scaffold. *Journal of Medicinal Chemistry* **2006**, *49*, (21), 6209-6221.

147. Riedinger, C.; Endicott, J. A.; Kemp, S. J.; Smyth, L. A.; Watson, A.; Valeur, E.; Golding, B. T.; Griffin, R. J.; Hardcastle, I. R.; Noble, M. E.; McDonnell, J. M., Analysis of Chemical Shift Changes Reveals the Binding Modes of Isoindolinone Inhibitors of the MDM2-p53 Interaction. *Journal of the American Chemical Society* **2008**, *130*, (47), 16038-16044.
148. Galatin, P. S.; Abraham, D. J., A nonpeptidic sulfonamide inhibits the p53-mdm2 interaction and activates p53-dependent transcription in mdm2-overexpressing cells. *Journal of Medicinal Chemistry* **2004**, *47*, (17), 4163-4165.
149. Lu, F.; Chi, S.-W.; Kim, D.-H.; Han, K.-H.; Kuntz, I. D.; Guy, R. K., Proteomimetic Libraries: Design, Synthesis, and Evaluation of p53-MDM2 Interaction Inhibitors. *Journal of Combinatorial Chemistry* **2006**, *8*, (3), 315-325.
150. Jianhua, Z.; Mijuan, W.; Jie, C.; Aiping, L.; Xiuqin, W.; Min, W.; Dali, Y.; Zhihua, L., The initial evaluation of non-peptidic small-molecule HDM2 inhibitors based on p53-HDM2 complex structure. *Cancer letters* **2002**, *183*, (1), 69-77.
151. Yin, H.; Lee, G.-i.; Sedey, K. A.; Kutzki, O.; Park, H. S.; Orner, B. P.; Ernst, J. T.; Wang, H.-G.; Sebt, S. M.; Hamilton, A. D., Terphenyl-Based Bak BH3 \pm -Helical Proteomimetics as Low-Molecular-Weight Antagonists of Bcl-xL. *Journal of the American Chemical Society* **2005**, *127*, (29), 10191-10196.
152. Yin, H.; Lee, G.-i.; Park, H. S.; Payne, G. A.; Rodriguez, J. M.; Sebt, S. M.; Hamilton, A. D., Terphenyl-Based Helical Mimetics That Disrupt the p53/HDM2 Interaction. *Angewandte Chemie International Edition* **2005**, *44*, (18), 2704-2707.
153. Chen, L.; Yin, H.; Farooqi, B.; Sebt, S.; Hamilton, A. D.; Chen, J., p53 α -Helix mimetics antagonize p53/MDM2 interaction and activate p53. *Molecular Cancer Therapeutics* **2005**, *4*, (6), 1019-1025.
154. Raboisson, P.; Marugan, J. J.; Schubert, C.; Koblisch, H. K.; Lu, T.; Zhao, S.; Player, M. R.; Maroney, A. C.; Reed, R. L.; Huebert, N. D., Structure-based design, synthesis, and biological evaluation of novel 1,4-diazepines as HDM2 antagonists. *Bioorganic & Medicinal Chemistry Letters* **2005**, *15*, (7), 1857-1861.
155. Stoll, R.; Renner, C.; Hansen, S.; Palme, S.; Klein, C.; Belling, A.; Zeslawski, W.; Kamionka, M.; Rehm, T.; Mühlhahn, P.; Schumacher, R.; Hesse, F.; Kaluza, B.; Voelter, W.; Engh, R. A.; Holak, T. A., Chalcone Derivatives Antagonize Interactions between the Human Oncoprotein MDM2 and p53. *Biochemistry* **2000**, *40*, (2), 336-344.
156. Achanta, G.; Modzelewska, A.; Feng, L.; Khan, S. R.; Huang, P., A Boronic-Chalcone Derivative Exhibits Potent Anticancer Activity through Inhibition of the Proteasome. *Molecular Pharmacology* **2006**, *70*, (1), 426-433.
157. Issaeva, N.; Bozko, P.; Enge, M.; Protopopova, M.; Verhoef, L. G. G. C.; Masucci, M.; Pramanik, A.; Selivanova, G., Small molecule RITA binds to p53, blocks

- p53-HDM-2 interaction and activates p53 function in tumors. *Nature Medicine* **2004**, *10*, (12), 1321-1328.
158. Tsukamoto, S.; Yoshida, T.; Hosono, H.; Ohta, T.; Yokosawa, H., Hexylitaconic acid: A new inhibitor of p53-HDM2 interaction isolated from a marine-derived fungus, *Arthrinium* sp. *Bioorganic & Medicinal Chemistry Letters* **2006**, *16*, (1), 69-71.
159. LUK, K.-C.; SO, S.-S.; Zhang, J.; Zhang, Z. Oxindole derivatives. WO 2006/136606 A3, 2006.
160. Chen, L. S., (CN), Han, Xingchun (Shanghai, CN), He, Yun (Shanghai, CN), Yang, Song (Shanghai, CN), Zhang, Zhuming (Hillsborough, NJ, US) Spiroindolinone derivatives. 2010.
161. Rothweiler, U.; Czarna, A.; Krajewski, M.; Ciombor, J.; Kalinski, C.; Khazak, V.; Ross, G.; Skobeleva, N.; Weber, L.; Holak, T. A., Isoquinolin-1-one inhibitors of the MDM2-p53 interaction. *Chemmedchem* **2008**, *3*, (7), 1118-1128.
162. Zheleva, D. I.; McInnes, C.; Baxter, C.; Gibson, D.; Maccallum, D.; Powers, H.; Duncan, K.; Bailey, K.; Cummings, L.; Thomas, M.; Wang, S.; Turner, N.; Uhrinova, S.; Uhrinova, S.; Barlow, P.; Taylor, P.; Walkinshaw, M.; Lane, D.; Fischer, P., Bisarylsulfonamides -novel small molecule inhibitors of p53-Mdm2 interaction. *AACR Meeting Abstracts* **2004**, 2004, (1), 1281-d-1282.
163. Wu, S. Y.; McNae, I.; Kontopidis, G.; McClue, S. J.; McInnes, C.; Stewart, K. J.; Wang, S. D.; Zheleva, D. I.; Marriage, H.; Lane, D. P.; Taylor, P.; Fischer, P. M.; Walkinshaw, M. D., Discovery of a novel family of CDK inhibitors with the program LIDAEUS: Structural basis for ligand-induced disordering of the activation loop. *Structure* **2003**, *11*, (4), 399-410.
164. Gudkov, A. V.; Komarova, E. A., The role of p53 in determining sensitivity to radiotherapy. *Nature Reviews Cancer* **2003**, *3*, (2), 117-129.
165. Donehower, L. A., Does p53 affect organismal aging? *Journal of Cellular Physiology* **2002**, *192*, (1), 23-33.
166. Mendrysa, S. M.; McElwee, M. K.; Michalowski, J.; O'Leary, K. A.; Young, K. M.; Perry, M. E., mdm2 Is Critical for Inhibition of p53 during Lymphopoiesis and the Response to Ionizing Irradiation. *Mol. Cell. Biol.* **2003**, *23*, (2), 462-472.
167. Mendrysa, S. M.; O'Leary, K. A.; McElwee, M. K.; Michalowski, J.; Eisenman, R. N.; Powell, D. A.; Perry, M. E., Tumor suppression and normal aging in mice with constitutively high p53 activity. *Genes & Development* **2006**, *20*, (1), 16-21.
168. O'Leary, K. A.; Mendrysa, S. M.; Vaccaro, A.; Perry, M. E., Mdm2 Regulates p53 Independently of p19ARF in Homeostatic Tissues. *Molecular and Cellular Biology* **2004**, *24*, (1), 186-191.

169. Vassilev, L. T., MDM2 inhibitors for cancer therapy. *Trends in Molecular Medicine* **2007**, 13, (1), 23.
170. Shangary, S.; Ding, K.; Qiu, S.; Nikolovska-Coleska, Z.; Bauer, J. A.; Liu, M. L.; Wang, G. P.; Lu, Y. P.; McEachern, D.; Bernard, D.; Bradford, C. R.; Carey, T. E.; Wang, S. M., Reactivation of p53 by a specific MDM2 antagonist (MI-43) leads to p21-mediated cell cycle arrest and selective cell death in colon cancer. *Molecular Cancer Therapeutics* **2008**, 7, (6), 1533-1542.
171. Shangary, S.; Qin, D. G.; McEachern, D.; Liu, M. L.; Miller, R. S.; Qiu, S.; Nikolovska-Coleska, Z.; Ding, K.; Wang, G. P.; Chen, J. Y.; Bernard, D.; Zhang, J.; Lu, Y. P.; Gu, Q. Y.; Shah, R. B.; Pienta, K. J.; Ling, X. L.; Kang, S. M.; Guo, M.; Sun, Y.; Yang, D. J.; Wang, S. M., Temporal activation of p53 by a specific MDM2 inhibitor is selectively toxic to tumors and leads to complete tumor growth inhibition. *Proceedings of the National Academy of Sciences of the United States of America* **2008**, 105, (10), 3933-3938.
172. Shangary, S.; Wang, S. M., Targeting the MDM2-p53 interaction for cancer therapy. *Clinical Cancer Research* **2008**, 14, (17), 5318-5324.
173. Shangary, S.; Wang, S., Small-Molecule Inhibitors of the MDM2-p53 Protein-Protein Interaction to Reactivate p53 Function: A Novel Approach for Cancer Therapy. *Annual Review of Pharmacology and Toxicology* **2009**, 49, (1), 223-241.
174. Shangary, S.; Qin, D.; McEachern, D.; Miller, R. S.; Nikolovska-Coleska, Z.; Liu, M.; Qiu, S.; Ding, K.; Wang, G.; Chen, J.; Lu, Y.; Bernard, D.; Gu, Q.; Sun, Y.; Shah, R. B.; Pienta, K. J.; Lin, X.; Kang, S.; Zhu, S.; Guo, M.; Yang, D.; Wang, S., A novel orally active MDM2 inhibitor (MI-219) activates the p53 pathway and is selectively toxic to tumor cells. *Molecular Cancer Therapeutics* **2007**, 6, 3518S-3518S.
175. Carvajal, D.; Tovar, C.; Yang, H.; Vu, B. T.; Heimbrook, D. C.; Vassilev, L. T., Activation of p53 by MDM2 antagonists can protect proliferating cells from mitotic inhibitors. *Cancer Research* **2005**, 65, (5), 1918-1924.
176. Kranz, D.; Dobbelstein, M., Nongenotoxic p53 Activation Protects Cells against S-Phase-Specific Chemotherapy. *Cancer Research* **2006**, 66, (21), 10274-10280.
177. Stuhmer, T.; Chatterjee, M.; Hildebrandt, M.; Herrmann, P.; Gollasch, H.; Gerecke, C.; Theurich, S.; Cigliano, L.; Manz, R. A.; Daniel, P. T.; Bommert, K.; Vassilev, L. T.; Bargou, R. C., Nongenotoxic activation of the p53 pathway as a therapeutic strategy for multiple myeloma. *Blood* **2005**, 106, (10), 3609-3617.
178. Secchiero, P.; Barbarotto, E.; Tiribelli, M.; Zerbinati, C.; di Iasio, M. G.; Gonelli, A.; Cavazzini, F.; Campioni, D.; Fanin, R.; Cuneo, A.; Zauli, G., Functional integrity of the p53-mediated apoptotic pathway induced by the nongenotoxic agent nultin-3 in B-cell chronic lymphocytic leukemia (B-CLL). *Blood* **2006**, 107, (10), 4122-4129.

179. Kastan, M. B., Our cells get stressed too! Implications for human disease. *Blood Cells, Molecules, and Diseases* 39, (2), 148-150.
180. Lowe, S. W.; Schmitt, E. M.; Smith, S. W.; Osborne, B. A.; Jacks, T., p53 is required for radiation-induced apoptosis in mouse thymocytes. *Nature* 1993, 362, (6423), 847-849.
181. Potten, C. S.; Wilson, J. W.; Booth, C., Regulation and Significance of Apoptosis in the Stem Cells of the Gastrointestinal Epithelium. *Stem Cells* 1997, 15, (2), 82-93.
182. Shvarts, A.; Steegenga, W. T.; Riteco, N.; vanLaar, T.; Dekker, P.; Bazuine, M.; vanHam, R. C. A.; vanOordt, W. V.; Hateboer, G.; vanderEb, A. J.; Jochemsen, A. G., MDMX: A novel p53-binding protein with some functional properties of MDM2. *Embo Journal* 1996, 15, (19), 5349-5357.
183. Ramos, Y. F. M.; Stad, R.; Attema, J.; Peltenburg, L. T. C.; van der Eb, A. J.; Jochemsen, A. G., Aberrant Expression of HDMX Proteins in Tumor Cells Correlates with Wild-Type p53. *Cancer Research* 2001, 61, (5), 1839-1842.
184. Hu, B.; Gilkes, D. M.; Chen, J., Efficient p53 activation and apoptosis by simultaneous disruption of binding to MDM2 and MDMX. *Cancer Research* 2007, 67, (18), 8810-8817.
185. Hu, B. L.; Gilkes, D. M.; Farooqi, B.; Sebti, S. M.; Chen, J. D., MDMX overexpression prevents p53 activation by the MDM2 inhibitor nutlin. *Journal of Biological Chemistry* 2006, 281, (44), 33030-33035.
186. Patton, J. T.; Mayo, L. D.; Singhi, A. D.; Gudkov, A. V.; Stark, G. R.; Jackson, M. W., Levels of HdmX expression dictate the sensitivity of normal and transformed cells to nutlin-3. *Cancer Research* 2006, 66, (6), 3169-3176.
187. Popowicz, G. M.; Czarna, A.; Rothweiler, U.; Szwagierczak, A.; Krajewski, M.; Weber, L.; Holak, T. A., Molecular basis for the inhibition of p53 by Mdmx. *Cell Cycle* 2007, 6, 2386-2392.
188. McCoy, M. A.; Gesell, J. J.; Senior, M. M.; Wyss, D. F., Flexible lid to the p53-binding domain of human Mdm2: Implications for p53 regulation. *Proceedings of the National Academy of Sciences of the United States of America* 2003, 100, (4), 1645-1648.
189. Bottger, A.; Bottger, V.; Sparks, A.; Liu, W. L.; Howard, S. F.; Lane, D. P., Design of a synthetic Mdm2-binding mini protein that activates the p53 response in vivo. *Current Biology* 1997, 7, (11), 860-869.
190. Taylor, P.; Blackburn, E.; Sheng, Y. G.; Harding, S.; Hsin, K. Y.; Kan, D.; Shave, S.; Walkinshaw, M., Ligand discovery and virtual screening using the program LIDAEUS. *British Journal of Pharmacology* 2008, 153, S55-S67.

191. Blattner, C.; Sparks, A.; Lane, D., Transcription factor E2F-1 is upregulated in response to DNA damage in a manner analogous to that of p53. *Molecular and Cellular Biology* **1999**, 19, (5), 3704-3713.
192. Martin, K.; Trouche, D.; Hagemeyer, C.; Sorensen, T. S.; Lathangue, N. B.; Kouzarides, T., Stimulation of E2f1/Dp1 Transcriptional Activity by Mdm2 Oncoprotein. *Nature* **1995**, 375, (6533), 691-694.
193. O'Connor, D. J.; Lu, X., Stress signals induce transcriptionally inactive E2F-1 independently of p53 and Rb. *Oncogene* **2000**, 19, (20), 2369-2376.
194. Pompella, A.; Visvikis, A.; Paolicchi, A.; Tata, V. D.; Casini, A. F., The changing faces of glutathione, a cellular protagonist. *Biochemical Pharmacology* **2003**, 66, (8), 1499-1503.
195. Bondi, A., van der Waals Volumes and Radii. *The Journal of Physical Chemistry* **1964**, 68, (3), 441-451.
196. Tsunoda, T.; Otsuka, J.; Yamamiya, Y.; Ito, S., N,N,N',N'-Tetramethylazodicarboxamide (Tmad), a New Versatile Reagent for Mitsunobu Reaction - Its Application to Synthesis of Secondary-Amines. *Chemistry Letters* **1994**, (3), 539-542.
197. Tsunoda, T.; Yamamoto, H.; Goda, K.; Ito, S., Mitsunobu-type alkylation of p-toluenesulfonamide. A convenient new route to primary and secondary amines. *Tetrahedron Letters* **1996**, 37, (14), 2457-2458.
198. Mader, M. M.; Shih, C.; Considine, E.; Dios, A. D.; Grossman, C. S.; Hipskind, P. A.; Lin, H.-S.; Lobb, K. L.; Lopez, B.; Lopez, J. E., Acyl sulfonamide anti-proliferatives. Part 2: Activity of heterocyclic sulfonamide derivatives. *Bioorganic & Medicinal Chemistry Letters* **2005**, 15, (3), 617-620.
199. Lachman, A., Benzophenone Oxime. *Organic Synthesis, Coll. Vol. 2*, 70.
200. Abiraj, K.; Gowda, D. C., Magnesium-Catalyzed Proficient Reduction of Oximes to Amines Using Ammonium Formate. *Synthetic Communications: An International Journal for Rapid Communication of Synthetic Organic Chemistry* **2004**, 34, (4), 599 - 605.
201. Smith, A. E.; Orton, K. J. P., Acids as accelerators in the acetylation of amino-groups. *Journal Of The Chemical Society* **1908**, 93, 1242-1250.
202. Smith, A. E.; Orton, K. J. P., Acids as accelerators in acetylation Part II. *Journal Of The Chemical Society* **1909**, 95, 1060-1064.
203. Justik, M. W.; Koser, G. F., Oxidative rearrangements of arylalkenes with [hydroxy(tosyloxy)iodo]benzene in 95% methanol: a general, regioselective synthesis of [alpha]-aryl ketones. *Tetrahedron Letters* **2004**, 45, (32), 6159-6163.

204. Kirkpatrick, P.; Ellis, C., Chemical space. *Nature* **2004**, 432, (7019), 823-823.
205. Irwin, J. J.; Shoichet, B. K., ZINC - A free database of commercially available compounds for virtual screening. *Journal Of Chemical Information And Modeling* **2005**, 45, (1), 177-182.
206. Oprea, T. I.; Matter, H., Integrating virtual screening in lead discovery. *Current Opinion in Chemical Biology* **2004**, 8, (4), 349-358.
207. Shoichet, B. K., Virtual screening of chemical libraries. *Nature* **2004**, 432, (7019), 862-865.
208. Muegge, I.; Oloff, S., Advances in virtual screening. *Drug Discovery Today: Technologies* **2006**, 3, (4), 405-411.
209. Wang, R. X.; Lu, Y. P.; Wang, S. M., Comparative evaluation of 11 scoring functions for molecular docking. *Journal of Medicinal Chemistry* **2003**, 46, (12), 2287-2303.
210. Verdonk, M. L.; Berdini, V.; Hartshorn, M. J.; Mooij, W. T. M.; Murray, C. W.; Taylor, R. D.; Watson, P., Virtual screening using protein-ligand docking: Avoiding artificial enrichment. *Journal of Chemical Information and Computer Sciences* **2004**, 44, (3), 793-806.
211. Huang, N.; Shoichet, B. K.; Irwin, J. J., Benchmarking sets for molecular docking. *Journal of Medicinal Chemistry* **2006**, 49, (23), 6789-6801.
212. OpenEye Scientific Software, I., Santa Fe, NM, USA, www.eyesopen.com, 2007.
213. Dror, O.; Schneidman-Duhovny, D.; Inbar, Y.; Nussinov, R.; Wolfson, H. J., Novel Approach for Efficient Pharmacophore-Based Virtual Screening: Method and Applications. *Journal of Chemical Information and Modeling* **2009**, 49, (10), 2333-2343.
214. Klabunde, T., Chemogenomic approaches to drug discovery: similar receptors bind similar ligands. *British Journal of Pharmacology* **2007**, 152, (1), 5-7.
215. Rognan, D., Chemogenomic approaches to rational drug design. *British Journal of Pharmacology* **2007**, 152, (1), 38-52.
216. Rush, T. S.; Grant, J. A.; Mosyak, L.; Nicholls, A., A shape-based 3-D scaffold hopping method and its application to a bacterial protein-protein interaction. *Journal Of Medicinal Chemistry* **2005**, 48, (5), 1489-1495.
217. Hawkins, P. C. D.; Skillman, A. G.; Nicholls, A., Comparison of shape-matching and docking as virtual screening tools. *Journal Of Medicinal Chemistry* **2007**, 50, (1), 74-82.

218. Moffat, K.; Gillet, V. J.; Whittle, M.; Bravi, G.; Leach, A. R., A comparison of field-based similarity searching methods: CatShape, FBSS, and ROCS. *Journal of Chemical Information and Modeling* **2008**, 48, (4), 719-729.
219. McGaughy, G. B.; Sheridan, R. P.; Bayly, C. I.; Culberson, J. C.; Kreatsoulas, C.; Lindsley, S.; Maiorov, V.; Truchon, J. F.; Cornell, W. D., Comparison of topological, shape, and docking methods in virtual screening. *Journal of Chemical Information and Modeling* **2007**, 47, (4), 1504-1519.
220. Cummings, M. D.; Gibbs, A. C.; DesJarlais, R. L., Processing of small molecule databases for automated docking. *Medicinal Chemistry* **2007**, 3, (1), 107-113.
221. Oprea, T. I., Current trends in lead discovery: Are we looking for the appropriate properties? *Molecular Diversity* **2000**, 5, (4), 199-208.
222. Oprea, T. I., Property distribution of drug-related chemical databases. *Journal of Computer-Aided Molecular Design* **2000**, 14, (3), 251-264.
223. Lipinski, C. A., Lead- and drug-like compounds: the rule-of-five revolution. *Drug Discovery Today: Technologies* **2004**, 1, (4), 337-341.
224. Lipinski, C. A.; Lombardo, F.; Dominy, B. W.; Feeney, P. J., Experimental and computational approaches to estimate solubility and permeability in drug discovery and development settings. *Advanced Drug Delivery Reviews* **1997**, 23, (1-3), 3-25.
225. Bostrom, J.; Greenwood, J. R.; Gottfries, J., Assessing the performance of OMEGA with respect to retrieving bioactive conformations. *Journal of Molecular Graphics & Modelling* **2003**, 21, (5), 449-462.
226. Escalante, J.; Ortíz-Nava, C.; Flores, P.; Priego, J.; Garc a-Mart nez, C., Synthesis, NMR and Crystallographic Studies of 2-Substituted Dihydroquinazolines Derived from (S)-Phenylethylamine. *Molecules* **2007**, 12, (2), 173-182.
227. B hm, H.-J.; Flohr, A.; Stahl, M., Scaffold hopping. *Drug Discovery Today: Technologies* **2004**, 1, (3), 217-224.
228. Lee, J.; Gauthier, D.; Rivero, R. A., Solid-phase synthesis of 3,4,5-substituted 1,5-benzodiazepin-2-ones. *Journal of Organic Chemistry* **1999**, 64, (9), 3060-3065.
229. Costantino, L.; Barlocco, D., Privileged structures as leads in medicinal chemistry. *Current Medicinal Chemistry* **2006**, 13, (1), 65-85.
230. Lipinski, C. A. In *Synergy between advances in screening methodology and computational chemistry*, 1st Joint ELRIG/SBS meeting, East Midland Conference Centre, University of Nottingham, 2007; ELRIG: East Midland Conference Centre, University of Nottingham, 2007.

231. Ertl, P.; Jelfs, S.; Muhlbacher, J.; Schuffenhauer, A.; Selzer, P., Quest for the rings. In silico exploration of ring universe to identify novel bioactive heteroaromatic scaffolds. *Journal of Medicinal Chemistry* **2006**, *49*, (15), 4568-4573.
232. Awouters, F.; Niemegeers, C. J. E.; Van den Berk, J.; Van Nueten, J. M.; Lenaerts, F. M.; Borgers, M.; Schellekens, K. H. L.; Broeckaert, A.; De Cree, J.; Janssen, P. A. J., Oxatomide, a new orally active drug which inhibits both the release and the effects of allergic mediators. *Cellular and Molecular Life Sciences* **1977**, *33*, (12), 1657-1659.
233. Swann, I. L.; Thompson, E. N.; Qureshi, K., Domperidone or Metoclopramide in Preventing Chemotherapeutically Induced Nausea and Vomiting. *British Medical Journal* **1979**, *2*, (6199), 1188-1188.
234. Borsini, F.; Evans, K.; Jason, K.; Rohde, F.; Alexander, B.; Pollentier, S., Pharmacology of Flibanserin. *CNS Drug Reviews* **2002**, *8*, (2), 117-142.
235. Kawamoto, H.; Ozaki, S.; Itoh, Y.; Miyaji, M.; Arai, S.; Nakashima, H.; Kato, T.; Ohta, H.; Iwasawa, Y., Discovery of the first potent and selective small molecule opioid receptor-like (ORL1) antagonist: 1-[(3R,4R)-1-cyclooctylmethyl-3-hydroxymethyl-4-piperidyl]-3-ethyl-1,3-dihydro-2H-benzimidazol-2-one (J-113397). *Journal of Medicinal Chemistry* **1999**, *42*, (25), 5061-5063.
236. Barreca, M. L.; Rao, A.; De Luca, L.; ZappalÀ , M.; Monforte, A.-M.; Maga, G.; Pannecouque, C.; Balzarini, J.; De Clercq, E.; Chimirri, A.; Monforte, P., Computational Strategies in Discovering Novel Non-nucleoside Inhibitors of HIV-1 RT. *Journal of Medicinal Chemistry* **2005**, *48*, (9), 3433-3437.
237. Yu, K.-L.; Sin, N.; Civiello, R. L.; Wang, X. A.; Combrink, K. D.; Gulgeze, H. B.; Venables, B. L.; Wright, J. J. K.; Dalterio, R. A.; Zadjura, L.; Marino, A.; Dando, S.; D'Arienzo, C.; Kadow, K. F.; Cianci, C. W.; Li, Z.; Clarke, J.; Genovesi, E. V.; Medina, I.; Lamb, L.; Colonna, R. J.; Yang, Z.; Krystal, M.; Meanwell, N. A., Respiratory syncytial virus fusion inhibitors. Part 4: Optimization for oral bioavailability. *Bioorganic & Medicinal Chemistry Letters* **2007**, *17*, (4), 895-901.
238. Hammach, A.; Barbosa, A.; Gaenzler, F. C.; Fadra, T.; Goldberg, D.; Hao, M.-H.; Kroe, R. R.; Liu, P.; Qian, K. C.; Ralph, M.; Sarko, C.; Soleymanzadeh, F.; Moss, N., Discovery and design of benzimidazolone based inhibitors of p38 MAP kinase. *Bioorganic & Medicinal Chemistry Letters* **2006**, *16*, (24), 6316-6320.
239. Ghelardini, C.; Galeotti, N.; Casamenti, F.; MalmbergAiello, P.; Pepeu, G.; Gualtieri, F.; Bartolini, A., Central cholinergic antinociception induced by 5HT(4) agonists: BIMU 1 and BIMU 8. *Life Sciences* **1996**, *58*, (25), 2297-2309.
240. Hopkins, A. L.; Groom, C. R.; Alex, A., Ligand efficiency: a useful metric for lead selection. *Drug Discovery Today* **2004**, *9*, (10), 430-431.

241. LUK Kin-Chun, S. S.-S., Zhang Jing, Zhang, Zhuming WO 2006/136606 A3, 2006.
242. Huber, V. J.; Arroll, T. W.; Lum, C.; Goodman, B. A.; Nakanishi, H., (1-Benzimidazolonyl)alanine (Bia): preliminary investigations into a potential tryptophan mimetic. *Tetrahedron Letters* **2002**, 43, (38), 6729-6733.
243. Zou, B. L.; Yuan, O. L.; Ma, D. W., Cascade Coupling/Cyclization process to n-substituted 1,3-dihydrobenzimidazol-2-ones. *Organic Letters* **2007**, 9, 4291-4294.
244. Thomas Sander *OSIRIS Property Explorer, Actelion Pharmaceuticals Ltd., Gewerbestrasse 16, 4123 Allschwil, Switzerland, Email: thomas.sanderactelion.com*
245. Taber, D. F., <http://www.organic-chemistry.org/>
In Taber, D. F., Ed.
246. Richmond, M. L.; Sprout, C. M.; Seto, C. T., Enantioselective Addition of Vinylzinc Reagents to Aldehydes Catalyzed by Modular Ligands Derived from Amino Acids. *The Journal of Organic Chemistry* **2005**, 70, (22), 8835-8840.
247. Robak, M. T.; Herbage, M. A.; Ellman, J. A., Synthesis and Applications of tert-Butanesulfinamide. *Chemical Reviews* **110**, (6), 3600-3740.
248. Lin, G. Q.; Xu, M. H.; Zhong, Y. W.; Sun, X. W., An advance on exploring N-tert-butanesulfinyl imines in asymmetric synthesis of chiral amines. *Accounts of Chemical Research* **2008**, 41, (7), 831-840.
249. Ellman, J. A., Applications of tert-butanesulfinamide in the asymmetric synthesis of amines. *Pure and Applied Chemistry* **2003**, 75, (1), 39-46.
250. Hunt, C. A.; Mallorga, P. J.; Michelson, S. R.; Schwam, H.; Sondey, J. M.; Smith, R. L.; Sugrue, M. F.; Shepard, K. L., 3-Substituted thieno[2,3-b][1,4]thiazine-6-sulfonamides. A novel class of topically active carbonic anhydrase inhibitors *Journal of Medicinal Chemistry* **1994**, 37, (2), 240-247.
251. Mohamadi, F.; Spees, M. M.; Grindey, G. B., Sulfonylureas: a new class of cancer chemotherapeutic agents. *Journal of Medicinal Chemistry* **1992**, 35, (16), 3014-3016.
252. Kurosawa, W.; Kan, T.; Fukuyama, T., PREPARATION OF SECONDARY AMINES FROM PRIMARY AMINES VIA 2-NITROBENZENESULFONAMIDES. *Organic Synthesis Collective Volume* **2004**, 10, 482.
253. Lazny, R.; Nodzevska, A.; Wolosewicz, K., New Simple Polymeric Supports with Hydrazone Linkers for Solid-Phase Synthesis of Ketones and Primary Amines. *Synthesis* **2003**, 2003, (18), 2858,2864.

254. Kamm, O., Ethyl Phenylacetate. *Organic Synthesis, Coll. Vol.* **1941**, 1, 270.